# The Marine Geochemistry of the Rare Earth Elements

by

Hein J.W. de Baar

Ingenieur Chemische Technologie
Technische Hogeschool Delft

1977

Submitted in partial fulfillment
of the requirements for the
degree of

Doctor of Philosophy

at the

Massachusetts Institute of Technology
and the
Woods Hole Oceanographic Institution

September 1983

Signature of Author _____
Department of Earth, Atmospheric, and Planetary Sciences, Massachusetts Institute of Technology and the Joint Program in Oceanography, Massachusetts Institute of Technology / Woods Hole Oceanographic Institution, 12 December 1983

Certified by _____
Peter G. Brewer, Thesis Supervisor

Accepted by _____
Cindy Lee, Chairman, Joint Committee for Chemical Oceanography, Massachusetts Institute of Technology / Woods Hole Oceanographic Institution

ABSTRACT

Novel methods were developed for the determination of 12 of the 14 Rare Earth Elements (REE) in seawater. Initial extractions of the REE by chelating ion exchange chromatography is followed by cation exchange for removal of co-extracted U and remaining traces of major ions. Finally traces of U are removed by anion exchange before irradiation for 8 hours at a flux of $5 \times 10^{13}$ neutrons.$cm^{-2}$.$sec^{-1}$. After post-irradiation separation of $^{24}Na$, the gamma spectra are recorded over four different time intervals with a Ge(Li) detector. An internal standard ($^{144}Ce$) is carried all along the procedure for improved precision by avoidance of counting geometry errors.

Vertical profiles are reported for three stations in respectively the Northwest Atlantic Ocean, the Eastern Equatorial Pacific Ocean and the Cariaco Trench, an anoxic basin. This data set represents the first detailed profiles of Pr, Tb, Ho, Tm and Lu in seawater, together with profiles of La, Ce, Nd, Sm, Eu, Gd and Yb. The first observations of positive Ce anomalies in seawater are ascribed to regeneration of Ce under reducing conditions. The first reported positive Gd anomalies are ascribed to the unique chemical properties of the Gd(III)-cation, which has an exactly half-filled 4f electron shell.

Concentrations of the REE range from 0.3 pmol.$kg^{-1}$ (Lu) to 86 pmol.$kg^{-1}$ (Ce) and are among the lowest reported so far for trace elements in seawater. The REE as a group typically exhibit a quasi-linear increase with depth. In the deep water there appears to be some degree of correlation with silicate. Concentration levels in the deep Pacific Ocean are 2-4 times those in deep Atlantic waters. Ce has an opposite behaviour, with very strong depletions in deep Pacific waters. In the Cariaco Trench all REE, but especially Ce, are strongly affected by the chemical changes across the oxic/anoxic interface.

The REE distributions normalized versus shales (crustal abundance) exhibit four major features:

i) a gradual enrichment of the heavy REE, most strongly developed in the deep Pacific Ocean. This is compatible with the stabilization of heavy REE by stronger inorganic complexation in seawater as predicted by the TURNER- WHITFIELD-DICKSON speciation model.

ii) the first description of positive Gd anomalies, in agreement with the anomalously strong complexation of the Gd(III)-cation predicted by the same speciation model.

iii) most commonly negative, but sometimes positive, Ce anomalies.

iv) a linear Eu/Sm relation for all samples.

Distributions of the dissolved REE in ocean waters seem to be dominated by their internal cycling within the ocean basins. With a few notable exceptions, the ultimate external sources (riverine, aeolian, hydrothermal) and sinks (authigenic minerals) appear to have little impact on the spatial distribution of the REE in oceanic water masses. Analogies with distributions of other properties within the oceans suggest that the REE as a group are controlled by two simultaneous processes:

A) cycling like or identical to opal and calcium-carbonate, with circumstantial evidence in suport of the latter as a possible carrier.

B) adsorptive scavenging, possibly by manganese-oxide phases on settling particles.

The latter mechanism is strongly supported by the parallels between REE(III) speciation in seawater and the 'typical' seawater REE pattern. This general correspondence is highlighted by the very distinct excursions of Gd in both Gd(III) speciation and the observed seawater REE patterns.

Combination of both apparent mechanisms, for instance scavenging of REE by adsorptive coatings (Mn oxides) on settling skeletal material, is very well conceivable. Upon dissolution of the shells at or near the seafloor the adsorbed REE fraction would be released into the bottom waters.

The observations of

- positive Ce anomalies in Northwest Atlantic surface waters,
- enhanced Ce anomalies and Mn levels in the $O_2$-minimum zone of the Eastern Equatorial Pacific Ocean, and
- enhanced Ce concentrations in anoxic waters

all support the contention that a vigorous cycling driven by oxidation and reduction reactions dominates both Ce and Mn in the ocean basins.

Under conditions of thermodynamic equilibrium, Ce tends to become depleted in well-oxygenated open ocean waters, and normal or enriched in waters below a $pO_2$ threshold of about 0.001-0.010 atm partial pressure. The latter threshold level generally lies below the sediment/water interface.

However, the kinetics of oxidation (and reduction) of Ce appears to be slow relative to various transport processes. This leads to disequilibria, i.e. a major uncoupling of the $pO_2$ threshold level and the Ce anomaly distribution.

The REE are definitely non-conservative in seawater and in general the REE pattern or $^{143}Nd/^{144}Nd$ isotopic ratio cannot be treated as ideal water mass tracers. The continuous redistribution of Ce within the modern ocean, combined with the likelihood of active diagenesis, precludes the use of Ce anomalies as indicators of oxic versus anoxic conditions in ancient oceans. On the other hand, the Eu/Sm ratio, possibly combined with $^{143}Nd/^{144}Nd$, would have potential as a tracer for understanding modern and ancient processes of hydrothermal circulation.

ACKNOWLEDGEMENTS

The research described in this thesis really is a joint effort of many people. Peter Brewer initially suggested to consider the Rare Earth Elements as a possible thesis topic. Moreover he did follow up by being a real adviser indeed, providing elegant solutions and witty moral support whenever difficulties were encountered. At all times Michael Bacon could be counted on for advice on chemical and practical matters, for sincerely probing yet another one of my brilliant misconceptions, for running his cruises in a very smooth and enjoyable manner, and most of all for trying, probably desperately, to transfer some of his own talents in writing clear and concise manuscripts. Mike delivers. Fred Frey opened my eyes for rare earths geochemistry and also provided advice on very many details of neutron activation analysis. For the first activations we were allowed to use several detectors in his laboratory. Hugh Livingston provided valuable advice on both geochemical and analytical matters. In the process he managed to fill major gaps in my knowledge of radiochemistry. In several occasions I was also granted generous time-slots for the detectors in his laboratory. Given the many analytical stumbling blocks I am most grateful to all my advisers for providing lots of sincere encouragement which prevented an almost certain career in the Foreign Legion.

During the first two years Cindy Lee guided a blatantly ignorant alien through the delicate network of U.S. academia. I still like to believe Cindy is the one person whom dutifully read all 1000 or so pages of my assorted thesis proposals on the marine geochemistry of the periodic table. Her bargaining skills are demonstrated by the fact that I finally settled for only about ten percent of Mendeleyev's menu. I am most grateful to John Farrington for setting an example of professionalism by turning a once vigorous scientific debate into a loyal friendship for years to come.

Deborah Shafer provided various programs for data processing, and taught me how to use them. Alan Fleer taught me very many laboratory skills, helped tremendously with all kinds of tasks in the laboratory, and maintained the counting equipment as well as my good spirits, the latter by allowing me to win some of our tennis games. Rebecca Belastock provided much assistance in and around the laboratory and advised me on small craft oceanography. Peter Sachs adviced on the construction of all kinds of equipment and gave me full access to his collection of tools. Most of all I would like to thank Debbie, Becky, Alan and Pete for their generous friendship, of which the continuous supply of home baked goodies during coffee break is just one example.

Without the advice and cooperation of Bill Fecych, John Bernard and Kwan Kwok of the MIT Nuclear Reactor Laboratory there would have been no data in this thesis. Ken Bruland collected the Pacific samples (ch.4) during the VERTEX II expedition. Ed Boyle taught me various techniques as used for analyses of trace elements. Ernie Charette, Ed Phares and his crew of skilled carpenters, Tom Rennie and Gordon Rose all helped with the construction of a clean laboratory. Communications with my fellow students always proved to be most enjoyable and served, if nothing else, for dispelling the notion that I was the only one struggling with an awful thesis project. I am particularly grateful to Bob Anderson for his

advice and moral support. Dave Graham kindly provided access to his insights in geochemistry, as well as his well organized reprint collection. Abbie Alvin, Dixie Berthel, Connie Brackett and Jake Peirson not only beautifully managed my persistent bureaucratic foul ups with the education system, but also provided serious reminders that nothing should be taken absolutely serious.

Ik ben zeer dankbaar aan mijn ouders voor het leggen van een degelijke fundatie in mijn opleiding. Door hun stimulans en steun in mijn scholing was deze laatste fase mogelijk. Maar vakkennis alleen zou niet toereikend zijn. Meest dankbaar ben ik mijn ouders daarom ook voor wat ze zelf aan mij geleerd hebben.

Zonder de bereidwilligheid van Pieternel om over zichzelf heen in dit wilde avontuur te stappen was er natuurlijk nooit iets gelukt. Vanwege mijn onbegrijpelijke voorliefde voor de al even onbegrijpelijke scheikunde werd een ballingschap met volstrekte afwezigheid van een, al was het maar een wankele, economische basis op de koop toe genomen. Ondanks de radicaal moderne inzichten van haar ega zag ze zich de laatste drie jaar toch weer gedwongen het negentiende eeuwse rolpatroon op te vatten, hierbij gelukkig gesteund door de huidige achttiende eeuwse federale regering. Pieternel zonder je geloof in mijn dromen, en al je hulp, was dit luchtkasteel nooit van de grond gekomen. Van de hele Ph.D. verdien je de P van Pieternel en de h.D. van h.eleboel Dank.
Jouke maakte me elke dag zonneklaar duidelijk dat hij me zo mist als ik met mijn vriendjes op het werk ben, dat windsurferen een doorslaggevend stuk zeeonderzoek is, dat mijn leerproces op gevorderde leeftijd maar een trage bedoening is, maar bovenal dat het belang van zeldzame aarden in zee ook maar betrekkelijk is.

Last but not least I would like to thank all those people whom helped us setting up in Woods Hole. Especially the friendship of the Brewer, Cowles, VanderKolk, and Wakeham families and the support of the playgroup 'cooperative' really made us feel at home.

This research was supported by Department of Energy contract DE-AS02-76EV03566 and Office of Naval Research Contract N00014-82-C-0019 NR 083-004.

TABLE OF CONTENTS

List of Figures

List of Tables

# 1. GENERAL INTRODUCTION

## 1.1. Properties and Abundances of the Rare Earth Elements.

The Rare Earth Elements (REE) are the element lanthanum (La) and the fourteen elements that follow La in the periodic table (the lanthanides) in which the fourteen 4f electrons are successively added to the La-configuration (Table 1.1). Their most attractive properties are the romantic names, whose origins are discussed by HAMMOND (1981).

Nuclides of the REE and other elements are continuously synthesized during stellar evolution (BURBIDGE et al.,1957; ALLER, 1961; CLAYTON, 1968). The various stages of nucleosynthesis can be related to cosmic abundance patterns, and vice versa (HENDERSON, 1982). Actually the abundances of REE-nuclides have been instrumental in the development of current theory for nucleosynthesis. The concentrations of REE in sedimentary rocks, thought to represent crustal abundance, show two features (Figure 1.1):

i) the elements with even atomic number Z are more stable than those with odd atomic number (the ODDO-HARKINS rule);
ii) there is a systematic decrease in abundance with increasing atomic number.

Later work led to the current understanding that the same principles hold for the abundance of all elements in the solar system (Figure 1.1).

Within the REE series the element Pm (Z=61) is the ultimate example of the Oddo-Harkins rule. It does not exist on earth, except for negligible amounts of short-lived (few years) radionuclides produced upon spontaneous fission of $^{238}U$. Compilations of isotopic abundances of the REE have been given by HERRMANN(1970); WALKER et al.(1977) and LEDERER & SHIRLEY(1978). Four naturally occurring unstable isotopes decay with long half-lives ranging from $10^{10}$ to $10^{15}$ years (Table 1.2). The Sm-Nd isotopic system has been studied extensively in geochemistry (DePAOLO & WASSERBURG, 1976). Applications of the Sm-Nd system to the marine environment will be dealt with in chapter 7. Measurements of the Lu-Hf

| Z | Symbol | Element | ←——REE$^0$——→ | | | | | | ←REE$^{3+}$→ | | |
|---|---|---|---|---|---|---|---|---|---|---|---|
| | | | 4f | 5s | 5p | 5d | 6s | 7s | 4f | 5s | 5p |
| 57 | La | Lanthanum | | 2 | 6 | 1 | 2 | | | 2 | 6 |
| 58 | Ce | Cerium | 1 | 2 | 6 | 1 | 2 | | 1 | 2 | 6 |
| 59 | Pr | Praesodymium | 3 | 2 | 6 | | | 2 | 2 | 2 | 6 |
| 60 | Nd | Neodymium | 4 | 2 | 6 | | 2 | | 3 | 2 | 6 |
| 61 | Pm | Promethium | 5 | 2 | 6 | | 2 | | 4 | 2 | 6 |
| 62 | Sm | Samarium | 6 | 2 | 6 | | 2 | | 5 | 2 | 6 |
| 63 | Eu | Europium | 7 | 2 | 6 | | 2 | | 6 | 2 | 6 |
| 64 | Gd | Gadolinium | 7 | 2 | 6 | 1 | 2 | | 7 | 2 | 6 |
| 65 | Tb | Terbium | 9 | 2 | 6 | | 2 | | 8 | 2 | 6 |
| 66 | Dy | Dysprosium | 10 | 2 | 6 | | 2 | | 9 | 2 | 6 |
| 67 | Ho | Holmium | 11 | 2 | 6 | | 2 | | 10 | 2 | 6 |
| 68 | Er | Erbium | 12 | 2 | 6 | | 2 | | 11 | 2 | 6 |
| 69 | Tm | Thulium | 13 | 2 | 6 | | 2 | | 12 | 2 | 6 |
| 70 | Yb | Ytterbium | 14 | 2 | 6 | | 2 | | 13 | 2 | 6 |
| 71 | Lu | Lutetium | 14 | 2 | 6 | 1 | 2 | | 14 | 2 | 6 |

Table 1.1. The Rare Earth Elements with 'outer' shell electron configurations for the metals and REE(III)-ions. All REE have the same 'inner' shell configuration as Xe: $1s^2$, $2s^2$, $2p^6$, $3s^2$, $3p^6$, $3d^{10}$, $4s^2$, $4p^6$, $4d^{10}$. The given electron shell configurations are not all known with complete certainty because of the exceedingly complex emission spectra.

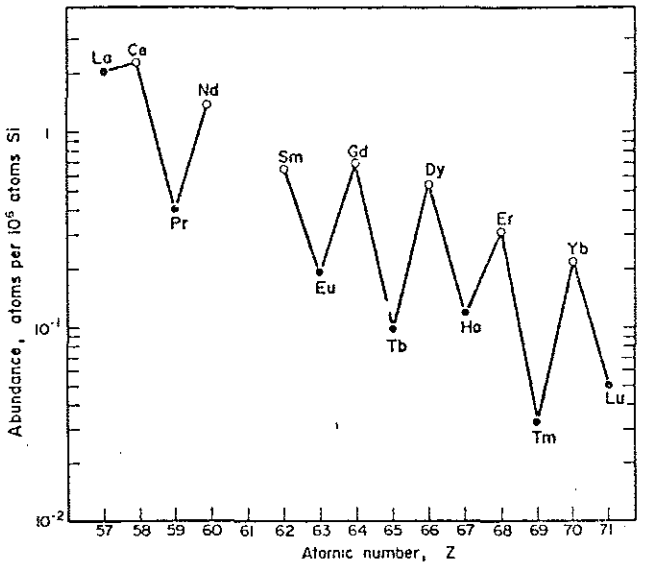


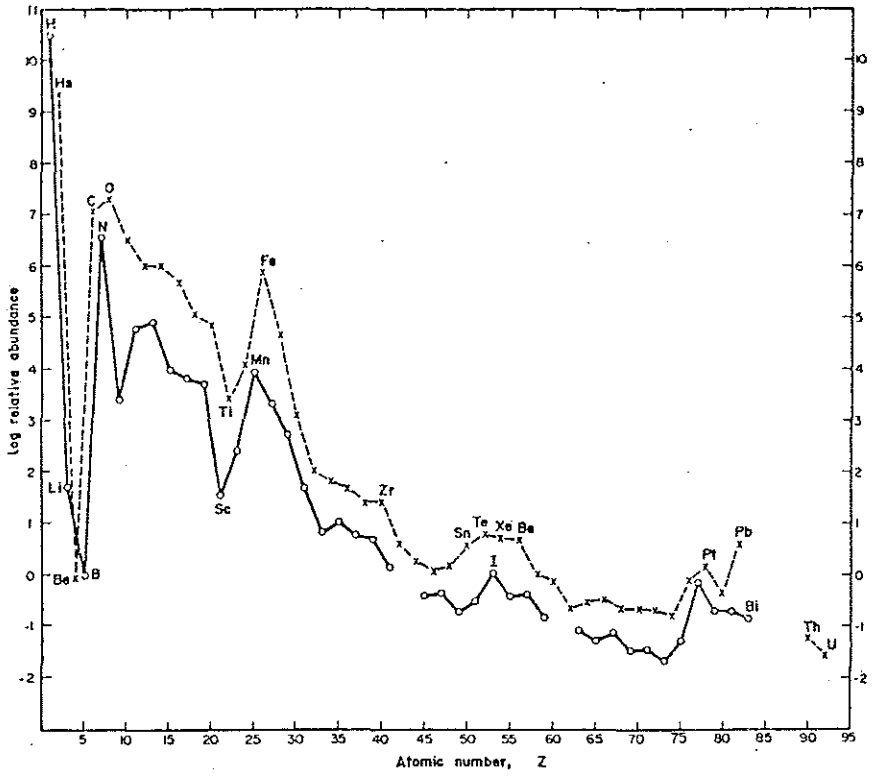


Figure 1.1. ABOVE: The REE abundance pattern in sedimentary rocks as used by SUESS & UREY (1956) to produce their estimate of element abundances in the solar system. Open circles even, filled circles odd Z.

BELOW: The abundances of the elements, normalized to Si=$10^6$ atoms, in the solar system (CAMERON, 1973). Crosses: elements of even atomic number; circles: elements of odd atomic number.

| | DECAY REACTION | HALF-LIFE |
|---|---|---|
| (i) | $^{138}La \xrightarrow{EC} {}^{138}Ba$ 70%; $^{138}La \xrightarrow{-\beta} {}^{138}Ce$ 30% | $1.6 \times 10^{11}$ years |
| (ii) | $^{144}Nd \xrightarrow{\alpha} {}^{140}Ce$ | $2.1 \times 10^{15}$ years |
| (iii) | $^{147}Sm \xrightarrow{\alpha} {}^{143}Nd$ | $1.15\text{-}1.28 \times 10^{11}$ years |
| (iv) | $^{176}Lu \xrightarrow{-\beta} {}^{176}Hf$ | $2.2 \times 10^{10}$ years |

Table 1.2. The decay schemes of four naturally occurring long-lived radionuclides (HERRMANN, 1970). Short-lived isotopes $^{145}Pm$ and $^{147}Pm$ produced from spontaneous $^{238}U$ fission have not yet been detected on earth.

isotopic couple in rocks are now routinely achieved (PATCHETT & TATSUMOTO, 1980). Most recently isochron dating with the La-Ce system has been reported (TANAKA & MASUDA, 1982). The variations in the $^{138}Ce/^{140}Ce$ ratio resulting from radioactive decay of $^{138}La$ are potentially very interesting with respect to marine chemistry. The oxidation and reduction of Ce occurs exclusively within the marine environment and the corresponding strong La/Ce fractionations may very well affect the $^{138}Ce/^{140}Ce$ isotopic signature.

The most stable oxidation state of all lanthanides is the $REE^{3+}$-form. The $La^{3+}$-, $Gd^{3+}$- and $Lu^{3+}$-cations with exactly empty, half (7/14) and completely (14/14) filled 4f electron shell (Table 1.1) are particularly stable (Figure 6.7). The only other oxidation states relevant for geological processes are the $Ce^{4+}$ and $Eu^{2+}$ cations. Unstable cations like $Sm^{2+}$, $Yb^{2+}$ and others are known to exist in solution but are irrelevant for geochemical purposes.

The trivalent ionic radii decrease very gradually with increasing atomic number (Table 1.3). This is the well-known lanthanide-contraction, which results from the filling of the 4f subshell. At close inspection there appears to be a minor discontinuity between Gd and Tb, possibly as a result of the stabilization of the exactly half-filled 4f shell of Gd(III). One geochemical effect of the lanthanide contraction is to cause the heavier REE to be similar in ionic radius to much lighter elements (e.g., Y). There appears to be a coherence between Y(III) and the suite Gd(III)-Lu(III), often called the 'yttrium earths'. The large REE cations La(III)-Eu(III) are often referred to as 'cerium earths'. During evolution of igneous rocks the REE are often fractionated according to ionic radii into roughly these two groups.

Cations in aqueous solution (e.g., REE(III)), are all surrounded by a given number of weakly bound water molecules (hydration), some of which may further condensate to form hydrolysed species:

$$REE^{3+} + nH_2O \rightleftharpoons [REE\ O\begin{smallmatrix}H\\H\end{smallmatrix}]^{3+}[H_2O]_{n-1} \rightleftharpoons [REE\text{-}OH]^{2+}[H_2O]_{n-1} + H^+$$

(hydration) (hydrolysis)

Both hydration and hydrolysis are known to depend on numerous factors that are still poorly understood (WILLIAMS, 1982; BAES & MESMER, 1976).

| Ca | | Sc | |
|---|---|---|---|
| 2 VI | 1.00 | 3 VI | 0.745 |
| VII | 1.06 | VIII | 0.870 |
| VIII | 1.12 | | |
| IX | 1.18 | | |
| X | 1.23 | | |
| XII | 1.34 | | |

| Sr | | Y | |
|---|---|---|---|
| 2 VI | 1.18 | 3 VI | 0.900 |
| VII | 1.21 | VII | 0.96 |
| VIII | 1.26 | VIII | 1.019 |
| IX | 1.31 | IX | 1.075 |
| X | 1.36 | | |
| XII | 1.44 | | |

| Ba | | La | | Ce | | Pr | | Nd | | Pm | |
|---|---|---|---|---|---|---|---|---|---|---|---|
| 2 VI | 1.35 | 3 VI | 1.032 | 3 VI | 1.01 | 3 VI | 0.99 | 2 VIII | 1.29 | 3 VI | 0.97 |
| VII | 1.38 | VII | 1.10 | VII | 1.07 | VIII | 1.126 | IX | 1.35 | VIII | 1.093 |
| VIII | 1.42 | VIII | 1.160 | VIII | 1.143 | IX | 1.179 | 3 VI | 0.983 | IX | 1.144 |
| IX | 1.47 | IX | 1.216 | IX | 1.196 | 4 VI | 0.85 | VIII | 1.109 | | |
| X | 1.52 | X | 1.27 | X | 1.25 | VIII | 0.96 | IX | 1.163 | | |
| XI | 1.57 | XII | 1.36 | XII | 1.34 | | | XII | 1.27 | | |
| XII | 1.61 | | | 4 VI | 0.87 | | | | | | |
| | | | | VIII | 0.97 | | | | | | |
| | | | | X | 1.07 | | | | | | |
| | | | | XII | 1.14 | | | | | | |

| Ra | |
|---|---|
| 2 VIII | 1.48 |
| XII | 1.70 |

| Sm | | Eu | | Gd | | Tb | | Dy | |
|---|---|---|---|---|---|---|---|---|---|
| 2 VII | 1.22 | 2 VI | 1.17 | 3 VI | 0.938 | 3 VI | 0.923 | 2 VI | 1.07 |
| VIII | 1.27 | VII | 1.20 | VII | 1.00 | VII | 0.98 | VII | 1.13 |
| IX | 1.32 | VIII | 1.25 | VIII | 1.053 | VIII | 1.040 | VIII | 1.19 |
| 3 VI | 0.958 | IX | 1.30 | IX | 1.107 | IX | 1.095 | 3 VI | 0.912 |
| VII | 1.02 | X | 1.35 | | | 4 VI | 0.76 | VII | 0.97 |
| VIII | 1.079 | 3 VI | 0.947 | | | VIII | 0.88 | VIII | 1.027 |
| IX | 1.132 | VII | 1.01 | | | | | IX | 1.083 |
| XII | 1.24 | VIII | 1.066 | | | | | | |
| | | IX | 1.120 | | | | | | |

| Ho | | Er | | Tm | | Yb | | Lu | |
|---|---|---|---|---|---|---|---|---|---|
| 3 VI | 0.901 | 3 VI | 0.890 | 2 VI | 1.03 | 2 VI | 1.02 | 3 VI | 0.861 |
| VIII | 1.015 | VII | 0.945 | VII | 1.09 | VII | 1.08 | VIII | 0.977 |
| IX | 1.072 | VIII | 1.004 | 3 VI | 0.880 | VIII | 1.14 | IX | 1.032 |
| X | 1.12 | IX | 1.062 | VIII | 0.994 | 3 VI | 0.868 | | |
| | | | | IX | 1.052 | VII | 0.925 | | |
| | | | | | | VIII | 0.985 | | |
| | | | | | | IX | 1.042 | | |

Table 1.3. The ionic radii (Angstrom) for different coordination numbers (roman numerals) and oxidation states (arabic numerals) of group 2a and group 3b elements. Values from SHANNON (1976). See HENDERSON (1982) for a discussion of differences with other compilations.

The simplest treatment is the electrostatic description of BORN, who predicted that the free energy of hydration of an ion of charge z and radius r would be proportional to $z^2/r$ (TURNER, WHITFIELD & DICKSON, 1981). Although this approach is overly simplistic one would expect the heavier REE(III) with smaller ionic radii to be more strongly hydrolysed. Apparently the aqueous geochemistry of the REE(III) is indirectly also a function of their ionic radii. Such gradual changes of properties in aqueous solution would make the REE-series a unique group of elements in marine chemistry.

The occurrence of different oxidation states for Ce and Eu leads to anomalies of either element versus their neighbors La-Pr and Sm-Gd in the series. Reduction of Eu is thought to occur often during the evolution of igneous rocks. The larger ionic radius of Eu(II) leads to its fractionation from the rest of the series (Table 1.3). Anomalies of Eu have been reported in various types of igneous and sedimentary rocks. However reduction and subsequent fractionation of Eu does not seem to occur within the ocean basins, with hydrothermal solutions being the notable exception (see section 4.3). The other redox element Ce exhibits an opposite behaviour. Development of Ce anomalies (i.e. the Ce(IV) state) during formation of igneous rocks can be largely ruled out (SCHREIBER et al.,1980) with one exception ascribed to recycling of oceanic lithosphere (HEMING & RANKIN, 1979). On the other hand Ce anomalies have been found exclusively within the ocean basins. Seawater is typically depleted in Ce relative to La-Pr, whereas such phases as ferromanganese nodules often exhibit a Ce enrichment. Many other trace elements in seawater (e.g. Mn, Fe, Cu, As, Sb, Se and I) are also affected by their multiple oxidation states. Yet Ce and Eu are unique because anomalies can be defined by comparison with their 'non-redox' neighbors in the REE-series. In principle one can single out oxidation-reduction reactions of Ce and Eu from all other processes affecting their oceanic distributions.

## 1.2. Normalization.

The even/odd predominance with atomic number Z (Oddo-Harkins) is the prominent feature for abundances of the REE-series in such reservoirs as

the solar system, the bulk earth, the crust, or for that matter, the ocean basins. Unfortunately it masks any fractionations due to secondary effects such as differences in ionic radii, different valencies of Ce and Eu, and differences in chemical bonding. Many schemes have been tried to overcome the zig-zag effect which would appear in a plot of raw abundance data (HASKIN, FREY, SCHMITT & SMITH, 1966). Any type plot designed to overcome this problem should be simple and relevant, in that order.

The elements are usually ranked on the horizontal axis, according to atomic number. Less simple but more relevant would be a ranking according to a parameter which actually controls the abundance. For instance fractionations during evolution of igneous rocks are largely controlled by ionic radius (Table 1.3).

MASUDA(1965) has pointed out that the reciprocals of ionic radii (i.e. 1/r) are a linear function of atomic number, provided the ionic radii values of TEMPLETON & DAUBEN (1954) are used. However the linear relation between ionic radii themselves and atomic number is almost as good. In other words, plots versus Z, r or 1/r would all look essentially the same.

For our purposes a parameter controlling the oceanic distribution of the REE would be ideal. Quite paradoxically a major objective of this study is to find exactly such controlling parameter(s). In doing so one can only rely on the simple ranking according to atomic number. However it is interesting to note that the simple $z^2/r$ relation of the BORN-model (see above) for all trivalent REE (z=3) would again suggest the reciprocal of the ionic radius (1/r) as an important controlling parameter.

The zig-zag pattern disappears when abundance ratios for each element rather than simple concentrations [pmol/kg] are plotted on the vertical axis. In other terms our measured values are to be normalized versus a reference abundance pattern. Two types reference pattern are conceivable:

i) Those representing a complete reservoir like bulk earth, crustal abundance, average marine sediments, or, most specifically, mean ocean water. The last named reference would be most suitable for resolving differences between various water masses. North Pacific Deep Water, the single largest water mass according to the census

method of WORTHINGTON(1981), would be a suitable reference. However REE data for NPDW are not available. Also, for comparison of the bulk oceans with, for instance, the continents, one would still employ a different reference representative of both reservoirs.

ii) Those representing ultimate inputs into the reservoir. Terrestrial (aeolian, riverine) as well as minor localized hydrothermal inputs are the most relevant ultimate sources for the ocean basins.

The bulk earth as a reservoir has a relative REE distribution similar to that of chondritic meteorites (HENDERSON, 1983). The relative REE abundances in igneous rocks in the earth's crust vary widely relative to chondrites. Lighter REE are sometimes enriched and sometimes depleted, while Eu exhibits both positive and negative anomalies. However during the processes of weathering, soil formation and sedimentation this variability is mostly evened out. As a result the relative abundance patterns of shales (HASKIN & HASKIN, 1966), marine sediments (WILDEMAN & HASKIN, 1963) and other sedimentary rocks (HASKIN, FREY, SCHMITT & SMITH, 1966) are surprisingly similar. In other words, the REE contents of sediments in general, and of 'shales' in particular, can be taken to represent the well mixed average REE content of the crust, or at least the upper crust. Abundances in a composite of 40 North American shales (NASC), or the arithmetic mean of abundances in three different shale composites (NASC, European shales, Russian platform; HASKIN & HASKIN, 1966), are commonly used as reference for crustal abundance. Relative to chondrites (bulk earth) the crust exhibits an enrichment of the lighter REE, and also a distinct negative Eu anomaly (Figure 1.2).

For the purpose of this thesis, the shale pattern is preferred over the chondritic pattern. Shales represent more relevant reservoirs:

- average crustal abundance;
- average abundance in terrestrial and marine sediments;

and also relevant inputs of:

- terrestrial material transported either by rivers or as aerosols.

Moreover seawater has a Eu depletion versus chondrites similar to that of shales. In other words, the Eu anomaly disappears when seawater/shale ratios are plotted. Of course the idealized concept of fully homogenized

sedimentary rocks is only a first approximation. Excursions from the shale pattern are observed upon close inspection of various terrestrial sedimentary basins. For instance a negative Eu anomaly versus shales for Sahara dust and aerosols (RAHN, 1976) is also reflected in recently reported surface seawater values (ELDERFIELD & GREAVES, 1982). Finally, in case of a perceived hydrothermal source, a 'typical' Mid Ocean Ridge Basalt reference pattern might be more advantageous.

Analytical considerations also play a role in selection of the most suitable reference. So far all abundance data for various chondrites or shale composites is based on oxide type analytical standards instead of more accurate standards made up from pure REE metals (see section 2.14). Neither of the two analytical methods, Instrumental Neutron Activation Analysis (INAA) and Isotope Dilution Mass Spectrometry (IDMS), yields data for all fourteen elements. Most INAA data does not include values for Dy and Er, whereas monoisotopic elements Pr, Tb, Ho and Tm cannot be determined by IDMS. Quite often values for La and Lu are also missing from IDMS data sets. On the other hand IDMS yields a higher precision.

The chondritic average based on INAA data by HASKIN, HASKIN, FREY & WILDEMAN (1968) is a good reference for relative bulk earth abundances. Subsequent IDMS results for the Leedey chondrite have a higher precision (MASUDA et al., 1973). An average of the Leedey results and additional IDMS analyses of other chondrites has been reported by NAKAMURA (1974). The most suitable chondritic reference is a weighted mean of all available INAA and IDMS data for CI chondrites as calculated by EVENSEN et al.(1978)(Table 1.4). The latter mean values are very consistent with the precise values for Leedey and the NAKAMURA average (Figure 1.2). Moreover by combination of both INAA and IDMS data all fourteen elements are included.

The various shale references all exhibit a very uniform relative trend versus chondrites (Figure 1.2). Following the example of PIPER(1974) the arithmetic mean of three shale composites (Table 1.4) was arbitrarily selected as the most suitable shale reference for normalization of the data in this thesis.

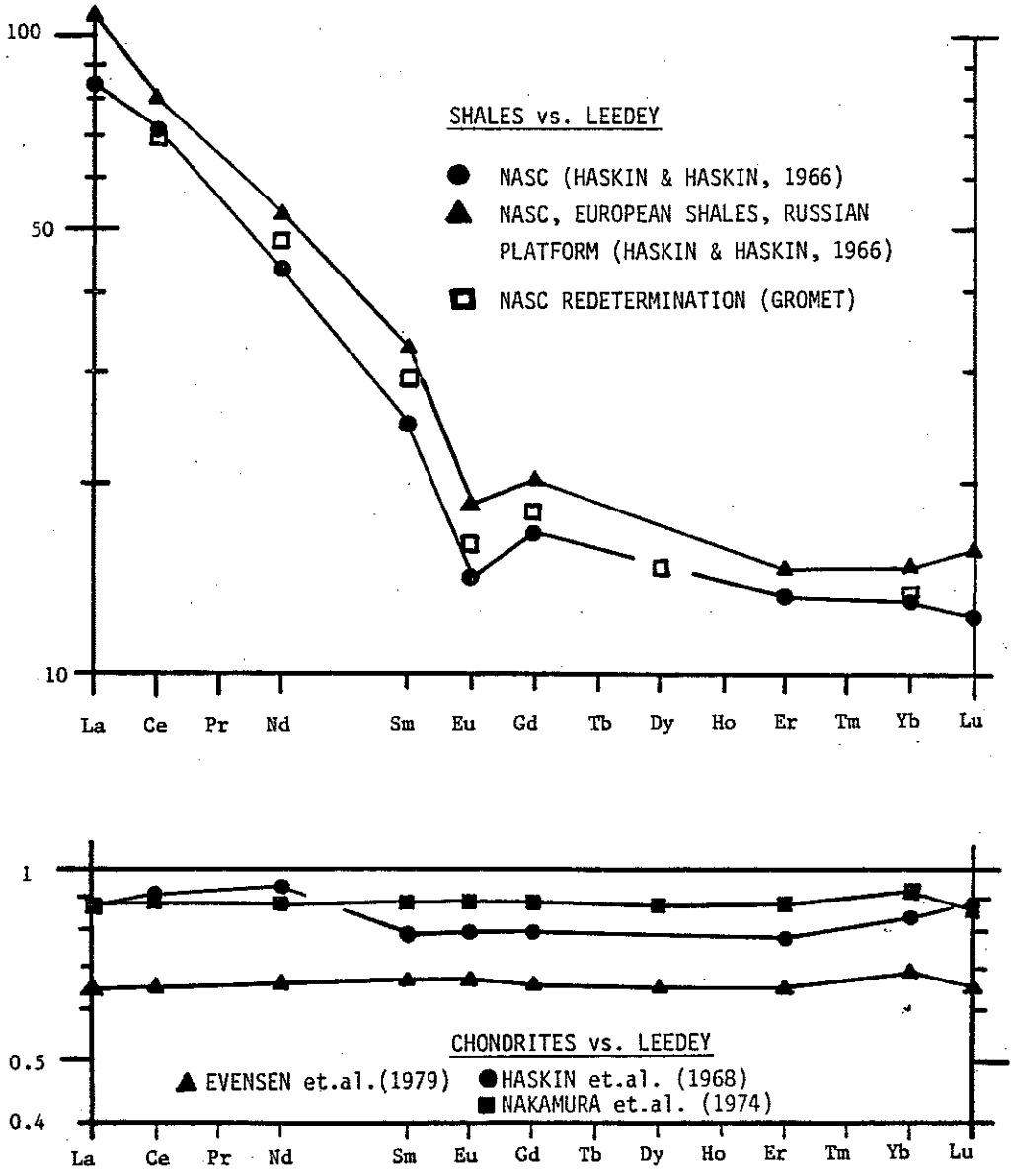


Figure 1.2. ABOVE: The abundances of REE in North American Shales Composite and an arithmetic mean of NASC, European shales and Russian platform (HASKIN & HASKIN, 1966), both normalized versus Leedey chondrite (MASUDA et al., 1973). Redetermination of NASC yields essentially the same trend, although minor inhomogeneities of the NASC-mixture have been reported (GROMET, pers.comm.).

BELOW: The abundances of REE in chondritic averages by HASKIN, HASKIN, FREY & WILDEMAN (1968), NAKAMURA et al.(1974) and EVENSEN et al.(1979) normalized versus the Leedey chondrite values of MASUDA et al. 1973).

| | CHONDRITES | NASC | MEAN SHALES |
|---|---|---|---|
| La | 1.716 | 230 | 295 |
| Ce | 4.55 | 500 | 592 |
| Pr | 0.684 | 56 | 71.7 |
| Nd | 3.285 | 215 | 263 |
| Sm | 1.024 | 37.9 | 49.9 |
| Eu | 0.382 | 8.16 | 10.6 |
| Gd | 1.30 | 33.1 | 40.4 |
| Tb | 0.236 | 5.35 | 7.74 |
| Dy | 1.564 | --- | (33.8) |
| Ho | 0.344 | 6.306 | 8.12 |
| Er | 0.992 | 20.3 | 22.4 |
| Tm | 0.152 | 2.96 | 3.73 |
| Yb | 0.954 | 17.9 | 20.4 |
| Lu | 0.145 | 2.74 | 3.49 |

Table 1.4. Concentrations [micromol.kg$^{-1}$] of REE in CI chondritic average (EVENSEN at.al., 1978), North American Shales Composite and an arithmetic mean of NASC, European shales and Russian platform (HASKIN & HASKIN, 1966).

## 1.3. The Marine Geochemistry of the Rare Earth Elements, A.D. 1980

### Seawater

Until recently virtually no data was available on the REE in seawater. Early work by BALASHOV & KITROV(1961), HOOD(1966), SHIGEMATSU et al. (1967), HAYES(1969), NAGATSAKU et al. (1971) and KOLESOV et al.(1975) is of historical interest only. Values reported by GOLDBERG et al.(1963), HOGDAHL et al.(1968), MASUDA & IKEUCHI(1979) and PIEPGRAS et al.(1979) fall within the range reported in this thesis and recently by ELDERFIELD & GREAVES(1982). However both GOLDBERG et al.(1963) and MASUDA & IKEUCHI(1979) report values for only one sample, which cannot be checked for oceanographic consistency. The results of HOGDAHL et al.(1968) exhibit considerable scatter when plotted properly as six different 'profiles' of 3-4 sampling depths each. Finally concentrations in two Pacific samples for Nd and Sm only (PIEPGRAS, WASSERBURG & DASCH, 1979), and later reported Nd-Sm values of the same laboratory (PIEPGRAS & WASSERBURG, 1982, 1983), agree well with determinations reported in this thesis.

Despite these shortcomings of the earlier data, two major features consistently appeared in shale-normalized patterns:

i) A large depletion of Ce, most likely caused by the oxidation of dissolved Ce(III) to insoluble Ce(IV) forms.
ii) An enrichment of the heavier REE, which are expected to be stabilized in seawater due to formation of stronger inorganic complexes.

Neither one of these features had been observed in rivers or aerosols.The dissolved and suspended loads of the Garonne and Dordogne rivers (MARTIN et al.,1976) show a flat shale type pattern. Recent results for five rivers in the Pacific Northwest region of the U.S. exhibit similar patterns (KEASLER & LOVELAND, 1982). Shale patterns were also found in atmospheric (RAHN, 1976) and marine (La, Ce, Sm and Eu only; BUAT-MENARD, 1979) aerosols. Suspended particulate La concentrations measured during the GEOSECS expeditions (BREWER et al.,1978) vary considerably but are typically less than 10 percent of the above mentioned total

concentrations. Additional values for suspended particulate La, Ce, Sm and Eu fall in the same 10 percent range (BUAT-MENARD, 1979). The La/Al, Sm/Al and Eu/Al ratios were typically close to crustal abundance ratios. However the Ce/Al-ratios in the same particles were found to be about twice as high as in aerosols and shales. Moreover a strong correlation between Ce and Mn was found (BUAT-MENARD, pers.comm.).
A simple box model for particulate Mn (BUAT-MENARD & CHESSELET, 1979) and particulate Ce (DE BAAR, unpublished manuscript, 1980) in surface waters of the North Atlantic Ocean would require an additional source next to the aerosol input in order to match the output along with settling particles. This result and the well-known positive Ce anomaly in ferromanganese nodules indicate that both elements Mn and Ce are regenerated in organic-rich, reducing shelf sediments after which the dissolved Mn and Ce diffuse upward and are transported to the center of ocean basins.

Radionuclides

SUGIHARA & BOWEN (1962) and BOWEN & SUGIHARA (1965) reported distributions of fallout $^{144}Ce$ and $^{147}Pm$ in parts of the Atlantic Ocean between 1956 and 1961. Compared with the 1000 days postproduction estimates of the original activity ratios both $^{144}Ce$ and $^{147}Pm$ were strongly depleted relative to $^{90}Sr$, which is a conservative tracer.

Vertical profiles of $^{144}Ce$ and $^{147}Pm$ showed secondary maxima at about 700-1000m which were interpreted as being local concentrations of zooplankters or settling particles. Presumably the $^{144}Ce$ and $^{147}Pm$ become associated with sinking particles, and SUGIHARA & BOWEN (1962) suggest settling velocities of about 1200 $m.yr.^{-1}$.

NAGAYA et al.(1965; 1974) studied the distribution of fallout $^{144}Ce$ between the dissolved and suspended particulate phases of seawater. Their observation of significant interaction with particles is consistent with results of laboratory studies with $^{144}Ce$ and other REE radionuclides (DAWSON & DUURSMA, 1973; DUURSMA & EISMA, 1974; CORMACK & BOWEN, 1967).

OSTERBERG, CAREY & CURL (1963) measured $^{141-144}Ce$ in sea cucumbers collected at 200m and 2800m depth in the Pacific Ocean. They concluded that the radiocerium was transported downward with velocities around

40-200 $m.day^{-1}$, probably with rapidly sinking fecal pellets. Uptake of $^{144}Ce$ by primary producers and herbivores, but not by carnivores, was reported by OSTERBERG, PEARCY & CURL (1964).

Zooplankton culture experiments have shown repeatedly that 99% of radiocerium available in seawater or phytoplankton is incorporated into fecal pellets (FOWLER et al. 1973). Rapid vertical transport by fecal pellets might be a major mechanism for the removal of Ce from ocean waters. CHIPMAN (1958) had shown earlier that algae in laboratory cultures rapidly accumulate $^{144}Ce$ many thousands of times above seawater concentrations. Subsequent feeding by copepods would rapidly remove nearly all $^{144}Ce$ in seawater and algal food. When the radioactive particles were no longer available, the accumulated radioactivity of the zooplankters was rapidly lost, depending on the time for clearing the digestive tract. Radiocerium is poorly absorbed across the gut wall and therefore does not accumulate in soft tissues (BOROUGHS et al., 1957). RICE & WILLIS (1959) and RICE (1963) also demonstrated significant uptake of $^{144}Ce$ by phytoplankton.

The $^{144}Ce$ released form nuclear fuel reprocessing plants has repeatedly been shown to be strongly retained by the finest size fractions of sediments (HETHERINGTON & JEFFERIES, 1974; GUEGUENIAT et al.,1979).

## Marine Deposits

The analysis of picomolar REE concentrations in seawater is more difficult than the determination of micromolar REE concentrations in various marine deposits. However the resulting values for REE in (filtered) seawater represent a single phase of great geochemical significance. On the other hand the REE data for bulk marine deposits currently available in the literature, may not be very useful for a study of their marine geochemistry. Four major reasons for this skepticism:

1) detritus;
2) coatings;
3) time-scale discrepancies;
4) integrated fractionations;

are discussed below.

1) Within the marine environment two different pools of REE can be recognized:

i) The refractory (lithogenous) pool. The REE in this pool are thought to be strongly bound within the crystal lattices of detrital material. This inert terrestrial detritus (e.g., clays) is transported as aerosols, or the suspended load of rivers, from the continents into the ocean basins. Some of this material may reside for a while in the suspended particulate phase of the oceanic water column, but eventually all this material would be deposited in marine sediments. Throughout these transport steps the refractory material retains the same shale-type REE pattern.

ii) The reactive pool, which in itself consists of several reservoirs:
- the dissolved or dissolvable fraction of the river load;
- the dissolvable fraction of aerosols;
- the truly dissolved fraction of seawater, pore waters and hydrothermal effluents;
- the authigenic and biogenic phases of fine suspended particles and larger size fractions, the latter typically collected in sediment traps;
- the REE contents of authigenic (hydrogenous) and biogenic marine mineral deposits.

The first, refractory, pool would be closely associated with the transport and inventories of particulate Al. Yet the focus of this study is the marine geochemistry of the REE, i.e. the second, reactive pool, with a strong emphasis on water column processes. However fluxes and inventories of the latter reactive pool are probably an order of magnitude lower than for the refractory pool. In other words, bulk analyses of suspended particles or marine deposits may yield no information other than the shale type REE pattern of the dominant refractory component. Only for deposits with concentrations well above those of shales (e.g. nodules) would bulk analyses yield valuable insight.

2) In a 100-cm sediment column the authigenic REE inventory would be twenty times that of the overlying water column (see 3 below). Then REE fractionations during diagenesis are expected to override any fractionations which had occurred earlier in the overlying water column before deposition of the material at the sediment/water interface. For example the reactive pools of Fe and Mn are thoroughly redistributed during diagenesis. As a result many detrital and authigenic minerals are coated with a layer of Fe/Mn oxides (BOYLE, in prep.). Given the high REE concentrations in nodules (ELDERFIELD et al.,1981) and finely dispersed micronodules (ELDERFIELD, 1977) one would also expect high REE concentrations in these coatings. For example SPIRN(1965) reports that more than half of the REE content of marine clays is apparently adsorbed on the clay particle surfaces, and this is probably still a lower limit. Concentration values for a number of cleaned calcareous tests reported by SPIRN (1965) are much higher than those measured more recently in carefully picked and cleaned shells (ELDERFIELD et al.,1981). Very recent determinations in the same laboratory for even more scrupulously cleaned shells are again considerably lower (PALNER & ELDERFIELD, pers.comm.), i.e. the earlier estimates of REE contents of foraminifera (SPIRN, 1965), pteropods (TUREKIAN et al., 1973) and diatoms (PIPER, 1975) may be largely ascribed to Fe/Mn 'contamination'. Matters may be further complicated by recrystallisation of the original biogenic phase. In analogy with Sr (ELDERFIELD & GIESKES, 1982), this could lead to ejection of REE from the original crystal matrix.

The same argument as above for Fe/Mn phases can be made with respect to phosphorous. The often observed correlation of REE with sedimentary P contents, combined with the likelihood of diagenetic redistribution of P (see below) would lead to similar 'contamination' problems for REE in bulk authigenic minerals.

Thus any REE concentrations reported for bulk mineral deposits are most likely flawed by 'contamination' with detritus and/or (ferromanganese) coatings.

Finally the possibility of true analytical contamination cannot always be ruled out.

3) Even if the detrital component and coatings could be avoided, the resulting values for the truly authigenic phase of marine deposits may still be irrelevant for understanding water column processes. First of all, the total dissolved REE inventory of the oceanic water column would correspond to a sediment layer with a thickness of only 5 millimeter, or about 5 centimeter if 90 percent of the sediment consists of the refractory phase (PIPER, 1974). Thus it would be very difficult to set up a meaningful mass balance with matching ultimate sources (dissolved river load, dissolvable aerosol fraction, hydrothermal and low temperature submarine weathering) and sinks (bulk authigenic minerals) for the reactive REE in the oceans (PIPER, 1974; MARTIN et al., 1976). Moreover the inherent steady-state assumption of such a mass balance may be invalid. The residence times of dissolved REE(III) in the oceanic water column are probably on the order of 100-1000 years and are definitely shorter than the time scale of oceanic mixing for which 2000 years is a generous upper limit. On the other hand, the time variability for formation and dissolution of ferromanganese nodules, phosphorites and other REE bearing minerals takes place over much longer time scales. For instance any suggestion to match the (integrated) negative Ce anomaly in the water column with the positive Ce anomaly of (slow growing) nodules would be misleading (PIPER, 1974; HOLLAND, in press).

4) Even if all these 'contamination' problems could be avoided one still has to be very careful with interpretation of an observed REE pattern. Any observed pattern is the integrated result of <u>all</u> fractionations that a given sample has gone through. Of course this is not only true for mineral deposits, but for any type of sample, including filtered seawater. For example an observed anomaly in a nodule does not necessarily arise from the last process before sampling (i.e., nodule formation) but can also be the reflection of any previous processes. Anomalies of Ce may not solely be indicators of the redox conditions during nodule formation (GLASBY 1973; PIPER, 1974b), but may also reflect the anomaly pattern of the local sedimentation which occurred earlier (GLASBY et al., 1978; RANKIN & GLASBY, 1979). The aforementioned Eu depletions in seawater (ELDERFIELD & GREAVES, 1982) most likely do not result from marine chemistry, but from earlier fractionations during

evolution of igneous rocks.

Finally the common practice of assigning a direct seawater source to any deposit with a 'seawater-type' pattern is overly simplistic.

Notwithstanding the above reservations, the existing data for various REE bearing authigenic minerals was searched for evidence related to water column processes (DE BAAR, unpublished manuscript, 1980). More recently FLEET (1983) also reviewed the sedimentary geochemistry of the rare earths. Submarine weathering at low temperature may alter the surface REE contents of igneous rocks (HUMPHRIS, 1983) but is unlikely to have a major impact on the water-column inventory.
Among authigenic REE-bearing minerals like

- calcareous oozes (SPIRN, 1965)
- phosphorites (ALTSCHULER, 1980)
- barites (GUICHARD et al.,1979)
- phillipsite (BERNAT, 1975)
- montmorillonites or smectites (COURTOIS & HOFFERT, 1977)
- ocean-ridge metalliferous sediments (ROBERTSON & FLEET, 1976; TOTH, 1980; BONNOT-COURTOIS, 1981)
- ferromanganese nodules (ELDERFIELD et al., 1981)
- cherts (SHIMIZU & MASUDA, 1977)

only phosphorites, some metalliferous sediments and nodules consistently have higher REE levels than shales. Given the 'contamination' problems, all other minerals with REE levels around those of shales would yield little information on water column processes. Nevertheless it is interesting to note that deep sea cherts have negative Ce anomalies but ones in shelf sediments do not. This led SHIMIZU & MASUDA (1977) to postulate that Ce is depleted in open ocean waters but not those of shallow seas, in accordance with our expectations. The Eu(II) cation which prevails under strongly reducing conditions has ionic radii (for various coordination numbers, see Table 1.3) very similar to those of the Ba(II) ion. This is expected to lead to preferential uptake of Eu in barites formed under reducing conditions. Continental barites are closely associated with hydrothermal events and indeed exhibit strong positive Eu anomalies. However most deep sea barites are not Eu enriched (GUICHARD et al., 1979).

High REE levels in biogenic phosphorites (shark teeth, fish bone apatite) are almost certainly caused by diagenesis (BLOKH, 1961) whereby a coupled replacement of two $Ca^{2+}$-ions by one $Na^{+}$-ion and one $REE^{3+}$-ion has been suggested (KOCHENOV & ZINOV'EV, 1960). The bones of recent fish have much lower concentrations (HERRMANN, 1970) and massive scavenging of REE from seawater by settling fish debris (BERNAT, 1975) is unlikely. The formation of various types of abiogenic phosphorites is not completely understood (FROELICH et al., 1982). Most likely they are precipitated during diagenesis within sediments, or at best at the sediment surface, rather than in the open ocean water column. Thus REE contents of abiogenic phosphorites would not yield much information on water column processes. Nevertheless, the often observed interrelations between REE, P and Fe are intriguing (ELDERFIELD et al., 1981).

Scavenging of REE from ambient seawater by finely dispersed freshly formed Mn-oxides in hydrothermal plumes may account for high REE concentrations in metalliferous ridge-crest sediments. Whether or not this removal process has a major impact on the total ocean water inventory of the REE remains to be seen. Ridge-crest deposits often exhibit a 'seawater' pattern with normal Eu levels and a Ce depletion (TOTH, 1980; BONNOT-COURTOIS, 1981), not inconsistent with such direct scavenging of REE from seawater. However a positive Eu anomaly in some deposits of the Red Sea (COURTOIS & TREUIL, 1977) and the Galapagos area (CORLISS et al., 1978) points at a truly hydrothermal component.

Most significant for water column processes is the strong correlation between Mn and REE, and even more Mn and Ce, in nodules. The relation, if any, of nodule formation with water-column budgets would be hard to assess (see above). On the other hand, one would expect to find a similar correlation for:

- suspended particles in the water column;
- dissolved levels of Mn, Ce and other REE under anoxic conditions prevailing in interstitial waters or anoxic basins.

## 1.5. Summary

The available evidence, albeit very limited, led to the following original hypotheses (DE BAAR, unpublished manuscript, 1980):

1) Dissolved cerium and manganese are released from the continental shelves and slopes along the margins of ocean basins.

2) Removal of dissolved cerium takes place by adsorptive scavenging and/or incorporation in rapidly settling large particles like fecal pellets. The residence time of cerium is very short, around 10 - 30 years.

3) The redox mobilization of cerium in pore waters is almost identical to its behavior in anoxic basins. High dissolved Ce(III) concentrations are expected in anoxic waters.

4) Following recommendations of CHAMBERLIN (1897) we propose multiple hypotheses for the cycling and removal of strictly trivalent REE:
    a) incorporation in soft tissue of planktonic organisms
    b) incorporation in shells of planktonic organisms
    c) removal by adsorptive scavenging
    d) a combination of a)b)c)

5) If, and only if, hypothesis 4c is correct:
    The oceanic residence times of the trivalent REE are controlled by the stability of their dissolved complexes, both increasing with increasing atomic number (GOLDBERG et al., 1963)

## 2. METHODS

### 2.1. Introduction

Studies of trace elements in the open ocean environment have for a long time been hampered by analytical problems: contamination, interference of ubiquitous major ions, and the requirement of sensitive methods for detection of concentrations in the nanomolar to picomolar range. However, in the past few years reliable data sets have been obtained for some, mostly first row, transition metals( Cr, Mn, Fe, Co, Ni, Cu, Zn, Pd, Ag, Cd), and metalloid elements(Ge, Sn, Pb, As, Sb, Bi)(BRULAND, 1983; WONG et al.,1983; QUINBY-HUNT & TUREKIAN, 1983; LEE, 1983; MARTIN et al., in press).

Only recently reliable methods have been developed for the determination of the REE in seawater. The Caltech group has focused strictly on two elements: Nd with its isotopic ratio, and Sm (PIEPGRAS et al., 1979, 1980). Analytical schemes for the determination of the REE series have been developed both by our group (De BAAR et al., 1982,1983) and ELDERFIELD & GREAVES (1982, 1983). The latter employ the classical incomplete iron-coprecipitation method followed by Isotope Dilution Mass Spectrometry (IDMS).

A novel extraction and purification procedure with an overall 100 % yield was developed, thus ruling out artificial fractionations within the REE-series itself. While complete extraction is more elegant when used in conjunction with isotope dilution, it is absolutely essential when final determination is by any other method such as Instrumental Neutron Activation Analysis (INAA) or Inductively Coupled Plasma spectroscopy (ICP) (WALSH, BUCKLEY & BARKER, 1981; CROCK & LICHTE, 1982). An initial extraction of the REE by chelating ion exchange chromatography (2.6.) is followed by cation exchange (2.7.) and anion exchange (2.8.) purification. An internal standard ($^{144}$Ce) is added for improving the precision by avoidance of counting geometry errors.

For final determination both GOLDBERG et al.(1963) and HOGDAHL et al. (1967) had to combine neutron activation with beta-spectrometry. The latter necessitates a difficult and laborious separation of the REE among themselves. At the time our research started all IDMS methods also

required separation of the REE, either as individual elements or in two or three groups. More recently IDMS determination of nine elements La, Ce, Nd, Sm, Eu, Gd, Dy, Er, Yb as one group have been reported (THIRLWALL, 1982; ELDERFIELD & GREAVES, 1982). By combining gamma-spectrometry(2.11, 2.12, 2.13) with neutron activation (2.9) the twelve elements La, Ce, Pr, Nd, Sm, Eu, Gd, Tb, Ho, Tm, Yb, Lu can be determined as a group. Two mono-isotopic elements Pr and Tb which cannot be determined by IDMS are significant with respect to observed anomalies of neighboring elements Ce and Gd in the series. Anomalies are neither observed nor expected among the heavy REE (Tb, Dy, Ho, Er, Tm, Yb, Lu) and omission of Dy and Er from our data seems tolerable. The simultaneous determination of all 14 naturally occurring REE certainly is an advantage of the ICP method, but its sensitivity is not adequate for seawater analyses.

The expenses for gamma ray detection equipment are substantially lower than for a mass spectrometer, provided one has access to a research reactor with high neutron flux facility (2.9). On the other hand determination of twelve elements in one sample occupies about 4 days detector time. This would be reduced to about one day per sample upon installation of a high purity germanium-well detector with much higher efficiency. For IDMS a run of about 4 hours for nine elements per sample is needed. However IDMS facilities are almost always operated on a time-sharing basis. For instance if a time slot of one day a week is allocated then the productivity of both methods would be very close again. Yet the potential precision of about 1 percent for IDMS is unsurpassed and considerably better than the the 2 - 10 percent (varying from element to element, see 2.15) typical for neutron activation. Precision of ICP is reported to be about 1-2 % (WALSH et al., 1981) or 1-4 % (CROCK & LICHTE, 1982) for standard rocks. At least for the next few years precision in the five percent range is deemed adequate for establishing a first outline of the marine geochemistry of the rare earths, as well as most other trace elements.

Concentrations of the REE are extremely low. Our observations so far range from 0.3 (Lu) to 86 (Ce) picomol.kg$^{-1}$ seawater. Crustal abundances are more than six orders of magnitude higher. Evidently one has to employ ultraclean methods for all pre-irradiation steps of the

procedure. Clean sampling(2.2.) is a prerequisite, although requirements are not as utmost rigorous as sometimes advocated for elements like Fe, Hg or Pb which are more common in the shipboard environment. On the other hand the possibility of interferences due to fission products of uranium leads to extremely stringent specifications (2.3.) for the separation of U from the REE in seawater, as well as the avoidance of U contamination afterwards. When extracting the REE from a 10 ltr. seawater sample one has to reduce the total amount of U from 140 x $10^3$ pmol. to well below 1 pmol. in order to avoid interferences. The same extract would contain 3 to 860 pmol. of each individual REE.
All pre-irradiation separations are done in a clean air laboratory(2.4.). During post-irradiation procedures (2.10.) above contamination hazards have become redundant, yet one still follows the protocols for careful handling of radioisotopes.

This chapter is the culmination of three years development of analytical techniques. During the past 18 months actual INAA measurements of the REE in seawater have been made. Yet in that same period the procedures were continuously improved and upgraded. As a consequence the various data sets (chapters 3, 4, 5) were produced along somewhat different lines. In the remainder of this chapter the most recent procedures will be highlighted, yet operational differences between data sets will be pointed out either in this chapter 2 or in their related chapters 3, 4 and 5. With few exceptions the many unsuccessful trials, aborted failures and assorted dead end roads will not be discussed.

2.2. Sampling and shipboard filtration.

Before each cruise polyethylene containers with caps were cleaned following recommendations of Dr. E. Boyle:

- storage for 24 hours at 60 $^{o}$C, each container filled to the rim with 1N HCl (ACS Reagent Grade) in Pyrex water.
- 24 hours at room temperature in upside down position.
- threefold rinse with Pyrex water after pouring out the dilute acid.
- weighing.
- packaging inside plastic bags to prevent dust collection around bottle necks.

Before and after sampling the containers were stored inside clean plywood boxes.

Water samples were collected by deployment of PVC Niskin bottles (30 ltr.) with Teflon coated stainless steel internal springs on a steel hydrowire. During cruise 86/2 aboard R.V. Oceanus (August 1980) complete profiles of about 20 sampling depths each were collected at four stations along a Gulf of Maine - Bermuda transect in the Northwest Atlantic Ocean. PE gloves were worn when drawing samples from the Niskin bottles. Each LPE container (4 ltr.) was rinsed threefold with the seawater and filled to almost capacity. A suite of 500 ml. bottles for trace metal analyses was filled similarly. No attempts were made at shipboard filtration. The 4 ltr. samples for REE analyses were acidified on shipboard with 7 ml. double Vycor distilled 6N HCl each from a Repipet dispenser. The 500 ml. trace metal samples were acidified with 1 ml. 6N HCl, using an Eppendorf pipette with hot acid cleaned tips. Results of the REE analyses for one station are reported in chapter 3.

During R/V KNORR cruise 99/2 in November 1982 profiles were collected in the western basin of the Cariaco Trench (31 sampling depths), and in the deep center of the Carribean Basin (20 sampling depths). This time all samples were filtered through specially designed filtration units(Figure 2.2.1). Ten metal-free filter holders had been manufactured with all PE bodies, PE inlet and outlet, PE porous support

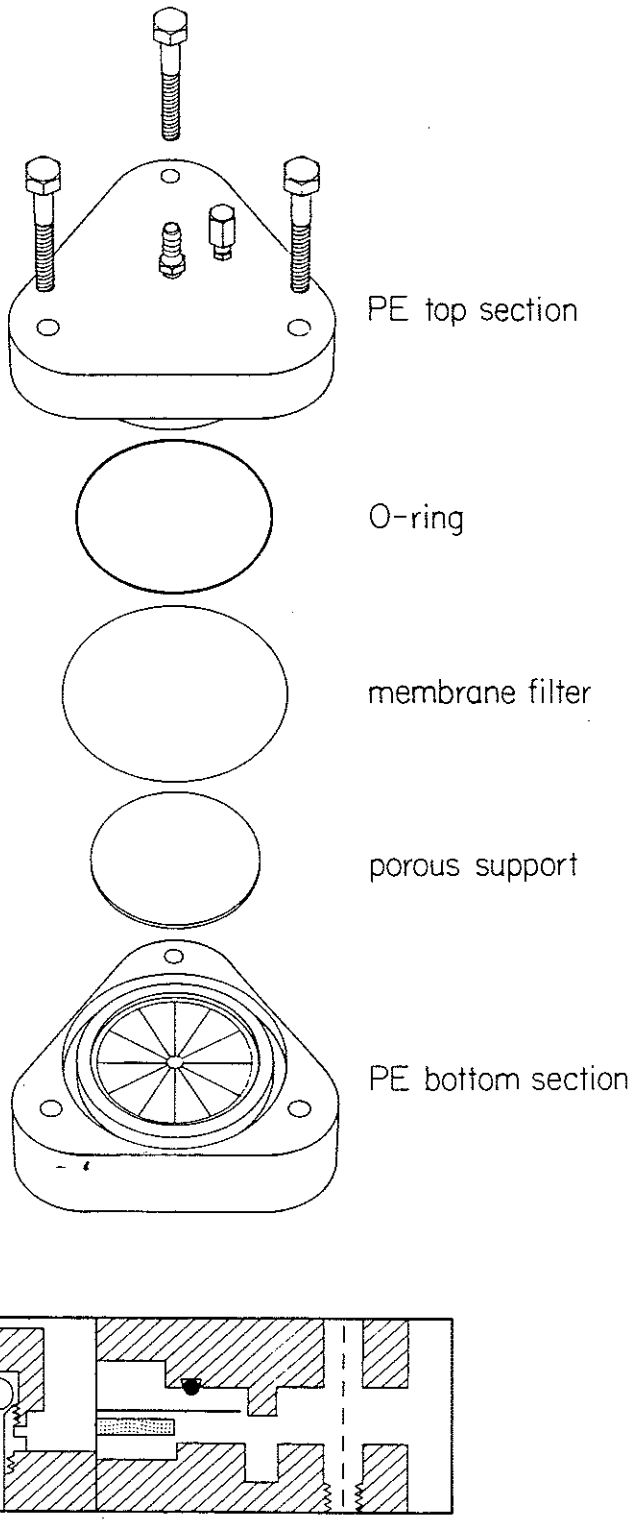


Figure 2.2.1. Metal-free filtration apparatus. Inserts: air bleeding valve (left) and detail of O-ring seal with 'dirt-barrier' groove and tongue(right).

frit, Teflon PTFE air bleeding valve and Teflon FEP encapsulated O-ring seals. The effective area of 142mm. diameter Nuclepore membrane filters had been optimized to 80 % by selecting a 126mm diameter of the support frit. Concentric mounting of the membrane filter was envisioned, most often achieved, but proved not mandatory for a tight seal. Three feet PE inlet tubing and four feet silicone outlet tubing were attached permanently to the filter housing. The silicone tubing was chosen primarily for possible forcing of the flow with a peristaltic pump, which proved to be unnecessary. A short silicone tubing connector was employed for easy attachment of the filter inlet to the outlet spigot of a Niskin bottle. All components were soaked for at least 48 hours in 1N HCl at room temperature, rinsed thoroughly with Pyrex water and allowed to dry inside a laminar flow bench. After assemblage each unit was packed in a plastic bag and stowed in a clean PE pail with lid.

A separate clean area in a laboratory van was dedicated for shipboard mounting of the membrane filters. Plastic gloves were worn during filter changes, and during filtration and acidification. The outlet tubing of each filter unit was attached, via a spigot, to an evacuated flask in line with a continuously running vacuum pump. Using two clean Teflon FEP forceps (Nalgene) a new, untreated , Nuclepore membrane filter (142mm diameter, 1 micron pore size) was positioned onto the support frit and kept in place by applying slight vacuum suction. Then the top half of the housing with permanently installed O-ring was put in place. Three nylon bolts were carefully tightened such as to equalize the force applied to the O-ring seal. Then the inlet tube was attached to a reservoir of Pyrex water which had been acidified to pH=2 with double quartz distilled 8N HCl. Manipulation of the vacuum spigot and bleeding valve allowed filling the filter housing and tubing, after which a five minute 'acid soak' was instated. Then the acidified water was pumped out. This was followed by a threefold flush with Pyrex water(4 pH 6) and one flush with Pyrex water which had been adjusted to pH=8 with ultrapure 2N $NH_4OH$. After this treatment the units and filters themselves were thought to be clean and at the proper pH, and they were stored again inside bags and pails, ready for use.

Upon recovery of a cast of 8 Niskin bottles a $N_2$-gas line was attached to their top bleeding valves. During sampling the void space

overlying the anoxic seawater was flushed continuously with filtered $N_2$-gas in order to maintain reducing conditions. Filter units were attached to the bottom spigot after which the system was flushed by gravity flow with 10-15 liters of sample seawater. Subsequently jerryjugs (10 ltr.) were rinsed threefold and filled to almost capacity with filtered water for REE analyses. Then three bottles of respectively 125ml., 500ml. and 1000ml. capacity were filled similarly for analyses of respectively Al (Dr. D. Hydes), trace metals (our group) and Be (Dr. C. Measures). The flush and rinse water was collected in a seperate container, weighed and discarded. Its net weight was recorded in order to keep track of the amount of water represented by the particulate matter on the filters. Afterwards the filters were flushed with pH=8 Pyrex water to wash off excess salt. Then the filter housing was opened. The filter was folded in four, placed inside a clean PE zip-lip bag and stored in a freezer. New filters were mounted as described above.

The water samples were finally acidified with 10 ml.(REE), 1 ml.(Be), 0.5 ml.(trace metals) and 0.1ml.(Al) 8N HCl using a Repipet dispenser (REE) and Eppendorf pipettes with hot acid cleaned tips. Results of REE analyses for the Cariaco Trench station are reported in chapter 5.

A profile of 27 filtered samples was collected by Dr. K.W. Bruland during the VERTEX II expedition in the Eastern Equatorial Pacific Ocean, using Teflon coated GoFlo bottles(30 ltr.) mounted on a inch diameter Kevlar hydrowire. Upon recovery $N_2$-pressure was applied to the bottle in order to force the seawater through a 0.3 micron pore size Nuclepore filter mounted in a Teflon PTFE filter holder (Millipore YY42 14200, out of production). The water was stored in 30 ltr. capacity PE cubitainers and acidified with 27 ml. double quartz distilled 8N HCl from a Repipet dispenser. These VERTEX procedures have proven to be succesful with respect to analyses of such contaminant-prone elements as Mn, Fe, Co, Ni, Cu, Zn, Ag and Cd. Results of REE analyses for this station are given in chapter 4.

## 2.3. Interferences.

Given the picomolar concentrations of the REE in our samples one is inclined to consider all remaining elements of the periodic table as plausible sources of interference. In reality only uranium (U) would give rise to serious interferences, while the silicon (Si) of the quartz irradiation vials as well as omnipresent sodium (Na) give rise to high initial radiation levels.

### Sodium.

The major constituents of seawater (S = 35.00 $^{o}/oo$) are alkaline and earthalkaline cations $Na^{+}$, $Mg^{++}$, $Ca^{++}$, $K^{+}$ and anions $Cl^{-}$ and $SO_4^{--}$ (WILSON, 1975). In 10 kg. seawater as required for our determinations these would correspond to about 300 gr. salt which by its sheer bulk would interfere with any analytical method. Our extraction of the REE from seawater solution is based on cation retention (2.6., 2.7.) which allows replacement of the $Cl^{-}$ and $SO_4^{--}$ by any desired anion. Quantitative ($>$ 99.9%) separation of the REE from above major cations is routinely achieved by our chelating ion exchange procedure (2.6.). However trace impurities of these (earth)alkaline metals remaining in the REE fraction might still give rise to unacceptable radiation levels. This proves to be true for Na which is the most common element in seawater (0.47 $mol.kg^{-1}$), and also very ubiquitous in reagents, glassware or fingertips. Moreover Na has an unfavourably high thermal neutron cross section in the reaction

$$^{23}Na\ (n,\gamma)\ ^{24}Na \xrightarrow{-\beta} {}^{24}Mg \qquad (2.3.1)$$

and the short 15.02 hours halflife of its activation product $^{24}Na$ gives rise to high initial radiation levels. The activity of an irradiation produced isotope is described by

$$A = -\frac{dN}{dt} = \lambda N = (N_{AV} \times \phi)[\sigma \times \theta\,(1 - e^{-\lambda T})](M)\ e^{-\lambda t} \qquad (2.3.2)$$

with A = activity [disintegrations per second, dps] at time t after the end of the irradiation

N = number of atoms of radioisotope

$N_{AV}$ = $6.02 \times 10^{23}$ = Avagadro's Number

$\phi$ = $5 \times 10^{13}$ neutrons.$cm^{-2}$.$sec^{-1}$ = thermal neutron flux

T = 8 hours = 28,800 sec = irradiation time

t = time past end of irradiation.

In the case of sodium:

$\sigma$ = 0.53 barns = $0.53 \times 10^{-24}$ $cm^2$ = thermal neutron cross section of $^{23}Na$

$\lambda$ = $12.81 \times 10^{-6}$ $sec^{-1}$ = decay constant of $^{24}Na$

$\theta$ = 1.00 = abundance of $^{23}Na$ isotope

M = 4.7 moles = moles of Na in 10 kg. seawater

For naturally occurring assemblages of the REE the highest initial radioactivity is caused by radioisotopes of La, Sm and Eu. For example the activity of $^{140}La$ is given by the same equation (2.3.2) where

$\sigma$ = 8.94 barns = $8.94 \times 10^{-24}$ $cm^2$ = thermal neutron cross section of $^{139}La$

$\lambda$ = $4.78 \times 10^{-6}$ $s^{-1}$ = 0.0172 $h^{-1}$ = decay constant of $^{140}La$

$\theta$ = 0.9991 = abundance of $^{139}La$ isotope

M = $150 \times 10^{-12}$ moles = moles of La in 10 kg. seawater

Combination of the two equations leads to a simple activity ratio

$$\frac{A(^{24}Na)}{A(^{140}La)} = \frac{0.53}{8.94} \times \frac{1.00}{0.9991} \times \frac{(1-0.6916)}{(1-0.8715)} \times \frac{4.7}{150 \times 10^{-12}} \times \frac{e^{-0.0461t}}{e^{-0.0172t}} = 4.5 \times 10^{9} \quad (2.3.3)$$

Directly after activation (t=0) the activity of $^{24}Na$ would be almost ten orders of magnitude higher than for $^{140}La$. In other words, the mass of Na in our original sample has to be reduced from 4.7 moles to about $10^{-10}$ moles in order to arrive at comparable activities for $^{140}La$ and

$^{24}Na$. By employing a two step pre-irradiation separation (2.6., 2.7.) the $^{24}Na$ radiation level is reduced to well below safety levels. However in sample extracts and overall reagent blanks its activity is routinely still about hundred times higher than for the combined REE activity, at 24 hours postirradiation. This is not the case for irradiated standards, which would suggest that $^{24}Na$ activity mostly results from reagent impurities. The 1368.5 keV gamma peak of $^{24}Na$ does in itself not interfere with any peaks of REE-isotopes. Yet detector deadtimes greatly exceeding 10 % and a very high background due to Compton effects and brehmsstrahlung would still prevent recording of gamma spectra. With respect to $^{140}La$ and $^{153}Sm$, one could allow a 3-4 days cooling time. However for determination of short-lived isotopes $^{142}Pr$ (19.2 hrs. halflife), $^{152ml}Eu$ (9.3 hrs.), $^{159}Gd$ (18.6 hrs.) and $^{166}Ho$ (26.8 hrs.) a post irradiation separation of $^{24}Na$ is required. The first spectra recorded immediately after this clean-up routinely exhibit comparable sized peaks of $^{24}Na$ and $^{140}La$. According to the ratio :

$$\frac{A(^{24}Na)(dpm)}{A(^{140}La)(dpm)} = \frac{\epsilon_{abs(1592keV)}}{\epsilon_{abs(1369keV)}} \times \frac{960}{1000} \times \frac{^{24}Na\text{-counts (cpm)}}{^{140}La\text{-counts (cpm)}} \qquad (2.3.4)$$

where $\epsilon$ = absolute detector efficiency at 1369 respectively 1592 keV

1000 =number of 1369 keV gamma events per 1000 decays of $^{24}Na$

960 =number of 1592 keV gamma events per 1000 decays of $^{140}La$

with $$\epsilon_{abs(1369)} \approx \epsilon_{abs(1592)}$$

it is suggested that comparable activities [d.p.m.] of $^{24}Na$ and $^{140}La$ have indeed been achieved.

Silicon.

The irradiation vials had been especially manufactured from synthetic ultrapure quartz glass. In other words, they consist of only silicon and oxygen. Unfortunately the minor (3.1 % abundance) stable isotope $^{30}Si$ has a very high thermal neutron cross section of 107 barns and its activation product $^{31}Si$ with a 2.62 hours half-life causes a vigorous initial radiation level. After 24 hours cooling time the $^{31}Si$ still accounts for over 90 % of the total activity, with almost all of the remaining 10 % contributed by above discussed $^{24}Na$. For the sake of early counts of short-lived REE isotopes, one has to remove the activated sample extract from the vial, as done in conjunction with the post irradiation separation (2.10.).

Uranium.

For our purposes U can be considered as a conservative element in seawater. Concentrations are about $14 \times 10^{-9}$ $mol.kg^{-1}$ in the open ocean, consisting of almost all $^{238}U$ (99.3 %) and only a small fraction $^{235}U$ (0.57%). The latter isotope may give rise to interferences in our determinations by neutron activation.

Upon bombardment with neutrons the isotope $^{235}U$ yields a suite of fission products with a mass distribution as illustrated in Figure 2.3.1. Some of the heavy products with mass numbers comparable to the light REE exhibit significant fission yields in the range of 6.29 % ($^{140}I$), 5.8 % ($^{141}I$), 5.89 % ($^{142}I$), 5.95 % ($^{143}Xe$), 5.48 % ($^{144}Ce$), 2.23 % ($^{147}La$), 0.268 % ($^{152}Nd$) and 0.161 % ($^{153}Pm$). Each of these initial products decays along isobaric chains until final transformation into a stable isotope (Table 2.3.1). In the process $^{140}La$, $^{141}Ce$, $^{143}Ce$, $^{144}Ce$, $^{147}Nd$ and $^{153}Sm$ are produced. These are the very same radioisotopes as intended to produce for determination of the REE by $(n,\gamma)$ activation of stable isotopes $^{139}La$, $^{140}Ce$, $^{142}Ce$, $^{146}Nd$ and $^{152}Sm$. Also $^{144}Ce$ is used in our procedures as a radiotracer spike. On the other hand the isobaric fission chains 142 and 152 are terminated at $^{142}Ce$ respectively $^{152}Sm$ without a chance for interference with the determinations of $^{142}Pr$ and $^{152}Eu$.

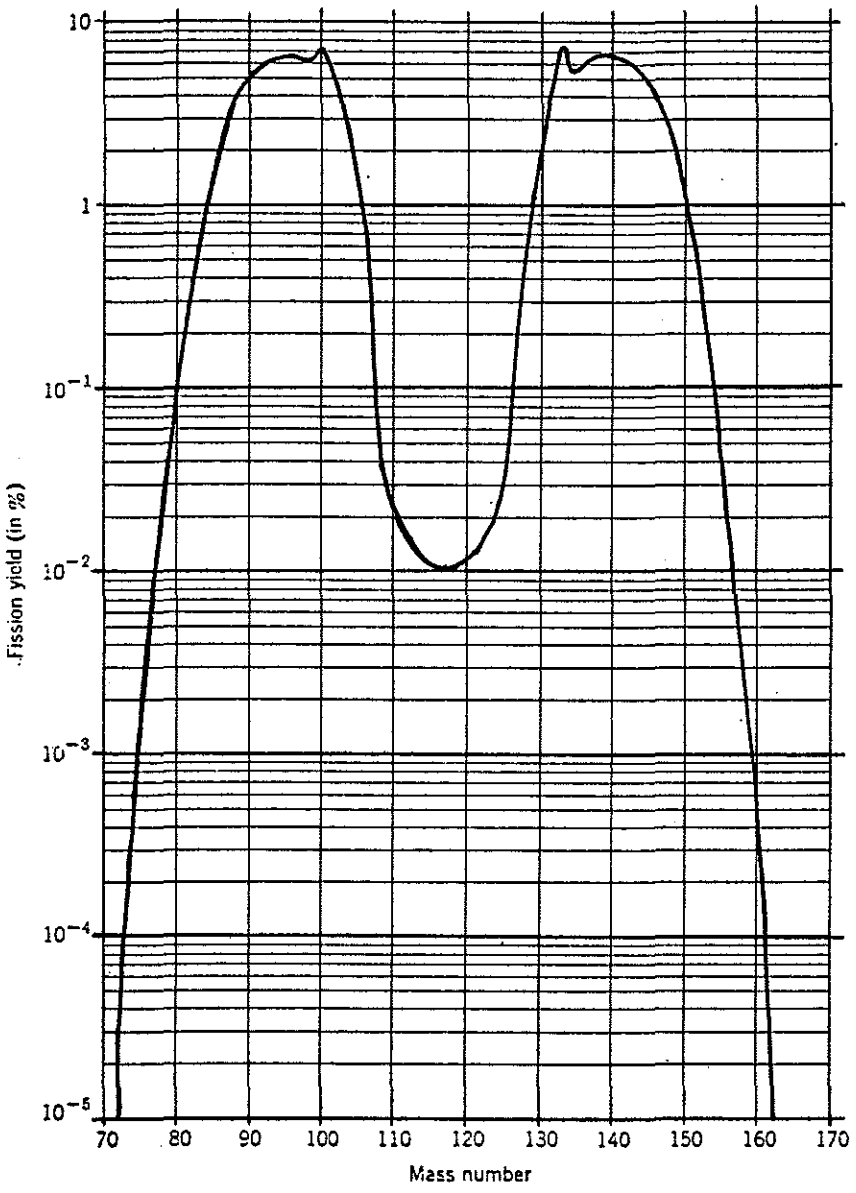


FIGURE 2.3.1. Yields of fission produced decay chains as a function of mass number for the slow-neutron fission of $^{235}U$ (Taken from FRIEDLANDER, KENNEDY & MILLER, 1966).

$$^{140}_{53}\mathrm{I} \xrightarrow{0.86\ \mathrm{s}} {}^{140}_{54}\mathrm{Xe} \xrightarrow{13.7\ \mathrm{s}} {}^{140}_{55}\mathrm{Cs} \xrightarrow{65\ \mathrm{s}} {}^{140}_{56}\mathrm{Ba} \xrightarrow{12.79\ \mathrm{d}} {}^{140}_{57}\mathrm{La} \xrightarrow{40.2\ \mathrm{h}} {}^{140}_{58}\mathrm{Ce}$$

$$^{141}_{53}\mathrm{I} \xrightarrow{0.46\mathrm{s}} {}^{141}_{54}\mathrm{Xe} \xrightarrow{1.72\mathrm{s}} {}^{141}_{55}\mathrm{Cs} \xrightarrow{25.1\mathrm{s}} {}^{141}_{56}\mathrm{Ba} \xrightarrow{18.2\mathrm{m}} {}^{141}_{57}\mathrm{La} \xrightarrow{3.9\mathrm{h}} {}^{141}_{58}\mathrm{Ce} \xrightarrow{32\mathrm{d}} {}^{141}_{59}\mathrm{Pr}$$

$$^{142}_{53}\mathrm{I} \xrightarrow{0.2\mathrm{s}} {}^{142}_{54}\mathrm{Xe} \xrightarrow{1.22\mathrm{s}} {}^{142}_{55}\mathrm{Cs} \xrightarrow{1.7\mathrm{s}} {}^{142}_{56}\mathrm{Ba} \xrightarrow{10.7\mathrm{m}} {}^{142}_{57}\mathrm{La} \xrightarrow{92.5\mathrm{m}} {}^{142}_{58}\mathrm{Ce}$$

$$^{143}_{54}\mathrm{Xe} \xrightarrow{0.3\mathrm{s}} {}^{143}_{55}\mathrm{Cs} \xrightarrow{1.78\mathrm{s}} {}^{143}_{56}\mathrm{Ba} \xrightarrow{13.7\mathrm{s}} {}^{143}_{57}\mathrm{La} \xrightarrow{14.1\mathrm{m}} {}^{143}_{58}\mathrm{Ce} \xrightarrow{33.0\mathrm{h}} {}^{143}_{59}\mathrm{Pr} \xrightarrow{13.6\mathrm{d}} {}^{143}_{60}\mathrm{Nd}$$

$$^{144}_{54}\mathrm{Xe} \xrightarrow{1.1\mathrm{s}} {}^{144}_{55}\mathrm{Cs} \xrightarrow{1.0\mathrm{s}} {}^{144}_{56}\mathrm{Ba} \xrightarrow{11\mathrm{s}} {}^{144}_{57}\mathrm{La} \xrightarrow{40\mathrm{s}} {}^{144}_{58}\mathrm{Ce} \xrightarrow{284\mathrm{d}} {}^{144}_{59}\mathrm{Pr} \xrightarrow{7.2\mathrm{m}} {}^{144}_{60}\mathrm{Nd}$$

$$^{147}_{57}\mathrm{La} \xrightarrow{5\mathrm{s}} {}^{147}_{58}\mathrm{Ce} \xrightarrow{56\mathrm{s}} {}^{147}_{59}\mathrm{Pr} \xrightarrow{13.6\mathrm{m}} {}^{147}_{60}\mathrm{Nd} \xrightarrow{11\mathrm{d}} {}^{147}_{61}\mathrm{Pm} \xrightarrow{2.6\mathrm{y}} {}^{147}_{62}\mathrm{Sm}$$

$$^{152}_{60}\mathrm{Nd} \xrightarrow{11.5\mathrm{m}} {}^{152}_{61}\mathrm{Pm} \xrightarrow{18\mathrm{m}} {}^{152}_{62}\mathrm{Sm}$$

$$^{153}_{61}\mathrm{Pm} \xrightarrow{5.4\mathrm{m}} {}^{153}_{62}\mathrm{Sm} \xrightarrow{46.7\mathrm{h}} {}^{153}_{63}\mathrm{Eu}$$

TABLE 2.3.1. Relevant isobaric decay chains produced from heavy thermal neutron fission products of $^{235}U$. Production of $^{140}La$, $^{141}Ce$, ($^{143}Ce$), $^{147}Nd$, and $^{153}Sm$ would interfere with REE determinations. The $^{144}Ce$ production would interfere with an added internal standard of the same isotope. Note absence of interferences for determinations of $^{142}Pr$ and $^{152}Eu$.

Below the maximum possible interferences of U with determinations of respectively Ce, Nd, Sm and La, as well as the radiotracer $^{144}Ce$ will be assessed.

The activity produced by neutron irradiation of any given element is described by the equation (2.3.2), where in the case of determination of Ce in seawater:

$\sigma$ = 0.58 barns = 0.58 x $10^{-24}$ $cm^2$ = thermal neutron cross section of $^{140}Ce$

$\lambda$ = 0.2468 x $10^{-6}$ $sec^{-1}$ = decay constant of $^{141}Ce$

$\theta$ = 0.8848 = abundance of $^{140}Ce$ isotope

M = 100 x $10^{-12}$ = moles of Ce in 10 kg. seawater.

The undesirable fission produced activity of $^{141}Ce$ is described by a similar equation which includes the additional 5.8 % yield term of the 141-chain:

$$A[dps] = -\frac{dN}{dt} = \lambda N = (N_{AV} \times \phi)[\sigma \times \theta (1-e^{-\lambda T}) \eta\ ] (M) e^{-\lambda t} \qquad (2.3.5)$$

where

$\sigma$ = 580 barns = 580 x $10^{-24}$ $cm^2$ = thermal neutron fission cross section of $^{235}U$

$\lambda$ = 0.2468 x $10^{-6}$ $sec^{-1}$ = 0.887 x $10^{-3}$ $h^{-1}$ = decay constant of $^{141}Ce$

$\theta$ = 0.0072 = abundance of $^{235}U$ isotope

M = 140 x $10^{-9}$ mols = mols of U in 10 kg. seawater

$\eta$ = 0.058 = fission yield of mass=141 decay chain.

Combination of equations (2.3.2.) and (2.3.5.) leads to a very simple ratio

$$\frac{A\ (^{141}Ce)(fission)}{A\ (^{141}Ce)(n,\gamma)} = \frac{580 \times 0.058}{0.54} \times \frac{0.0072}{0.8848} \times \frac{140 \times 10^{-9}}{100 \times 10^{-12}} = 710 \qquad (2.3.6)$$

This implies that the $^{141}Ce$ activity to be measured from desired $^{140}Ce$ activation would be about three orders of magnitude smaller than the undesired fission produced $^{141}Ce$-activity. In order to keep the latter below a one percent interference level, one has to remove the U with a yield exceeding 99.999 %. A similar interference would occur for $^{143}Ce$, but the latter isotope is not being used for our Ce determinations (see section 2.11.).

In the case of $^{147}Nd$ the analog of the last equation (2.3.6) with different parameters for Nd:

$\sigma$ = 1.3 barns = 1.3 x $10^{-24}$ $cm^2$ = thermal neutron cross section of $^{146}Nd$

$\theta$ = 0.172 = abundance of $^{146}Nd$ isotope

M = 200 x $10^{-12}$ = mols of Nd in 10 kg. seawater

$\eta$ = 0.0223 = fission yield of mass=147 decay chain;

would yield an activity ratio of 292 for the interfering fission produced $^{147}Nd$ versus the desired activation produced $^{147}Nd$. This again calls for a better than five orders of magnitude reduction of the U in our original sample.

In the analogous case for Sm [3 pmol.$kg^{-1}$ seawater] the 0.16 % yield would make fission produced $^{153}Sm$ only about 0.6 times the desired (n,$\gamma$) production from $^{152}Sm$, also as a result of the high cross section of $^{152}Sm$.

The case of $^{140}La$ is somewhat more complicated because of the long lived intermediate $^{140}Ba$ (half-life = 12.8 d) in the fission chain. The activity of $^{140}Ba$ at termination time t=0 of the activation is expressed by the above equation (2.3.5), where:

$\sigma$ = 580 barns = 580 x $10^{-24}$ $cm^2$ = thermal neutron fission cross section of $^{235}U$

$\lambda$ = 0.627x$10^{-6}$ $s^{-1}$ = 0.00226 $h^{-1}$ = decay constant $^{140}Ba$

$\theta$ = 0.0072 = abundance of $^{235}U$

M = 140 x $10^{-9}$ = mols of U in 10 kg seawater

$\eta$ = 0.0629 = fission yield of mass=140 decay chain

t = 0

Neglecting the small amount of $^{140}La$ produced from $^{140}Ba$ decay during the activation period, one can assume that all $^{140}La$ is produced from decay of above given amount of $^{140}Ba$ at t=0

$$A_{140La} = A_{140Ba} \times \frac{\lambda_{140La}}{\lambda_{140La} - \lambda_{140Ba}} (e^{-\lambda_{Ba}t} - e^{-\lambda_{La}t}) \qquad (2.3.7)$$

Combination of both equations leads to the term

$$A(140La)_{fission} = (N_{AV} \times \phi)[\sigma \times \theta \times \eta (1-e^{-\lambda T})](M)\left(\frac{\lambda_{La}}{\lambda_{La}-\lambda_{Ba}}\right)(e^{-\lambda_{Ba}t} - e^{-\lambda_{La}t}) \qquad (2.3.8)$$

which describes fission derived $^{140}La$ activity (VOBECKY, 1980). The desired $(n,\gamma)$ activation of $^{139}La$ has been described above in the discussion of sodium, and can be combined with (2.3.8) in order to arrive at the activity ratio at any given time past irradiation:

$$\frac{A(fission)}{A(n,\gamma)} = \frac{\sigma_u \times \theta_u \times \eta_{140} (1-e^{-\lambda_{Ba}T})}{\sigma_{La} \times \theta_{La} (1-e^{-\lambda_{La}T})} \times \frac{M_u}{M_{La}} \times \frac{\lambda_{La}}{(\lambda_{La}-\lambda_{Ba})} \times \frac{(e^{-\lambda_{Ba}t} - e^{-\lambda_{La}t})}{e^{-\lambda_{La}t}} \qquad (2.3.9)$$

$$= \frac{580 \times 0.0072 \times 0.0629 (1-0.9821)}{8.94 \times 0.9991 (1-0.8715)} \times \frac{140 \times 10^{-9}}{150 \times 10^{-12}} \times \frac{0.0172}{0.0172-0.0023} \times \frac{(e^{-\lambda_{Ba}t} - e^{-\lambda_{La}t})}{e^{-\lambda_{La}t}}$$

At times t=24 hrs and t=36 hrs post irradiation ratios of 1.9 respectively 3.1 have been estimated. The continuing production of $^{140}La$ from $^{140}Ba$ would make above ratio (2.3.9) more and more unfavourable with increasing time beyond irradiation. For instance the counting for $^{140}La$ lasts about one week post activation, at which time (t=168h) the ratio would have increased to about 50. However the

postactivation clean-up takes place between 24 to 36 hours after irradiation and would separate parent $^{140}Ba$ from its daughter $^{140}La$, the latter remaining in the REE fraction. From there on the ratio $^{140}La_{fission} / {}^{140}La_{desired}$ would not change anymore. Therefore above values of 1.9 - 3.1 at 24-36 hours can be considered as a worst case. In other words, the amount of U has to be reduced more than two orders of magnitude in order to keep interference with La determination below the 1 percent level.

The fission production of $^{144}Ce$ would again be described by equation (2.3.5) with

$\lambda = 101.55 \times 10^{-6}\ h^{-1}$ = decay constant of $^{144}Ce$

$\eta = 0.0548$ = fission yield of mass=144 decay chain

leading to

$$A[dps] = (6.02\times10^{23} \times 5\times10^{13})(580\times10^{-24} \times 0.0072(1-e^{-\lambda T})0.0548)(140\times10^{-9})e^{-\lambda t}$$

$= 783\ (e^{-\lambda t})$ dps $= 46{,}980\ (e^{-\lambda t})$ dpm for the fission produced $^{144}Ce$ activity at time t after irradiation.

On the other hand a typical dose of $^{144}Ce$ tracer added to each sample or standard has an activity of about $20\times10^{3}$ d.p.m. (halflife=284.4 d). The resulting activity ratio of about 2.34 again requires removal of U well over two orders of magnitude, in order to avoid interference with $^{144}Ce$ tracer.

The worst of all above cases is undoubtedly the possible interference with $^{141}Ce$, and this sets the criterion for a very efficient elimination of U from our samples. This necessary removal of $140 \times 10^{-9}$ mol U from 10 kg. seawater down to an amount well below $10^{-12}$ mol in the final extract is achieved by a combination of cation exchange (2.7) and anion exchange (2.8) chromatography. Fortunately there is a very sensitive quality control in case this scheme fails for a given sample. Any $^{238}U$ which would inadvertently have slipped through the separation steps would give rise to a strong $^{239}Np$ signal:

$$^{238}U\ (n,\gamma)\ ^{239}U \xrightarrow[23.5\ m]{-\beta} {}^{239}Np \xrightarrow[2.35\ d]{-\beta} {}^{239}Pu \qquad (2.3.10)$$

The neutron activation produced $^{239}Np$ activity can again be calculated with equation (2.3.2) where

$\sigma$ = 2.71 barns = 2.71 x $10^{-24}$ $cm^2$ = thermal neutron cross section of $^{238}U$

$\lambda$ = 3.41 x $10^{-6}$ $s^{-1}$ = 0.0123 $h^{-1}$ = decay constant of $^{239}Np$

$\theta$ = 0.9927 = abundance of $^{238}U$ isotope

M = 140 x $10^{-9}$ = mols of U in 10 kg seawater

Combination with above described equation (2.3.5) for fission produced $^{141}Ce$ leads to an activity ratio

$$\frac{A(239Np)}{A(141Ce)} = \frac{2.71x0.9927x(1-0.9063)}{580x0.0072x(1-0.993)x0.058} \times \frac{e^{-\lambda_{Np}t}}{e^{-\lambda_{Ce}t}} = 147\ \frac{e^{-\lambda_{Np}t}}{e^{-\lambda_{Ce}t}} \qquad (2.3.11)$$

The resulting count ratio for each useful gamma peak is given in Table 2.2., assuming that the absolute detector efficiencies are about the same in this narrow gamma energy region.

In fact the above $(n,\gamma)$ reaction 2.3.10 for $^{239}Np$ production is the one case where the minor fraction of about 0.2 percent epithermal neutrons would lead to an enhanced yield (see section 2.9). The reaction rate per atom is given by (2.3.12)

$$r = \phi_{th} x \sigma_{th} + \phi_{epi}(I + 0.44\,\sigma_{th}) \qquad (2.3.12)$$

where $\phi_{th}$ = 4.9879 x $10^{13}$ neutrons.$cm^{-2}$.$sec^{-1}$=thermal neutron flux

$\sigma_{th}$ = 2.71 barns = 2.71 x $10^{-24}$ $cm^2$ = thermal neutron cross section of $^{238}U$

$\phi_{epi}$ = 0.01207x$10^{13}$neutrons.$cm^{-2}$.$sec^{-1}$=epithermal neutron flux

I = 270 barns=270 x $10^{-24}$ $cm^2$. = resonance integral of $^{238}U$

This leads to an effective rate of $17.8 \times 10^{-9}$, compared to

$$\phi_{th} \times \sigma_{th} = 5 \times 10^{13} \times 2.71 \times 10^{-24} = 13.6 \times 10^{-9}$$

as used above when all neutrons were assumed to be strictly in the thermal energy region. Consequently the counting ratios in Table 2.1 are also enhanced in favour of better diagnostic use of $^{239}Np$ as indicator of incomplete U separation.

These predicted ratios were determined experimentally by irradiation during 8 hours at $5 \times 10^{13}$ neutrons.cm$^{-2}$sec$^{-1}$ of a U standard (0.00539 dpm $^{238}U$ = 30 pmol) with normal 235/238 isotopic ratio. The sample was counted after ten days cooling with an 18 % nominal efficiency Ge(Li) detector (Canberra). After this period of about four halflives roughly 94 % of the $^{239}Np$ has already decayed away, yet very distinct peaks were still recorded(Table 2.3.3). The measured count rate ratios of $^{239}Np$ versus fission produced $^{141}Ce$ agree well with the predicted ratios (Table 2.3.2).

| Isotope | Gamma Peak (keV) | Number of Gamma events per 1000 decays | Gamma count ratio at time t after irradiation | | |
|---|---|---|---|---|---|
| | | | t=0 | t=24h | t=253h (10.5 days) |
| $^{141}Ce$ | 145.4 | 490 | --- | --- | --- |
| For strictly thermal neutrons: | | | | | |
| $^{239}Np$ | 106.1 | 219 | 65 | 49.5 | 3.7 |
| | 228.2 | 113 | 33.6 | 25.5 | 1.9 |
| For thermal and epithermal neutrons: | | | | | |
| $^{239}Np$ | 106.1 | 219 | 85 | 65 | 4.8 |
| | 228.2 | 113 | 44 | 33 | 2.5 |

Table 2.3.2. Predicted count rate ratios of $(n,\gamma)$ produced $^{239}Np$ and fission produced $^{141}Ce$, both resulting from a hypothetical U impurity in activated REE extract. Absolute detector efficiencies were assumed to be about constant as function of energy in the narrow 100 - 250 keV range. More favourable ratios are predicted when the minor 0.2 % fraction of epithermal neutrons is taken into account. These values are intended to be only rough estimates. Actual ratios may differ depending on detector efficiency, which really varies with energy, as well as various uncertainties in the epithermal/thermal neutron flux ratio.

| Nuclide | keV | Total counts over 20,000 sec interval | |
|---|---|---|---|
| | | net peak area | gross=peak area + background |
| 144Ce | 134 | 8447 | 16233 |
| 141Ce | 145 | 6773 | 17459 |
| 239Np | 106 | 63455 | 86093 |
| 239Np | 228 | 10609 | 16594 |
| 239Np | 277 | 9674 | 13455 |
| 140La | 329 | 3188 | 8050 |
| 140La | 487 | 1698 | 3014 |
| 140Ba | 537 | 453 | 1623 |
| 140La | 816 | 665 | 1205 |
| 140La | 1596 | 1266 | 1378 |

Count rate ratio of $^{239}Np$ versus $^{141}Ce$ at 253 hours postactivation:

| | |
|---|---|
| 239Np(106) / 141Ce(145) | 9.4 |
| 239Np(228) / 141Ce(145) | 1.6 |

Table 2.3.3. Gamma counts of nuclides produced from irradiation of 30 pmol U. The spectrum was recorded over 20,000 sec interval, beiginning 10 days, 10 hours and 11 minutes postactivation. The midpoint (10,000 sec) of counting corresponds to 253 hours postactivation. Various REE nuclides produced from $^{235}U$ fission were observed. The measured $^{239}Np/^{141}Ce$ count rate ratios are in fair agreement with predicted ratios (Table 2.3.2).

## 2.4. Laboratory

Concentrations of REE to be measured are very low. Moreover stringent requirements have been set (2.3) for separation of U and Na. Ultraclean working conditions are essential. Various precautions can be taken to avoid contamination, yet it is hard to prove which of those are truly necessary. In this respect the scientific method had to give way to intuition and common sense. Our precautions described below have been selected in a somewhat arbitrary manner.

An existing radionuclide laboratory was converted to a clean laboratory. The siting within a larger complex of radioisotope laboratories (Figures 2.4.1, 2.4.2) has several advantages:

i) use of a radionuclide ($^{144}Ce$) as internal standard is allowed
ii) restricted access of personnel, i.e. less chance of contamination
iii) easy access to high level radioisotope area for postactivation work (2.10).

First the destined area, with two existing workbenches, was separated off by erecting a wall with entrance door, and construction of a lowered ceiling. All seams were carefully sealed to permit maintaining positive pressure within the clean laboratory. Then one of the counters was converted to a combined Class-100 laminary flow bench / fumehood assembly (Figure 2.4.3).

Class-100 specifications (in non-S.I. units) are as follows:

- greater than 99.97 % arrestance of 0.3 micron diameter particles
- clean air flow velocity greater than 100 feet per minute (FPM).

The first requirement was met by installation of a High Efficiency Particle Arrestance filter (American Air Filter, ASTROCEL I HEPA, 24x30x 5&7/8 inch) which is warranted to meet such specifications. The second requirement can be met by an air blower which delivers sufficient capacity at an acceptable noise level. The pressure drop over a new 5&7/8 inch thick filter is 0.5 inch water gauge, slowly building up to 1.0 inch by clogging with particles, at which point the filter has to be replaced. Given the 5 square feet (24x30 inch) area of the filter the blower has to deliver at least 500 cubic feet per minute (CFM) at 0.5"

respectively 1.0" pressure drop. Actually a larger capacity multispeed blower is preferable because it would run much more quietly at a low speed setting, while excessively high flow rates can easily be reduced by simply shutting of part of the air inlet.

The selected four-speed blower(Dayton 4C352) is specified to deliver 1670 CFM at 0.7" pressure drop at lowest speed, and 2340 CFM at 1.0" at highest speed setting. Upon complete installation flow velocities of 160±20 FPM, well exceeding the 100 FPM specification, were measured with blower speed at its lowest setting. The corresponding displacement of 900 CFM at 0.5" pressure drop is lower than specified for the blower, possibly as a result of additional resistance in the ductwork and glassfibre prefilter (10x20x1").

The fibreglass fumehood (LABCONCO) was modified for attachment to a rooftop exhaust blower via about 30 feet of 10" diameter fibreglass pipe. Maximum exhaust capacity roughly matched the 900 CFM clean air input. However the exhaust flow was routinely reduced by closing the sash window of the fume hood. In this way a positive pressure is maintained in the laminary flow bench, while allowing distillations and sample evaporations under clean air conditions inside the fume hood. Excess clean air spills out between the acrylic sliding doors of the laminary flow bench into the clean laboratory, and from there via leaks around the entrance door back into the radioisotope laboratory. At maximum particle free input of 900 CFM (somewhat less when the fume hood is running), the residence time in the clean laboratory is on the order of five minutes. Therefore the clean laboratory is expected to be clean indeed, although it does not meet the Class-100 conditions inside the laminary flow bench.

General cleanliness is further enhanced by several Astroturf floormats in the radioisotope laboratory. The complete radioisotope laboratory complex was cleaned routinely. Finally all work in the clean lab was done while wearing PE gloves, lintfree labcoats and special shoes.

N.B. Above units (different from the S.I. system) are used for easy comparison with commercial brochures.

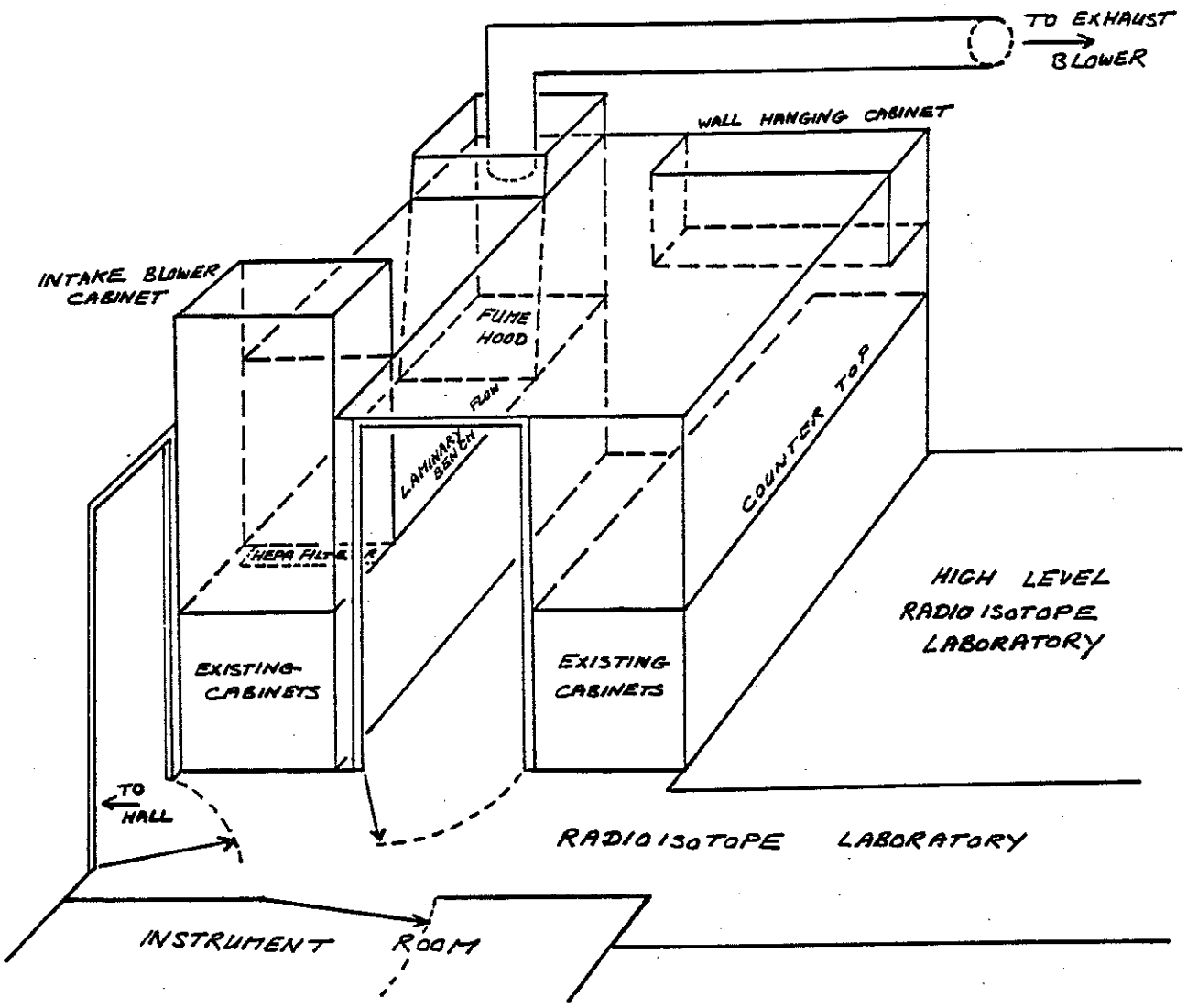


Figure 2.4.1. Perspective view sketch of clean laboratory with combined laminary flow bench / fume hood assembly. The radioisotope laboratory with ample ASTROTURF floormats serves as an extra dirt-barrier. Adjacent high level radioisotope laboratory is used for postactivation procedures (2.10).

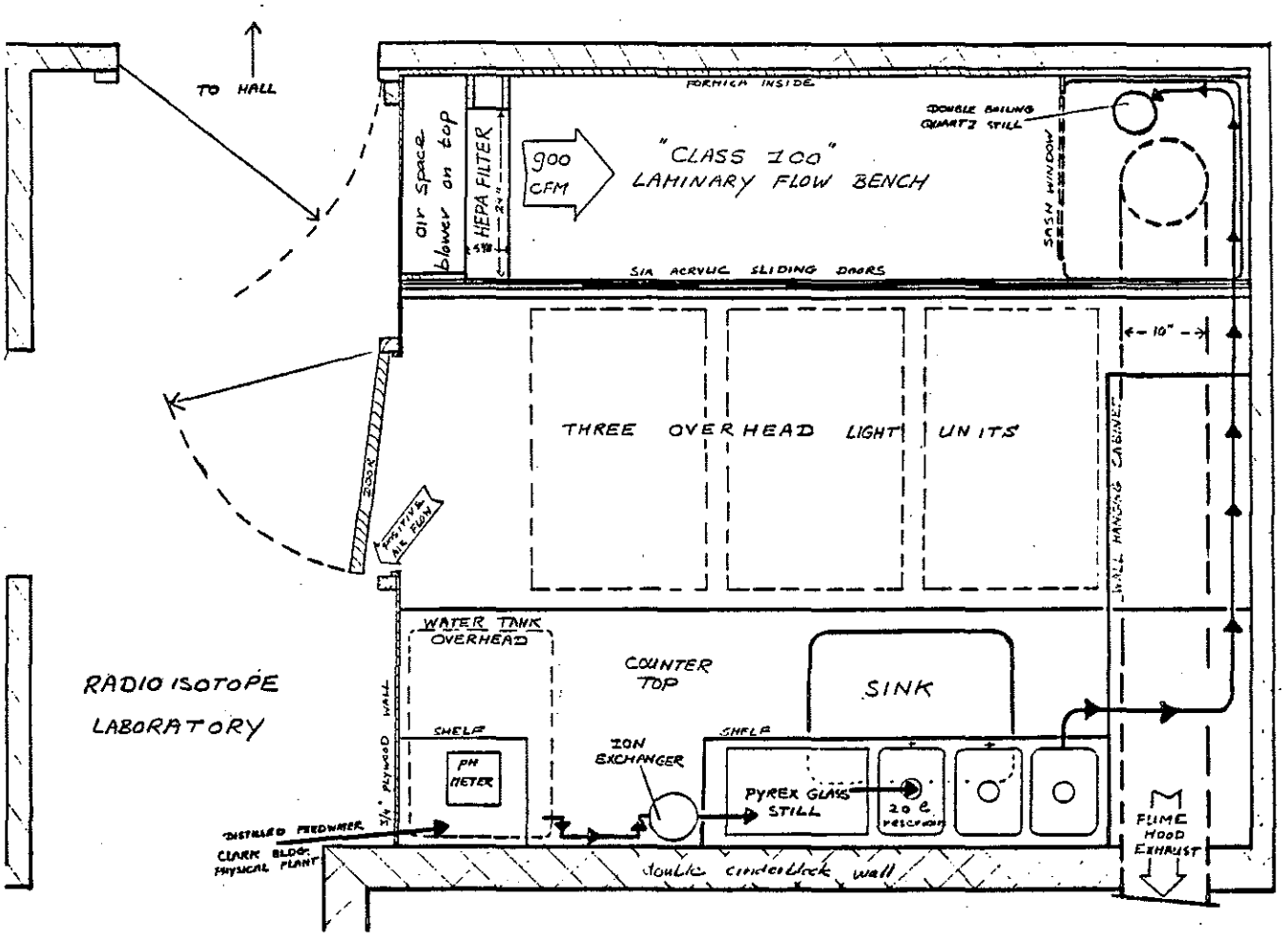


Figure 2.4.2. Plan view of clean laboratory, mostly at bench top level. Double boiling quartz still is permanently installed in fume hood for production of highest purity water and acids (2.5). Two shelves over other bench support pH-meter and pure water still with reservoirs, the latter behind acrylic window to keep dust out. Note pure water lines (arrows) running from overhead tank via ion exchanger, Pyrex glass still, into storage reservoirs, and from there into quartz still. Wall hanging cabinet with sliding doors for storage of purified reagents. Three overhead light units flush with ceiling. Non metal material was used whenever possible for fittings, door handles, etc.

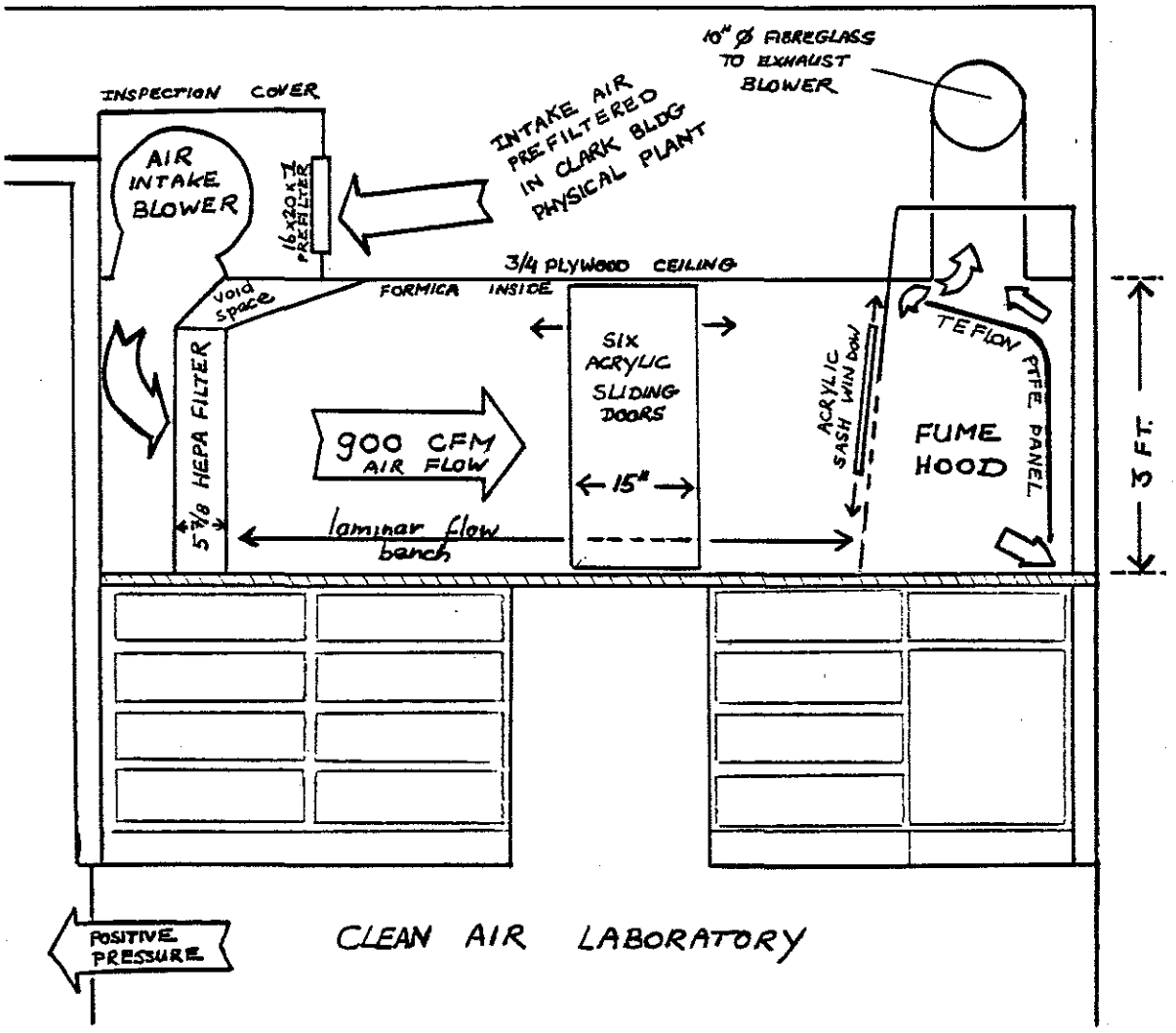


Figure 2.4.3. Section view of combined laminary flow bench / fume hood assembly, built on existing counter with cabinets underneath. Teflon PTFE panel inside fume hood directs air flow and diverts condensation from exhaust pipe. Air flow into fume hood controlled by sash window position.

## 2.5. Labware and Reagents.

### Labware

With few exceptions, the samples, and their various REE-extracts during processing, would only come in contact with hot acid cleaned polyethylene (PE), polypropylene (PP) and Teflon (PTFE, PFA, FEP) labware. The only exceptions are the acid cleaned Pyrex glass combination pH electrode used for neutralization of the seawater (2.6), the hot acid cleaned Pyrex pasteur pipettes used for final transfers (2.9), and of course the fused quartz activation vials. The hydrophobic properties of Teflon make it an excellent material for evaporation beakers. Very little, if any, of the sample remains on the vessel walls during evaporation.

For cleaning all PE bottles and reservoirs were filled to the rim with 1N HCl (ACS Reagent Grade in Pyrex water), kept in a stove at 60°C for 24 hours, allowed to cool upside down for 24 hours, and finally stored (still containing the dilute acid) until use. Teflon FEP bottles (1000ml, Nalgene 1600-0032) as well as wash bottles (500ml, Nalgene 2403-0500), were taken through the same routine, using 2N nitric acid instead. Smaller PE and PP labware was soaked in dilute acid for 24 hours, rinsed with Pyrex water, and then soaked in 1N HCl inside 2000ml containers (Nalgene 2120-0005). These were then kept in an oven at 60°C for 24 hours and stored at room temperature until use. The glass (Pyrex and quartz) and Teflon (except bottles) labware was first soaked in 8N $HNO_3$ (1/1) baths at 60°C for 24 hours. This labware was then taken out, rinsed thoroughly with Pyrex water, and soaked in 1N HCl in the same 2000ml containers. These were also taken through the 24 hour hot cycle and then stored until use.

Almost all the time all labware, bottles and reservoirs are immersed in 1N HCl solution, only to be taken out just before use. Then the bottles or labware would be rinsed thoroughly with Pyrex water. All labware was subsequently rinsed with 0.1N HCl in quartz water respectively quartz water, and allowed to dry upside down in the laminary flow bench. Directly after use the various Teflon beakers and vials were filled with 8N $HNO_3$ and heated at about 60°C on the hot plate to bring any (unexpected) residual REE or $^{144}Ce$ radiotracer into solution.

This 8N $HNO_3$ was discarded, and after a thorough rinse the beakers were placed in the 8N $HNO_3$ bath, to be further treated as described above.

Ultrapure Reagents

Whenever possible all purified reagents were directly collected into Teflon FEP bottles or wash bottles. Linear and conventional PE bottles were occasionally used for less corrosive reagents such as water or 1N buffer solution.

WATER. Distilled water produced by the physical plant in Clark Laboratory (WHOI) has a fairly high purity with trace metal concentrations around 1 microgram per liter (Cu=0.2; Fe=3; Ni=0.4; Co=0.2; Mn=0.3 $ug.l^{-1}$; Bill Martin, pers. comm.). This water was pumped into a PE storage reservoir (Figure 2.4.2) and then fed by gravity flow through an ion exchanger (Sybron/Barnstead Ultrapure Cartridge D 0809) directly into a Pyrex glass single boiling still (Corning AG1B). The still was run almost daily, and occasionally overnight, at production rates of about 1200ml per hour. The so-called 'Pyrex-water' that was produced was collected in 20 ltr. carboys and used routinely for making up postirradiation reagents, dilute acid soaking solutions, and rinsing of labware. However, for preparation of ultrapure reagents and final rinses of labware, this water was further purified by passing it over a double boiling fused quartz still (Heraeus-Amersil). This still is set up permanently in the clean air fume hood (Figure 2.4.2) and also used for distillation of acids (see below). Production rates are about 100-200ml per hour. This so-called 'quartz-water' was collected directly into the reagent or washing bottle.

ACIDS. Glacial acetic acid (15.9N) and concentrated nitric acid (15.8N) were produced with the double boiling quartz still from ACS reagent grade starting materials. Three initial portions of about 50ml each were used for a thorough rinse of the 1000ml Teflon FEP bottle, after which collection started. Hydrochloric acid with normalities up to about 10N HCl can be produced by distillation, simply by feeding the double still with acid of the same strength. We have chosen to produce 8N HCl routinely because it is the optimum normality for extraction of uranium with the AG1X8 separation step (Figure 2.8.1).

Distillation of sulphuric acid is an extremely difficult and dangerous enterprise. Extensive heating is required in order to reach the high boiling point of concentrated $H_2SO_4$ (338 $^{o}$C at 1 atm), and one must avoid the notoriously exothermous reaction upon mixing of water into already very hot concentrated sulphuric acid. Initially a few 100 ml concentrated acid were produced from the same double still. Dilutions from this batch were used for the Atlantic samples (Chapter 3). Yet sudden 'bumping' of the acid due to delayed boiling seemed outright dangerous. Also extensive insulation and alufoil 'mirrors' were necessary in order to achieve any production at all. Attempts with sub-boiling distillation, using the 'two-bottle still' (Figure 2.5.1) proved fruitless as no $H_2SO_4$ was carried over at all. Only by using a modified version of the prohibitively expensive quartz subboiling still (QUARTZ & SILICE, France) it seems feasible to produce moderate amounts of sulphuric acid (MOODY & BEARY, 1982). For all other samples Ultrex $H_2SO_4$ (Baker) was used instead, but not until an upper limit of REE blanks in the latter was assessed (see below). The sulphuric acid is used only in the cation exchange step, whereby all REE from a 1N $H_2SO_4$ solution are retained by the resin (2.7). Initially the columns were pre-conditioned with some 4N $H_2SO_4$, yet in the final procedure only the 1N $H_2SO_4$ was used. In further work the 1N $H_2SO_4$ prepared from Ultrex $H_2SO_4$ may be further purified by taking advantage of the same cation exchange scheme. Alternatively ultrapure $H_2SO_4$ in precleaned Teflon bottles can be purchased from the National Bureau of Standards (MOODY & BEARY, 1982).

Dilute acids of various strength were made by addition of quartz water directly from the still. The glacial acetic acid was used for making up buffer solutions.

AMMONIUM HYDROXIDE Concentrated $NH_4OH$ (15.9N) was produced by saturation of quartz water with $NH_3$-gas (Figure 2.5.2). After about 6-8 hours when the solution seemed saturated (no more bubbles emanating from frit) the pressure was taken off by opening the outer container, carefully avoiding reverse flow of liquid into the gas lines. After complete decompression gas bubbles would form in situ in the apparently

oversaturated solution. Therefore the screwcap of the Teflon bottle was only tightened the next morning. Normalities of 16± 0.5 were determined by backtitration of small aliquots. This concentrated ammonia was used to make up 2N $NH_4OH$, as well as the 1M and 8M buffer solutions.

2N $NH_4OH$ About 125 ml of ultraclean concentrated ammonia was diluted to 1000 ml with quartz water. The resulting 2N $NH_4OH$ was further purified over a 15x200mm CHELEX-100 (200-400, $NH_4^+$-form) resin column, which was preconditioned as described in section 2.6. The first 3x30ml product was used to rinse the bottle threefold, and discarded.

1M BUFFER About 126 ml concentrated ammonia and 120 ml glacial acetic acid were added to about 1500 ml quartz water in a 2000 ml bottle, while mixing with a magnetic stirrer. The acidity was adjusted to pH=5.4 with additional glacial acetic acid. Then the bottle was filled to the 2000 ml mark. The solution was further purified over the same column as described above, now in the $H^+$-form (15x100mm), directly after above passage of the 2N $NH_4OH$ reagent. The first effluents were discarded until the pH was stabilized at 5.4, upon which collection started in Teflon FEP bottles.

8M BUFFER About 440ml concentrated ammonia and 400ml glacial acetic acid in separate 1000ml LPE bottles were kept in the freezer overnight. Precooling is necessary to counteract the exothermic reaction upon mixing which otherwise would lead to vigorous boiling. The next morning the viscous ammonia was added to the frozen glacial acetic acid, and the whole bottle placed in ice. After cooling to room temperature the pH was adjusted to an apparent reading of 6.9 with about 40ml additional glacial acetic acid. The viscous reagent was further purified over the same CHELEX-100 column, directly after the 1N buffer had passed. Flow rates were extremely low. The effluent was collected in 500ml Teflon FEP bottles.

Addition of 0.500 ml 8M buffer (pH=6.9) to 100ml neutralized seawater (pH between 6 and 8) was repeatedly found to bring the final pH to 6.0 ± 0.1. The final molality of the buffer in seawater is about 0.4M. Further experiments indicated excellent buffer capacities for final

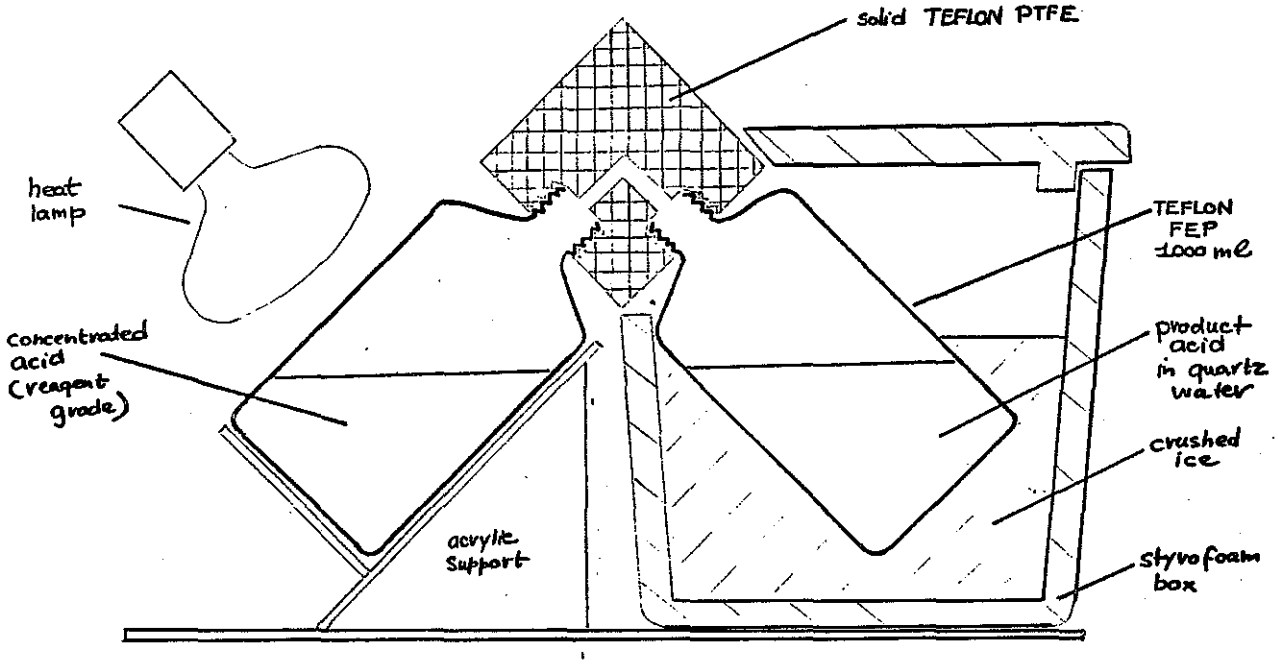


Figure 2.5.1. Sub-boiling two bottle still for preparation of small batches ultrapure dilute acid from concentrated reagent grade substrates.

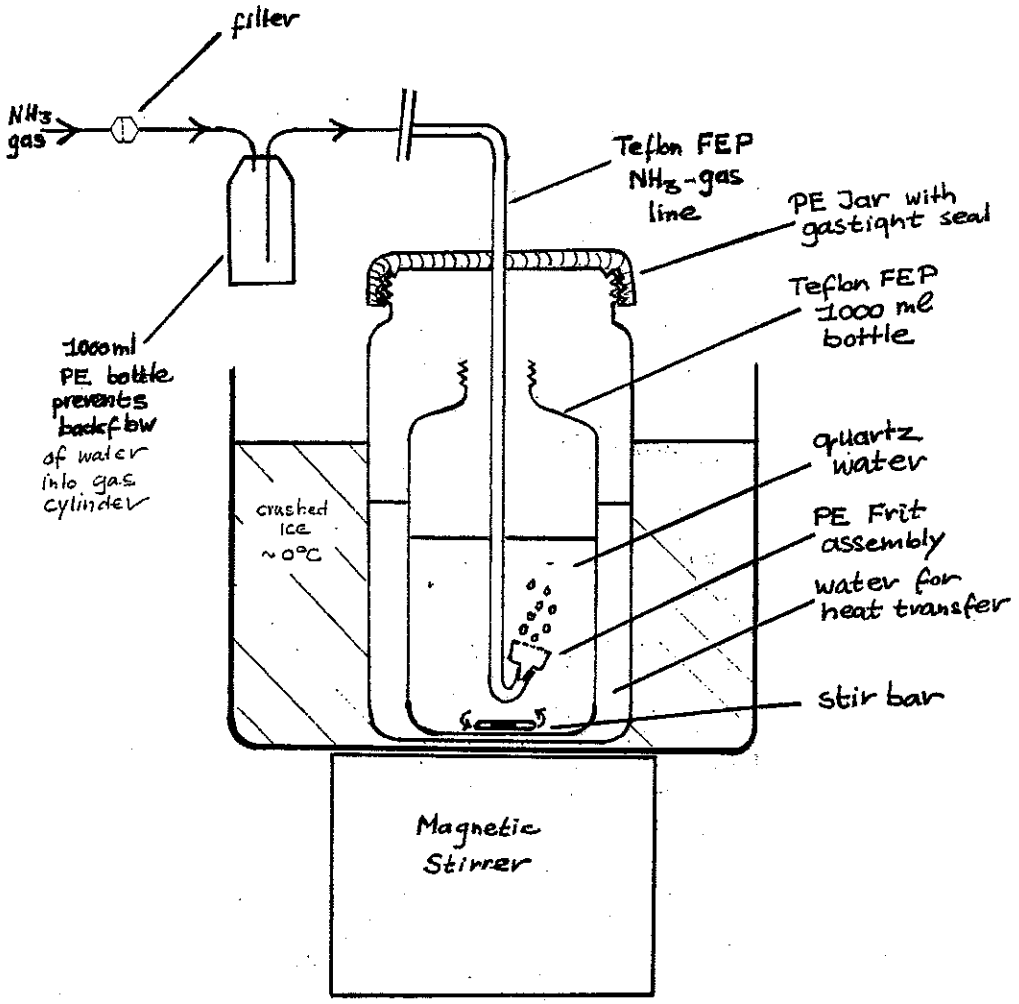


Figure 2.5.2. Setup for production of concentrated ammoniumhydroxide from ammonia gas. All work was done inside the clean air fume hood.

molalities ranging between 0.2 and 1.0 molar. For 10 ltr. seawater samples actual additions of only 30ml, rather then 50ml, were made.

BLANKS Routine analysis of REE blanks in all reagent batches is not feasible. Yet in the first stages REE blanks were determined once for a number of reagents. Some of these reagents were prepared by somewhat different procedures than described above. The 1M and 8M buffers as well as the 2M $NH_4OH$ were made up from untreated ACS reagents, and then purified over a CHELEX-100 column. 3.3M $HNO_3$ was made up in the sub-boiling 'two-bottle' still (Figure 2.5.1). Various volumes of these reagents were evaporated to dryness in Teflon PTFE beakers. Two $H_2SO_4$ lots (Baker Ultra respectively Instra grades) were evaporated separately in Pyrex beakers at much higher temperature. Resulting REE blanks, especially for the sulphuric acid lots, really are upper limits. For instance an empty beaker carried along the procedure also gave rise to REE blanks. After evaporation all beakers were spiked with $^{144}Ce$ internal standard, an equal amount of internal standard was also transferred directly into a quartz vial. Samples were taken up in 3.3M $HNO_3$, transferred into quartz vials, and irradiated (see 2.9). Only one set of counts was done for short lived isotopes.

For all reagents the highest blanks seemed to occur for the light REE, especially La and Ce. The highest contribution for latter elements would come from the sulphuric acid reagents, both contributing about one percent to the total amount expected in ten liters of seawater. At the time it was thought that the enhanced La and Ce blanks (relative to the other REE) resulted from U fission. In the overall procedure such U would have been taken out. Upon closer inspection (2.3, 2.16) it seems that these blanks were more likely resulting from true REE contamination, after all.

Later on all reagent batches were routinely monitored for blanks of Mn and Ni. The absence of both from distilled reagents indicates purity for other non-volatile elements, like the REE, as well. Also Mn has a much lower affinity for CHELEX-100 than the REE (2.6). Its absence from reagents purified over CHELEX-100 would suggest their purity for REE as well. Aliquots of 30ml of each reagent were poured into Teflon FEP vials,

evaporated to dryness and taken up in 0.500 ml 0.2N $HNO_3$. With GFAAS detection limits for Mn and Ni of about 0.1 respectively 0.2 ug.$l^{-1}$, and a factor 60 for preconcentration, the levels of Mn and Ni in our reagents were below about 20 respectively 40 nanogr.$l^{-1}$. Batches with levels of Mn or Ni above detection limits were either rejected or further purified and again checked. Initially such blanks would quite often appear in any reagents made up from reagent grade $NH_4OH$, even after purification over CHELEX-100 columns. After that was discovered, all concentrated ammonia was made by gas saturation as described above.

INTERNAL STANDARD The radionuclide $^{144}Ce$ was selected from various other possible REE nuclides as the most suitable internal standard. Its major gamma peak at 133 keV is in a somewhat crowded region of the REE spectrum, but nevertheless well separated from other peaks. Also the $^{144}Ce$ generated Compton background would be well below 133keV. Most importantly $^{144}Ce$ is produced from fission of $^{235}U$ (see 2.3). The latter can easily be highly purified before the irradiation. Various other shorter lived REE radionuclides produced upon fission can be allowed to decay away. Therefore commercially available $^{144}Ce$ is guaranteed to be carrier-free, i.e. free of stable isotopes of Ce (and other REE). This was verified by activation of a large dose of the aquired batch of $^{144}Ce$, about 100-fold the amount of radiotracer spike typically added to each sample. Small but distinct $^{140}La$ peaks in the resulting gamma spectra would correspond to a negligible contamination of a seawater sample (less than 0.01 percent).
Typical $^{144}Ce$ spikes would correspond to about 200 cpm for the 133keV peak in the final gamma spectra. This way it is the largest peak in the spectra of third and fourth count sets. For the first count set one would like to have a stronger $^{144}Ce$ signal, yet this would also lead to greater interferences of its secondary 80.1 keV peak with the determination of $^{166}Ho$ (see 2.13).

Post-irradiation Reagents

These were made up from ACS grade reagents in Pyrex water.

## 2.6. Chelating ion exchange chromatography.

### Introduction.

The chelating resin Dowex-A1 (MORRIS et al., 1958) is better known by the trade name CHELEX-100 (BIORAD LABORATORIES, 1978) of its analytical grade. The resin consists of a cross-linked styrene-divinylbenzene matrix with iminodiacetic acid substituted onto some of its benzene rings (Figure 2.6.1.). The selectivity of CHELEX-100 for metal ions corresponds to that of free iminodiacetic acid in solution (Table 2.6.1.). Actual selectivity values depend on pH, ionic strength (I) and composition of a given solution. For instance the approximate selectivity for cations in an acetate buffer system at pH=5 is:

$$Pd^{2+} > Cu^{2+} \gg Fe^{2+} > Ni^{2+} > Pb^{2+} > Mn^{2+} \gg Ca^{2+} = Mg^{2+} \ggg Na^{+} \quad (2.6.1)$$

Chelex-100 chromatography has been found to be highly efficient for the analytical extraction of transition metals from seawater, while exhibiting very low analytical blanks (RILEY, 1975). Some initial unpublished studies (LAI et al., 1966; CALLAHAN et al., 1966) were followed by systematic investigations of RILEY & TAYLOR (1968[a]; see also 1968[b,c]; 1972). The latter reported a 99-100 % retention of radiotracer spikes and/or standard additions from seawater solution at pH values ranging from 5 to 9 for a suite of elements (Bi, Cd, Ce, Co, Cu, In, Mn, Mo, Ni, Pb, Re, Sc, Th, W, V, Y and Zn) including the lanthanide Ce and lanthanide analogs Sc and Y. However their final analyte still contained considerable amounts of major cations Na, K, Mg and Ca which would give rise to serious interferences in the subsequent final analysis by GFAAS or any other method. This serious disadvantage has been well recognized, although some accurate determinations with low blanks have been made (MOORE, 1978; BRULAND et al., 1979). Other pre-concentration methods such as solvent extraction (8-hydroxyquinoline, KLINKHAMMER, 1980; Freon/APDC/DDDC, DANIELSSON et al., 1978; APDC/DDDC, BRULAND et al., 1979) and coprecipitation (Co/APDC, BOYLE & EDMOND, 1976) were employed instead when the first accurate determinations were made of oceanographically consistent profiles for such transition metals as Mn (BENDER et al., 1977), Co (KNAUER et al., 1982; Ni (SCLATER, BOYLE &

| Ion | Selectivity coefficient relative to $Zn^{2+}$ |
|---|---|
| $Hg^{2+}$ | 1060 |
| $Cu^{2+}$ | 126 |
| $UO_2^{2+}$ | 5.7 |
| $Ni^{2+}$ | 4.4 |
| $Pb^{2+}$ | 3.88 |
| $Zn^{2+}$ | 1.000 |
| $Co^{2+}$ | 0.615 |
| $Cd^{2+}$ | 0.39 |
| $Fe^{2+}$ | 0.13 |
| $Mn^{2+}$ | 0.024 |
| $Ba^{2+}$ | 0.016 |
| $Ca^{2+}$ | 0.013 |
| $Sr^{2+}$ | 0.013 |
| $Mg^{2+}$ | 0.009 |
| $Na^{+}$ | 0.000 000 1 |

Table 2.6.1. The selectivity factors of CHELEX-100 for various cations, relative to its affinity for a reference cation, in this case $Zn^{2+}$. (Taken from BIORAD, 1978).

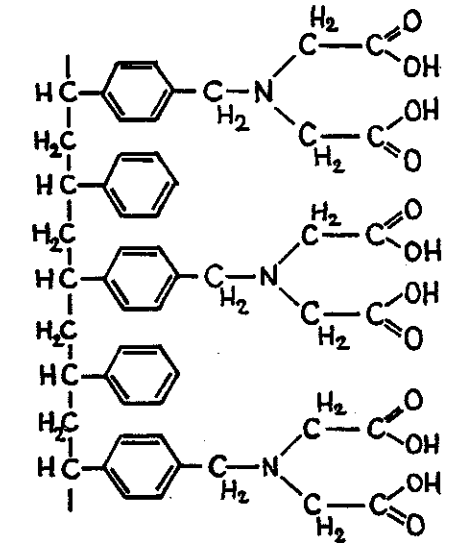

CHELEX-100

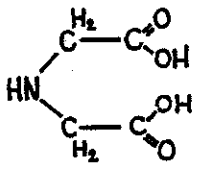

Iminodiacetic acid

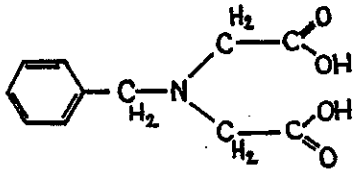

N-benzyliminodiacetic acid

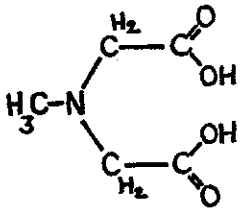

N-methyliminodiacetic acid

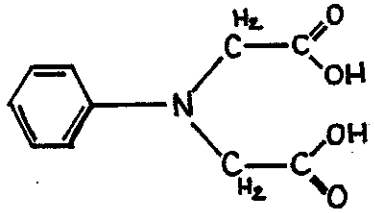

N-phenyliminodiacetic acid

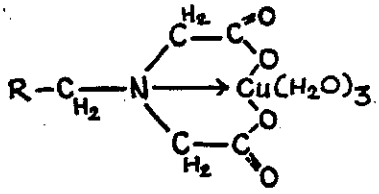

Two-ring structure of chelated $Cu^{2+}$-ion with iminodiacetic group

Figure 2.6.1. The structures of CHELEX-100, iminodiacetic acid and some of its derivatives like N-benzyldiaminoacetic acid. All are shown in fully protonated form such as commonly encountered at pH values below 2. The complete chelation of a $Cu^{2+}$-ion is shown as example. Such complete chelation is favoured at higher pH (greater than 5) when the second proton becomes fully neutralized.

EDMOND, 1977), Cu (BOYLE, SCLATER & EDMOND, 1977), Zn (BRULAND et al., 1978) and Cd (BOYLE, SCLATER & EDMOND, 1976). All of the latter methods are single step batch equilibrations. Thus very high and specific affinity of the complexing agent for the metal(s) of interest is a prerequisite. On the other hand chromatography can be envisioned as an almost infinite suite of equilibrated batches (whose total is expressed as the number of theoretical plates). Complete extractions or separations can be achieved at relatively low and non-specific affinities.

Chelex-100 selectivity for various elements is known to be strongly dependent on pH and ionic strength. The pH dependence is not surprising given the proton dissociation of the iminodiacetic group (Figure 2.6.2.). Only at or above pH=4 do both carboxylic groups become available for the chelation reaction with metal ions. However chelation becomes effective at lower pH as ionic strength increases.

KINGSTON and co-workers (1978; 1979) realized the existence of an optimum pH range for the separation of transition metals from alkaline earth elements at the given ionic strength (I=0.7) of seawater. At higher ionic strength (0.5 to 1.0) the chelation of transition metals Mn, Fe, Co, Ni, Cu, Zn, Cd had been demonstrated to increase rapidly from pH=3 upward, to level off at pH=5 and to remain at constant level at higher pH (LEYDEN & UNDERWOOD, 1964; HOLYNSKA, 1974; LAI et al., 1966; CALLAHAN et al., 1966). The behaviour of Co and Cu is somewhat different. At pH values over 6 their chelation seems to decrease again.

At similar ionic strengths chelation of the alkaline earth metals Ca, Mg, Sr, Ba also exhibits a plateau at pH between 4 and 5, possibly slightly lower chelation between pH=5 and pH=6 (LUTTRELL et al., 1971) and then a steep increase at higher pH-values. The plateau between pH=5 and pH=6 would then be most suitable for quantitative separation. Also at higher pH values the competition between alkaline earths and transition metals for the iminodiacetic functional group might lead to less than completetrace element yields.

Experimental results for radiotracer spikes as well as standard additions of Mn, Co, Ni, Cu, Zn and Cd to 100ml. samples of coastal seawater buffered at pH=5.0-5.5 indeed suggest essentially complete recoveries (KINGSTON et al., 1978). Moreover the alkaline and alkaline earth elements were quantitatively removed from the 6.5cm length column by

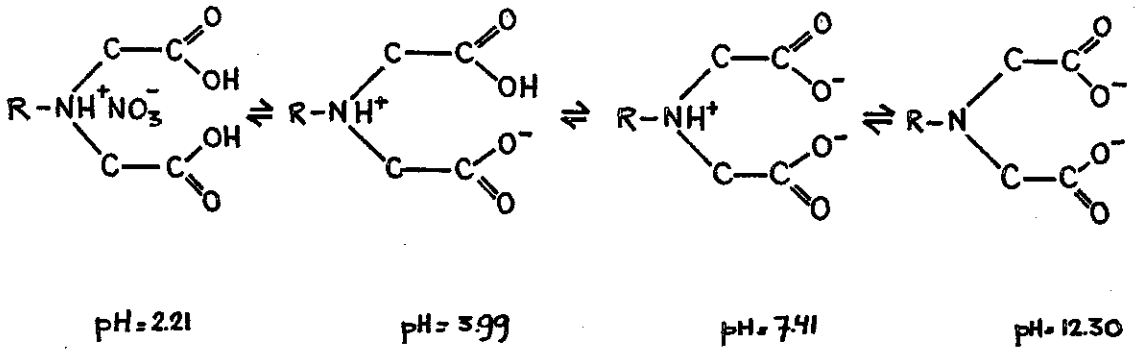


Figure 2.6.2. Proton dissociation reactions of the iminodiacetic acid functional group of CHELEX-100 at low ionic strength (Taken from KINGSTON, 1979). At low and intermediate pH the nitrogen atom becomes protonated to form a zwitterion which would also hinder formation of two-ring chelates by metal-ions. Only at or above pH=4 both carboxylic groups become available for the chelation reaction with metal ions. The half-neutralization point (50 % fully dissociated) occurs at pH of about 5.6 $\pm$ 0.2 (LEYDEN & UNDERWOOD, 1964). At higher ionic strength all equilibria shift and chelation becomes effective at lower pH (LUTTRELL et al., 1971). Of course the pH range for chelation is ultimately also a function of the specific affinity of the given metal ion ($Mg^{2+}$, $Cu^{2+}$, $Gd^{3+}$, $Th^{4+}$) for the resin.

washing with ammonium acetate/acetic acid buffer (pH=5), before elution of the trace metal fraction with 2.5N nitric acid. However the method has not yet been used for accurate determination of vertical profiles of the given transition metals.

With few exceptions (CHRISTELL. et al., 1961; RILEY & TAYLOR, 1968; LEE et al., 1977) no information is available on the chelation of Rare Earth Elements by CHELEX-100. However its free functional group in solution, N-benzyliminodiacetic acid (Figure 2.6.1) has been reported to exhibit very high formation constants with the REE-series (Table 2.6.2). Comparably high formation constants were also reported for somewhat differently substituted iminodiacetic groups (Figure 2.6.1), including iminodiacetic acid itself (Table 2.6.2). In all cases the chelation is observed to increase with atomic number of the REE.

One would expect to find a very high affinity of CHELEX-100 for the REE, thus enabling quantitative chromatographic extraction from seawater. Buffering of the seawater at carefully selected pH, and subsequent washings of the column would also allow separation from the major cations, in analogy with the results of KINGSTON et al.(1978). Moreover the generally reported ultra-low trace metal blank of CHELEX-100 is promising with respect to REE determinations.

Outline of research

An initial set of experiments was designed to simply confirm the separations reported by KINGSTON et al.(1978). The tracer of choice was $^{54}Mn$. The affinity of CHELEX-100 for Mn is expected to be less than for any other trace metal, and also very close to the affinity for undesired alkaline earths Ca and Mg (Table 2.6.1). In other terms $^{54}Mn$ serves as the 'bottom line' with respect to complete (100 %) extraction as well asquantitative separation from the major cations. After these $^{54}Mn$ experiments proved successful, a suite of batch experiments served to determine the pH dependence of the distribution of radiotracers $^{144}Ce$ and $^{153}Gd$ between CHELEX-100 and seawater. Subsequent small scale chromatography studies at optimum pH=6 with both tracers $^{144}Ce$ and $^{153}Gd$ proved very successful. Then the method was scaled up, first by using larger diameter column beds for larger volumes of seawater, and finally by enhancing the flow rate for 10 ltr. samples spiked with a

| Metal ion | Iminodiacetic acid | | N-benzyliminodiacetic acid | |
|---|---|---|---|---|
| | $pk_1$=2.58 | $pk_2$=9.33 | $pk_1$=2.04 | $pk_2$=8.89 |
| | log $K_1$ | log $K_2$ | log $K_1$ | log $K_2$ |
| $La^{3+}$ | 5.88 | 4.09 | 5.42 | 3.99 |
| $Ce^{3+}$ | 6.18 | 4.53 | 5.75 | 4.26 |
| $Pr^{3+}$ | 6.44 | 4.78 | 5.84 | 4.51 |
| $Nd^{3+}$ | 6.50 | 4.89 | 5.99 | 4.44 |
| $Sm^{3+}$ | 6.64 | 5.24 | 6.06 | 4.64 |
| $Eu^{3+}$ | 6.73 | 5.38 | 6.07 | 4.60 |
| $Gd^{3+}$ | 6.68 | 5.39 | 6.09 | 4.60 |
| $Tb^{3+}$ | 6.78 | 5.46 | 6.33 | 4.85 |
| $Dy^{3+}$ | 6.88 | 5.43 | 6.36 | 4.85 |
| $Ho^{3+}$ | 6.97 | 5.50 | 6.35 | 4.90 |
| $Er^{3+}$ | 7.09 | 5.59 | 6.54 | 5.09 |
| $Tm^{3+}$ | 7.22 | 5.68 | 6.59 | 5.15 |
| $Yb^{3+}$ | 7.42 | 5.85 | 6.69 | 5.26 |
| $Lu^{3+}$ | 7.61 | 6.12 | 6.70 | 5.32 |
| $Y^{3+}$ | 6.78 | 5.25 | 6.18 | 4.75 |
| $Zn^{2+}$ | | | 7.06 | |
| $Ca^{2+}$ | | | 3.21 | |

$$k_1 = \frac{[H][HA]}{[H\ A]} \qquad k_2 = \frac{[H][A]}{[HA]} \qquad K_1 = \frac{[LnA]}{[Ln][A]} \qquad K_2 = \frac{[LnA_2]}{[A][LnA]}$$

Table 2.6.2. Formation constants for iminodiacetic acid and N-benzylimino- diacetic acid with Rare Earth ions at 25°C and I = 0.1 ionic strength ($KNO_3$ medium)(Taken from THOMPSON et al., 1961; 1967). The complete chelation reaction: Ln + 2A = $LnA_2$ would be represented by the product $K_1.K_2$.

mixture of radiotracers $^{144}Ce$, $^{152}Eu$ and $^{153}Gd$. In conjunction with these experiments some estimates were made of the retention of U from seawater by the CHELEX-100 resin under given conditions.

The ultimate extraction procedure as used for 'real' samples is described at the end of this section.

Manganese tracer experiments.

Procedures were as follows: The CHELEX-100 resin (200-400 mesh) was soaked in 6N HCl for one week, the HCl was renewed daily. The resin slurry was poured into 7mm diameter Pyrex glass barrels with Pyrex bottom frit and PE funnel reservoir (BIORAD EconoColumns) until a 7-8 cm length resin bed was obtained. The beds were washed with about 50 ml 6N HCl, 10 ml Pyrex water, and preconditioned with 10 ml 2N $NH_4OH$ after which the excess ammonia was washed off with 10 ml Pyrex water. The change into the ammonia-form was accompanied by a swelling of the resin such that the length (volume) of the bed doubled to about 15 cm. Surface seawater (100ml, S=32 $^{o}/oo$) was acidified to pH=2 with 6N HCl. If desired the water was subsequently spiked with 20 nanoCurie $^{54}Mn$ radiotracer and allowed to equilibrate for at least 24 hours. After neutralization with 2N $NH_4OH$ the water was buffered at pH=5.0 by addition of 0.500 ml 8N buffer solution (see section 2.5. for preparation and buffer capacity). A few milliliters seawater were carefully loaded onto the resin bed in order to allow complete shrinkage of the column to its original 7-8cm length. Then the remaining seawater was added. The effluent was collected in 10ml. aliquots in precleaned Pyrex test tubes. Subsequently 4 x 10ml 1N buffer wash solution (pH=5.0) was passed over the column and collected in 2.0ml aliquots. After 3 x 2ml Pyrex water washes the columns were eluted with 4 x 2ml 2.5N $HNO_3$. All $^{54}Mn$ in the 10ml. aliquots was completely precipitated by addition of 0.10ml Mn carrier solution (1.0 $mg.ml^{-1}$) and 0.30ml 6N NaOH. After centrifugation the supernatant was transferred into another test tube. The precipitate was redissolved by addition of 6N HCl up to the 2.0ml mark. All samples were counted twice over one minute intervals for gamma radiation with a N.M.C. Sodium Iodide Crystal Counter set at a 1100V plateau. The precision under given conditions was about 5 % (mostly as a result of counting geometry errors) and was deemed adequate.

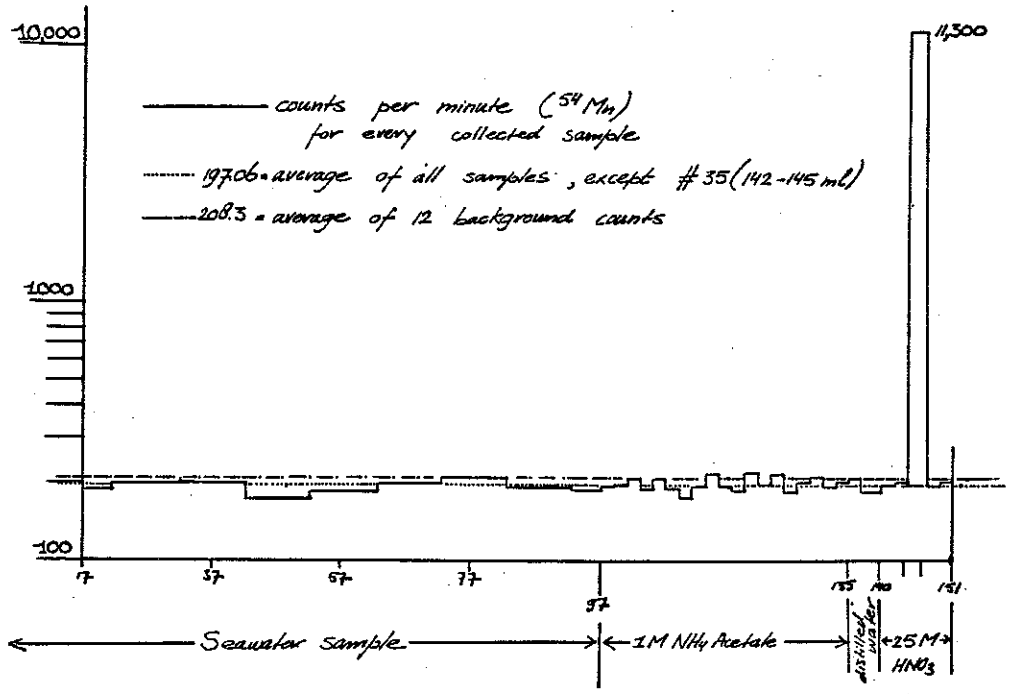


Figure 2.6.3. CHELEX-100 chromatography of 20 nanoCurie $^{54}Mn$ radiotracer in 100ml seawater (pH=5.04) with 40ml buffer wash (pH=5.0). Logarithmic vertical axis, typical background 208 ($\pm$ 12) cpm. All (97 $\pm$ 5 %) $^{54}Mn$ is recovered in the 2.5N nitric acid eluate.

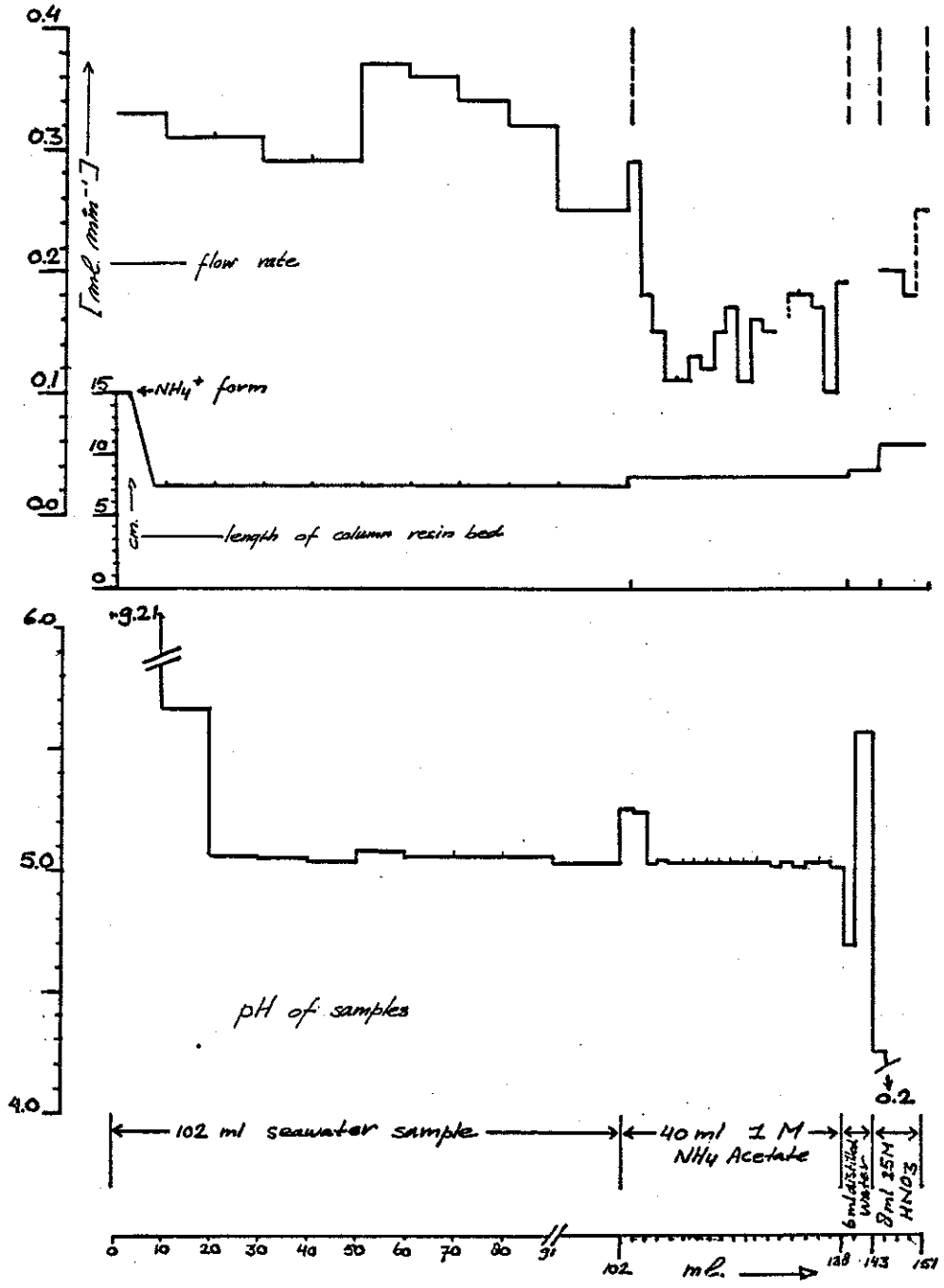


Figure 2.6.4. Gravity flow rates and resin bed contraction (above) and effluent pH (below) of the $^{54}Mn$ radiotracer experiment with a 7x70mm CHELEX-100 (200-400) resin bed.

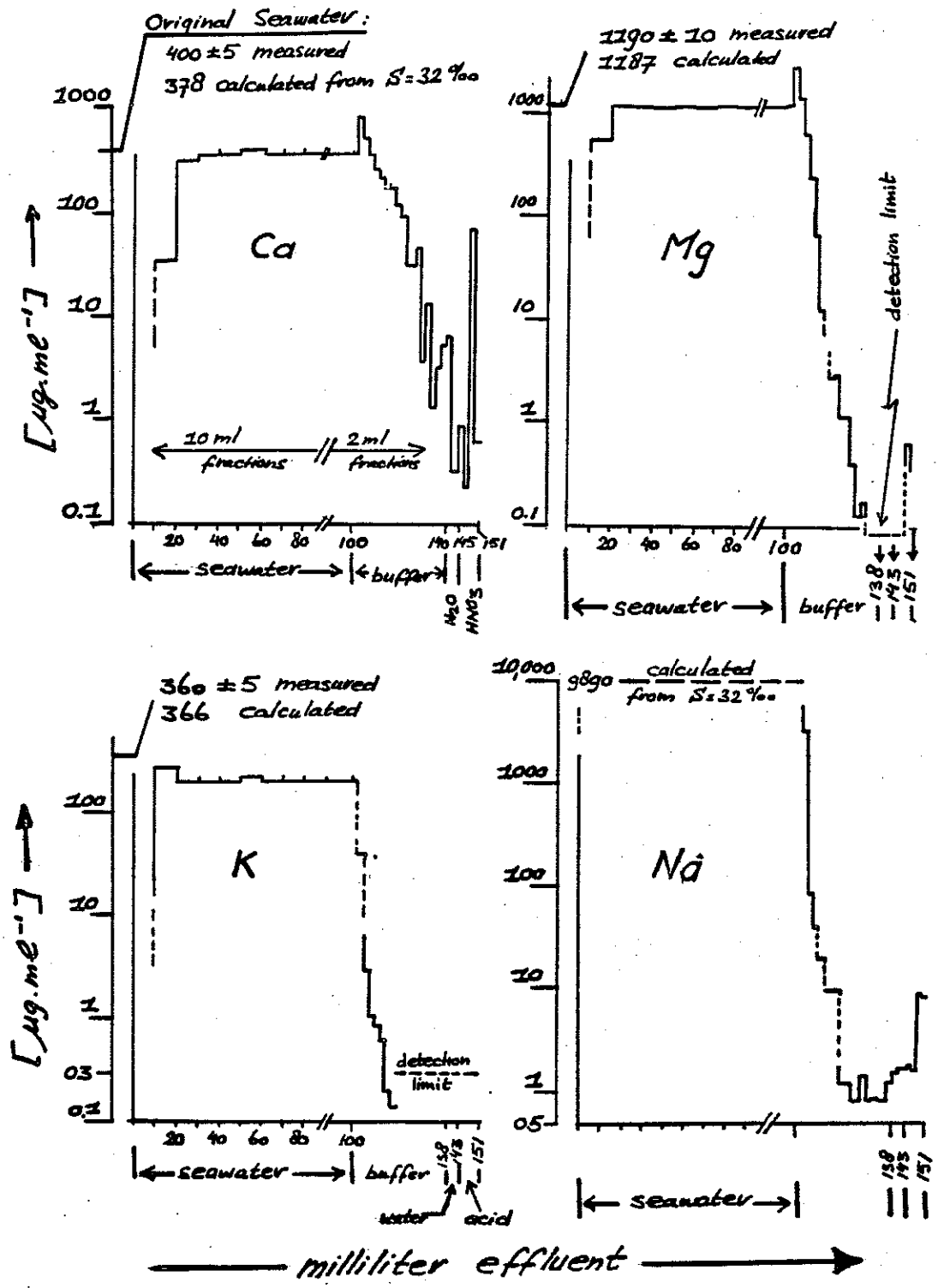


Figure 2.6.5 CHELEX-100 chromatography of Na, K, Mg and Ca along with the $^{54}Mn$ radiotracer experiment. Note dropoff during washing stages and distinct peak for all elements in nitric acid fraction.

One $^{54}Mn$ chromatogram resulting from a duplicate experiment is depicted in Figure 2.6.3. After background correction the net peak area of the nitric acid eluate corresponds to 97 $\pm$ 5 % of the original amount of tracer added. More importantly no $^{54}Mn$ activity is observed in the seawater effluent or washes. The detection limit defined as twice the standard deviation of the background is about 30 cpm or 0.3 % of the total amount of tracer. Flow rates vary between 0.3 and 1.3 $ml.cm^{-2}.min^{-1}$. After initial high values due to ammonia released from the resin bed, the effluent pH remains remarkably constant until the final elution step with nitric acid (Figure 2.6.4.). The corresponding chromatograms for Na, K, Mg and Ca show no concentration change for the seawater fraction, a dramatic dropoff during the washing stages, yet a distinct peak in the nitric acid eluate (Figure 2.6.5). The latter is especially significant for Ca, which is known to have the higher affinity for CHELEX-100 (Table 2.6.1). However the total amount of Ca is still reduced two orders of magnitude (Table 2.6.3). The other major ions are reduced even further to four and five orders of magnitude below the contents of the original 100ml seawater.

The experiments were repeated in duplicate at pH=5.2 and pH=5.4 (Figure 2.6.6.). After background correction the net peak area's of the $^{54}Mn$ tracer correspond to a yield of 99.6 $\pm$ 5 % and 99.7 $\pm$ 5 % at pH=5.2 respectively pH=5.4. No radiotracer was found in the other effluents, with detection limits again at about 0.3 percent. Acidity remains constant all along the procedure, with slight but distinct increases at the beginning of the buffer wash (proton exchange with K, Na, Ca, Mg) and during the Pyrex water washing (Figure 2.6.7). This time only the final washes and the nitric acid fractions were monitored just for Mg and Ca (Figure 2.6.8). The Mg levels are consistently very low, at about 1 $microgr.ml^{-1}$, in the nitric acid fraction. The Ca exhibits considerable variation between 1 and 15 $microgr.ml^{-1}$ for the peak concentrations of the nitric acid eluate, but the values are always below those of the earlier experiment (Figure 2.6.5, Table 2.6.3).

Finally the method was employed for determination of Mn in a suite of unfiltered seawater samples collected in the Panama Basin. Special Pyrex glass column supports (Figure 2.6.9) were manafactured in order to

avoid contamination. The 100ml. water samples had been acidified to pH=2 and were neutralized with 0.5ml 2N $NH_4OH$ and buffered with 0.5ml 8N buffer. The pH of effluent seawater was found to be between 5.6 and 6.0 for the various samples. The columns were washed with 3 x 10ml 1N buffer (pH=5.2) and 2 x 5ml. Pyrex water. Then the metal fraction was eluted with 4 x 5ml. 3N $HNO_3$ and collected into a 30ml capacity Teflon PFA vial with conical bottom (SAVILLEX 0201C). After evaporation under UV light inside the laminar flow bench the samples were taken up in 1.0ml 0.1N $HNO_3$, generally considered an ideal matrix for GFAAS analyses. The Mn concentrations in this final analyte were determined with a Perkin-Elmer 4000 Graphite Furnace Atomic Absorption Spectrophotometer. Despite less than ideal sampling conditions (steel hydrowire, ordinary NISKIN bottles) the resulting profile (Figure 2.6.10) looks promising. Concentration values are comparable to those reported recently for filtered seawater collected at a nearby station (MARTIN & KNAUER, 1983). One radiotracer spiked sample run along the procedure again showed no losses of $^{54}Mn$ in the various effluents and a 100 $\pm$ 5 % overall yield.

Provided that clean techniques for sampling (BRULAND et al.,1979; BOYLE, in press), shipboard filtration (section 2.2) and laboratory extraction are used, the modified CHELEX-100 method (KINGSTON et al., 1978) is very promising indeed for accurate determination of Mn (Co, Ni, Cu, Zn, Cd, etc.?) in open ocean waters.

Distributions of REE between CHELEX-100 and seawater.

The distribution coefficient of a radiotracer between the CHELEX-100 resin and seawater solution is described by

$$D = \frac{\text{Activity [cpm] / gram resin}}{\text{Activity [cpm] / ml. solution}} \qquad (2.6.2)$$

Assuming complete equilibration, a value for D determined in radiotracer experiments also applies for (pico)molar ratios of the corresponding element. Procedures were as follows:

| | Total Amounts in Microgram | | Percentage of original | Concen-tration | Matching matrix |
|---|---|---|---|---|---|
| | 100ml seawater S=32 o/oo | 2.5N HNO3 fraction | seawater in final 2.5N | in 1 ml analyte [ug/ml] | (BRULAND et al.,1979) [ug/ml] |
| Na | 989,000 | 40 | 0.004 | 40 | 150 |
| K | 36,600 | less than 3 | 0.008 | 3 | 20 |
| Mg | 118,700 | 1.3 | 0.001 | 1.3 | 1700 |
| Ca | 37,800 | 160 | 0.4 | 160 | 1800 |

Table 2.6.3. The amount of major cations in original seawater and the final 2.5N $HNO_3$ fraction for trace metal analysis. The major cations are reduced 2 to 5 orders of magnitude. A final GFAAS analyte taken up in e.g. 0.1N $HNO_3$ (after evaporation of the 2.5N $HNO_3$) would contain considerably less of the cation matrix than reported earlier (BRULAND et al., 1979).

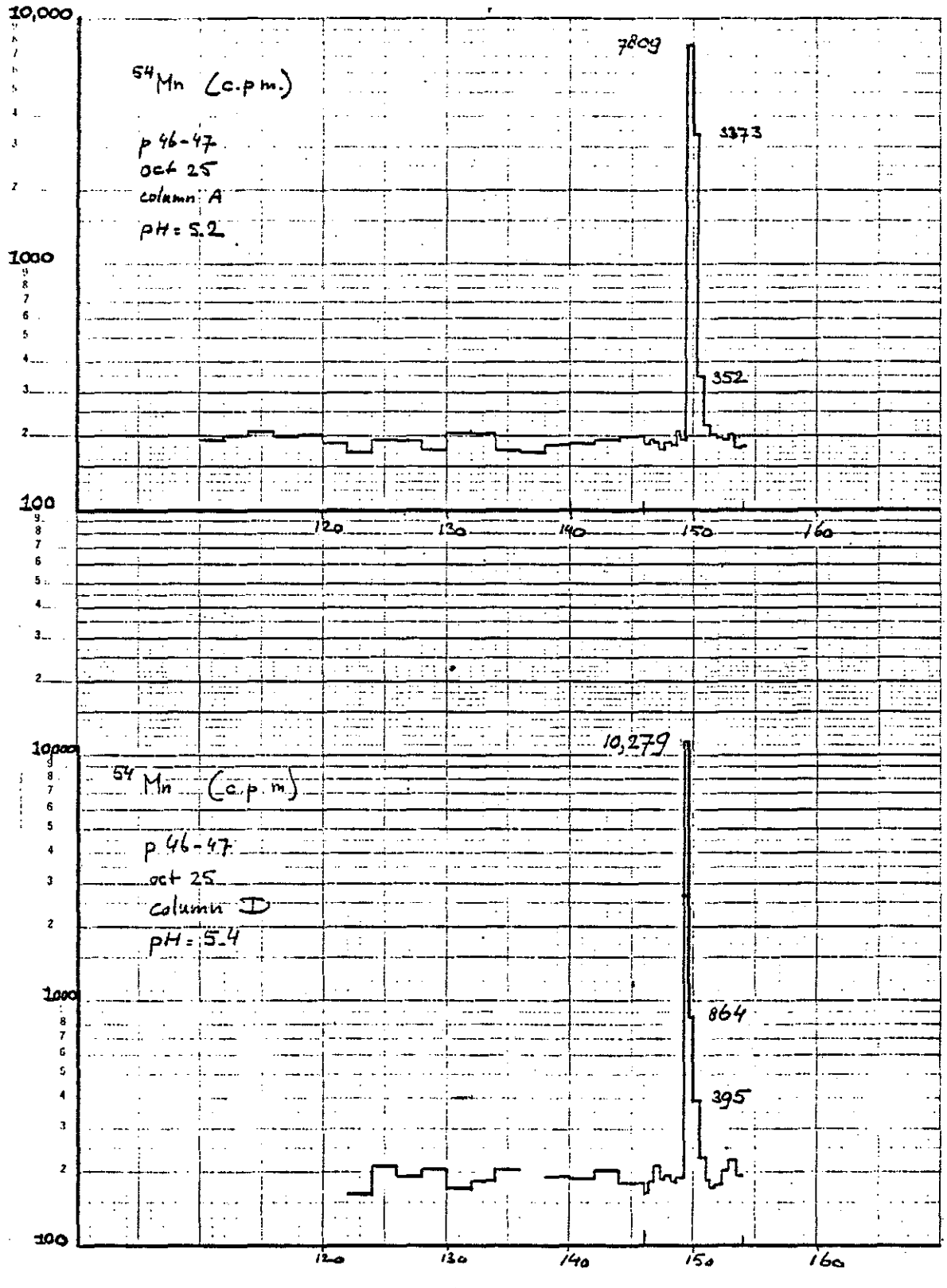


Figure 2.6.6. CHELEX-100 chromatography of $^{54}$Mn radiotracer in 100ml seawater at pH=5.2 (above) and pH=5.4 (below).

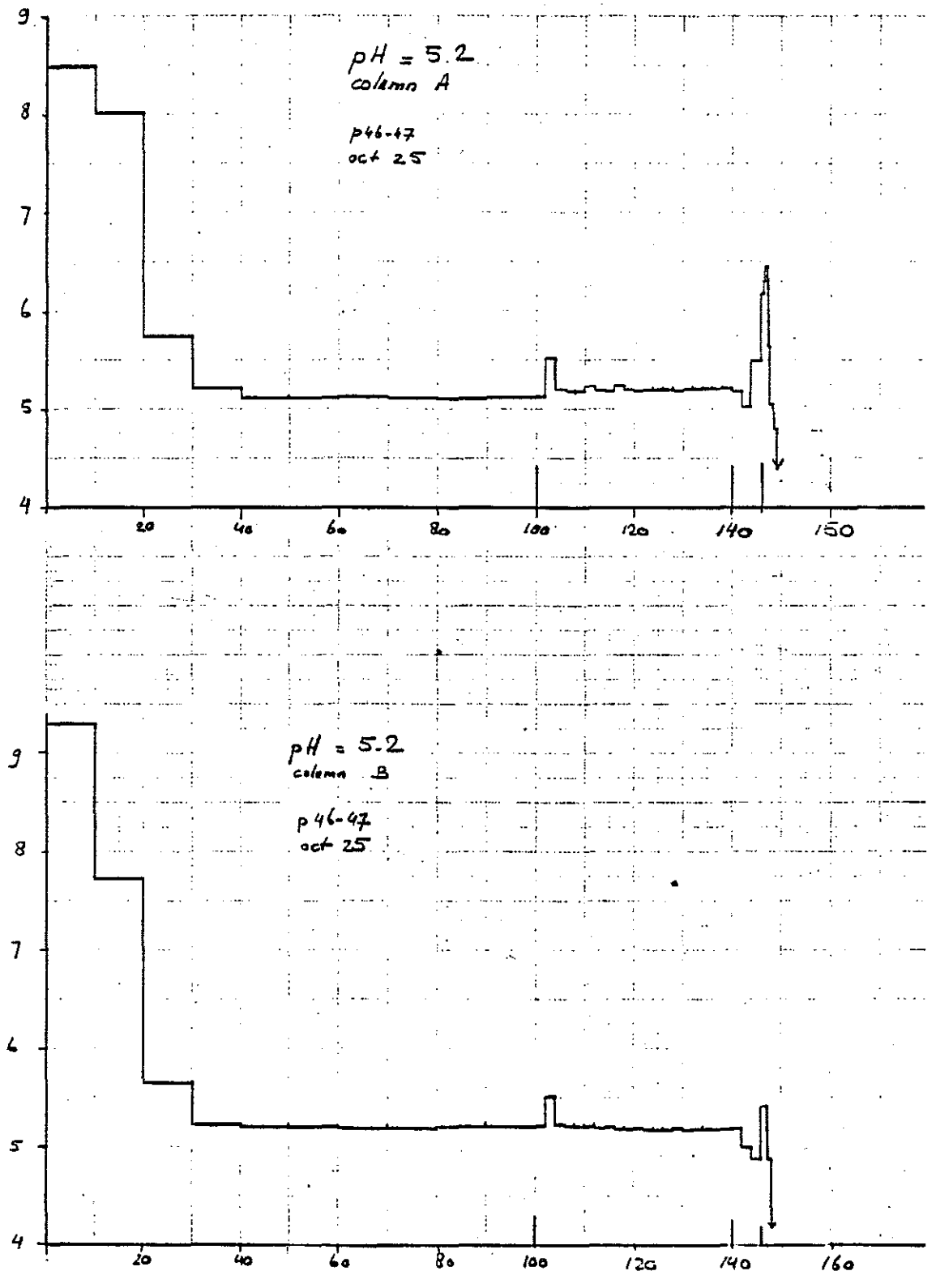


Figure 2.6.7. Effluent pH of $^{54}Mn$ radiotracer experiments at pH=5.2 and pH=5.4.

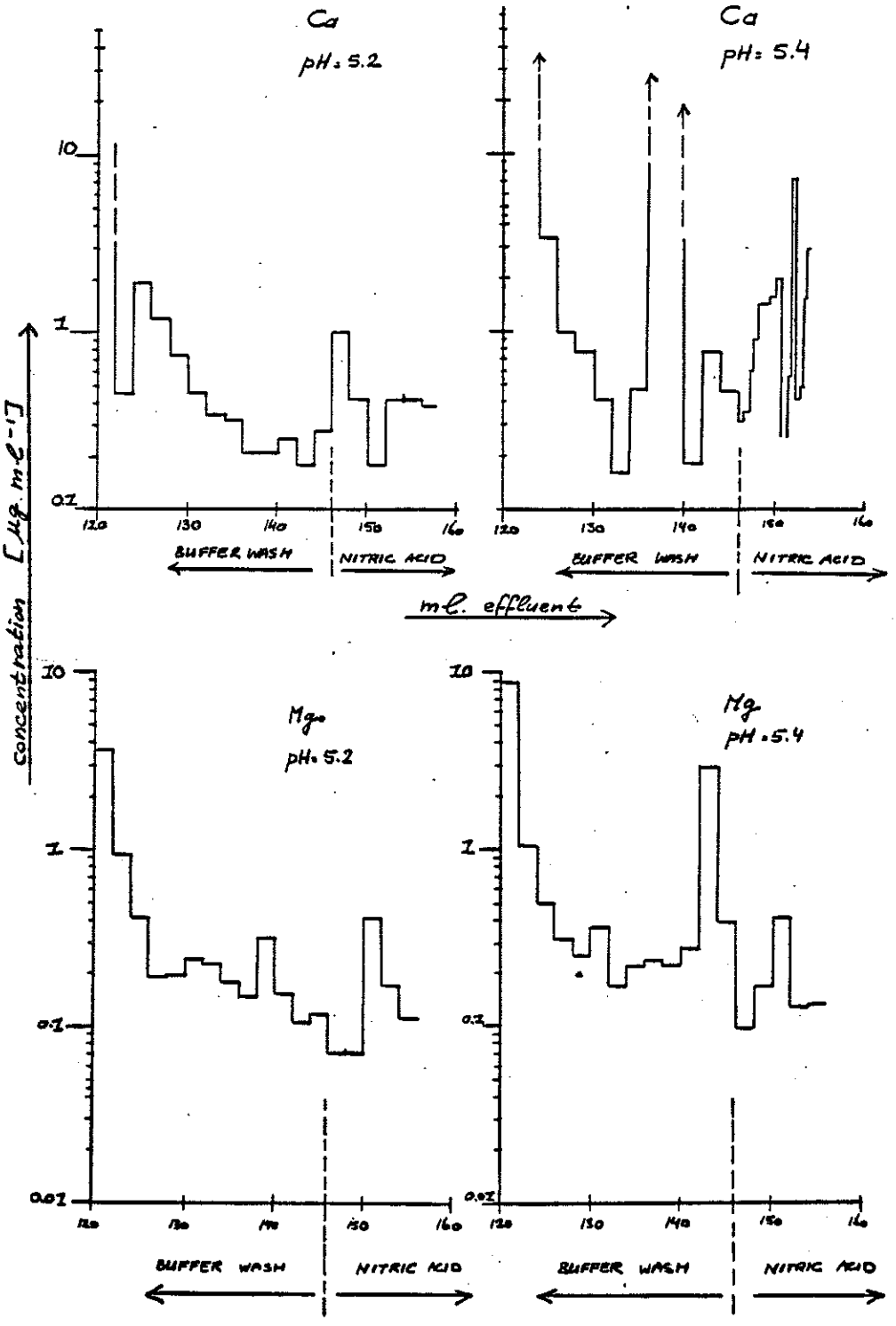


Figure 2.6.8. Concentrations of Ca and Mg in final washings and nitric acid eluate of duplicate CHELEX-100 chromatography experiments at pH=5.2 and pH=5.4

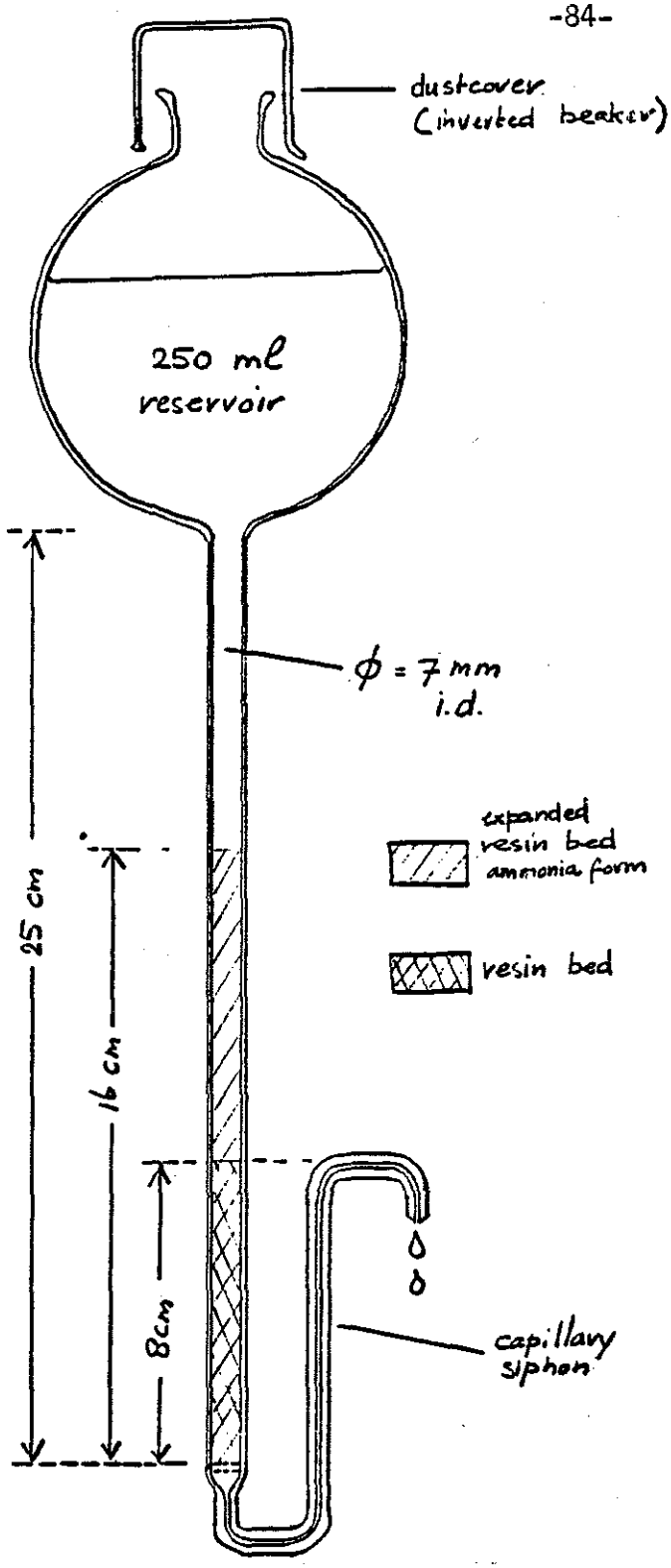


Figure 2.6.9. All Pyrex chromatography column and reservoir (modified after MOORE, 1977). Siphon prevents the resin bed from running dry, while small dead volume of its capillary tubing does not affect peak width of elution bands. Total column length of 25cm provides room for resin bed expansion as well as hydrostatic head for higher flow rates.

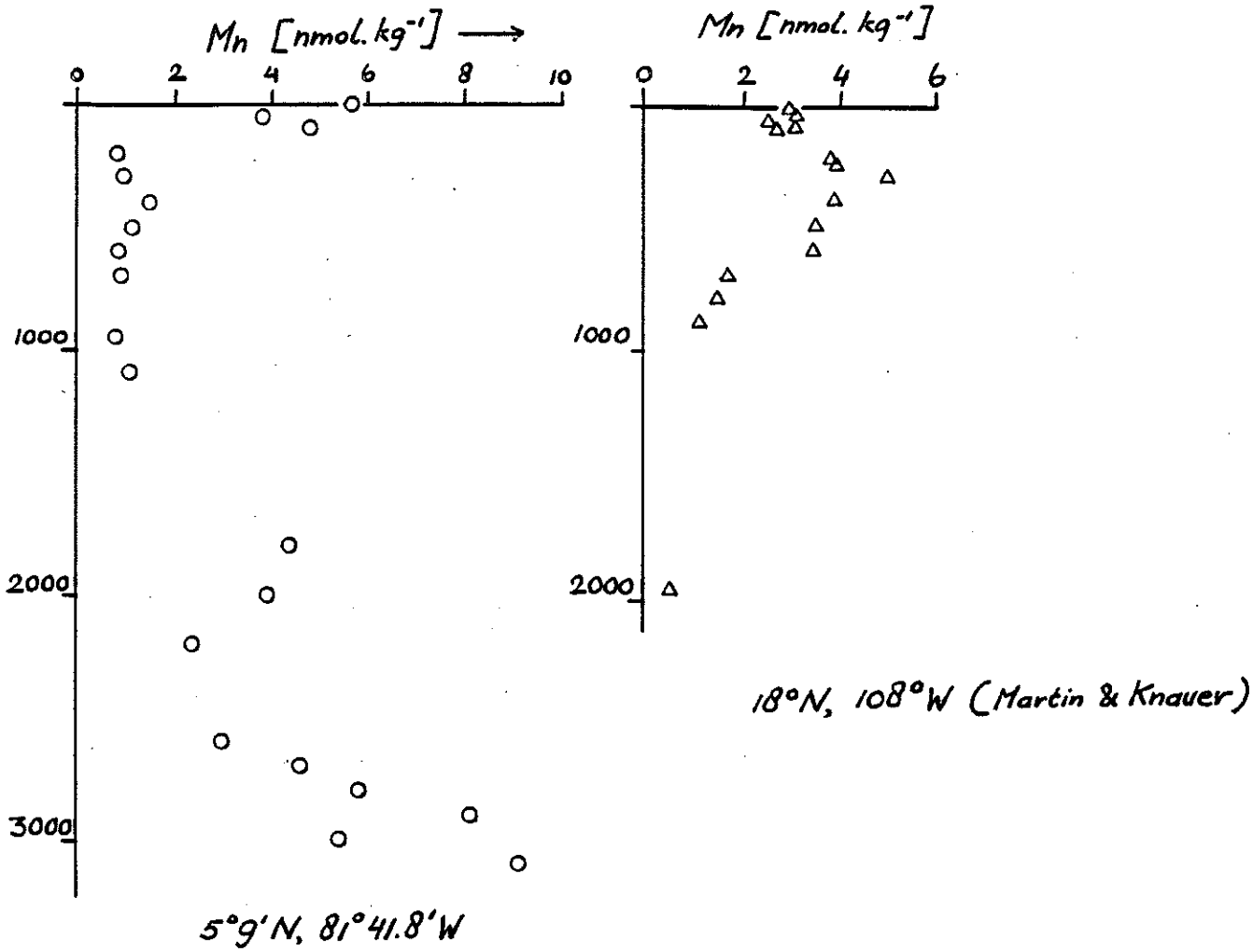


Figure 2.6.10. Vertical profile of manganese in the Panama Basin ($5^{o}9.0'N$, $81^{o}41.8'W$)(KNORR 73-16, station 1110). Recent data for filtered seawater collected at $18^{o}N$, $108^{o}W$ during VERTEX II expedition is shown for comparison (Taken from MARTIN & KNAUER, in press).

Pyrex glass test tubes with Teflon PTFE lined screwcaps had been hot acid cleaned, rinsed and dried. The vials were weighed before and after addition of 400mg. dry CHELEX-100 (200-400) resin. Two 200ml batches of acidified seawater (S=32 o/oo, pH=2) were spiked, one with $^{144}Ce$ and one with $^{153}Gd$ radiotracer, and were allowed to equilibrate. Then the seawater was neutralized with $NH_4OH$, and 10 ml aliquots were pipetted into the test tubes. Finally 0.500 ml aliquots of different 8N buffer solutions were added to the test tubes. The range of pH values ( 6.2 to 9.3 ) of the 8N buffers led to a corresponding range (4.8 to 7.8) in the seawater/resin mix.

The mixture was allowed to equilibrate on a shaker table at 25°C for 72 hours (HEITNER-WIRGIN & MARKOVITS,1963; LEYDEN & UNDERWOOD, 1964). After centrifugation 2ml subsamples of the supernate were transferred into new test tubes. The remaining supernate was carefully sucked out and discarded after pH determination. The volume of the resin fraction was adjusted to 2.0ml with 6N HCl. Activities of both fractions were counted with the NaI detector set at a 1200V plateau (Figure 2.6.11). The activity of $^{144}Ce$ and $^{153}Gd$ in the seawater fraction clearly dropped off with increasing pH until at about pH=5.7 background levels were reached (Figure 2.6.12). The large uncertainty in the less than 4 % activity found in the seawater fraction led to very erratic, albeit high (greater than 1000) values for the distribution coefficient.

The experiment was repeated with smaller 10-20mg amounts of resin and higher radiotracer doses in order to arrive at better overall precision. The resulting distribution coefficients for $^{153}Gd$ now exhibit a fairly smooth pattern with maximum values of about $10^5$ around pH=6 (Figure 2.6.13). Corresponding results for $^{144}Ce$, although more noisy, exhibit a similar trend with distribution coefficients around $10^4$, somewhat lower than for $^{153}Gd$ as expected from the formation constants (Table 2.6.2). The latter analogy of CHELEX-100 with free iminodiacetic acid or its derivatives (Table 2.6.2), combined with the proportionality of D and the product $K_1K_2$, would predict values for La which are fourfold lower (i.e. $D_{La}=2x10^3$) than those of Ce. Values for Lu would be twentyfold higher (i.e. $D_{Lu}=2x10^6$) than those of Gd. Parallel experiments without tracer spikes served for a study of the behaviour of the major ions. Under the given conditions only Ca exhibited

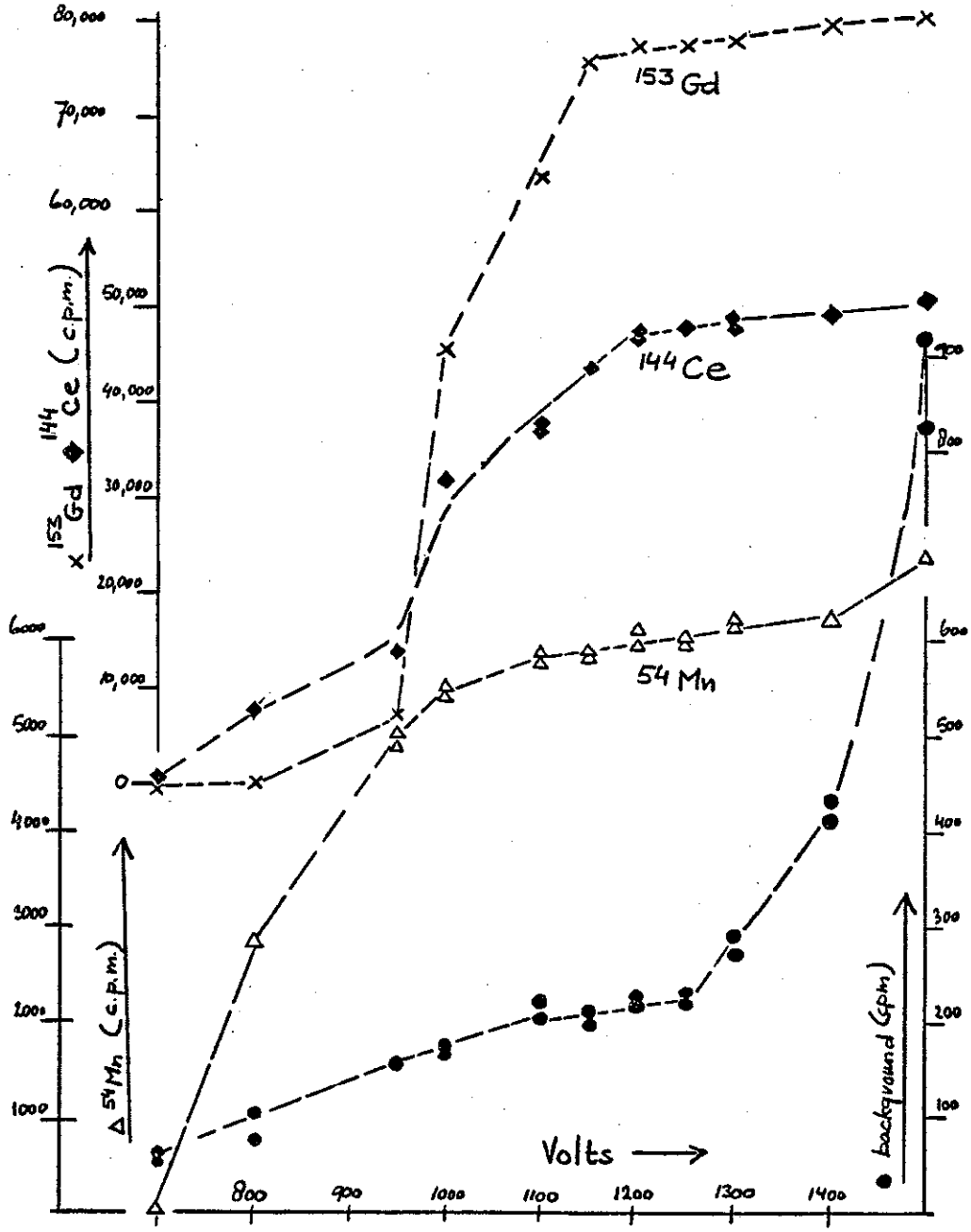


Figure 2.6.11. Response of the NaI detector system as a function of voltage. Gamma counts for $^{54}Mn$ and $^{144}Ce$, $^{153}Gd$ were routinely done at 1100V respectively 1200V.

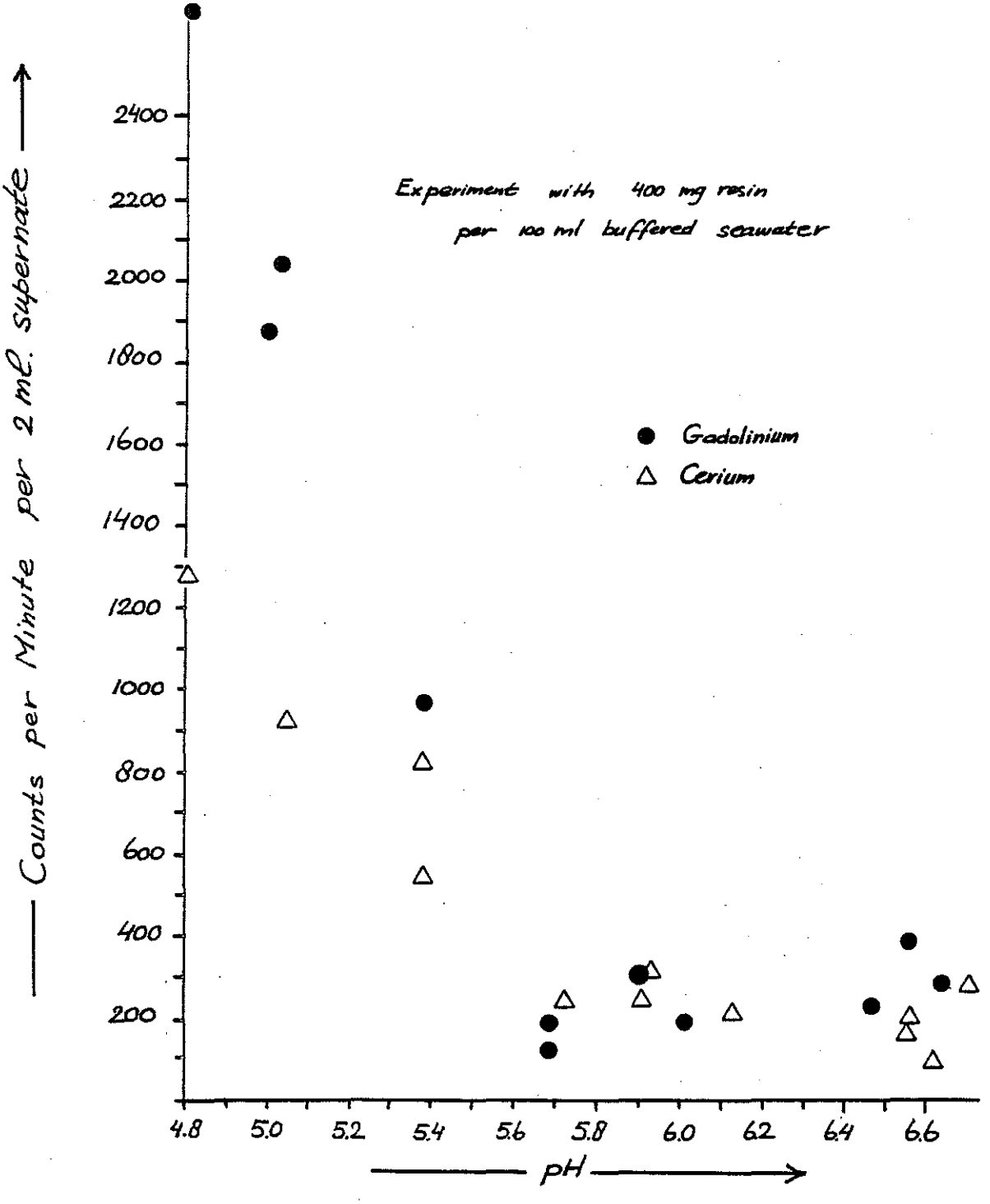


Figure 2.6.12. Activities (cpm) of $^{144}Ce$ and $^{153}Gd$ in 2.0 ml of seawater supernate after 72 hours equilibration with CHELEX-100 at various pH. Note dropoff with increasing pH to background levels at about pH=7

a detectable change in its seawater concentration (Figure 2.6.12), in agreement with the observed (Table 2.6.3.) and predicted (Table 2.6.1) stronger chelation of Ca relative to Mg, Na and K.

Although a more thorough study including other REE would be of interest, the results so far, showing

1) high values of D at pH values over 5; and
2) optimum pH=6 for 100 % yield and separation from Ca, Mg

are sufficient for our immediate needs.

Chromatography with REE radiotracers

Initial experiments were similar to those described above for manganese, except for the use of radiotracers $^{144}Ce$ and $^{153}Gd$ rather than $^{54}Mn$. The resulting chromatograms (Figure 2.6.14) demonstrate that both tracers are retained by the columns until final elution with nitric acid. After background correction the integrated net peak areas correspond to essentially complete recoveries of 97 $\pm$ 5 % and 93 $\pm$ 5 % for $^{144}Ce$ respectively $^{153}Gd$.
The next gravity flow experiments were done at about pH=6, with larger diameter (15mm) resin columns and 6-10 ltr. seawater. The seawater was added in 2000ml batches, and only the first batch had been spiked with tracers, such as to create unfavourable conditions for complete retention. In a duplicate set of experiments (6 ltr.) two separate spikes were used for two different columns. In the other experiment (10 ltr.) a mixed $^{144}Ce/^{153}Gd$ spike was added to the first 2000ml batch seawater. In all cases the overall yield proved to be very good (Table 2.6.4).

Operations so far were at very low gravity flow rates in the 0.3 to 1.6 $ml.cm.^{-2}min.^{-1}$ range. For a 15mm diameter resin bed this corresponds to 0.5 to 2.8 $ml.min.^{-1}$ or 750-4000 $ml.day^{-1}$, i.e. extraction of 10 ltr. seawater would take several days. Enhanced flow rates of about 14 $ml.cm^{-2}.min.^{-1}$ (1500 $ml.hour^{-1}$) are now routinely achieved by peristaltic pumping from the bottom of the column (Figure 2.6.15). Under these conditions considerable pressure gradients build up along the resin bed, and the limiting factor with respect to even higher

| Column dimensions [mm] | Flow Rate [ml.cm$^{-2}$ min$^{-1}$] | Seawater volume [ml] | pH | Buffer-Wash volume [ml] | pH | Radiotracer Yield $^{144}$Ce [%] | $^{153}$Gd [%] |
|---|---|---|---|---|---|---|---|
| 7x70 | 0.9 | 100 | 5.5 | 40 | 5.4 | 97±5 | 93±5 |
| 14x70 | 0.8 - 1.6 | 3x2000 | 5.9 | 140 | 5.8 | 99±5 | 99±5 |
| 14x70 | 0.8 - 1.6 | 5x2000 | 6.0 | 200 | 5.4 | Combined tracer 108±5 | |

| Enhanced flow rate experiment: | | | | | | Tracer | keV | yield |
|---|---|---|---|---|---|---|---|---|
| 14x80 | 14 | 15,000 | 6.0 | 200 | 5.4 | 153Gd | 97 | 102 ±5 |
| | | | | | | 153Gd | 103 | 100.2±5 |
| | | | | | | 152Eu | 122 | 109 ±5 |
| | | | | | | 144Ce | 134 | 106 ±5 |
| | | | | | | 152Eu | 245 | 99.8±5 |
| | | | | | | 152Eu | 344 | 103 ±5 |

Table 2.6.4. Conditions and yields of REE radiotracers experiments for CHELEX-100 chromatography. In the second and third experiments the tracers were added only to the first 2000ml seawater. A tracer mixture was used in the third and fourth experiment. For the latter, yields of individual tracers were determined with the Ge(Li)detector system. The NaI detector was used for the first three experiments.

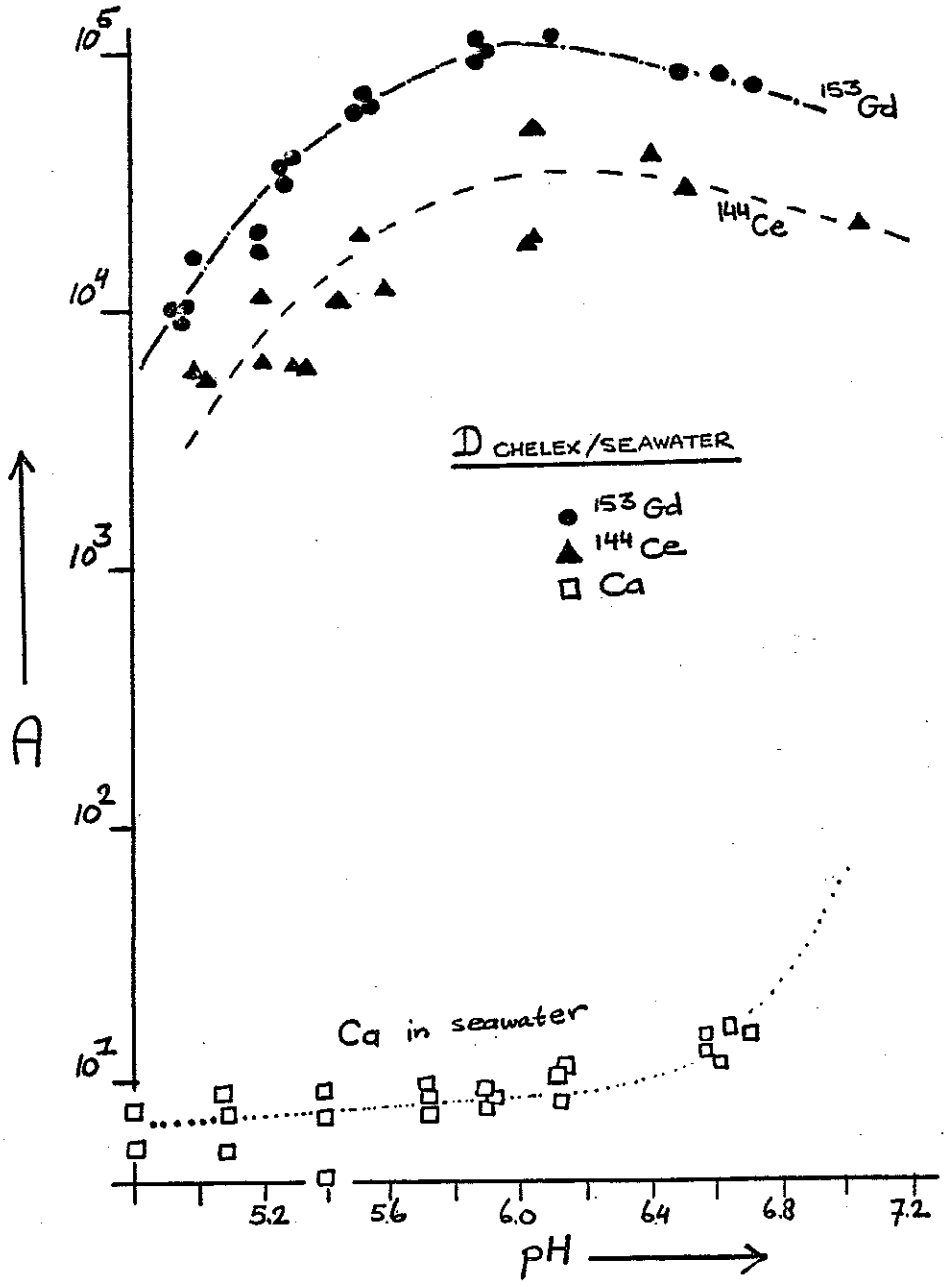


Figure 2.6.13. Distribution coefficients D between CHELEX-100 and seawater at various pH for $^{144}Ce$, $^{153}Gd$ and Ca. At about pH=6 the separation coefficient $D_{Gd}/D_{Ca}$ is optimal.

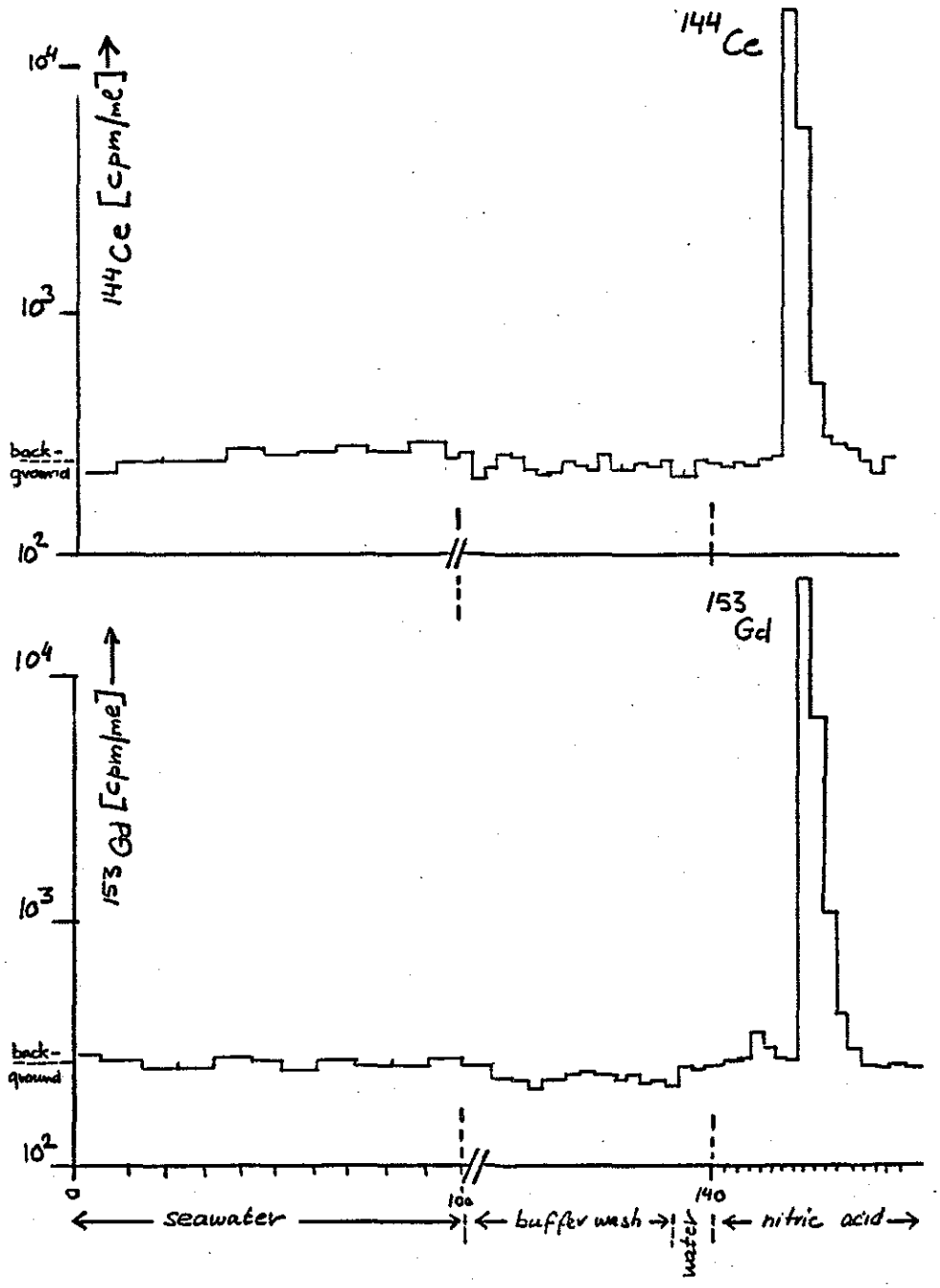


Figure 2.6.14. CHELEX-100 chromatography of $^{144}Ce$ and $^{153}Gd$ in 100ml seawater (pH=5.5) with 40ml buffer wash (pH=5.4).

flow rates appears to be leakage of air bubbles at the connection between the column outlet and the silicone rubber tubing of the peristaltic pump.

Extraction efficiency of REE was tested by an experiment with two resin columns hooked up in series. The first column (15x80mm) was intended to retain quantitatively a $^{144}Ce/^{152}Eu/^{153}Gd$ tracer mixture. The second column (15x100mm) would certainly retain most, if not all, of any radiotracer amount which inadvertently would have passed through the first column. The seawater (pH=2) was spiked with 2.0ml tracer mix and allowed to equilibrate for 24 hours. Two other 2.0ml aliquots were pipetted, one into a Teflon PFA vial and one into a test tube for use as standards. After neutralization with $NH_4OH$, the pH of the seawater was adjusted to 6.0 and the array of two columns was hooked up to the reservoir. During an initial 90 minute period a few hundred ml. water passed by gravity flow, to allow the resin beds to shrink from the ammonia-form (16-20cm length) to the 'normal' 8-10cm length. Then the pumps were started, and ten hours later all seawater had passed through. The reservoir was rinsed with 200ml. 1N buffer wash, which was then pumped through the resin beds. After a 60ml water wash the resin columns were detached and each of them eluted with ample 3N $HNO_3$ into Teflon PFA vials. The original reservoir was rinsed with 200ml and then with 400ml 4N HCl. All washes and rinses were evaporated down to a small volume and transferred into counting vials. The nitric acid eluates as well as one tracer mix standard (in PFA vial) were each spiked with a $^{54}Mn$ internal standard, evaporated to dryness and taken up in 2.0ml nitric acid. The results of 60,000 second counts with the Ge(Li) detector suggest a complete retention by the first resin column of each individual radioisotope (Table 2.6.5). In similar spectra of the nitric acid eluate of the second column, as well as from the various washes and rinses, no gamma peaks of $^{144}Ce$, $^{152}Eu$ or $^{153}Gd$ were observed. The latter fractions (and the other standard) had previously been counted with the more efficient NaI detector and no activity had been observed, with the detection limit at about 0.1 % of the total mixture of radiotracers.

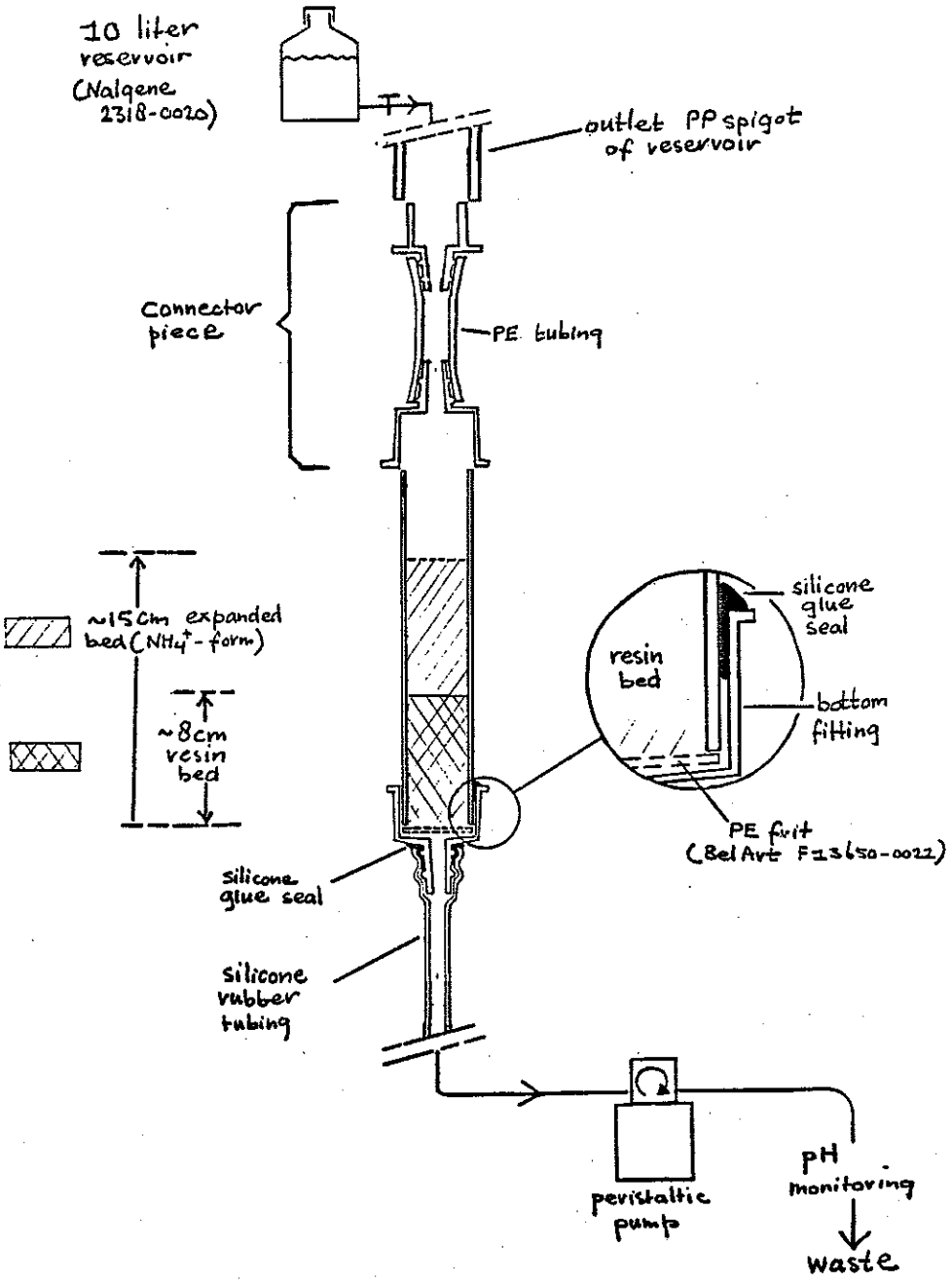


Figure 2.6.15. Set up as used routinely for CHELEX-100 extraction of REE from 10 liter seawater samples with flow rates enhanced by peristaltic pump.

Uranium extraction

The behaviour of U on the CHELEX-100 resin columns under the conditions described above is important with respect to U interferences in the final determinations (see section 2.3). The affinity of CHELEX-100 for U in seawater is strongly pH-dependent (Figure 2.6.16). On the one hand complete retention of U has been reported for acidified seawater with pH-values in the 3-5 range (MIYAKE et al., 1966; HIROSE & ISHII, 1978). On the other hand RILEY & TAYLOR (1968) report no retention at all for seawater at pH=7.6 . The reason for this pH-functionality is the stabilization of U in solution by formation of a carbonate complex:

$$UO_2^{2+} + 3\ CO_3^{2-} = UO_2[CO_3]_3^{4-} \qquad (2.6.3)$$

where

$$K = \frac{\left[UO_2^{2+}\right]\left[CO_3^{2-}\right]^3}{\left[UO_2\ (CO_3^{2-})_3^{4-}\right]} = 10^{-24} \qquad \text{(GARRELS \& CHRIST,1965)} \quad (2.6.4)$$

From a description of the carbonate system in seawater (BROECKER & PENG,1982; their Table 3-7) we derive:

$$\frac{\alpha\, K_1' . K_2' . pCO_2}{\left[a_{H^+}\right]^2} = [CO_3^{2-}] \qquad (2.6.5)$$

where

$\alpha$ = 2.84 x $10^{-2}$ (moles.kg$^{-1}$.atm$^{-1}$) at 25°C and 1 atm.
$K_1'$ = 10.00 x $10^{-7}$ at 25°C and 1 atm.
$K_2'$ = 7.69 x $10^{-10}$ at 25°C and 1 atm.
$pCO_2$ = 320 x $10^{-6}$ atm.

leads to

$$\log[CO_3^{2-}] = 2pH + \log(\alpha . K'_1 . K'_2 . pCO_2) = 2pH - 20.156 \qquad (2.6.6)$$

In other words, for a one unit drop in pH the carbonate concentration drops two orders of magnitude. Combination with equation (2.6.4) for uranylcarbonate formation demonstrates that for every unit drop in pH the

U-complexation would drop six orders of magnitude. In natural seawater (pH=8.2) or at slightly lower pH=7.6 (RILEY & TAYLOR, 1968) all U is stabilized as an anion which would not readily interact with the carboxylic groups of the resin (Table 2.6.5). On the other hand at or below pH=5 all U is in the free cationic $UO_2^{2+}$-form which has a high affinity for CHELEX-100 (Table 2.6.1). The break-even point is at pH=6.1, exactly the working range for our REE extraction. The latter implies that under our working conditions (pH=6.0±0.2) the overall U yield may vary dramatically depending on slight changes in pH, volumes and flow rates of various solutions, kinetics, etc.

In the above a perfect equilibration with atmospheric $pCO_2$ was assumed. This is probably correct for the acidified seawater which had been stored several months at pH=2 and then would be virtually depleted with respect to its total $CO_2$ content. The stirring during neutralization and buffering would help replenishing some total $CO_2$. However an equilibrium with the atmosphere is almost certainly not achieved. In other terms, above estimates of $CO_3^{2-}$-concentration are upper limits. For a given pH the concentration of free $UO_2^{2+}$ would shift to higher values than under above assumed equilibrium with the atmosphere.

The actual yield of U extraction was determined in conjunction with above REE radiotracer experiments. The nitric acid eluate from the CHELEX-100 column was spiked with a known amount of $^{236}U$ internal standard, upon which the U fraction was separated from the REE fraction by anion exchange chromatography (section 2.8). After elution of the AG1X8 columns, the U was electroplated on a silver disc and its activity determined by alpha spectrometry (ANDERSON & FLEER, 1982). Resulting $^{238}U/^{236}U$ activity ratios led to yield estimates varying anywhere in between 30 and 90 percent for the CHELEX extraction of U (2.5 $dpm.kg^{-1}$ $^{238}U$ = 14 $nmol.kg^{-1}$ at S=35 o/oo) from seawater.

For our purposes it is simply assumed that most, if not all, U is retained by the CHELEX resin. Complete U removal has to be achieved in subsequent chromatography separations (sections 2.7, 2.8). Alternatively one might conceive of a scheme where U is washed off the CHELEX resin with alkaline carbonate solutions, but no attempts have been made in this direction.

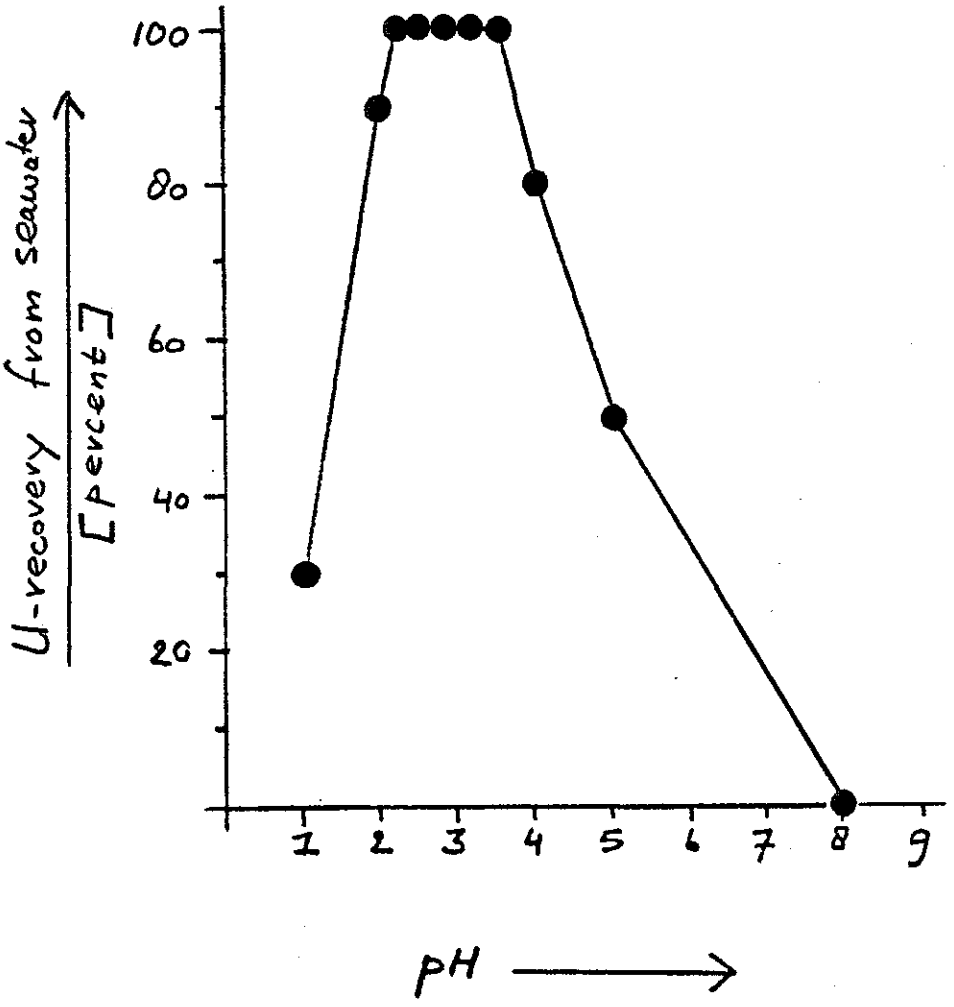


Figure 2.6.16. The pH dependence of U recovery from seawater with CHELEX-100 resin chromatography (Taken from MIYAKE, SUGIMURA & UCHIDA, 1972). Below pH=2 the iminodiacetic functional groups of the resin are fully protonated. At pH values over 5 the $UO_2^{2+}$ becomes stabilized in solution as a carbonate anion.

| pH | $[CO_3^{2-}]$ [mol/kg] | | Ratio = $\frac{[UO_2^{2+}]}{[UO_2(CO_3)_3]^{4-}}$ | |
|---|---|---|---|---|
| 8.2 | 0.175 | $10^{-3}$ | 0.2 | $10^{-12}$ |
| 7.6 | 0.011 | $10^{-3}$ | 0.8 | $10^{-9}$ |
| 7 | 0.7 | $10^{-6}$ | 2.9 | $10^{-6}$ |
| 6.08 | 1.0 | $10^{-8}$ | 1.0 | |
| 6 | 0.7 | $10^{-8}$ | 3 | |
| 5 | 0.7 | $10^{-10}$ | 3 | $10^{6}$ |

Table 2.6.5. The carbonate ion concentration and U-speciation ratio predicted as a function of pH in seawater (T=25°C; 1 atm) in equilibrium with the atmosphere ($pCO_2$=320x$10^{-6}$atm). For every unit drop in pH the U-species ratio is lowered six orders of magnitude. Numerical values may be shifted somewhat due to various effects of additional reagents (HCl, $NH_4OH$, 8N buffer). Further shifts would occur upon equilibration with the CHELEX-100 resin. Actual equilibration with atmospheric $CO_2$ is also rather unlikely, see text.

Final Procedure

Hot acid cleaned PE reservoirs (10 liter) with PP spigots (Nalgene 2318-0020) were rinsed with Pyrex water and weighed on a 20kg capacity triple beam balance (Ohaus 1119D) which had been calibrated ($\pm$ 1 gram) versus NBS Class S weights. Inside the laminar flow bench the seawater samples (pH=2) were carefully poured from their storage containers into this reservoir. An initial few hundred milliliters was used to rinse possible contaminants off the neck of the storage container, and was discarded. After recording the gross weights a suite of 10 reservoirs (9 samples and 1 overall blank) were spiked with 0.500ml (about 200cpm at 134keV on the 18% efficiency Ge(Li) detector) $^{144}Ce$ internal standard each, and allowed to equilibrate for at least 48 hours.

About 200 gram dry CHELEX-100 resin (200-400 mesh, Biorad 142-2842) was transferred into a clean 125ml PE bottle and soaked in about 100ml 4N HCl under continuous stirring with a clean Teflon stir bar. After about 12 hours the stirring was discontinued in order to allow the resin to settle down such that the supernate could be poured off and replaced with a new aliquot of 4N HCl. This was repeated four times over a 48 hours period (prolonged storage in acid may cause detioration of the resin and should be avoided). During the same period the 20cm length, 15mm diameter PE barrels and PE end fittings (BelArt F19962), porous PE frits (35micron pores,1.6mm thick, BelArt F13650-0022), and PE dustcovers of the column supports were taken out of the 1N HCl storage solution, rinsed with Pyrex water and allowed to dry in the laminar flow bench. The columns were assembled with silicone glue in between the outside of the barrel and the inside of the bottom fitting in order to obtain an airtight seal (Figure 2.6.15). A set of ten columns with dustcovers was placed in acrylic racks and thoroughly rinsed with 0.1 N HCl. Subsequently the resin beds were washed with 4 x 10ml 4N $HNO_3$ and 3 x 5ml quartz water. Then about 2 x 5ml 2N $NH_4OH$ was passed over the columns until complete expansion of the resin bed. Excess $NH_4OH$ was washed off with about 3 x 3ml quartz water. All along the procedures PE gloves were worn. Manipulation of dustcovers etc. was done with clean Teflon FEP forceps (Cole-Parmer K-6442-00).

The next morning each seawater sample was neutralized and buffered. Hot acid cleaned 6cm length PTFE stir bars (Cole Parmer K-4770-70) were

rinsed thoroughly and dropped into the reservoir. While stirring gently the tip of a combination pH electrode was immersed just below the surface. Then the seawater was neutralized by squeezing 2N $NH_4OH$ from a Teflon FEP spray bottle into the reservoir. About 30ml 8M buffer was measured into a clean PFA vial and added to the seawater. Stirring continued for about one more minute until pH=6.0 $\pm$ 0.1 was well established. In between samples the pH electrode was rinsed extensively with 0.1 N HCl and quartz water.

Then a PE connector piece was fitted to the spigot of the reservoir and the column was attached (Figure 2.6.15). Silicone rubber pump tubing was connected to the bottom of the column with silicone glue for an airtight seal. During the first 60-120 minutes the seawater was fed through the resin bed by gravity flow in order to allow complete shrinkage to the original 8cm length of the bed. Then the peristaltic pumps (HARVARD Apparatus 1200) were started to run for about six hours with flow rates of about 1500ml per hour. At the end the reservoirs were tilted in order to recover all the seawater. Each column was disconnected and returned to the acrylic racks, complete with dustcovers. Resin beds were washed with 10 x 8ml 1N buffer, 4 x 5ml quartz water and finally eluted with 6 x 5ml 3N $HNO_3$ into clean 100ml capacity Teflon PTFE beakers (Chemplast 15001). The pH of seawater, buffer wash and water wash effluents were monitored all along the procedure. The nitric acid was allowed to evaporate overnight by leaving the beakers on a hotplate under UV light in the laminary flow hood. The resulting extract contains:

- all $^{144}Ce$ internal standard
- the dissolved REE from the original seawater
- 100 % or less, i.e. 140 nanomoles or less, of the U in the original seawater
- about 100 micromoles Na; five orders of amgnitude below the original amount
- minor amounts of Mg, Ca and K

The next morning this extract is processed further (section 2.7).

## 2.7. Cation exchange chromatography.

### Introduction

During the initial phases of this project a two step separation scheme was envisioned. CHELEX-100 separation (2.6) of the REE from major cations Na, K, Mg, Ca would be followed by the removal of U with the classical anion exchange method (2.8). However the CHELEX-100 reduces the total amount of Na only about four to five orders of magnitude (2.6), rather than the ten orders specified for avoidance of high $^{24}Na$ radioactivity (2.3). Also the large amount of 140 nanomoles U to be retained by the anion exchanger may cause overloading of latter resin column (2.8), possibly leading to incomplete U removal.

The following criteria were taken into consideration when searching for a suitable additional separation step :

- optimum separation of U, and Na (K, Mg, Ca), from the REE.
- simple, well tested reliable method
- small number of easily purified reagents.

For the latter reason the large variety of mixed solvent chromatography methods (KORKISCH, 1969) was excluded. Cation exchange chromatography with a sulfonated polystyrene resin and 1N sulphuric acid medium was selected. This is a rather simple method which offers high separation factors for REE versus U, Na (Mg)(Table 2.7.1). Lower separation factors are reported for hydrochloric or nitric acid media. The picomolar amounts of REE are easily retained by the resin bed, while unlimited quantities of U, Na can in principle be washed off the column (STRELOW, 1963). This is the opposite of anion exchange chromatography where all U is supposed to be retained by the resin while the REE fraction passes freely.
The major disadvantage of the cation exchange method is the required use of sulphuric acid, which is difficult to purify by distillation (see section 2.5).

### Procedure

The resin (BIORAD AG50WX8, 200-400 mesh) was soaked in 8N HCl under continuous stirring with a Teflon PTFE coated magnetic stirrer. Every 12 hours the supernate was poured off and replaced with a new aliquot of 8N HCl. This was repeated four times over a 48-hour interval. The 8x40mm

| Cation | D coefficients between AG50WX8 and medium | | | | | Separation factor |
|---|---|---|---|---|---|---|
| | 0.1N $H_2SO_4$ | 0.2N $H_2SO_4$ | 0.5N $H_2SO_4$ | 1.0N $H_2SO_4$ | 4.0 N HCl | $D_{Gd}$ / D in 1.0 N $H_2SO_4$ |
| $La^{3+}$ | $>10^4$ | $>10^4$ | 1860 | 329 | 10.4 | |
| $Ce^{3+}$ | $>10^4$ | $>10^4$ | 1800 | 318 | 10.5 | |
| $Sm^{3+}$ | $>10^4$ | $>10^4$ | 1460 | 269 | | |
| $Gd^{3+}$ | $>10^4$ | $>10^4$ | 1390 | 246 | | 1.00 |
| $Er^{3+}$ | $>10^4$ | $>10^4$ | 1300 | 242 | | |
| $Yb^{3+}$ | $>10^4$ | $>10^4$ | 1330 | 249 | | |
| $Y^{3+}$ | $>10^4$ | $>10^4$ | 1380 | 253 | 8.6 | |
| $Mg^{2+}$ | 1300 | 484 | 124 | 41.5 | 3.5 | 5.9 |
| $UO_2^{2+}$ | 596 | 118 | 29.2 | 9.6 | 3.3 | 25.6 |
| $Na^{+}$ | 81 | 47.7 | 20.1 | 8.9 | --- | 27.6 |

Table 2.7.1. Distribution coefficients D between AG50WX8 resin and dilute sulphuric acid medium (Taken from STRELOW et al., 1965). High separation factors $D_{Gd}/D$ versus Gd in 1.0 N $H_2SO_4$ medium would allow complete separation of Mg, U, Na from the REE. Subsequent elution of the REE fraction by 8N HCl is achieved easily, given the low D values in 4N HCl medium (Taken from STRELOW, 1960).

polypropylene columns (BIORAD 731-1550) and PE dustcovers were taken out of the 1N HCl storage solution, rinsed with Pyrex water and placed in acrylic racks. Then ten 40±5 mm length resin beds were poured and washed with 3 x 5ml 8N HCl. The resin was conditioned with 3 x 3ml 0.2N $H_2SO_4$. In the meantime the residual CHELEX-100 extract in its PTFE beaker was taken up in 3ml 0.2N $H_2SO_4$, evaporated to near dryness in order to drive off chloride and nitrate, and taken up in another 3ml. 0.2N $H_2SO_4$. The latter volume was loaded on the column. Subsequently the PTFE beakers were rinsed with 3 x 5ml 1N $H_2SO_4$, and each of these rinses was also loaded on the column after each previous volume had completely passed the bed. Subsequently the resin was washed with 7 x 7ml 1N $H_2SO_4$ in order to remove U and Na (Mg, Ca, K). The REE fraction was finally eluted with 5 x 3 ml 8N HCl into clean 50ml capacity Teflon PTFE beakers (CHEMPLAST 15001). The complete procedure took about 8 hours and was done the day directly following the CHELEX-100 extraction. The samples were then allowed to evaporate overnight in order to reduce their volume before loading onto the next (anion exchange) column (2.8).

Radiotracer experiments

An initial experiment was designed to test the separation of U, Na and Mg from a $^{153}Gd$ radiotracer. The following amounts of elements

1000 microgram (43.5 micromol) Na
1000 microgram (41.1 micromol) Mg
607 nanomol (107.8 dpm) $^{238}U$

were added to three Teflon beakers each. One beaker was also spiked with $^{153}Gd$ radiotracer. The samples were evaporated to dryness and further processed as described above, except that a total volume of only 18ml 1N $H_2SO_4$ was used. The effluents of each of the three columns were collected in 2.0 ± 0.2 ml aliquots. The $^{153}Gd$ is completely retained by the resin (Figure 2.7.1) with a 98 ± 5 % yield after background subtraction. Both Na and Mg are washed off quantitatively by the 1N $H_2SO_4$, with Mg lagging behind Na as expected from their distribution coefficients (Table 2.7.1). The integrated peak areas of 970 and 950 microgram for Na and Mg indicate quantitative recovery. With the detection limit of $5 \times 10^{-3}$ microgram.$ml^{-1}$ for Na (Figure 2.7.1) the

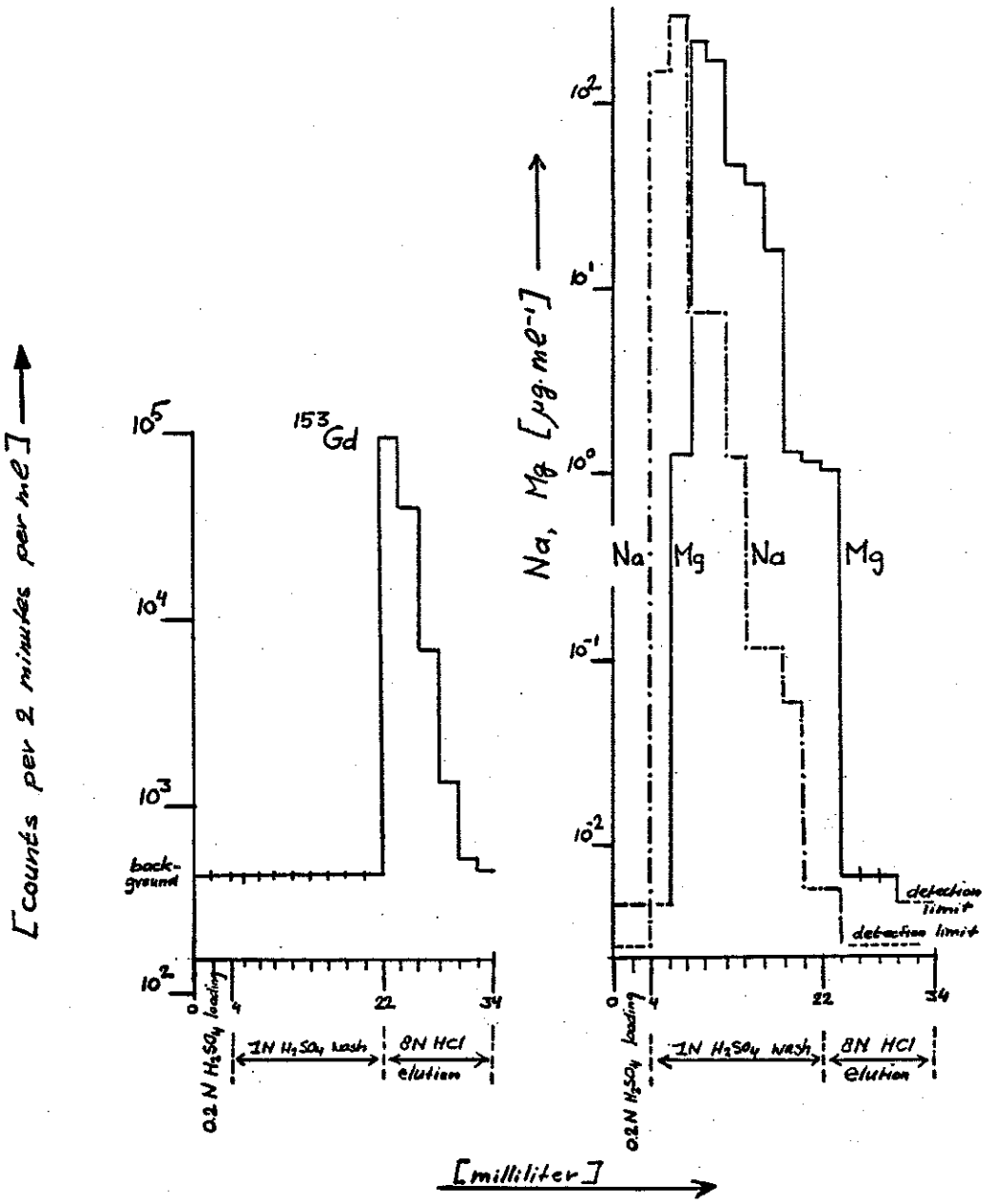


Figure 2.7.1. Quantitative AG50WX8 / H2SO4 separation of REE tracer $^{153}$Gd from the elements Na and Mg. The latter elements were employed because they are expected to elute before (Na) and after (Mg) the U peak. Moreover removal of Na is the other main objective of this separation.

total 8N HCl fraction contains less than 2 nanomoles (50 nanogram) Na, more than nine orders of magnitude below the Na contents of a ten liter seawater sample.
Determinations of U in each individual subfraction would be impractical. For our purposes the laborious alpha spectrometry method has restricted detection limits. Yet from the distribution coefficients (Table 2.7.1) one would expect to find the U peak sandwiched between those of Na and Mg. Also the U yield of the combined 1N $H_2SO_4$ effluents from one of the columns was determined at 99 $\pm$ 5 % by alpha spectrometry. These findings are in excellent agreement with the original results for separation of U from the REE as reported by STRELOW (1963).

In the actual procedure a total of 80ml 1N $H_2SO_4$ washings is used in order to achieve an even better removal of U and Na. Complete retention of the REE fraction during these extensive washings was demonstrated as follows:

Six Teflon PTFE beakers were each loaded with the same Na-Mg-U mixture as in the previous experiment. Then three sets of two beakers were each spiked in duplicate with respectively $^{144}Ce$, $^{152}Eu$ and $^{153}Gd$. The samples were further processed as in the above procedure, except that a total of 100ml 1N $H_2SO_4$ was used. Effluents were collected in 5ml ($H_2SO_4$) and 2ml (HCl) aliquots.
All along the washing stage the tracers were completely retained by the resin columns (Figure 2.7.2), with quantitative recovery after 8N HCl elution (Table 2.7.2). No measurements were made of Na, U or Mg. Yet in analogy with the previous experiment (Figure 2.7.1) these elements are expected to elute within the first 20-30ml of 1N $H_2SO_4$ effluent (Figure 2.7.2, lowermost panel).

Despite this very good Na separation the irradiated extracts still produce some $^{24}Na$ activity. It is most likely that this is caused by minor traces of Na in those reagents which are used during or after this separation step. The latter necessitates a postactivation cleanup (2.10) for which the very same AG50WX8 / $H_2SO_4$ system has been employed routinely. The resulting 1N $H_2SO_4$ effluent usually contained about 99 % of the $^{24}Na$ activity, while no gamma peaks of any of the produced REE radioisotopes were detected. On the other hand, the 8N HCl fraction

always contained all REE, including such radioisotopes as $^{140}La$, $^{141}Ce$, $^{142}Pr$, $^{153}Sm$, $^{175}Yb$, $^{177}Lu$, etcetera. In other words, during postactivation cleanup the radioisotopes of all REE were quantitatively retained by the resin bed during the $H_2SO_4$ washing stages.

Summary

The cation exchange separation of U, Na, Mg (Ca, K) from the REE, has been proven to be successful for radiotracers $^{144}Ce$, $^{152}Eu$ and $^{153}Gd$. Additional evidence from radioisotopes of all other REE is provided by the excellent results of post-activation separation.

After CHELEX-100 and cation exchange chromatography a typical extract contains:

- all $^{144}Ce$ internal standard
- all dissolved REE from the original seawater sample
- ultralow (less than 2 nmol ?) amounts of Na
- trace amounts, if any, of U.

The next day this extract is further purified by anion exchange (2.8).

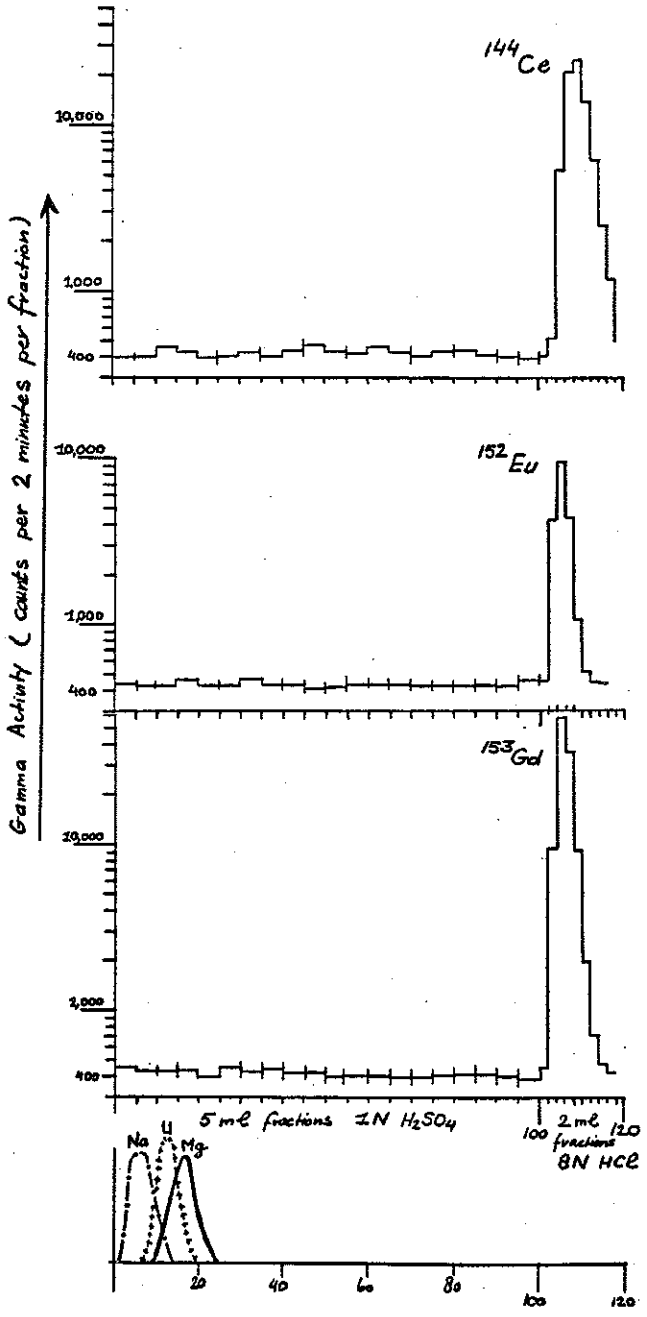


Figure 2.7.2. Quantitative retention of REE tracers $^{144}Ce$, $^{152}Eu$, $^{153}Gd$ during 100ml 1N H2SO4 washing of AG50WX8 resin beds. Detection limits for the washing stage are around 0.1 percent (Table 2.7.2). No determinations of elements Na, U, Mg were made, yet their peaks are expected to elute within the first 20-30ml washing, as depicted in the lowermost panel.

| Isotope | Net peak area (counts/2 min.) | Typical background (standard deviation) (cnts./2min.) | Yield ( % ) | Detection limit (2 st.deviations of background) ( % ) |
|---|---|---|---|---|
| 144Ce | 70661 | 423 (22) | 98.7 ±5 | 0.1 |
| 144Ce | 70564 | 423 (22) | 98.5 ±5 | 0.1 |
| 152Eu | 17783 | 423 (22) | 99.7 ±5 | 0.3 |
| 152Eu | 17280 | 423 (22) | 96.9 ±5 | 0.3 |
| 153Gd | 113218 | 423 (22) | 100.2 ±5 | 0.04 |
| 153Gd | 113826 | 423 (22) | 100.8 ±5 | 0.04 |

Table 2.7.2. Yields of radiotracer experiments with the AG50WX8/H2SO4 system, as determined from the given net peak areas after background correction. The detection limits apply to the 1N $H_2SO_4$ washing stages during which no loss of tracers was observed.

2.8. Anion exchange chromatography.

Introduction

The cation exchange method described above seems quite adequate for the removal of uranium. Most likely the U contents of its final REE extract are below the specified 1 picomole ($10^{-12}$moles) upper limit (section 2.3), i.e. five orders of magnitude below the total amount of U in 10 ltr. seawater. However the U detection limit of alpha spectrometry (and many other analytical methods) is above this picomolar level (see below). So far the evidence for complete removal by cation exchange of U to below picomolar levels is certainly convincing, yet not conclusive.

Therefore an extra U separation was instated as a precaution against possible remaining U impurities. For this final purification the classical anion exchange separation with strong hydrochloric acid medium was selected (KRAUS & NELSON, 1955). In 6N to 12N HCl medium the uranyl cation $UO_2^{2+}$ forms anions $(UO_2Cl_3)^-$ and $(UO_2Cl_4)^{2-}$ which are strongly adsorbed by the quaternary amine functional groups $R\text{-}N(CH_3)_3^+$ of the strongly basic anion exchanger AG1X8 (DOWEX-1 is the commercial grade)(Figure 2.8.1). Maximum adsorption occurs in about 8-9N HCl medium. On the other hand the REE are not adsorbed at all over the whole 0-12N range of HCl normalities.

In an earlier devised two step scheme (2.6 & 2.8) the cation exchange separation (2.7) was not included. During this early phase of the project numerous experiments were done, mostly to test the removal of U by anion exchange. Results of some of these experiments are given below, in support of the routinely employed final procedure which will be described first.

Procedure

The resin (BIORAD AG1X8, 200-400 mesh) was soaked in 8N HCl under continuous stirring. Every 12 hours the supernate was poured off and replaced with a new aliquot of 8N HCl. This was repeated four times over a 48-hour interval, except that the fourth time an aliquot of quartz water was added. This way the slurry would obtain a low (less than 1N HCl) molality in order to bring adsorbed U impurities into solution. The

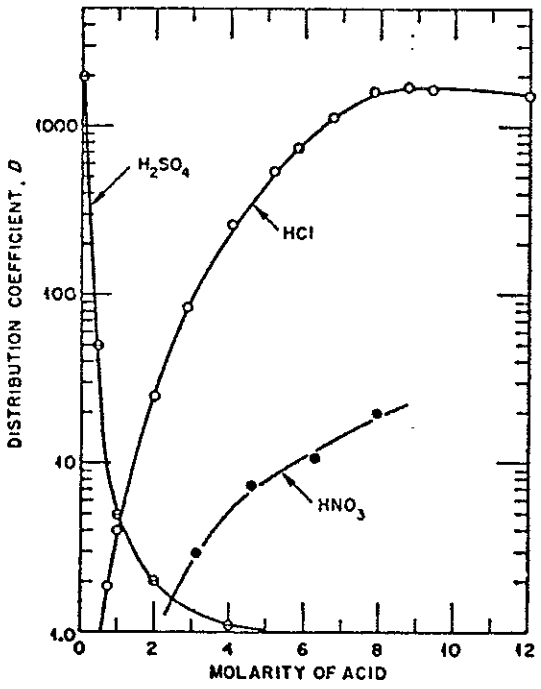


Figure 2.8.1. Adsorption of U(VI) by AG1X8 (DOWEX 1) from hydrochloric acid, as well as nitric and sulphuric acid media (Taken from KRAUS & NELSON, 1955). The REE exhibit no retention at all over the whole 0-12N HCl range. Our procedure employs 8N HCl in order to obtain maximum adsorption. Initial experiments were also done with 6N and 12N HCl media.

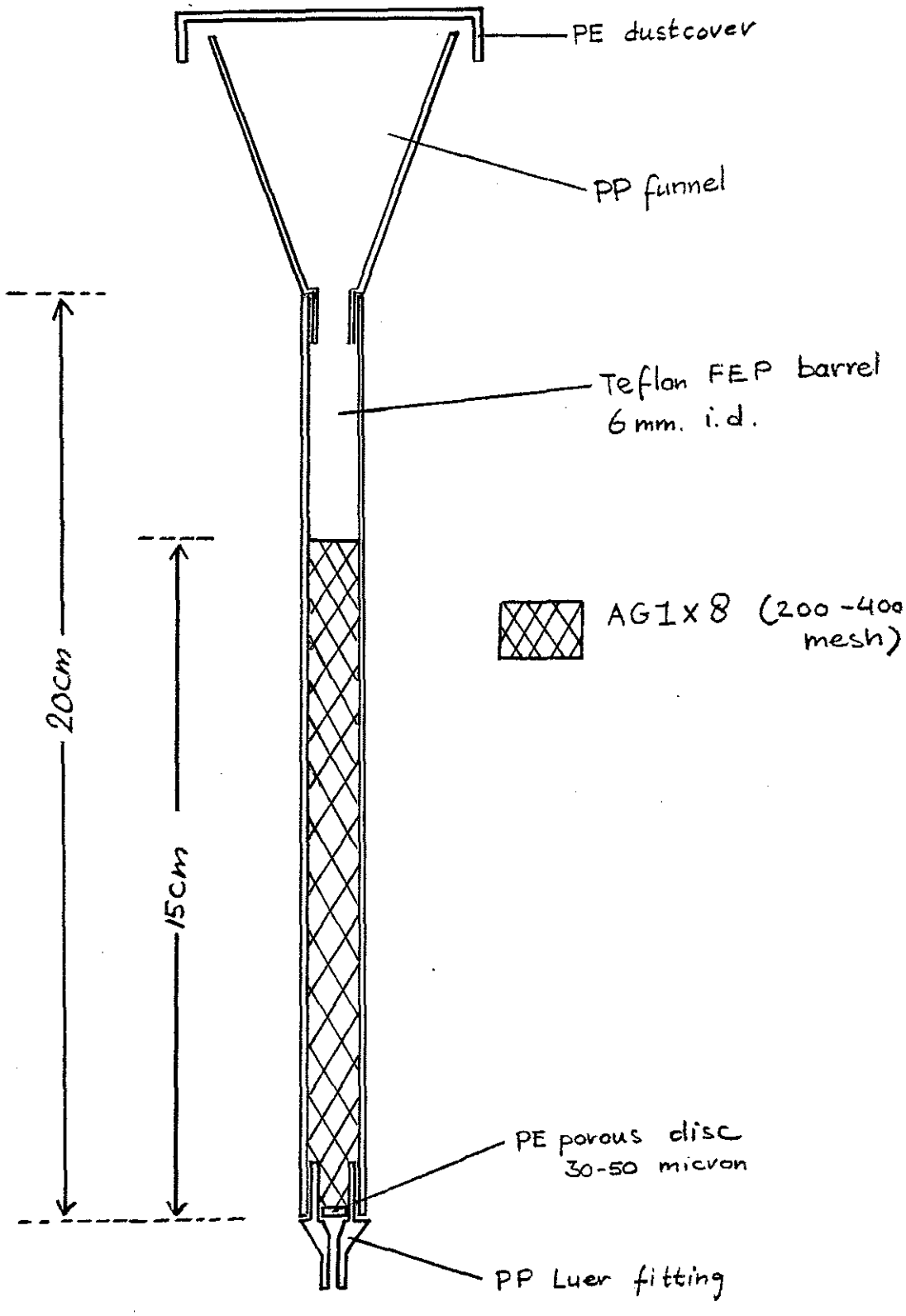


Figure 2.8.2. Column for AG1X8 separations. KONTES K420160 polypropylene and KONTES K420163 porous PE frit, with barrel replaced by 6mm i.d. Teflon FEP tubing (Cole-Parmer TJ-6406-72).

columns and dustcovers (Figure 2.8.2) were taken out of the 1N HCl storage solution, rinsed with Pyrex water, and placed in acrylic racks. Then ten 6x150mm resin beds were poured and washed with 4 x 6ml 0.1N HCl in order to remove U and REE impurities. The resin was conditioned with 4 x 6ml 8N HCl, further removing REE impurities in the process.

The residual AG50WX8 extracts (2.7) of nine samples and one overall blank were taken up in 3ml 8N HCl and loaded on the column. This and subsequent effluents were collected in 30ml capacity Teflon PFA vials with conical bottoms (and screwcaps, SAVILLEX 0201C). Then the PTFE beakers were rinsed with 3 x 3ml 8N HCl. Each of these rinses was also loaded on the column after the previous volume had completely passed the bed. After another 2 x 3ml 8N HCl additions directly to the columns, the combined 18ml effluent was allowed to evaporate to dryness under UV light in the laminary flow bench. This evaporation took about three hours. The complete procedure of about 8 hours was done the day after the cation exchange step (2.7). Then the residue was taken up in 2-3ml 12N $HNO_3$, the vials were closed with their PFA screwcaps, and the samples were allowed to reflux overnight on the hot plate at about $60^{o}C$ setting. In this way any REE deposit on the vessel walls would be washed down. The next morning the nitric acid was allowed to evaporate and the residue was taken up in 1.0 ml 12N $HNO_3$. Now all samples have a fairly uniform ($\pm$ 10 %) geometry for gamma counting on the Ge(Li) detector. Each sample was counted over a 1000 seconds interval. Routinely a yield of 100$\pm$10 % was recorded, again confirming the completeness of the overall (2.6, 2.7, 2.8) procedure. Finally the vials with purified extracts were stored inside a clean PE box, awaiting subsequent transfer into quartz vials and irradiation (2.9).

Radiotracer experiments

An initial experiment was designed to check the 'free passage' of REE along the resin bed. Two spikes of $^{144}Ce$ and $^{153}Gd$ were separately taken up in 10ml 12N HCl and passed over 7x70mm resin beds preconditioned with 12N HCl. Then the columns were washed with 10 x 2ml 12N HCl. The effluents were collected in 2ml subfractions and counted twice over two minute intervals with the NaI system.

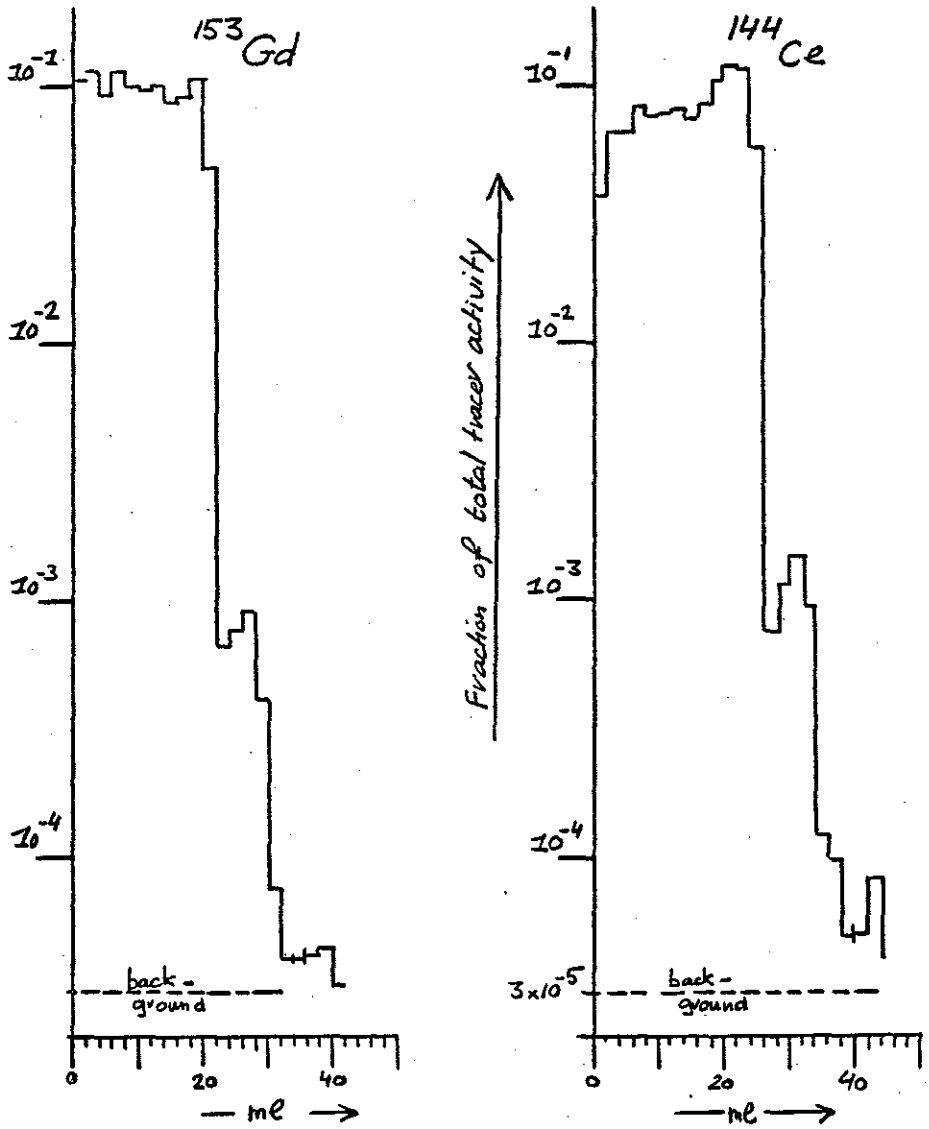


Figure 2.8.3. Radiotracers $^{144}Ce$ and $^{153}Gd$ in 6N HCl medium pass freely along 7x70mm AG1X8 (200-400 mesh) anion exchange resin beds.

| Resin (200-400 mesh) bed dimensions (mm x mm) | HCl medium (N) | Radiotracer Yield 144Ce (%) | 153Gd (%) | Detection Limit (2 sigma of background) [%] |
|---|---|---|---|---|
| Radiotracers only: | | | | |
| 7x70 | 6N | 105 ±5 | | 0.2 |
| 7x70 | 6N | | 106 ±5 | 0.2 |
| Radiotracers loaded with 6067 nmol U : | | | | |
| 7x120 | 7N | 103 ±5 | | |
| 7x120 | 7N | | 98 ±5 | |
| CHELEX-100 extracts of 6000ml seawater, the latter with radiotracers: | | | | |
| 7x140 (two in series) | 6.2N | 96 ±5 | | |
| 7x140 (two in series) | 6.2N | | 99 ±5 | |
| 7x140 (two in series) | 6N | | 101.3 ±5 | |

Table 2.8.1. Yields after background subtraction of REE radiotracer experiments with AG1X8 anion exchanger.

Quite obviously the REE are not retained at all by the resin (Figure 2.8.3). After background subtraction the integrated net peak areas correspond to 105 ± 5 % and 106 ± 5 % yields for $^{144}Ce$ and $^{153}Gd$ respectively (Table 2.8.1).

In the next experiment two Teflon PTFE beakers were loaded with 1078 dpm (6067 nmol !) $^{238}U$ each. One was spiked with $^{144}Ce$ and one with $^{153}Gd$. The mixtures were evaporated to dryness, taken up in 7N HCl and loaded on 7x120mm AG1X8 columns preconditioned with 7N HCl. The columns were washed with additional 7N HCl, after which the combined effluents were passed again over the same column. The overall yields were estimated at 103 ±5% and 98 ±5% for $^{144}Ce$ and $^{153}Gd$ respectively (Table 2.8.1).

In another experiment two 6000ml seawater samples were each spiked, with $^{144}Ce$, and one with $^{153}Gd$. Their CHELEX-100 extract was taken up in 6.2N HCl and passed directly over two different 7x140mm AG1X8 columns in series, using 6.2N HCl medium throughout. Yields were 96±5% and 99±5% for $^{144}Ce$ and $^{153}Gd$ respectively. The $^{153}Gd$ residue was again taken up in 6N HCl and passed over another two 7x140mm columns. The $^{153}Gd$ yield was now estimated at 101±5 %.

Uranium removal

Alpha spectrometry has been proven to be very useful for determinations of U in seawater (about 14 nmol = 2.5 dpm $^{238}U$ per liter) and other marine phases. For our purposes the method is less than ideal. For instance the 1 picomol benchmark would correspond to about $0.18 \times 10^{-3}$ dpm, i.e. about one disintegration event per four days, or one count per 40 days for a 10 % efficiency detector. Such a signal is at or below the detection limit of alpha detectors. For instance ANDERSON & FLEER (1982) report initial background count rates of about $0.1 \times 10^{-3}$ dpm, with significant increases over time as a result of contamination by daughter isotopes.

Also best precision is obtained when the activity of the $^{236}U$ internal standard matches that of the $^{238}U$ to be measured. This is easily achieved for seawater samples where the range of expected U concentrations is known, yet hard to accomplish in our studies where the U levels vary over five orders of magnitude. For instance with a factor 100 mismatch of $^{236}U$ versus $^{238}U$ the peak of one isotope in the alpha

spectrum gets lost in the background generated by the other isotope. On the other hand simple methods for determination of U at the picomolar level are scarce. Amounts as low as $10^{-12}$ to $10^{-14}$ moles of U can be determined by Isotope Dilution Mass Spectrometry (CHEN & WASSERBURG, 1981). In fact the $^{238}U\ (n,\gamma)\ ^{239}U \xrightarrow{-\beta} {}^{239}Np$ neutron activation scheme would also yield a very high sensitivity for U determination (see also 2.3, 2.9, 2.10).

Despite these drawbacks alpha spectrometry was used throughout for U determinations. Most experiments were designed with the original two step (2.6, 2.8) procedure in mind. During these early stages the clean air laboratory was not yet available and U blanks may have led to spurious results.

Several experiments were done with an initial load of 607 nmol U (four times the amount in 10 ltr. seawater), column lengths between 70 and 140mm and with both 6N and 12N HCl media (Table 2.8.2). As a result of detection limits and/or procedural blanks it is not possible to demonstrate that absolute amounts in the effluent REE fraction are below the 0.00018 dpm (1 picomol) specification. Yet evidence for U-free (less than 1 picomol) REE extracts is ultimately provided by the absence of any $^{239}Np$ activity from the gamma spectra of each irradiated extract (see sections 2.3, 2.10).

Nevertheless dilution factors (dpm of REE fraction / dpm spike) for the AG1X8 step are routinely around $10^{-4}$ - $10^{-5}$. In other terms, any U which would inadvertently have slipped through the cation exchange clean up (2.7) would be reduced by a factor $10^{4}$ - $10^{5}$ in the following anion exchange separation. For instance, assume that the CHELEX-100 co-extracts about half, i.e. 70 nmol, of the U from 10 ltr. seawater. If the cation exchanger removes only 99 % of that U, then the remaining 700 picomol would easily be reduced below 1 picomol by the final anion exchange step.

Summary

As a precaution against U impurities an extra separation is included in the procedure. While maintaining quantitative recovery of the REE fraction, this anion exchanger further reduces any U impurities by a factor $10^4$ to $10^5$.

The final extract contains:

- all $^{144}Ce$ internal standard
- all dissolved REE from the original seawater
- ultralow (less than 2 nmol ?) amounts of Na
- very little (less than 1 pmol ?), if any, U

| | Original 238U amount in spike (nmol)=(dpm) | Resin Bed (200-400) dimension (mm x mm) | HCl medium normality (N) | 238U detected in REE fraction (pmol) = | (dpm) | dilution factor (dpm/dpm) |
|---|---|---|---|---|---|---|
| CRITERIA FOR SEAWATER EXTRACTION: | | | | | | |
| | 140 | 25 (10 ltr. seawater) | | 1 | 0.00018 | $0.7 \times 10^{-5}$ |
| EXPERIMENTS: | | | | | | |
| 1) | 607 | 107.8 | 7x70 | 12N | 16 | 0.0029 | $2.6 \times 10^{-5}$ |
| 2) | 607 | 107.8 | 7x120 | 12N | 21 | 0.0037 | $3.4 \times 10^{-5}$ |
| | (twice over same column, HCl gas saturated) | | | | | | |
| 3) | 607 | 107.8 | 7x120 | 12N | 42 | 0.0075 | $7 \times 10^{-5}$ |
| | (twice over different columns, HCl gas saturated) | | | | | | |
| 4) | 607 | 107.8 | 7x120 (twice over same column) | 6.2N | 120 | 0.0213 | $20 \times 10^{-5}$ |
| | 607 | 107.8 | 7x120 (twice over same column) | 6.2N | 73 | 0.013 | $10 \times 10^{-5}$ |
| 5) | 607 | 107.8 | 7x120 | 6N | 47 | 0.0084 | $8 \times 10^{-5}$ |
| | two different columns in series) | | | | | | |
| 6) | blank | | 7x140 | 6N | < 17 | < 0.003 | |
| | blank | | 7x140 | 6N | < 17 | < 0.003 | |
| 7) | blank | | 7x120 | 6N | 5.6 | 0.001 | $4 \times 10^{-5}$ |

Table 2.8.2. Removal of U with AG1X8 (200-400 mesh) chromatography. Initial U spike of 607 nmol is fourfold the amount in 10 ltr. seawater. Trace amounts detected in the final extracts should be considered upper limits because of procedural blanks and/or detection limits. In experiment 2 the sample was passed twice over the same column, in exp. 3 over two different columns in series. In both exps. the samples were HCl gas saturated before the first and second loading. In exp. 4 samples were passed twice over the same column, in exp. 5 over two columns in series. For the blanks in exp. 6 actually zero counts (0 dpm) were recorded. The reported upper limits correspond to an assumed 1 count detection limit.

## 2.9. Neutron activation.

### Introduction

The activity of a radioisotope produced by neutron activation is described by the earlier given equation (2.3.2.). The constants $\sigma$, $\theta$ and $\lambda$ are specific for a given set of nuclides, e.g., $^{139}La\ (n, \gamma)\ ^{140}La$ (Table 2.9.1). Then the resulting activity is directly proportional to the neutron flux as well as the sample size M. In general the activity also increases with increasing irradiation time until a balance is reached when the production rate of a radioisotope equals its decay rate.

In a first trial a suite of REE standard mixtures with REE contents corresponding to those expected for 1 - 50 liters of seawater were irradiated for 8 hours at $8 \times 10^{12}$ neutrons.$cm^{-2}sec^{-1}$ at the M.I.T. Nuclear Reactor Laboratory. Numerous gamma spectra were recorded over various time intervals using both a 10 % nominal efficiency Ge(Li) detector as well as a planar Low Energy Photon Spectrometer. The somewhat higher resolution of latter LEPS detector proved to be of little value, and was largely offset by the much lower nominal efficiency. Even the stronger signals of short-lived $^{153}Sm$ and $^{152ml}Eu$ were barely discernible.

In the Ge(Li) spectra reasonable peaks were observed for Sm and Eu, weaker signals for La, Nd, Gd, Yb, and a very poor signal for Ce in the 1 ltr. standard. The 50 ltr. standard yielded good peaks for all above elements.

Better sensitivity for a reasonable sample size (10 ltr) can only be obtained by a higher neutron flux and/or a longer irradiation time. A set of two unfiltered 10 ltr. seawater samples was processed along the CHELEX-100 (2.6) and anion exchange (2.8) steps, omitting the cation exchange separation (2.7). Also no $^{144}Ce$ internal standard had been added. A blank was run along the procedure. The purified extracts were heat-sealed in quartz vials and together with some standards irradiated for 8 hours at a high neutron flux of $5 \times 10^{13}$ neutrons.$cm^{-2}sec^{-1}$ in port 2PH1 of the MIT Nuclear Reactor. During irradiation at this high flux the PE rabbit (Figure 2.9.1) becomes more and more brittle and it has to be replaced after 8 hours. This would necessitate repackaging of

| STABLE ISOTOPE | | | | ($n,\gamma$) PRODUCED NUCLIDE | |
|---|---|---|---|---|---|
| Atomic Number | Isotope | Thermal Neutron Cross Section (barn) | Isotopic Abundance (percent) | Nuclide | Half-life (hours, days or years) |
| 57 | 139La | 8.94 | 99.911 | 140La | 40.27h |
| 58 | 140Ce | 0.58 | 88.48 | 141Ce | 32.55d |
| 58 | 142Ce | 0.94 | 11.08 | 143Ce | 33.7h |
| 59 | 141Pr | 11.4 | 100 | 142Pr | 19.13h |
| 60 | 146Nd | 1.3 | 17.2 | 147Nd | 10.98d |
| 62 | 152Sm | 208 | 26.7 | 153Sm | 46.8h |
| 63 | 151Eu | 3200 | 47.9 | 152ml Eu | 9.3h |
| 63 | 151Eu | 5800 | 47.9 | 152Eu | 13.2y |
| 64 | 152Gd | 1100 | 0.20 | 153Gd | 241.6d |
| 64 | 158Gd | 2.4 | 24.8 | 159Gd | 18.56d |
| 65 | 159Tb | 23.5 | 100 | 160Tb | 72.4d |
| 67 | 165Ho | 62 | 100 | 166Ho | 26.8 |
| 68 | 170Er | 5.8 | 14.9 | 171Er | 7.52h |
| 69 | 169Tm | 105 | 100 | 170Tm | 129d |
| 70 | 168Yb | 3500 | 0.14 | 169Yb | 32.02d |
| 70 | 174Yb | 65 | 31.6 | 175Yb | 4.19d |
| 71 | 176Lu | 2050 | 2.6 | 177Lu | 6.71d |

Table 2.9.1. Thermal neutron cross sections and abundances of stable isotopes from which radionuclides are produced by ($n, \gamma$) activation. Half-life of product nuclide to be converted to decay constant $\lambda$ = (ln 2) / half-life before introduction in equation 2.3.2.

the highly radioactive quartz vials, leading to undesirable high radiation doses for reactor personnel. The 8-hour activation at 5 x $10^{13}$ neutrons.$cm^{-2}sec^{-1}$ is considered the maximum possible irradiation at the MIT Nuclear Reactor. By using an Al rabbit one might be able to extend the irradiation over longer time periods. High initial $^{24}Na$ activity necessitated a ten days cooling period, after which many gamma spectra were recorded with a Ge(Li) detector (Canberra, 18 % nominal efficiency, FWHM=1.8 at 1332keV, set at 2 ch/keV). Despite the loss of most of the short lived isotopes ($^{140}La$, $^{153}Sm$, $^{152ml}Eu$) good signals were still obtained for $^{140}La$, $^{141}Ce$, $^{147}Nd$, $^{153}Sm$, $^{152}Eu$, $^{153}Gd$, $^{160}Tb$, $^{175}Yb$ and $^{177}Lu$, with derived seawater concentrations in the expected range. No REE peaks were observed in the reagent blank. The absence of $^{239}Np$ (resulting from$^{238}U$) from any of the spectra demonstrated the effectiveness of the anion exchange separation (2.8) alone. Using high neutron flux good sensitivity seemed certainly possible. With additional removal of Na both before (2.7) and after activation (2.10), counting could start earlier, thus leading to increased sensitivity for some isotopes ($^{140}La$, $^{153}Sm$), as well as additional data for shorter lived isotopes such as $^{142}Pr$ and $^{177}Ho$.

Final Procedure

Special 75mm length , round bottom, activation vials were manufactured from high purity synthetic quartz tubing (HERAEUS AMERSIL, T21 Suprasil, 6mm i.d. x 8mm o.d.). Safety regulations require dry samples inside heatsealed ultrapure quartz tubes. Impurities in lower grade glass may lead to local heat sources upon irradiation, with the risk of breakage. Also the high purity quartz is helpful for avoidance of REE contamination. The vials had been cleaned extensively and were stored in 1N HCl solution. Ten vials were each rinsed, in order, with Pyrex water, 0.1N HCl in Pyrex water, and quartz water, and allowed to dry upside down in the laminar flow bench. Then the open end of a vial was welded onto a quartz holding rod, using a gas/oxygen blowtorch. For each sample transfer a clean Pyrex pasteur pipette (FISHER 13-678-20C) was taken out of its 1N HCl storage solution, rinsed with Pyrex water, 0.1N HCl in Pyrex water, and quartz water, and mounted on a PE pipetting pump (Pi-Pump, 2.0 ml cap.; Cole Parmer TJ-6221-02). Then the pipette was

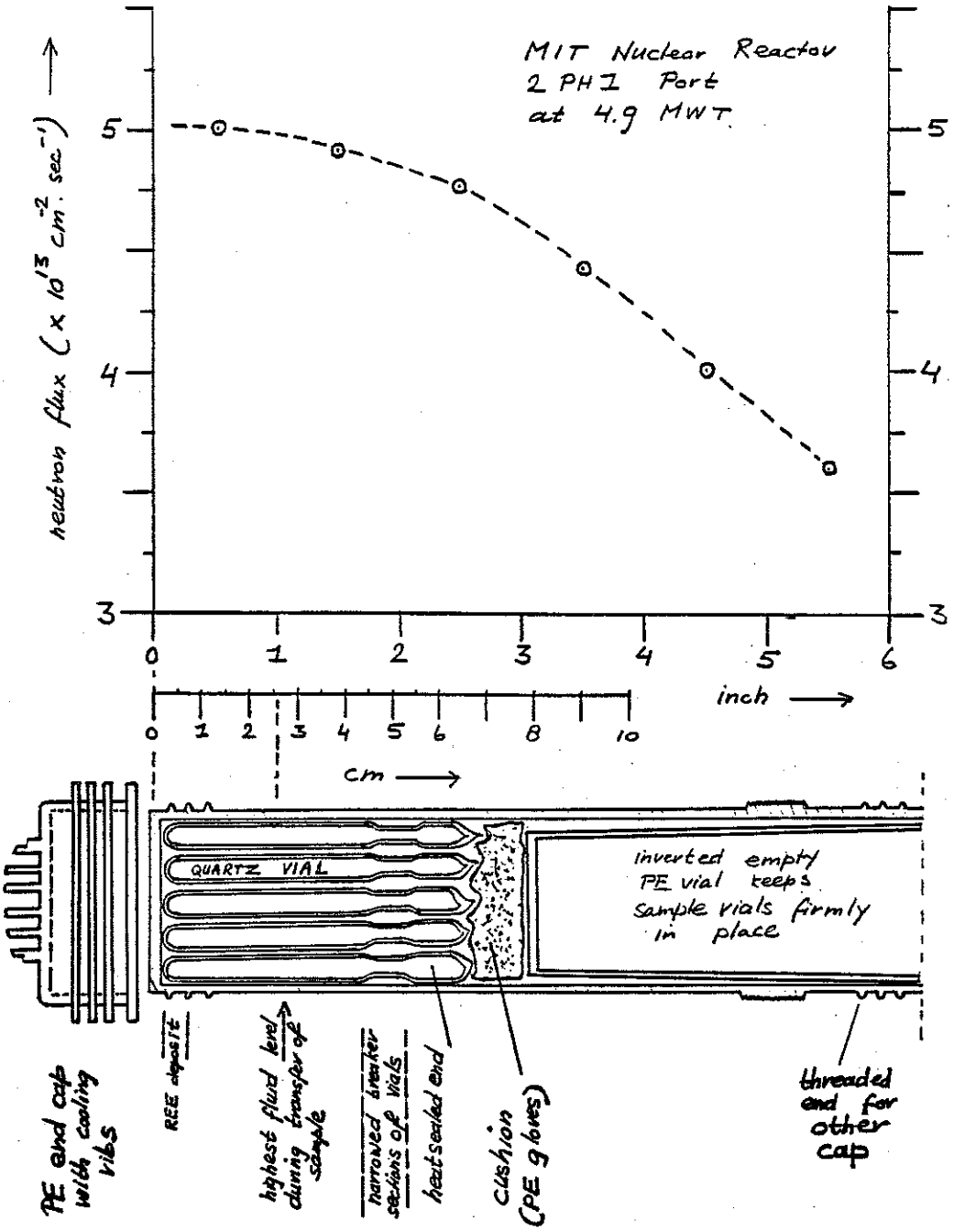


Figure 2.9.1. Polyethylene rabbit holding heatsealed quartz vials, as used in pneumatic tube system. Also shown is the neutron flux rate inside the rabbit when positioned in the 2PH1 port. The neutron flux decreases away from the reactor core along the length of the rabbit. In the first 25mm the decrease remains within about 1 percent (KHALIL, 1982).

rinsed two-fold with 12N $HNO_3$. Using this pipette, the final extract in 1.0 ml 12N $HNO_3$ (see section 2.8) was transferred in two 0.5 ml aliquots from the PFA vial into the quartz vial. The sample was evaporated to dryness by carefully heating the quartz vial just above the liquid interface with the blowtorch, so as to avoid any boiling. The gradual drop of the fluid level was followed by adjusting the height of the flame accordingly. In the meantime another 0.5 ml 12N $HNO_3$ had been added to the PFA vial in order to take up any remaining REE fraction. After complete evaporation of the first transfer, this 0.5 ml aliquot was transferred into the quartz vial with the same pipette, and evaporated to dryness. This was repeated for another 0.5 ml 12N $HNO_3$ aliquot. The fluid level in the quartz vial was always below 25mm. During evaporation almost all of the REE fraction is expected to deposit at the bottom of the vial, with very little remaining higher on the walls. The REE would be expected to be in the lower 5mm, and definitely below 25mm, during irradiation of the vial.
Complete evaporation is required because any remaining fluid may lead to high internal pressures during irradiation, with the possible risk of exploding vials.

Finally each vial was heatsealed with the blowtorch set at its highest temperature flame. In the process a narrow section was made in the quartz walls, in order to allow the vessels to be broken open after irradiation (Figure 2.9.2). After transfers, evaporations and heatsealing for nine samples, one blank (and two standards), numbers were engraved on the outside.
This is necessary because numbers written with feltpen markers are often obliterated during irradiation. The sealed and engraved vials were soaked in dilute acid in order to decontaminate the exterior. After rinsing with Pyrex water they were allowed to dry in the laminary flow bench. The interior of the PE rabbit (Figure 2.9.1) was also acid cleaned and dried. The twelve quartz vials were then stacked inside, with 2 PE gloves and a PE vial on top for cushioning and to firmly fix the vials in place. Afterwards the PFA vials were counted on the Ge(Li) detector to check for any $^{144}Ce$ (i.e. REE) which would inadvertently have been left behind.

The complete transfer procedure took about two days for each irradiation. A variety of other schemes for transfers and evaporations

has been tested, yet the current procedure, albeit very laborious, seemed most suitable.

The rabbit was inserted into the 2PH1 port of the MIT Nuclear Reactor, using the pneumatic tube system. Samples and standards were irradiated for 8 hours overnight (11.00pm-07.00am) at a $5 \times 10^{13}$ neutrons.$cm^{-2}sec^{-1}$ flux. The rabbit was taken out, and allowed to cool for about eight hours. Then the quartz vials were taken out, packed in a lead container, and transported by car to Woods Hole. There the samples were allowed to cool further until the next morning, when postactivation procedures (2.10) would start.

Irradiation Geometry

During the 8 hours irradiation period possible variations in time of the neutron flux are acceptable. However, at a given time, the spatial distribution of the neutron flux has to be homogenous in order to achieve precision. KHALIL (1982) determined flux gradients in the 2PH1 port. The results indicate that flux rates are at maximum near the reactor core, and decrease away from the core along the length of the rabbit (Figure 2.9.1). In the first 25mm the longitudinal decrease in flux remains within about 1 percent of the total flux. For this reason serious efforts were made to deposit the REE sample within the bottom 5mm of the vial. There is no data on radial flux gradients in this specific port, yet such variations are also expected to be within about 1 percent (FECYCH, pers.comm.). Sometimes flux monitors are used for each sample in order to allow correction for spatial flux gradients. However in our case the additional errors introduced by such corrections would probably be larger then the 1-2 % error arising from actual flux gradients themselves. The use of an internal standard (different than $^{144}Ce$), which would also cancel out such flux gradients, had been given some serious consideration. However likely candidates such as Sc or Y might also contain trace impurities of REE, thus leading to contamination of the samples. In fact it might be more advantageous to add a completely different element which can be better purified from REE, e.g. Co, directly after the three extractions/purifications (2.6, 2.7, 2.8) have been completed. On the other hand the $^{144}Ce$ standard is produced carrier free (i.e., without stable REE impurities) from $^{235}U$ fission.

Neutron Energy Spectrum

Neutrons produced in the fission process have an average energy of approximately 2 MeV ($2 \times 10^6$ eV). In a thermal reactor as used in our work, these are slowed down by collisions with the moderator atoms until they are in thermal equilibrium with the moderator material and have an average energy of about 0.025 eV, corresponding to a 2200 m/sec velocity. Therefore each irradiation port of a reactor has its own spectrum of neutron energies. While a function of such parameters as amount and type of moderator, capacity of the reactor, etc., a typical neutron energy spectrum would resemble Figure 2.9.2.A.
An arbitrary division of the spectrum consists of three regions:

- strictly thermal neutrons in thermal equilibrium with the moderator atoms, at energies below about 0.025 eV.
- fast neutrons as produced from fission without any moderation, at energies over 1 MeV
- intermediate neutrons which have slowed down somewhat, but not yet reached thermal equilibrium with the moderator.

For a given stable isotope (e.g., $^{139}La$) to be activated the probability of interaction with neutrons, or cross section, is a function of the energy of the neutrons (Fig. 2.9.2.B). Such a curve of the neutron activation cross section often has narrow peaks or 'resonances' where the cross section is exceptionally high. This usually occurs at neutron energies higher than 1 MeV, for isotopes with intermediate or high mass numbers, including many of the rare earths and $^{238}U$. The resonance integral I is an operationally defined measure of the cross section in such a narrow band. The total activity produced during irradiation can be envisioned as being proportional to the product of the neutron energy spectrum (Figure 2.9.2.A) and the cross section spectrum (Figure 2.9.2.B). For elements with high resonance integrals I the total activity produced may be enhanced considerably by even a small fraction of fast neutrons.

Parameters like a resonance integral can be determined experimentally by use of Cd filters. Cadmium is a unique element because it has a very high cross section for thermal neutrons, which can be adsorbed completely

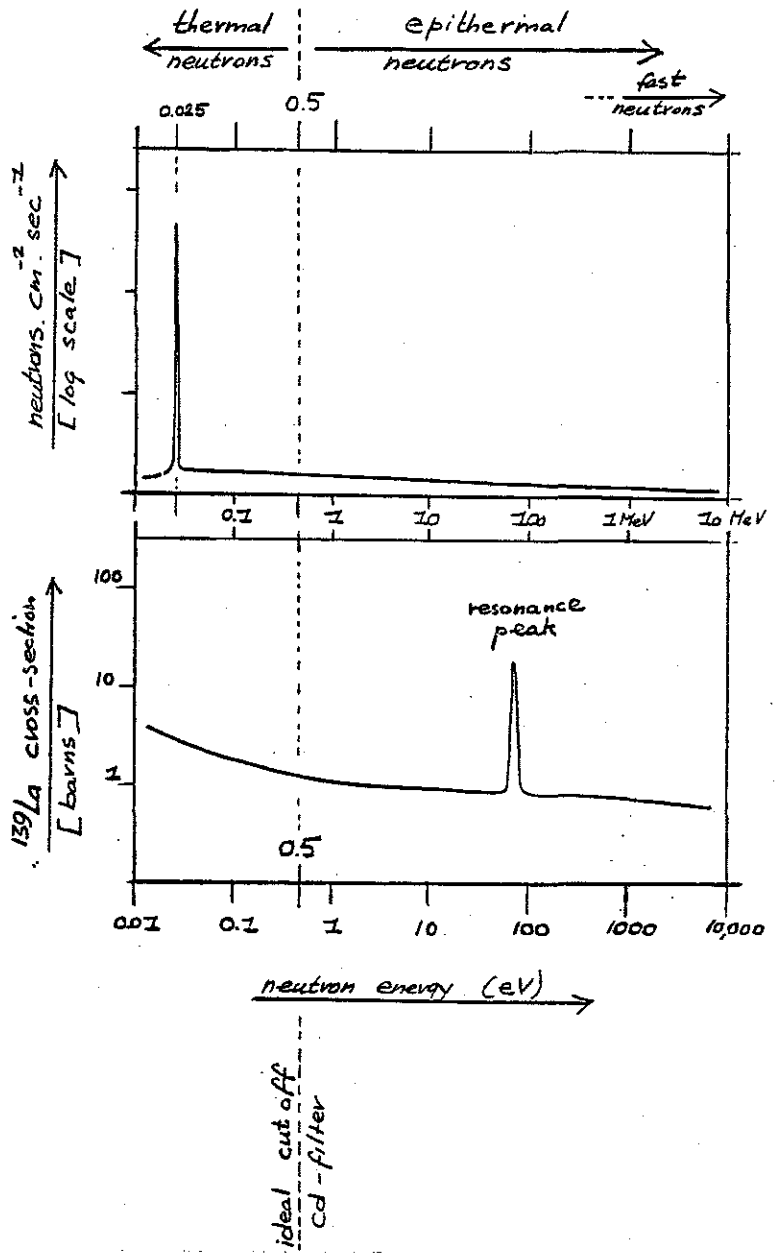


Figure 2.9.2. Sketches depicting:

A) Typical neutron energy spectrum of a thermal reactor.

B) The neutron activation cross section of $^{139}La$ as a function of neutron energy. Below 0.5 eV the area under the curve is quantified by the concept of a thermal neutron cross section. Note the resonance peak at about 70 eV, corresponding to resonance integral I in rate equation (2.3.12). The remainder of the area under the curve above 0.5 eV corresponds to the term $0.44\sigma_{th}$ in the same equation.

by a Cd shield of appropriate thickness. On the other hand fast neutrons pass freely through a Cd foil. When a sample is irradiated with a suitable Cd cover the thermal neutrons are ideally excluded and only neutrons with energies higher than about 0.5 eV will contribute to the activation process. For a given reactor port identical masses of an isotope, e.g. $^{197}Au$, can be irradiated with and without such a Cd filter. Activities are produced by strictly epithermal ( 0.5 eV) neutrons, and by the complete spectrum of both thermal and epithermal neutrons. In other words, the reaction rate r

$$r = \phi_{th} \times \sigma_{th} + \phi_{epi} (I + 0.44 \sigma_{th}) \qquad (2.3.12)$$

depends on both the thermal neutron flux $\phi_{th}$ and the epithermal neutron flux $\phi_{epi}$, where the first term $\phi_{th} \times \sigma_{th}$ can be eliminated by means of a Cd filter. The choice of a Cd filter then leads to operational definitions of

$\sigma_{th}$ = thermal neutron cross section (barn = $10^{24}$ $cm^2$)
I = resonance integral (barn = $10^{24}$ $cm^2$)

for a given isotope, as listed in many tabulations (LEDERER et al.,1978). The term $0.44\sigma_{th}$ in above equation (2.3.12) accounts for the activity produced by the flat, non-resonance, tailing of the epithermal region (Figure 2.9.3.B).

Determinations with and without Cd filter have been made for $^{197}Au$ (which has a high resonance integral) in reactor port 2PH1 of the MIT Nuclear Reactor (KHALIL, 1982). At a distance of 1.25 cm from the bottom of the rabbit, more or less the same location of our REE samples, the following result was obtained for the 'Cd-ratio' of $^{197}Au$:

$$R_{Cd} = \frac{\phi_{th} \times \sigma_{th} + \phi_{epi}( I + 0.44\sigma_{th})}{\phi_{epi} ( I + 0.44\sigma_{th})} \qquad (2.9.1)$$

$$= 26.38 \qquad \text{(KHALIL, 1982)}$$

At a total neutron flux $\phi_{th} + \phi_{epi} = 5 \times 10^{13}$ n.cm$^{-2}$s$^{-1}$

and with constants for $^{197}$Au

$\sigma_{th}$ = 99 barns
I = 1560 barns

the two components of the neutron flux are calculated at:

$\phi_{th}$ = 4.9879 x $10^{13}$ n.cm$^{-2}$.s$^{-1}$
$\phi_{epi}$ = 0.01207 x $10^{13}$ n.cm$^{-2}$.s$^{-1}$

Only about 0.2 percent of the neutrons have not been fully moderated. Further down along the rabbit this fraction is even smaller (KHALIL, 1982). As demonstrated in Table 2.9.2 the small fraction epithermal neutrons is negligible for nuclides of our interest, with the exception of a 25 % enhancement for production of $^{239}$Np from $^{238}$U (see also section 2.3). Yet in an irradiation port with ten percent or more epithermal neutrons the activity of many REE product nuclides would increase about threefold (STEINNES, 1971). In the latter case a strictly epithermal activation ( $\phi_{th}$=0) using Cd shielding would fully eliminate the troublesome activation of low mass elements Na and Si, because of their negligible resonance integrals.
However under our conditions such shielding would virtually eliminate all REE activity. The interfering activity of Na and Si has to be removed by a postactivation separation step (2.10) instead.

Summary

Irradiation of extracts from 10 ltr. seawater during 8 hours at 5 x $10^{13}$ neutrons.cm$^{-2}$.sec$^{-1}$ yields good sensitivity for REE determination. Spatial variations of the neutron flux lead to an error of about 1-2 percent. The potential of enhanced activity due to high resonance integrals of various REE nuclides cannot be exploited because of the virtual absence of fast neutrons at the reactor port.

| (n,γ) Reaction | CROSS SECTION TERMS $\sigma_{th}$ [barn] | $(I + 0.44\sigma_{th})$ [barn] | PRODUCTION RATES AT 2PH1 $\phi_{th}\sigma_{th}$ [neutrons/sec] | $\phi_{epi}(I + 0.44\sigma_{th})$ [neutrons/sec] |
|---|---|---|---|---|
| 139La(n,γ)140La | 8.8 | 11.8 | 43.9 | 0.142 |
| 140Ce(n,γ)141Ce | 0.58 | 0.48 | 2.89 | 0.0058 |
| 41Pr(n,γ)142Pr | 11.5 | 14.1 | 57.4 | 0.17 |
| 146Nd(n,γ)147Nd | 1.4 | 3.2 | 6.98 | 0.0039 |
| 152Sm(n,γ)153Sm | 210 | 2530 | 1047 | 30.54 |
| 151Eu(n,γ)152m1Eu | 2951 | 11410 | 14720 | 137.7 |
| 151Eu(n,γ)152Eu | 4410 | 3847 | 21997 | 46.4 |
| 152Gd(n,γ)153Gd | 1100 | 3100 | 5487 | 37.4 |
| 159Tb(n,γ)160Tb | 22 | 365 | 110 | 4.4 |
| 165Ho(n,γ)166Ho | 62 | 710 | 309 | 8.6 |
| 169Tm(n,γ)170Tm | 115 | 1550 | 574 | 18.7 |
| 168Yb(n,γ)169Yb | 3200 | 14700 | 15961 | 177 |
| 174Yb(n,γ)175Yb | 65 | 27 | 324 | 0.33 |
| 176Lu(n,γ)177Lu | 2050 | -- | 10225 | -- |
| 197Au(n,γ)198Au | 99 | 1550 | 493.8 | 18.7 |
| 235U fission | 580 | 280 | 2893 | 3.38 |
| 238(n,-β)239Np | 272 | 278 | 13.57 | 3.35 |

Table 2.9.2. Comparison of radioactivity produced by the strictly thermal neutron flux ( $\phi_{th}=4.988 \times 10^{13}$) and the epithermal neutron flux ( $\phi_{epi}= 0.01207 \times 10^{13}$) in reactor port 2PH1. Except for a 30 % increase for production of $^{239}$Np, the contribution by epithermal activation is negligible. (After STEINNES, 1971).

2.10. Postactivation chromatography.

Introduction

The REE-radionuclides have to be taken out of the highly radioactive quartz vials (see 2.3) in order to allow counting for short lived isotopes like $^{142}Pr$, $^{152ml}Eu$, $^{159}Gd$ and $^{166}Ho$. The necessary postactivation separation of $^{24}Na$ arising from persistent Na impurities is done immediately with the same cation exchange method as used before (2.7).

Procedure

The next morning, 24 hours postactivation, the first six sample vials were taken out of the containers, quickly broken open, and placed in 8mm diameter holes in a lead brick placed on a hot plate set at 60°C, all in a fumehood behind adequate shielding of lead, glass and acrylic materials. Throughout the procedure disposable PVC gloves were worn. Pliers and forceps were used for manipulation of the 'hot' quartz vials. Radiation levels were monitored with a portable counter, as well as by wearing badges on the labcoat, right wrist and as rings on one finger of each hand. Exposure times were minimized by working as quickly and efficiently as possible. Then each vial was filled with 1N $H_2SO_4$ and allowed to sit for two hours at 60°C to assure complete dissolution of the REE deposit. Then contents of each vial were transferred with a pasteur pipette to a 6 x 40mm AG50WX8 (200-400 mesh) cation exchange column which had been preconditioned with 0.2N $H_2SO_4$. Each vial was rinsed threefold with additional 1N $H_2SO_4$, and all rinses were also loaded on the column. The columns were set up outside the fume hood, behind leadglass screen. After this transfer any further personal radiation exposure is negligible. Subsequently the columns were washed with 4 x 5ml 1N $H_2SO_4$, each time after the previous volume had passed the bed. All 1N $H_2SO_4$ effluents were collected in a Teflon PFA vial. Then the REE fraction was eluted into a different PFA vial with 5 x 3ml 8N HCl. Both fractions were evaporated to dryness and taken up in 1.0 ml 8N HCl.

The remaining three samples and one blank were processed similarly. The REE standards usually contain very little $^{24}Na$ and were transferred

directly from the quartz tubes into the PFA vials. After evaporation and addition of 1.0 ml 8N HCl one of these standards was first counted during a two hour interval starting at about 30 hours post-activation. Then the REE fractions of all samples were also counted over 2-3 hour intervals each. About five days post-irradiation the 1N $H_2SO_4$ fractions were counted for 1000 second intervals each, in order to check for any $^{239}Np$ activity indicative of U impurities.

With the portable counter we usually found that the quartz vials themselves correspond to about 90 % of the total activity, with the $^{24}Na$ fraction and the REE fraction making up the remaining 10 percent. The REE fraction accounted for less than 1 % of the total activity at 24-36 hours after activation.

Uranium Products

The $^{239}Np$ activity to be used as indicator of any remaining U impurities (see 2.3) may be affected by the post-activation chromatography. We have not been able to find specific information on the behaviour of Np in the AG50WX8 / $H_2SO_4$ separation scheme (KORKISCH, 1969; BURNEY & HARBOUR, 1974). Np ions in dilute acid medium are generally expected to be strongly adsorbed by AG50WX8, with increasing adsorption for increasing charge, i.e.

$$Np(IV) > Np(III) > NpO_2^{2+} > NpO_2^{+}$$

Strong adsorption has indeed been reported for dilute hydrochloric acid solution (KORKISCH, 1969). However from analogy with Th, the adsorption of Np from dilute (1N) sulphuric medium is expected to be much lower.

The actual behaviour of Np was studied by activation of a known amount of $^{238}U$ (0.00539 dpm = 30 pmol) and subsequent post-activation separation as described above. Both the 1N $H_2SO_4$ washings and the 8N HCl eluate (which would normally contain the REE fraction) were evaporated to dryness, taken up in 1.0 ml 8N HCl and counted with the Ge(Li) detector. Results show that in this experiment about 80 % of the Np ended up in the $H_2SO_4$ washings, with the other 20 % remaining in the 8N HCl (REE) fraction. Apparently in 1N sulphuric medium Np has a moderate affinity for the resin. In such case the recovery in both

fractions may shift considerably depending on slightly varying conditions such as column length or acid strength. For instance, more extensive washing would probably remove all $^{239}Np$ from the columns.

Given these observations it is necessary to monitor both fractions for any $^{239}Np$ signal in order to guard effectively against any U impurities. Spectra of REE fractions are routinely checked for $^{239}Np$ peaks. Additional spectra of the 1N $H_2SO_4$ fractions are recorded over 1000-second intervals each, beginning about five days after irradiation when almost all $^{24}Na$-generated background has decayed away.

2.11. Gamma counting.

Procedure

Each sample and standard was counted over four different time intervals on a Ge(Li) co-axial detector (EG & G ORTEC, 16.9 % nominal efficiency and FWHM = 1.8keV at 1.33 MeV; Peak/Compton ratio = 49.1). The detector is interfaced with an 8192 channel analyzer (NORTHERN SCIENTIFIC 1710) adjusted to cover the 50-1500 keV range at a 5 channels/keV resolution. At a lower setting, e.g. 2 ch/keV, the high resolution signal of the Ge(Li) detector would detiorate. Each recorded spectrum was stored on magnetic tape for spectral analysis with the GAMANL program (2.12). The NS 1710 system also has an option for direct determination of gross and net peak areas. The latter values were also recorded, just in case of malfunctioning of the data processing. Yet with very few exceptions the output net peak areas determined by the GAMANL spectral analysis (2.12) were used for calculation (2.13) of final REE-concentration values. Visual scanning of each spectrum on the TN 1710 CRT-screen led to additional insight in the quality of the peaks with respect to such criteria as overlapping adjacent peaks, gaussian shape, etc. This has proven very helpful for selection of the best peak for determination of each element (2.13).

FIRST COUNTS. Beginning about 30 hours postactivation first one standard was counted, then all samples (and the blank), over 7,000 -10,000 second intervals (2-3 hours) each. Finally the other standard was counted for 12 hours, with the resulting spectrum serving as reference for both first and second count sets.

SECOND COUNTS. Immediately following the first set all samples and both standards were counted for 12-18 hour intervals. Second counts usually started about 60 hours postactivation and lasted until 9 days after irradiation. At 5 days after irradiation the second counts were temporarily suspended in order to count all $H_2SO_4$ fractions over 1000 sec intervals each to assess their $^{24}Na$ and $^{239}Np$ (if any) activities.

THIRD COUNTS would start 12 days postirradiation. Each standard and sample was counted over a 24-hour interval.

The above three count sets were done in a sequence, usually with a two day break between second and third counts. Then the samples were allowed to cool at least three more weeks before commencing the fourth, and final count set.
During the cooling period the first three count sets of a new irradiation, or the fourth set of a previous one, woiuld be recorded.

FOURTH COUNTS. beginning at least 6 weeks post irradiation each sample and standard was counted over a 48 hours interval.

For each spectrum the start time, live time and count time were recorded for the purpose of decay time corrections (2.13).

Complete counting for a set of nine samples, two standards and one blank occupies about 5-6 weeks of detector time and leads to concentration values for 12 out of the 14 naturally occurring rare earths. Detector time can be cut in half by abandoning the fourth count set. In this way results for Tm and $^{153}$Gd ($^{159}$Gd data of poorer quality were obtained in the first counts) are sacrificed, along with estimates of $^{152}$Eu and the best values for Tb.

2.12 Spectral Analysis.

Each spectrum is processed by the GAMANL program (HARPER, INOUYE & RASMUSSEN, 1968) on a VAX 11/780 (DIGITAL EQUIIPMENT CORP.) computer. In our 8192 channel spectra routinely 150-200 peaks are identified, for each of which is reported:

- peak center
- net peak area = gross peak area - background
- background
- error (%) of net peak area
- peak height (number of counts)
- height / background ratio
- Full Width Half Maximum (actual)
- FWHM from best fit of FWHM(keV) polynomial
- peak width at base
- area / gaussian area, a parameter which equals 1.000 for perfect gaussian peak
- type of peak (single, doublet, triplet)

Most important is of course the net peak area, which routinely was found to be in good to excellent agreement with the net peak area recorded manually from the NS 1710 analyzer. For the latter values the peak boundaries were arbitrarily assigned by the operator. On the other hand GAMANL would always employ exactly the same criteria and algorithms for all spectra and the resulting net peak areas are presumed to be of greater internal consistency, and thus superior.

Before routine use of GAMANL a few parameters, like expected FWHM, had to be chosen so as to match a typical spectrum. Very little change in the output data was observed when varying these parameters in different runs for the same given spectrum. From there on all spectra were processed with these parameters fixed at constant values.

Other output data such as error, gaussian shape, peak/background, were used for selection of the best peak for each element. Peaks classified as doublets or triplets were a priori excluded. The percentage error was used for overall precision estimates (2.15).

In the past decade GAMANL has been used extensively, both in our laboratory and by other workers, for resolving Ge(Li) spectra. Even for more complicated spectra of irradiated whole rock samples, often recorded with older, lower resolution detectors, GAMANL has proven to be quite adequate. Nevertheless for processing such spectra improved or completely different type programs have more recently been developed. However our relatively simple spectra are almost exclusively composed of peaks from REE radionuclides. Processing by other programs than GAMANL would probably yield little improvement, especially because only well resolved peaks of good quality were selected for further calculations.

## 2.13. Data Processing

### Introduction

For each count set concentration values are calculated from net peak areas (2.12). Most REE produce more than one radionuclide upon irradiation or multiple peaks for some nuclides. In such cases, the best peak is selected for final analysis. These selected peaks for a given count set are then fed into a computer program for decay time correction, internal standard correction and final calculation of concentrations. In some cases one still obtains more than one estimate from various count sets (e.g. three different values based on $^{177}$Lu(208) in first, second and third counts). For all these reasons some, presumably non-arbitrary, selection criteria are necessary.

### Peak Selection

In a first selection all peaks with spectral interferences were a priori excluded (unless no other peak is available). Earlier work by DENECHAUD, HELMKE & HASKIN (1970) and DUFFIELD & GILMORE (1979) proved quite helpful in sorting out these interferences. In several instances a number of good quality peaks remain, each one of them yielding an independent concentration estimate for that particular element. For instance four peaks (329, 487, 816, 1596 keV) of $^{140}$La in the second count set yield concentration values which routinely agree within 1-2 percent. Quite similarly two estimates based on strong $^{175}$Yb (283, 396) peaks in the second counts are in good agreement with three independent values based on $^{169}$Yb (177, 198, 308) in the third counts. Various of such peaks are routinely taken through the complete data processing procedure. Yet only the results based on the best quality peak are eventually reported. Selection criteria include such factors as percentage error, gaussian shape, peak/background ratio and total numberof counts. Concentration values based on all other, non-selected, peaks are used for consistency checks.

While our final reported values are definitely based on the best possible peaks, rejection of all the other data does not seem to be perfectly correct. Properly speaking one should have taken all these

second and third choice estimates into account, for instance by calculation of a weighted mean. The very same factors as used above for selection (% error, gaussian shape, peak/background ratio), and already provided by the GAMANL output, would determine the weighing factor. Most likely this approach would also yield improved overall precision. Development of such an additional data processing step would be rather straightforward, although so far time considerations have kept us from making such refinement.

The selected best peaks for each element are given in Table 2.13.1. Some aspects of the corresponding radionuclides are discussed below.

$^{144}$Ce (284.2d), Internal Standard. The major peak at 133 keV is used for geometry corrections in second, third and fourth counts. The small adjacent $^{169}$Yb (130.5) peak is well separated. In the first count set the $^{144}$Ce peak has a relatively large error. The very strong, perfectly gaussian peak of $^{140}$La at 1596 keV is used instead as internal standard of the first counts, by comparison with $^{140}$La(1596) / $^{144}$Ce(133) in the second counts as reference. The minor 80.1 keV peak of $^{144}$Ce coincides exactly with $^{166}$Ho (80.6), and a correction of the latter is necessary.

$^{140}$La(40.3d) All four peaks (329, 487, 816, 1596) in the second counts are excellent and yield very consistent results. Reported concentration values are based on the 1596 keV peak with perfect gaussian shape and superior peak/background ratio.

$^{141}$Ce(32.6d) The 145 keV peak in the fourth count set was used. The relative importance of an interfering $^{175}$Yb (4.2 days) peak at 144.9 keV was estimated from the count rate ratio derived from equation (2.3.2) with an additional gamma ray intensity term F, for each isotope:

$$\frac{\text{Count rate of } ^{144}\text{Ce at 145.4 keV}}{\text{Count rate of } ^{175}\text{Yb at 144.9 keV}} = 0.4392 \frac{\text{mole Ce}}{\text{mole Yb}} \exp(0.144\ t) \quad (2.13.1)$$

| COUNT SET | | | I | II | III | IV |
|---|---|---|---|---|---|---|
| Isotope | Halflife | keV | | | | |
| 144Ce (internal standard) | 284.2d | 133 | 0 | * | * | * |
| 140La | 40.3d | 329 | 0 | 0 | | |
| | | 487 | 0 | 0 | | |
| | | 816 | 0 | 0 | | |
| | | 1596 | 0 | * | | |
| 141Ce | 32.6d | 145 | o | o | o | * |
| 143Ce | 33.7h | 293 | o | | | |
| 142Pr | 19.1h | 1576 | * | | | |
| 147Nd | 11d | 91 | | + | * | |
| | | 531 | | | o | |
| 153Sm | 47h | 103 | 0 | * | | |
| 152m1Eu | 9.3h | 122 | 0 | | | |
| | | 344 | 0 | | | |
| 152Eu | 13.2y | 122 | (combined with 154Eu at 123) | | | 0 |
| | | 344 | | | | * |
| | | 1408 | | | | 0 |
| 154Eu | 8.5y | 123 | (combined with 152Eu at 122) | | | 0 |
| 153Gd | 241.6d | 97 | | | | * |
| mean | | 103 | | | | * |
| 159Gd | 18.6h | 364 | o | | | |
| 160Tb | 72.4d | 87 | | | 0 | 0 |
| | | 299 | | | 0 | * |
| | | 879 | | | 0 | 0 |
| | | 1178 | | | o | o |
| 166Ho | 26.8h | 81 | * | | | |
| 171Er | 7.5h | 308 | - | | | |
| 170Tm | 129d | 84 | | | 0 | * |
| 169Yb | 32d | 177 | | o | 0 | |
| | | 198 | | o | 0 | |
| | | 308 | | o | 0 | |
| 175Yb | 4.2d | 283 | o | 0 | | |
| | | 396 | o | * | | |
| 177Lu | 6.7d | 208 | o | * | 0 | |

* peaks used for final reported values  0 good agreement

o fair agreement  + reasonable agreement  - poor

Table 2.13.1. Selection of peaks (marked *) used for reported data. Peaks marked with good (0) or fair (o) agreement were routinely processed along for consistency checks. In future work the peaks with good agreement (0) would be suitable for calculation of a weighted mean (see text).

This amounts to a serious interference in seawater, which exhibits both a Ce depletion and an enrichment of the heavy REE, i.e. Yb (Figure 2.13.1). In the extreme case of deep Pacific water a cooling time of seven weeks was required before starting the fourth count set.

$^{143}$Ce(33.7h) The 293.3 keV signal in the first counts is rather weak, yet derived concentration values are consistent with those for $^{141}$Ce, making a systematic error in latter estimates unlikely.

$^{142}$Pr(19.1h) The 1576 keV peak in the first counts is small, yet free of interferences in an area with low background.

$^{147}$Nd(11d) The third count set is tailored for obtaining the 91 keV peak. Counts start after 12 days cooling, such that potential interferences of $^{153}$Sm(89.5, 97.4) have become negligible. Peaks of $^{160}$Tb(86.8) and $^{170}$Tm(84.3) are well separated. The 531.4 keV peak is free of interference but very weak, and serves as a consistency check.

$^{153}$Sm(47h) The 103 keV peak has no significant contributions of $^{153}$Gd (103.2) when counting within 12 days after activation. Reported values are based on the second counts, with first count values in excellent agreement.

$^{152m1}$Eu(9.3h) Both the 121.8 and 344 keV peak are free of interferences. Potential contributions of $^{152}$Eu(121.8, 344) and $^{154}$Eu(123) are negligible when counting within 2-3 days postactivation.

$^{152}$Eu(13.2y) Both the 344 and 1408 keV peaks in the fourth count set are free of interferences. The 122 keV peak has a significant shoulder of $^{154}$Eu (123 keV). The combined peak is processed as one, using the 13.2y halflife of $^{152}$Eu for decay corrections. The latter corrections are very small over the 3-4 weeks counting period, and the theoretical error due to a different 8.5y halflife of the minor $^{154}$Eu component is negligible. All three peaks, along with those of $^{152m1}$Eu (122, 344) yield consistent results and a weighted mean of all five

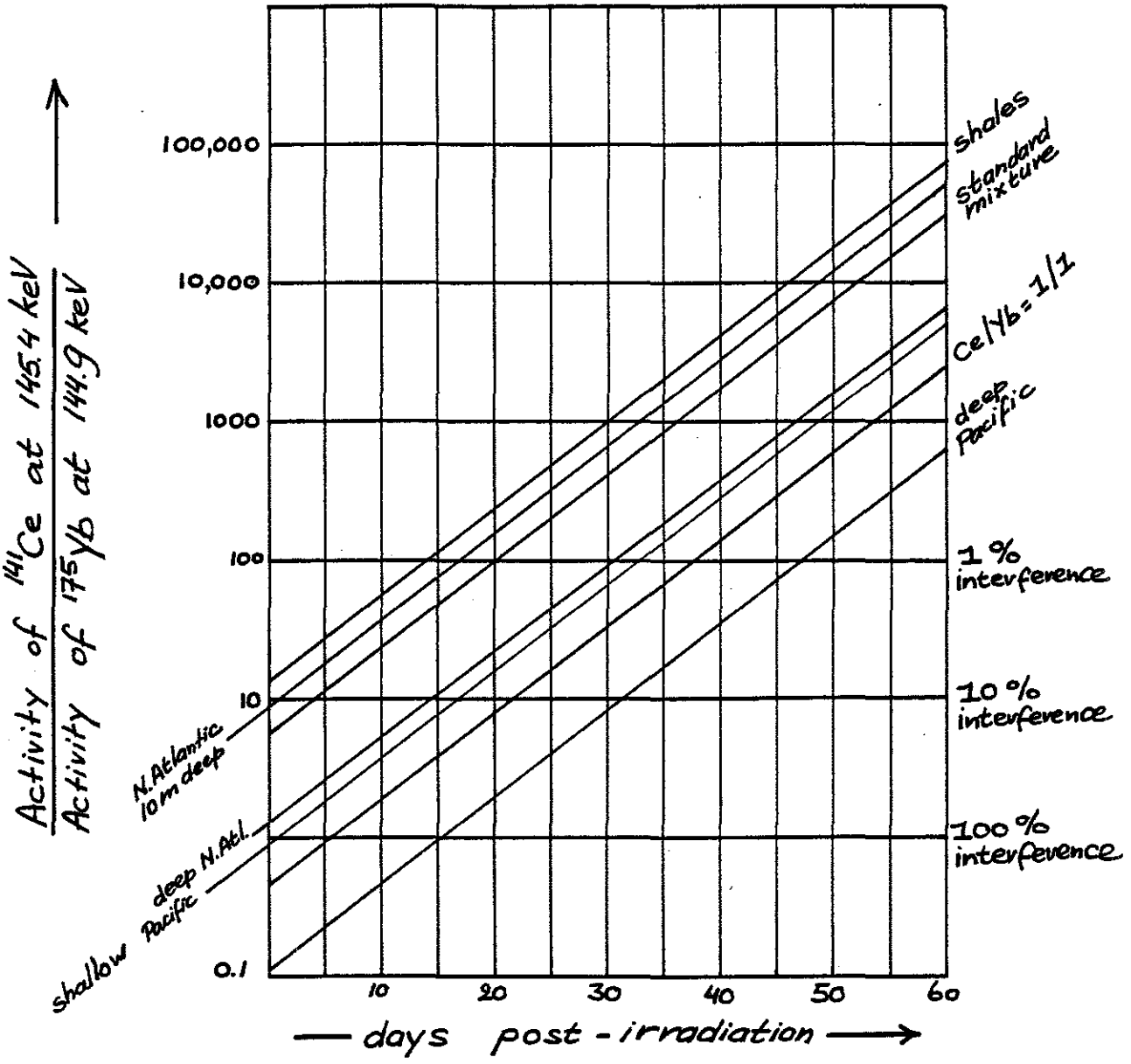


Figure 2.13.1. The count rate ratio $^{144}Ce$ / $^{175}Yb$ at 145 keV as a function of molar Ce/Yb ratio in various type samples, and time past irradiation. Note that about 7 weeks cooling time is required for a less than one percent interference with Ce determinations in deep Pacific waters.

estimates would be feasible. Yet data reported so far is based solely on the $^{152}$Eu(344) peak, which has more counts than the 1408 peak and lacks the ambiguity of the $^{152}$Eu-$^{154}$Eu(122) composite. Also the internal standard $^{144}$Ce of the fourth counts has better precision, relative to internal standard corrections for the first counts.

154Eu(8.5y) The 723 and 1274 keV peaks in the fourth counts are free of interferences, but very weak.

$^{153}$Gd(241.6d) The 97.4 and 103.2 keV peaks are very weak and necessitate a 48 hours count interval for each spectrum in the fourth count set. After six weeks cooling all $^{153}$Sm(103.2) has decayed away, while potential interferences of well separated $^{147}$Nd(91) and $^{169}$Yb(93.6) have become negligible. Both 97 and 103 keV peaks are comparably small. The reported concentration values represent the mean value based on both peaks.

$^{159}$Gd(18.6h) The 363.6 peak is weak, free of interferences, and serves as a consistency check for $^{153}$Gd derived results. Agreement is routinely within 20 %, enough to confirm the observed Gd anomalies (Chapter 6).

$^{160}$Tb(72.4d) When counting after 12 days there are no significant interferences for the peaks at 86.9, 298.6 and 879 keV. The 962 keV peak forms an unresolved doublet with $^{152}$Eu(964). Reported values are based on the the 299 keV peak in the fourth counts. A weighted mean of results from several peaks seems attractive.

$^{165m}$Dy(2.3h) During the 24 hours cooling period for the quartz vials this radionuclide has decayed away.

$^{166}$Ho(26.8h) The 80.6 keV peak in the first counts has a strong signal. Adjacent peaks of $^{153}$Sm(75.4, 83.4) are completely separated. This was verified by activation of a pure Sm standard and intercalibration of the resulting $^{153}$Sm spectrum with the sample spectra. On the other hand a minor peak at 80.1 keV of the $^{144}$Ce

internal standard coincides with the $^{166}$Ho peak. The following correction was applied:
From separate long counts of high doses $^{144}$Ce alone a count rate ratio

$$^{144}\text{Ce (80.1)} \;/\; ^{144}\text{Ce (133)} = 0.0097081$$

was established. The GAMANL net peak area of $^{144}$Ce (134) in the first counts was multiplied with this factor, and the resulting value for $^{141}$Ce (80.1) subtracted from the peak area reported for 80.6 keV by GAMANL. The final value of the true net peak area of $^{166}$Ho was used in further calculations. The correction routinely amounts to 1-2 %, and never exceeded 5 %, of the total peak area.

$^{171}$Er(7.5h) The 308 keV peak in the first counts coincides with a minor peak of $^{169}$Yb(307.7). The contribution of the latter was reconstructed from the $^{169}$Yb(307.7) / $^{169}$Yb(177) counting ratio in the third counts, and the $^{169}$Yb(177) peak in the first counts. With increasing time during the first count set it contributes 30 to 90 % to the total 308 keV peak. After this correction the first few counted

samples yield Er concentrations in the expected range, yet routine analyses of Er are not feasible. This Yb interference has not been reported in the literature. Occasionally published Er values based on gamma spectrometry are probably incorrect.

$^{170}$Tm(129d) The 84.3 keV peak in the fourth count set is rather small, but fully separated from the adjacent $^{160}$Tb(86.8) peak of similar magnitude.

$^{169}$Yb(32d) Estimates derived from the strong 177, 198, 308 keV peaks in the third counts are in good agreement with those derived from $^{175}$Yb.

$^{175}$Yb(4.2d) Strong peaks at 283 and 396 keV in the second counts are free of interferences and in excellent agreement with each other and the $^{169}$Yb derived estimates. The 396 keV peak is by far the largest of all and is used for the final data. Again a weighted mean of all five estimates would be feasible.

$^{177}$Lu(6.7d) The strong 208 keV peak in the second count is free of interference. Values for the same peak in the first and third counts serve as consistency checks.

Decay corrections

For a count set of nine samples, two standards and one blank, all net peak areas (including the $^{144}$Ce internal standard and the corrected $^{166}$Ho area) are converted to activities at a reference time $t_0$. Any point in time before the actual count set started would be suitable as a reference time. Yet for the sake of comparison with other count sets the endpoint of irradiation has been used consistently as reference time $t_0$.

For a given radionuclide the activity [dpm] at time $(t - t_0)$ past irradiation is given by

$$- \frac{dN}{dt} = \lambda N = \lambda N_0 \, e^{-\lambda(t - t_0)} \qquad (2.13.2)$$

which is a short version of equation 2.3.3, with

$N_o$ = number of radionuclide atoms at $t=t_o$

After multiplication with a factor ( $\epsilon$ x F ) for conversion from dpm to cpm,

where [cpm] = ( $\epsilon$ x F) x [dpm]
$\epsilon$ = absolute detector efficiency at keV of gamma peak
F = gamma ray intensity = number of gamma quanta per single decay event ($0<F\leq 1$) for given gamma peak of nuclide

one arrives at the corresponding activity [cpm]

$$-(\epsilon xF)\frac{dN}{dt} = (\epsilon xF)\lambda N = (\epsilon xF)\lambda N_o \; e^{-\lambda(t-t_o)} \qquad (2.13.3)$$

for a chosen gamma peak of the radionuclide of interest. This trivial factor ($\epsilon$xF) is eliminated again in below (2.13.7), and only carried along this derivation for the sake of correctness.
Rearrangement and integration with boundary conditions $(N_1,t_1)$, $(N_2,t_2)$ leads to

$$(\epsilon xF)\int_{N_2}^{N_1} dN = (\epsilon xF)\lambda N_o \int_{t_1}^{t_2} e^{-\lambda(t-t_o)} \qquad (2.13.4)$$

or

$$(\epsilon xF)(N_1 - N_2) = (\epsilon xF)N_o\,[e^{-\lambda(t_1-t_o)} - e^{-\lambda(t_2-t_o)}] \qquad (2.13.5)$$

where $t_1$ = begin of count interval
$t_2$ = end of count interval
$N_1-N_2$ = number of atoms decayed away during interval $(t_2-t_1)$

After multiplication with the ratio CT/LT for correction of dead time of the detector and rearrangement this leads to

$$(\epsilon xF)N_0 = \frac{(\epsilon xF)(CT / LT)(N_1 - N_2)}{[e^{-\lambda(t_1 - t_0)} - e^{-\lambda(t_2 - t_0)}]} \qquad (2.13.6)$$

Multiplication with decay constant $\lambda$ would yield an activity $\lambda(\epsilon xF)N_0$ (cpm) at $t_0$ for the chosen gamma peak. The above derivation is illustrated in Figure 2.13.2.

The first step of the computer program LANT/03 (see Appendix 9.1) is calculation of above term $(\epsilon xF)N_0$ from given values for

$(\epsilon xF)(CT / LT)(N_1 - N_2)$ = net peak area of chosen peak, as determined previously by GAMANL

$t_0$ = end of irradiation

$t_1$ = begin of counting

$t_2$ = $t_1$ + CT = end of counting interval

CT = count time [seconds]

LT = live time [seconds]

This is done for all chosen peaks (including the $^{144}Ce$ internal standard peak) in all spectra of samples, standards and blank from a given count set.

Internal standard corrections

Counting geometry errors are circumvented when the internal standard correction is made. Values of $(\epsilon xF)N_0$ for each activation produced gamma peak in a spectrum are divided by $(\epsilon xF)N_0$ of the $^{144}Ce$ in the same spectrum. The resulting ratio

$$\frac{(\epsilon xF)N_0 \text{ of REE-peak}}{(\epsilon xF)N_0 \text{ of } ^{144}Ce} = \frac{N_0(\text{REE-peak})}{N_0(^{144}Ce)} \qquad (2.13.7)$$

is proportional to the amount of the rare earth element in the sample or standard. The constant $(\epsilon xF)$ has also been eliminated from further calculations.

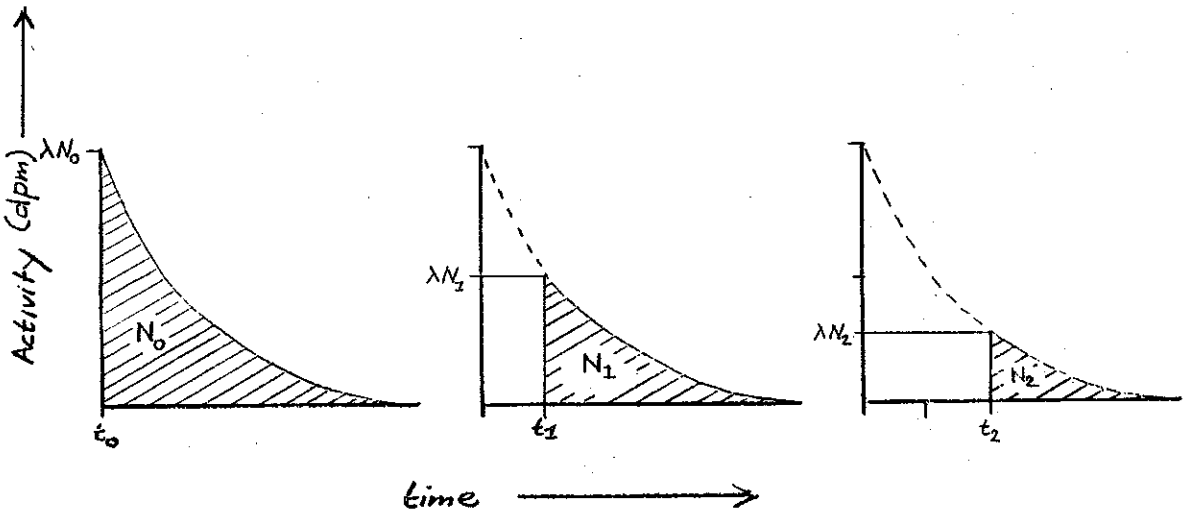


Figure 2.13.2. Exponential decay curve of a radionuclide. Activity $\lambda N$ (dpm) on the vertical axis as a function of time t. The area under the curve equals the number of atoms of radionuclide at given time t. Difference $(N_1-N_2)$ between areas under curve in second and third cartoon equals the number of atoms decayed away during count interval $(t_1-t_2)$. Multiplication with trivial factor $(\epsilon \times F)$ and dead time correction CT/LT yields the number of counts (net peak area) for chosen peak in gamma spectrum. Computer program back calculates $N_0$, or actually $(\epsilon \times F)N_0$, with equation (2.13.6).

Concentrations

Given two standards the program first takes the mean value of above ratio (2.13.6) for the two standards. Then the amount (pmol) of element in each sample (and blank) is calculated

$$\text{Amount(pmol)}_{\text{sample}} = \frac{[(N_0(\text{REE-peak}))/(N_0(144\text{Ce}))]_{\text{sample}}}{[(N_0(\text{REE-peak}))/(N_0(144\text{Ce}))]_{\text{mean (stds)}}} \times \text{Amount(pmol)}_{\text{standards}} \quad (2.13.8)$$

where the amount (pmol) in standards is a known quantity. Finally the concentration ($pmol.kg^{-1}$) is calculated by dividing by the weight (about 10kg) of the original seawater sample. Additional calculation of concentrations ratio's versus shales is optional.
The complete procedure is done for the second, third and fourth count sets. The program LANT/03 (Appendix 9.1) prints out the original input data, intermediate results like values for $(\epsilon \times F)N_0$ and the corrected $[N_0(\text{REE-peak})/N_0(144\text{Ce})]$, and finally concentration values as well as ratios versus shales.

Internal Standard Corrections First Counts

The first counts last only two hours and also have a high background. The $^{144}Ce$ internal standard signal is noisy, and calculation along above lines would yield limited precision. Therefore the high quality $^{140}La$ peak at 1596 keV is used instead as an internal standard, in combination with the $^{140}La/^{144}Ce$ ratio of the second count set. The underlying rationale is the fact that the number $N_0$ of $^{140}La$ atoms at $t_0$ should be the same in a given sample or standard, whether calculated from first count or second count. In this instance it is essential that both count sets are calculated back to the same reference time $t_0$.
Algorithms are as follows:
Values $(\epsilon \times F)N_0$ of each peak in each spectrum of the first counts, as calculated by the program LANT/03, are divided by $(\epsilon \times F)N_0(140\text{La}(1596))$ in the same spectrum. The resulting ratio is multiplied by the term

$$N_0(140\text{La}(1596))/N_0(144\text{Ce})$$

of the corresponding spectrum in the second counts, as provided by

LANT/03 output for the second count set. Then one arrives at a ratio

$$\frac{[(\epsilon \, xF)N_o(\text{REE-peak})]_{\text{first count}}}{[(\epsilon \, xF)N_o(^{140}\text{La}(1596))]_{\text{first cnt}}} \times \frac{[N_o(^{140}\text{La}(1596))]_{\text{second cnt}}}{[N_o(^{144}\text{Ce}]_{\text{second count}}} \qquad (2.13.9)$$

which is again proportional to the amount of rare earth element in the sample or standard. This value is then further processed just as described above under 'Concentrations' for the ratio (2.13.8) of the other count sets. Resulting concentration values ($pmol.kg^{-1}$) derived from $^{153}Sm$, $^{140}La(329)$, $^{140}La(487)$, $^{140}La(816)$ in the first counts are always in perfect agreement with corresponding values assessed from the second counts. This demonstrates that above somewhat indirect route for processing first count data is not only correct, but also yielding the desired good precision. After the decay corrections (equation 2.13.6) by the computer, the remaining calculations for first counts are rather simple. These were done with a small calculator, rather then setting up yet another program. While somewhat laborious, this procedure for the first counts is the only way to obtain good quality results for Pr and Ho, as well as important consistency checks for La, Ce, Sm, Eu, Gd, Yb, and Lu.

## 2.14. Standards

### Introduction

Standard solutions were prepared by dissolution of one gram chunks of each pure REE metal in about 1500 ml. dilute nitric acid. Aliquots of these solutions were combined into two different REE standard mixtures with elemental ratios resembling seawater and shales.

### Stock Solutions for Individual Elements

Wide neck, conventional PE, 2000 ml bottles (Nalgene, tar weight 220 ± 5 gram) were filled to the rim with 1N HCl (ACS reagent grade in Pyrex water), closed, and kept in a stove at 60 $^{o}$C for 24 hours. Then the bottles were stored upside down for 24 hours and allowed to cool to room temperature. After pouring out the dilute acid and a threefold rinse with Pyrex water the bottles and caps were allowed to dry overnight at 60$^{o}$C. Some 250 ml and 1000 ml LPE bottles (Nalgene) were treated similarly. Tare weights of the empty bottles with caps were determined on a Mettler PC 2200, Delta Range top loading balance, which was calibrated before and after the weighings versus NBS Class S weights (Table 2.14.1). Then the bottles were filled with approximately 800 ml. 1N $HNO_3$ (ACS Reagent Grade in Pyrex water). One gram chunks of each of the fourteen Rare Earth metals, stored under helium atmosphere in heatsealed Pyrex vials, were obtained from Ames Laboratory, Iowa State University. Each vial was broken open. The metal piece was taken out with cleaned plastic forceps and weighed quickly on a Mettler 10 gram capacity Microbalance in a room with constant temperature and humidity. The balance was calibrated before and after the weighings versus NBS Class S1 weights (Table 2.14.2.).

One would expect the metals to gain weight during handling due to surface formation of anion impurities (oxides, carbonates), but actually our values (WHOI) seem to be systematically lower than those reported by Ames (Table 2.14.2). Also the WHOI balance tends to give slightly elevated readings for the S1 calibration weights, which would further enhance the discrepancy. However in most cases the difference is still within the combined error limit of 2 x 0.00005 = 0.0001 gram. Differences of similar magnitude have previously been reported (WASSERBURG et al., 1981).

Then the metals were dumped in the dilute nitric acid in the 2000 ml bottles. With formation of bubbles the Eu dissolved within minutes, the La, Ce, Pr, Nd and Sm within about 30 minutes, and the remaining elements within 3-4 hours. Upon closer inspection the Ce solution contained very finely dispersed black particles which did not dissolve after addition of about 100 ml. concentrated (15.8 N) nitric acid and subsequent overnight storage of the whole bottle at 60°C. Drs. Gscheidner and Beaudry (Ames) did ascribe this persistent solid phase to an impurity, probably Ta, rather than a resistant oxide or nitrate of Ce, and kindly provided a new piece of refined Ce metal. This dissolved readily in 600 ml. 2.5N $HNO_3$ at 60°C within five minutes. The extra Ce solution with impurities was filtered over a 0.45 micron Nuclepore filter. The suspended matter was weighed and sent to Ames Laboratory for analyses (Table 2.14.3).
Then all solutions were diluted to about 1500 ml with Pyrex water and gross weights were determined with the top-loading balance (Table 2.14.4).

Minor calibration corrections ( 0.1 and 0.7 gram) of the top loading balance were made, but buoyancy corrections were deemed unnecessary as these effects are negligible. Molar concentrations of the stock solutions (Table 2.14.4) are based on the Ames values for weight and accuracy of the metal chunks. We further assumed that the NBS weights are absolute standards. Then the reproducibility of the top loading balance (0.01 gr. in 200 gram range, 0.1 gr. in 2200 gram range) and microbalance (0.00005gr., WHOI or Ames) can be treated as their accuracy which in further calculations was assumed to correspond with a one sigma standard deviation of a Gaussian distribution. Expected accuracy of the stock solutions, and any further dilutions or mixtures, were calculated with common methods for error propagation (BEVINGTON, 1969) and are listed as percentage standard deviation.

Standard Mixtures

In order to make up REE standard mixtures compatible with the naturally occurring even / odd predominance of atomic number (see 1.1), tenfold dilute (about 0.4 molar) stock solutions of Eu, Tb, Ho, Tm and Lu were prepared (Table 2.14.5). Aliquots of the 4M stock solutions were poured directly into clean, dry and preweighed 500 ml. or 1000 ml. LPE bottles, which were then filled with Pyrex water.

Subsequently two REE mixtures, 'Seawater Type' and 'Shale and Granite Type', were made up by pouring aliquots of the stock solutions (4N or 0.4N) of each element in 1000 ml bottles, which were then filled with Pyrex water and weighed (Tables 2.14.6 and 2.14.7). Distribution patterns of these mixtures are shown in Figure 2.14.1. The elements Pr, Nd, Gd, Ho and Tm with weaker signals in the INAA procedure are enhanced relative to their abundance in shales or seawater(Figure 2.14.1). At this point the elemental ratios of the standard mixtures are established. Further dilutions or transfers cause a further detioriation of the overall accuracy of each individual element. Yet the accuracy of elemental ratios will not be affected anymore.

The remainder of each of the 4N stock solutions was poured into five 250 ml LPE bottles, using a different clean and dry funnel for each element. Spilling of solution droplets on the bottle necks was avoided in order to prevent formation of deposits. Gross weights of full bottles with caps were recorded in order to guard against future evaporative weight loss. Then the caps were sealed with tape, and sets of fourteen stock solutions were delivered to Bacon, De Baar, Frey, Gromet and Thompson. The shale type REE mixture was divided similarly in four 250 ml aliquots and delivered to De Baar, Frey, Stockman and Thompson.

The seawater type mixture was diluted gravimetrically by pipetting 1012.5 $\pm$ 5 ug. (1000 $\pm$ 3 ul.) solution into a hot acid cleaned, dry and preweighed 500 ml. Teflon FEP bottle, using a 100 gram capacity Mettler microbalance which was calibrated versus Class S weights. Then the bottle was filled with 509.77 gram 0.5N $HNO_3$ and weighed on the top-loading balance (Table 2.14.8). The bottle is stored with a tape seal and its gross weight was recorded before and after aliquots were taken out in order to guard against evaporative losses.

Irradiation Standards

For each irradiation two standard were prepared by pipetting aliquots of this dilute solution into quartz vials. For each set of standards the pipette was calibrated gravimetrically with 0.5N $HNO_3$, for instance at 498.46 $\pm$ 1.67 mg., from which the amount [pmol.] of each element in the irradiation standards was calculated (Table 2.14.9). With the same pipette 500 ul aliquots of the $^{144}Ce$ internal standard spike solution

were added to both these standard vials and the seawater samples(see also section 2.6., final procedure). Combination of the two errors introduced by $^{144}$Ce-spike addition to standard and sample with the weighing error of the seawater sample leads to a lower limit representing the best possible accuracy for each element(Table 2.14.9). Of course the actual accuracy is lower, as a result of additional errors mostly arising from counting statistics, the latter also varying from element to element (section 2.15).

Old Standards

The above standards were used for the Pacific Ocean and Cariaco Trench data sets (chapters 4 and 5). For the Northwest Atlantic Ocean profile an older standard mixture, made available by Dr. F.A. Frey, was used. The results do not suggest a major deviation between the two standard mixtures. For instance, in all data the Gd anomaly is present. Nevertheless a future intercalibration between old and new standards would be of interest.

Calibration [grams] versus NBS Class S weights, before weighing:

| Nominal | Reading | Nominal | Reading | Nominal | Reading |
|---|---|---|---|---|---|
| 1.00 | 1.00 | 30.00 | 30.00 | 1000.0 | 999.6 |
| 2.00 | 2.00 | 50.00 | 49.99 | 1500.0 | 1499.4 |
| 5.00 | 5.00 | 100.0 | 99.96 | 1650.0 | 1649.3 |
| 10.00 | 10.00 | 150.0 | 149.94 | 1800.0 | 1799.2 |
| 20.00 | 20.00 | 300.0 | 299.99 | 2000.0 | 1999.2 |

Tare weights [gram] of 2000 ml. bottles after calibration corrections:

| | | | | | | | |
|---|---|---|---|---|---|---|---|
| La | 216.6 | Sm | 216.7 | Dy | 238.5 | Yb | 213.6 |
| Ce | 181.2 | Eu | 220.4 | Ho | 236.8 | Lu | 224.7 |
| Pr | 230.6 | Gd | 207.1 | Er | 225.2 | | |
| Nd | 218.1 | Tb | 225.7 | Tm | 210.3 | | |

Calibrations [grams] after weighing:

| Nominal | Reading | Nominal | Reading | Nominal | Reading |
|---|---|---|---|---|---|
| 150 | 149.9 | 215 | 214.9 | 225 | 224.9 |
| 200 | 199.9 | 220 | 219.9 | 230 | 229.9 |
| 210 | 209.9 | | | | |

TABLE 2.14.1. Tare weights of 2000 ml. bottles for REE stock solutions, corrected for shown calibration errors of toploading balance.

---

Calibration [gram] of WHOI microbalance versus NBS Class S-1 weights:

| Nominal | Reading | Nominal | Reading | Nominal | Reading |
|---|---|---|---|---|---|
| 0.020 | 0.02005 | 1.000 | 1.000015 | 1.050 | 1.050005 |
| 0.050 | 0.05000 | 1.001 | 1.001045 | 1.070 | 1.070055 |
| 0.100 | 0.09995 | 1.002 | 1.00201 | 1.100 | 1.0999995 |
| 0.200 | 0.20035 | 1.005 | 1.00505 | | |
| 0.500 | 0.50000 | 1.020 | 1.02007 | | |

Weights [gram] of chunks of Rare Earth metals:

| Element | Atomic weight | Ames | WHOI |
|---|---|---|---|
| La | 138.9055 | 1.07152 ± 0.00005 | 1.071545 |
| Ce | 140.12 | 1.03076 ± 0.00005 | 1.030525 |
| Pr | 140.9077 | 1.06704 ± 0.00005 | 1.06699 |
| Nd | 144.24 | 1.06510 ± 0.00005 | 1.06506 |
| Sm | 150.4 | 1.06760 ± 0.00005 | 1.067475 |
| Eu | 151.96 | 1.000 ± 0.005 | 0.9967 |
| Gd | 157.25 | 1.00829 ± 0.00005 | 1.00820 |
| Tb | 158.9254 | 1.05009 ± 0.00005 | 1.05000 |
| Dy | 162.50 | 1.08084 ± 0.00005 | 1.08072 |
| Ho | 164.9304 | 1.03735 ± 0.00005 | 1.03727 |
| Er | 167.26 | 1.09123 ± 0.00005 | 1.09122 |
| Tm | 168.9342 | 1.06600 ± 0.00005 | 1.06570 |
| Yb | 173.04 | 1.00717 ± 0.00005 | 1.007075 |
| Lu | 174.967 | 1.09282 ± 0.00005 | 1.09274 |

Calibration [gram] after weighing:

| Nominal | Reading | Nominal | Reading | Nominal | Reading |
|---|---|---|---|---|---|
| 1.000 | 1.0000 | 1.050 | 1.05000 | 1.100 | 1.099975 |
| 1.020 | 1.02004 | 1.070 | 1.07003 | | |

TABLE 2.14.2. Weights [gram] of pure Rare Earth metal pieces as estimated by Ames and WHOI. Atomic weights from LEDERER et al.(1978).

Weight [gram] Ce metal piece: Ames=1.01185 ± 0.00005 WHOI=1.01179
Weights [gram] of Nuclepore filters for removal of impurity:

| | Filter | Control Filter |
|---|---|---|
| Tare weight | 0.020712 | 0.02045 |
| Gross weight | 0.050381 | 0.02058 |
| Net impurity: | 0.029539 (after correction for control filter) | |

TABLE 2.14.3. The 3 % impurity in original piece of Cerium metal.

| Element | Gross weight bottle [gram] | Net weight of solution [gram] | Concentration [millimol/kg] | Accuracy as 1 sigma standard deviation [percent] |
|---|---|---|---|---|
| La | 1803.4 | 1586.8 | 4.861 | 0.029 |
| Ce | 1779.3 | 1598.1 | 4.602 | 0.028 |
| Pr | 1770.3 | 1539.7 | 4.918 | 0.029 |
| Nd | 1748.7 | 1530.6 | 4.824 | 0.030 |
| Sm | 1760.8 | 1544.1 | 4.597 | 0.029 |
| Eu | 1723.9 | 1503.5 | 4.36 | 0.50 |
| Gd | 1788.0 | 1580.9 | 4.056 | 0.029 |
| Tb | 1814.9 | 1589.2 | 4.157 | 0.029 |
| Dy | 1757.0 | 1517.9 | 4.381 | 0.030 |
| Ho | 1783.2 | 1546.4 | 4.067 | 0.029 |
| Er | 1787.2 | 1562.0 | 4.177 | 0.029 |
| Tm | 1785.0 | 1574.7 | 4.006 | 0.029 |
| Yb | 1761.0 | 1547.4 | 3.761 | 0.029 |
| Lu | 1789.2 | 1564.5 | 3.992 | 0.029 |

Balance calibration [gram] after weighing:

| Nominal | Reading | Nominal | Reading | Nominal | Reading |
|---|---|---|---|---|---|
| 1650 | 1649.3 | 1720 | 1719.3 | 1760 | 1759.3 |
| 1680 | 1679.3 | 1730 | 1729.3 | 1780 | 1779.3 |
| 1700 | 1699.3 | 1740 | 1739.3 | 1800 | 1799.3 |
| 1710 | 1709.3 | 1750 | 1749.3 | 1830 | 1829.2 |

Gross weights of bottles corrected for 0.7 gram balance calibration.

TABLE 2.14.4. Concentrations[mmol/kg] of REE stock solutions.

| Element | Net weight of 4N stock [gram] | Net weight after dilution [gram] | Concentration [millimol/kg] | Accuracy as 1 sigma [percent] |
|---|---|---|---|---|
| Eu | 50.98 | 462.5 | 0.481 | 0.58 |
| Tb | 50.92 | 483.5 | 0.438 | 0.29 |
| Ho | 103.06 | 986.8 | 0.425 | 0.14 |
| Tm | 100.97 | 1015.3 | 0.398 | 0.15 |
| Lu | 95.32 | 994.1 | 0.383 | 0.16 |

TABLE 2.14.5. Tenfold diluted stock solutions of REE in nitric acid.

| Element | Net weight of stock solution [gram] | Concentration [micromol/kg] | Accuracy as 1 sigma standard deviation [percent] |
|---|---|---|---|
| La | 54.62 | 259.3 | 0.26 |
| Ce | 125.73 | 565.1 | 0.12 |
| Pr | 25.42 | 122.1 | 0.56 |
| Nd | 88.43 | 416.6 | 0.17 |
| Sm | 11.22 | 50.4 | 1.26 |
| Eu | 16.76 | 7.87 | 1.02 |
| Gd | 32.55 | 128.9 | 0.44 |
| Tb | 22.44 | 9.596 | 0.69 |
| Dy | 12.40 | 53.1 | 1.14 |
| Ho | 76.96 | 31.9 | 0.24 |
| Er | 12.12 | 49.4 | 1.17 |
| Tm | 41.88 | 16.3 | 0.37 |
| Yb | 12.36 | 45.4 | 1.15 |
| Lu | 22.16 | 8.28 | 0.66 |

Net weight full bottle = (1122.0 - 98.1) = 1023.9 gram

TABLE 2.14.6. Concentrations [micromol./kg.] of REE in 'Seawater' type mixture.

---

| Element | Net weight of stock solution [gram] | Concentration [micromol/kg] | Accuracy as 1 sigma standard deviation [percent] |
|---|---|---|---|
| La | 120.21 | 574.9 | 0.129 |
| Ce | 199.78 | 904.5 | 0.088 |
| Pr | 44.81 | 216.8 | 0.32 |
| Nd | 160.02 | 759.5 | 0.10 |
| Sm | 36.84 | 166.6 | 0.39 |
| Eu | 44.24 | 20.93 | 0.66 |
| Gd | 29.27 | 116.8 | 0.49 |
| Tb | 34.86 | 15.02 | 0.50 |
| Dy | 20.91 | 90.13 | 0.68 |
| Ho | 57.70 | 23.99 | 0.29 |
| Er | 10.97 | 45.08 | 1.29 |
| Tm | 28.94 | 11.34 | 0.51 |
| Yb | 11.91 | 44.07 | 1.19 |
| Lu | 18.43 | 6.938 | 0.78 |

Net weight full bottle = (1116.9 - 100.46) = 1016.45 gram

TABLE 2.14.7. Concentrations [micromol./kg.] of REE in 'Shale and Granites Type' mixture.

| Element | Concentration [picomol./gram] | Accuracy as 1 sigma standard deviation [percent] |
|---|---|---|
| La | 515.02 | 0.57 |
| Ce | 1122.4 | 0.52 |
| Pr | 242.51 | 0.75 |
| Nd | 827.5 | 0.53 |
| Sm | 100.04 | 1.36 |
| Eu | 15.64 | 1.14 |
| Gd | 256.07 | 0.67 |
| Tb | 19.06 | 0.86 |
| Dy | 105.4 | 1.25 |
| Ho | 63.41 | 0.57 |
| Er | 98.20 | 1.27 |
| Tm | 32.36 | 0.63 |
| Yb | 90.18 | 1.25 |
| Lu | 16.45 | 0.83 |

1.0125 $\pm$ 0.005 gram 'Seawater Type' mixture in 509.77 gram 0.5N $HNO_3$.

Table 2.14.8. Concentrations [picomol. $gram^{-1}$] of Rare Earth Elements in 1000-fold dilution of 'Seawater Type' mixture.

| Element | Amount in each irradiation standard [picomoles] | Accuracy as 1 sigma standard deviation [percent] | Lower limit of overall accuracy as 1 sigma standard deviation [percent] |
|---|---|---|---|
| La | 256.75 | 0.60 | 0.64 |
| Ce | 559.5 | 0.55 | 0.60 |
| Pr | 120.9 | 0.77 | 1.10 |
| Nd | 412.5 | 0.77 | 1.09 |
| Sm | 49.87 | 1.37 | 1.58 |
| Eu | 7.79 | 1.15 | 1.39 |
| Gd | 127.6 | 0.69 | 1.04 |
| Tb | 9.50 | 0.88 | 1.17 |
| Dy | 52.53 | 1.26 | 1.48 |
| Ho | 31.61 | 0.58 | 0.98 |
| Er | 48.95 | 1.28 | 1.50 |
| Tm | 16.13 | 0.65 | 1.02 |
| Yb | 44.95 | 1.26 | 1.49 |
| Lu | 8.201 | 0.85 | 1.15 |

Table 2.14.9. Typical amounts of each Rare Earth Element in irradiation standards, calculated for 498.46 mg. of the 1000-fold dilute solution. The lower limit of overall accuracy includes additional errors resulting from $^{144}Ce$-spike additions to standard and sample, as well as the weighing error of the seawater sample.

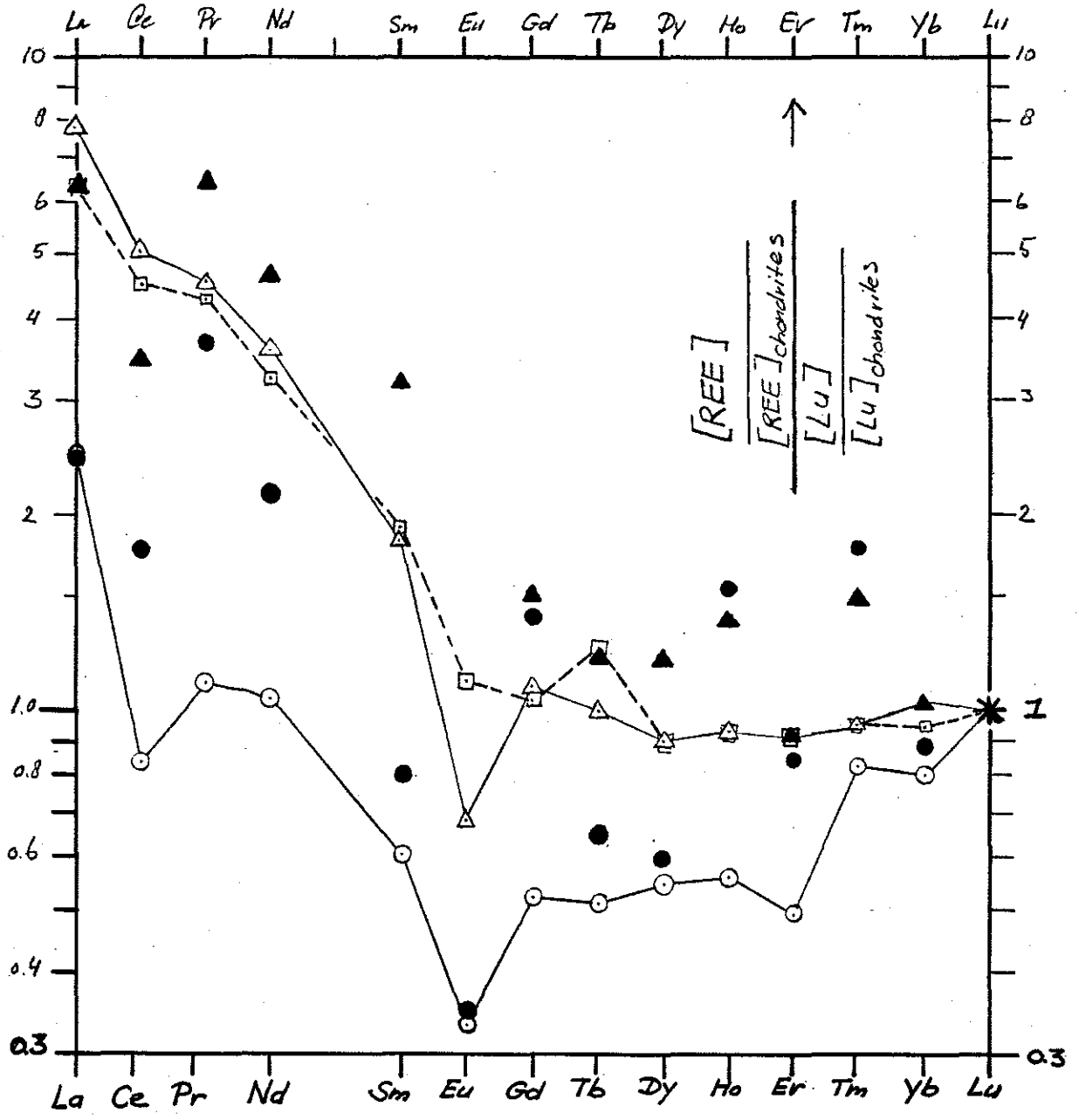


FIGURE 2.14.1. Abundances of Rare Earth Elements in two standard mixtures relative to a chondritic average (Herrmann, 1970) and normalized to Lu=1.0. The elements Pr, Nd, Gd, Ho and Tm with lower sensitivity in INAA determinations are enhanced in both standard mixtures, relative to the 'average' compositions of shales, granites respectively seawater.

- ⊡---⊡ Granitic average (Herrmann, 1970; his Table 39,57-71-E-4)
- △—△ Average of North American Shales Composite, European Shales Composite and Russian Platform Average, calculated from Haskin and Haskin, 1966.
- ▲ 'Shales and Granites Type' standard mixture.
- ⊙—⊙ Average concentrations in the North Atlantic Ocean(Elderfield and Greaves, 1982; De Baar, Bacon and Brewer, 1983).
- ● 'Seawater Type' standard mixture.

## 2.15. Precision and Accuracy

### Sources of Error

All water samples were acidified on shipboard with 10ml 8N HCl per about 10 liters of seawater. The corresponding correction of about 0.1 percent was deemed negligible and not applied.

The empty and filled reservoirs for extraction (section 2.6) were accurately weighed on a triple beam balance with 1 gram precision. The combined errors of tare (1 kg) and gross (11 kg) weights yield an almost negligible contribution to the overall error.

For each 500 ul REE standard the volumetric error is estimated at 0.3 percent. The same error applies to the 500 ul $^{144}Ce$ radiotracer spike added to each sample and standard. The sum of all above errors is very small compared to the errors arising from the actual Neutron Activation Analysis itself. Disregarding the NAA errors (which are discussed below) a lower limit can be set for overall precision (about 0.5 %) and overall accuracy (0.6 - 1.5 %, varying from element to element, Table 2.14.9).

The NAA method has two principle sources of error:

i) variability of about 1-2 % of the thermal neutron flux

ii) uncertainty in the net peak areas of the gamma spectra.

The latter standard counting error $\sigma_n/N_n$ [%] of the net peak area is the combined error

$$\frac{\sigma_n}{N_n} = \frac{\sqrt{\sigma_g^2 + \sigma_b^2}}{N_n} = \frac{\sqrt{N_g + N_b}}{N_g - N_b}$$

of the standard deviations $\sigma_g$ and $\sigma_b$ of the gross peak area and the background area, where

$\sigma_g^2 = N_g$ = gross number of counts

$\sigma_b^2 = N_b$ = number of counts in background

$N_n = N_g - N_b$ = net peak area.

Values for $\sigma_n/N$ as reported by GAMANL (2.12) vary between 0.1 and 5 percent for peaks of different elements. The overall counting statistics error in a reported concentration value consists of four such standard counting errors $\sigma_n/N_n$ from:

1) net area of given element peak in sample spectrum
2) net area of 144Ce internal standard peak in sample spectrum
3) net area of given element peak in standard spectrum
4) net area of 144Ce internal standard peak in standard spectrum

and varies from element to element. In other words:

$$\left(\frac{\sigma_n}{N_n}\right)_{counting}[\%] = \sqrt{\left(\frac{\sigma_n}{N_n}\right)_1^2 + \left(\frac{\sigma_n}{N_n}\right)_2^2 + \left(\frac{\sigma_n}{N_n}\right)_3^2 + \left(\frac{\sigma_n}{N_n}\right)_4^2} \quad (2.15.2)$$

Combination with above 0.5 % lower limit due to weighing and pipetting errors yields the overall precision:

$$\text{precision } [\%] = \sqrt{\left(\frac{\sigma_n}{N}_{counting}\right)^2 + (0.05)^2} \quad (2.15.3)$$

which again varies from element to element. Combination of the latter with the accuracy of the standards solution (Table 2.14.8) yields the overall accuracy.

The decay time corrections (section 2.13) are based on two measured time intervals:

CT = count time ($10^4$ - $10^6$ sec. $\pm$ 1 sec)

LT = live time ( same )

and the recorded point in time $t_1$ ($10^5 \pm 0.1$ minutes) when counting starts. Although values for CT and $t_1$ show up in exponentials (equation 2.13.5) their contribution to the overall error is deemed negligible.

Calculation along above lines of precision and accuracy for a given data set has yet to be done.

Replicate Analyses

The very first successful analyses were done on a set of six replicate samples of unfiltered Sargasso Sea surface water. Samples and standards were processed without $^{144}Ce$ internal standard. The errors arising from such internal standard are deemed smaller than the counting geometry errors. As a result the overall error in the set of replicates is probably higher than for the other data sets reported in chapters 3, 4 and 5. Also for the latter data the counting procedures were more refined.

| | 1 | 2 | 3 | 4 | 5 | 6 | SIGMA |
|---|---|---|---|---|---|---|---|
| | | | | [picomol/kg] | | | [%] |
| La | 13.9 | 10.9 | 13.0 | 13.0 | 13.4 | 13.1 | 3 |
| Ce | 14.1 | 13.1 | 12.1 | 13.2 | 12.4 | 12.7 | 6 |
| Nd | 12.6 | 7.7 | 17.6 | 12.9 | 13.4 | 13.7 | 4 |
| Sm | 2.9 | 1.9 | 2.2 | 2.8 | 2.7 | 2.8 | 3.5 |
| Eu | 0.79 | 0.51 | 0.61 | 0.76 | 0.77 | 0.79 | 2 |
| Gd | 4.7 | 0.83 | 3.2 | 4.6 | 4.3 | 4.6 | 4 |
| Tb | 0.73 | 0.47 | 0.51 | 0.69 | 0.72 | 0.72 | 2.3 |
| Yb | 3.9 | 2.5 | 2.8 | 3.6 | 3.6 | 3.7 | 3.8 |
| Lu | 0.61 | 0.42 | 0.47 | 0.59 | 0.56 | 0.60 | 3.4 |

Table 2.15.1. Replicate analyses of six (1 to 6) surface water samples of the Sargasso Sea. Values for samples 2 and 3 are consistently too low. The standard deviation SIGMA was calculated for the other four samples 1, 4, 5, 6 only.

The results (Table 2.15.1) agree well for four samples (1, 4, 5, 6) but are consistently too low for the other two (2, 3). Apparently some of the latter had been lost in one of the numerous sample transfers. Here again the internal standard would have been useful because such loss would have canceled out in the internal standard correction. Excluding the latter two samples, the standard deviations range between 2 and 5 percent. When normalized versus shales, this average of four samples (1, 4, 5, 6) has the typical seawater pattern (Figure 6.8).

Summary

Further efforts towards assessing overall precision are highly desirable. During the past period the procedures were continuously improved and upgraded. Therefore the overall precision is indeed expected to be better than 5 percent, yet further proof has to be provided by:

- error calculations from counting statistics
- another set of replicate analyses
- intercalibrations with Elderfield and co-workers.

## 2.16. Blanks

Low overall blanks (1-2 % for La, lower for the other REE) were usually, but not always achieved. For instance in the Cariaco Trench data set the blanks for La and Ce (Nd, Sm) are too high (chapter 5). Circumstantial evidence suggests that a batch of Ultrex sulphuric acid may have been the source of this blank. When blanks were encountered they always exhibited a smooth distribution vs. shales, with highest values for La and rapidly decreasing values for Ce, Pr, Nd, Sm, Eu and Gd. The heavier REE (Tb-Lu) were hardly discernible. This suggest that these are true REE blanks, rather than interferences produced from fission of $^{235}U$. In the latter case one would find a dominant $^{141}Ce$ signal, an absence of both $^{142}Pr$ and $^{152}Eu$ and also a very strong $^{239}Np$ peak. So far we have demonstrated that measurements of the REE in seawater can be made, although contamination occurred occasionally. The next step is another round of upgrading the laboratory so that contamination-free measurements can be achieved routinely.

## 2.17. Sensitivity

The detection limit for gamma counting is usually defined as two times the standard deviation of the background. However in our spectra the background is almost completely generated by REE isotopes themselves. In other words, at lower REE concentrations the background will also be lower, and although the relation is not proportional, the standard deviation of the background will also be smaller. In various spectra for reagent blanks, the stronger peaks of La, Sm, Eu, Yb and Lu were easily discernable at 1-2 percent of the levels in typical samples. Especially the four La peaks of about equal size are diagnostic, because they can be assigned unequivocally to La.

## 2.18. Summary

Methods have been developed for the determination of twelve out of fourteen REE in seawater. A large variety of problems was encountered during this period. As a matter of fact some problems were assigned highest priority and consequently other aspects still need some more attention. For instance the expected precision better than 5 % has to be verified.

# 3. RARE EARTH DISTRIBUTIONS WITH A POSITIVE CERIUM ANOMALY IN THE NORTHWEST ATLANTIC OCEAN *)

## 3.1. Abstract

From the vertical distributions of the rare earth elements (REE) in the Sargasso Sea we now report the first profiles of Pr, Tb, Ho, Tm and Lu in seawater, together with profiles for La, Ce, Sm, Eu and Yb. The first observations of positive cerium anomalies in seawater are ascribed to reducing inshore sediments as a source for Ce (DE BAAR et al., 1982). All vertical profiles are consistent with adsorption of trivalent rare earths by settling particles, possibly siliceous or calcareous, followed by their release at or near the seafloor on dissolution of the carriers. The very different Ce profile demonstrates the additional effects of oxidation and reduction reactions.

## 3.2. Introduction

The work reported here, earlier studies of Nd/Sm isotope systematics (PIEPGRAS et al., 1979; PIEPGRAS & WASSERBURG, 1980, 1982), and the recently reported profiles (ELDERFIELD & GREAVES, 1982) of nine REE demonstrate the renewed interest in the REE in the oceans. All REE exist essentially in the trivalent oxidation state, and their chemical properties vary gradually along the series (WEDEPOHL, 1978). However, unlike the other REE, Ce can be oxidized to a highly insoluble (BAES & MESMER, 1976) tetravalent state, and reduction of europium to a divalent state may also occur. Many other trace elements in seawater such as Mn (KLINKHAMMER, 1980; LANDING & BRULAND, 1980, 1981), Fe (LANDING & BRULAND, 1980, 1981; GORDON, MARTIN & KNAUER, 1982), Cr (EMERSON, CRANSTON & LISS, 1979), As (ANDREAE, 1981), Sb (ANDREAE, 1981), Se (MEASURES & BURTON, 1980) and I (WONG, 1980; ELDERFIELD &

*) This chapter, except for section 3.4. and the Gd-data (see also chapter 6) has previously been published (see Appendix 9.3).

TRUESDALE, 1980) are affected by their multiple oxidation states. Yet Ce and Eu are unique, because anomalies can be quantitatively defined by comparison with their neighbours within the REE series. Thus one can potentially single out oxidation-reduction reactions of Ce and Eu from all other processes affecting their distributions.

## 3.3. Methods

Seawater samples (4 l) were collected in August 1980. The water was pumped through a CHELEX-100 chromatography column for extraction of REE and separation from the major ions (KINGSTON et al., 1978). After subsequent purification by cation (STRELOW et al., 1965) and anion (KORKISCH & ARRHENIUS, 1964) exchange, the samples are analyzed with neutron activation followed by gamma spectrometry on a Ge(Li) detector. An overall chemical yield of 100.0% was demonstrated with radiotracer experiments. Precision (1 sigma) estimates for La, Ce, Sm, Eu, Tb, Yb and Lu range from 2 to 5 percent. Full details of methods and reproducibility are reported in chapter 2.

## 3.4. Hydrography.

Seawater samples (4 l) were collected, not filtered as to avoid contamination, and acidified to pH=2 during Oceanus cruise 86, August 1980. The 4460m deep station is located in the Sargasso Sea (33°58'N, 58°05'W) nearby GEOSECS (BAINBRIDGE, 1981) station 120 (33°16'N, 56°33'W). Major hydrographic features are depicted in Figure 3.1. Below the surface mixed layer the potential temperature ($\theta$) versus salinity (S) plot exhibits a linear section from 120m to about 800m, a distinct break at about 900m and another fairly linear section from 1000m downward. Most of the water beneath the Two Degree Discontinuity (S=34.905 $^{o}/oo$ at about 3650m) is of northern origin (Denmark Strait Overflow Water), as the central Atlantic water (AABW) is more or less bounded by a front (BROECKER & TAKAHASHI, 1980, 1981) extending southwestward from its 33°N, 50°W intersection with the GEOSECS transect (BROECKER, TAKAHASHI & STUIVER, 1980). Yet small but distinct decreases in oxygen ($O_2$), salinity, and an increase in silicate (Si) are

observed in plots versus θ, and less than one quarter (BROECKER & TAKAHASHI, 1981) of the bottom water may still be of Antarctic origin. The North Atlantic Deep Water (BROECKER & TAKAHASHI, 1980) proper, extending upward until about 4°C (S=34.996 °/oo at about 1580m) exhibits rather uniform profiles of θ, S, $O_2$ and nutrients. Yet plots versus θ reveal the core of DSW at 2.3° (3250m) by small maxima in S (34.996 °/oo) and $O_2$ (276μmol/kg) and a diffuse silicate minimum. The Iceland-Scotland overflow Water is characterized by a weak phosphate maximum (1.37umol/kg) at about 2.85° (S=34.95 at about 2800m). A very distinct Si-minimum (13.4 μmol/kg) in plots versus θ (4.08°) or S (34.996) labels the Labrador Sea Water at about 1600m depth. Although the Mediterranean Overflow Water has been traced as far as Bermuda (WORTHINGTON, 1976), we have no evidence for such a component at our station. The Western North Atlantic Water which spans the main thermocline up to 18° very closely follows the description of WORTHINGTON (1976). The distinct Si-maximum (15.5μmol/kg at 900m) is too small to be accounted for by any water (AAIW) of southern origin (BROECKER & TAKAHASHI, 1981). Only a thin slice of Eighteen Degree Water at about 110m depth seperates the main thermocline from the upper mixed layer. Salinity, temperature and the 50m depth of the mixed layer represent typical (ROBINSON et al., 1979) summer values for the Sargasso Sea. This water has been transported northward and warmed up along with the Gulfstream during the late spring/early summer (ROBINSON et al., 1979). Presumably a few months before the same parcel was travelling through the Florida Straits.

## 3.5. Results.

The first detailed profiles for Pr, Tb, Ho, Tm and Lu, as well as profiles for La, Ce, Sm, Eu, Gd, and Yb are shown in Figure 3.2. Concentrations of Lu, Tm and Tb, as well as Eu (ELDERFIELD & GREAVES, 1982), are typically less than 1 $pmol.kg^{-1}$ and are among the lowest reported thus far (MEASURES & EDMOND, 1982; LEE, 1982) for any non-radioactive element in seawater. The vertical profiles, except that of cerium, exhibit a consistent, fairly linear, increase with depth, as also observed in the eastern North Atlantic (ELDERFIELD & GREAVES,

1982). At both locations the lightest REE exhibit the strongest gradient with depth. The increasing trend with depth bears a faint resemblance (ELDERFIELD & GREAVES, 1982) to the distribution of nutrients, especially silicate. However, the following dissimilarities suggest that most of the processes governing the REE transport cycle are different from those controlling the nutrients. In the upper waters the REE and nutrient profiles diverge appreciably, the nutrients decreasing to very low values (Figure 3.1), whereas the REE continue their linear trend all the way up to the sea surface (Figure 3.2). Thus any incorporation of the REE into biogenic phases does not seem to exert a dominant control on their vertical distributions. For depths below 1000m, a plot of the heaviest rare earth, Lu, versus silicate (not illustrated) showed a linear relationship with a strong positive correlation ($r=0.997$, $P<0.001$). Because silicate is an approximately conservative tracer in the deep northwest Atlantic (BROECKER, TAKAHASHI & STUIVER, 1980; BROECKER & TAKAHASHI, 1980, 1981; EDMOND et al., 1979; NEEDELL, 1980; SPENCER, 1972), this result suggests that removal of Lu is slow compared to local renewal rates of the deep water masses. However, plots of the other REE versus silicate showed increasingly negative curvature with decreasing atomic number, indicative of efficient scavenging for the lighter REE relative to Lu. This observation and the heavy REE enrichment discussed below are consistent with adsorptive scavenging (CRAIG, 1974; SCHINDLER, 1976; BALISTRIERI et al., 1981) over the entire water column, combined with a release at or near the seafloor. The noted (ELDERFIELD & GREAVES, 1982) similarity with some profiles of Cu and Al, as well as Be, is also compatible with these abiotic processes (MEASURES & EDMOND, 1982; BOYLE, SCLATER & EDMOND,1977; BRULAND, 1980; HYDES, 1979).

Our Ce profile differs dramatically from that reported by ELDERFIELD & GREAVES (1982) and the profiles of the other REE. It shows high values in the mixed layer, a rapid decline to a minimum at mid depth, and then again an increase towards the seafloor (Figure 3.2).

3.6. Discussion.

Further discussion of our results for Ce and the other REE is best done with reference to their relative abundance patterns (Figure 3.3) which exhibit four major features:

1) An enrichment of the heavy relative to the light REE, in accordance with earlier observations (ELDERFIELD & GREAVES, 1982; GOLDBERG et al., 1963; HOGDAHL et al., 1968). The Lu/La ratio in the upper water column is about four times higher than in shales. Heavier REE are believed to be stabilized in seawater due to formation of stronger inorganic complexes (TURNER, WHITFIELD & DICKSON, 1981), so the lighter REE are expected to be scavenged more efficiently (SCHINDLER, 1976; BALISTRIERI et al., 1981) by adsorption on settling particles. This is the same effect as inferred from our comparisons with silicate discussed above and was first suggested by GOLDBERG et al. (1963). One would expect sinking particulate matter to exhibit light REE enrichments, but this has yet to be verified. With Ce disregarded, the REE patterns (Figure 3.3) in the upper 1,000m are very similar. However, from about 1,000m downward a minimum tends to develop at about Sm and Eu. This could be due to injection of a light REE enriched fraction released from dissolving biogenic particles at or near the seafloor. Most probably the relative rates of adsorption and desorption determine the shape and location of the minimum in the REE pattern for a given parcel of water.

2) Positive Gd anomalies at all depths, as discussed in chapter 6.

3) Absence of a significant Eu anomaly at all depths. Concentrations of Eu and Sm are almost perfectly correlated ($r=0.998$, $P<0.001$), with a ratio Sm/Eu=4.6, close to the value of 4.7 for shales (HASKIN & HASKIN, 1966). The small Eu anomaly reported recently (ELDERFIELD & GREAVES, 1982) appears to be related to a similar anomaly in a terrestrial aerosol source (RAHN, 1976). Thus far there is no clear evidence for reduction of Eu in seawater, although one might expect Eu

anomalies to develop in strongly reducing environments such as anoxic basins or hydrothermal vents (EDMOND et al., 1979).

4) The first observation of distinct positive Ce anomalies in seawater. Our neutron activation procedure yields data for both adjacent elements in the series, La and Pr, thus allowing us to define this anomaly quite precisely:

$$\text{Ce anomaly} = Ce/Ce^* = 2(Ce/Ce_{shale})/(La/La_{sh} + Pr/Pr_{sh}) \qquad (3.6.1)$$

where Ce* is the hypothetical concentration that a strictly trivalent Ce would have, as interpolated from La and Pr. In the mixed layer cerium is 2-3 times enriched (positive anomaly) relative to La and Pr. The anomaly drops off rapidly with depth until the transition from positive to negative values at about 250m (Figure 3.4). The ratio Ce/Ce* then gradually diminishes to produce the well known (ELDERFIELD & GREAVES, 1982; GOLDBERG et al., 1963; HOGDAHL et al., 1968) three- to four-fold depletion at depth. The negative Ce anomaly indicates enhanced removal of dissolved trivalent Ce as a result of oxidation to a highly insoluble (BAES & MESMER, 1976) tetravalent state. In principle one can quantify the net effect of this oxidation by employing a modified version of the vertical scavenging model (CRAIG, 1974). Scavenging rate constants $\Psi_{REE}/\Psi_{Lu}$ relative to the most conservative element Lu can be assessed. Thus various assumptions (e.g., an absolute value of the upwelling velocity w) necessary for derivation of an absolute scavenging rate constant $\Psi_{REE}$ [year$^{-1}$] are not required. Preliminary calculations (see appendix 9.2) for the deep water (below 1000m) suggest that La and Pr are removed about twice as fast as Lu, but that Ce is removed about four times as fast as Lu. From the following relationship

$$\frac{\Psi_{Ce(total)}}{\Psi_{Lu}} - \frac{\Psi_{Ce(oxid)}}{\Psi_{Lu}} = \frac{\Psi_{Ce(ads)}}{\Psi_{Lu}} = \frac{1}{2}\left(\frac{\Psi_{La}}{\Psi_{Lu}} + \frac{\Psi_{Pr}}{\Psi_{Lu}}\right) \qquad (3.6.2)$$

it is thus suggested that the change in oxidation state approximately doubles the removal efficiency for Ce at our station.

The positive Ce anomaly in surface waters is a new observation. The vertical profiles of Ce (Figure 3.1) and especially the Ce anomaly (Figure 3.3) are strikingly similar to open ocean profiles of Mn (KLINKHAMMER, 1980; LANDING & BRULAND, 1980, 1981), suggesting that similar mechanisms govern both elements. The surface maxima found for Mn have been attributed to either aeolian (KLINKHAMMER, 1980) (or riverine (LANDING & BRULAND, 1980, 1981)) inputs or an injection from reducing inshore sediments (LANDING & BRULAND, 1980, 1981). In the eastern North Atlantic there is good evidence (ELDERFIELD & GREAVES, 1982) for an aeolian input of REE, as characterized by a shale type pattern. At our station, however, an aeolian input would have to be enriched with both Ce and heavy REE in order to match the observed pattern in the surface waters (Figure 3.3). This is conceivable, but there is presently no evidence supporting this hypothesis. The current, albeit very limited, data for aerosols (RAHN, 1976; BUAT-MENARD, 1979) exhibit shale type patterns instead. In analogy the only available data for rivers also exhibits shale type patterns (MARTIN et al., 1976), although fractionations may very well occur during estuarine mixing. For instance, the fluvial component of inshore sediments might exhibit a positive Ce anomaly.

Cerium anomalies, both positive and negative, have been observed almost exclusively within the marine environment. Therefore Ce fractionations are more likely to be the result of strictly marine processes. The following explanation of the observed cerium enrichments in surface waters depends entirely on such cycling of cerium within the ocean basins. All trivalent REE, including $Ce^{3+}$, are removed from seawater by adsorption. Additional removal of dissolved Ce(III) by oxidation to solid Ce(IV) is suggested by the calculations described above and the well documented Ce depletion of deep waters in other areas (ELDERFIELD & GREAVES, 1982; GOLDBERG et al., 1963; HOGDAHL et al., 1968). One would expect to find a positive Ce anomaly for the authigenic fraction of particles settling toward the seafloor, but this has yet to be verified. Post-depositional reduction to Ce(III) may occur in organic rich inshore sediments, at which point Ce behaves again as the other, strictly trivalent, REE. Nevertheless a regenerative flux of all REE (including $Ce^{3+}$) from these sediments would still carry the memory of

a positive Ce anomaly. Relatively slow oxidation rates (CARPENTER & GRANT, 1967; HIRANO & KOYANAGI, 1978), in analogy with manganese (MURRAY & BREWER, 1977), would allow some diffusion of dissolved Ce(III) across oxic surface sediment layers and subsequent lateral transport into the centre of the basin, leading to the observed enrichments in the surface waters. Then margin sediments would act as a source for both the positive anomaly and Ce itself. In surface water transects one expects both these properties, like Mn (LANDING & BRULAND, 1980, 1981), to decrease in an offshore direction as a result of oxidative scavenging removal. Similar trends have been demonstrated (BREWER & SPENCER, 1975) for $^{228}Ra$, the latter being removed by radioactive decay (KAUFMAN et al., 1973; LI, FEELY & TOGGWEILER, 1980). The sharp gradient of the Ce anomaly near the seafloor (Figure 3.4) may be ascribed to essentially the same mechanisms. Studies of REE distributions in surface water transects, pore waters and anoxic basins are necessary for further testing of the above mechanisms.

| Depth (m) | La | Ce | Pr | Sm | Eu | Gd | Tb | Ho | Tm | Yb | Lu |
|---|---|---|---|---|---|---|---|---|---|---|---|
| 10 | 15.0 | 86 | 4.5 | 3.7 | 0.78 | 4.9 | 0.75 | 1.8 | 0.74 | 4.3 | 0.68 |
| 48 | 12.0 | 80 | 2.95 | 3.35 | 0.75 | 4.6 | 0.73 | 1.5 | 1.0 | 5.1 | 0.78 |
| 95 | 12.3 | 42 | 3.0 | 3.0 | 0.60 | 4.9 | 0.69 | 1.55 | 0.675 | 3.8 | 0.61 |
| 143 | 12.9 | 30 | 3.4 | 3.65 | 0.75 | 5.2 | 0.68 | 1.8 | 0.925 | 4.6 | 0.72 |
| 493 | 16.7 | 23 | 3.4 | 3.4 | 0.70 | 4.7 | 0.69 | 1.7 | 0.76 | 4.1 | 0.66 |
| 643 | 17.8 | 18 | 4.05 | 3.2 | 0.65 | 4.5 | 0.68 | 1.5 | 0.615 | 3.9 | 0.64 |
| 793 | 21.3 | 16 | 4.0 | 3.2 | 0.64 | 4.2 | 0.79 | 1.5 | 0.73 | 4.05 | 0.68 |
| 992 | 22.2 | 15 | 4.0 | 3.5 | 0.73 | 4.4 | 0.77 | 1.9 | 0.95 | 5.1 | 0.85 |
| 1184 | 27.2 | 23 | 5.3 | 3.6 | 0.76 | 4.9 | 0.82 | 1.9 | 0.88 | 4.9 | 0.82 |
| 1377 | 26.2 | 15 | 4.1 | 2.8 | 0.60 | 4.0 | 0.67 | 1.8 | 0.655 | 3.7 | 0.83 |
| 1729 | 26.2 | 14 | 3.8 | 3.05 | 0.65 | 4.5 | 0.65 | 1.2 | 0.70 | 3.9 | 0.88 |
| 2490 | -- | -- | (7.2) | 3.3 | 0.72 | 6.3 | 0.78 | 1.6 | 0.89 | 5.0 | 1.10 |
| 2870 | -- | 20 | 5.3 | 3.5 | 0.80 | 6.1 | 0.80 | 1.6 | 0.90 | 5.2 | 1.17 |
| 3253 | 46.6 | 16 | 4.6 | 4.5 | 1.04 | 7.1 | 0.97 | 2.0 | 1.03 | 6.1 | 1.36 |
| 4309 | 83.8 | 44 | 10.7 | 7.9 | 1.67 | 11.1 | 1.57 | 2.65 | 1.27 | 7.3 | 1.59 |
| 4378 | 80.8 | 44 | 10.4 | 7.6 | 1.66 | 10.6 | 1.53 | 2.6 | 1.21 | 7.35 | 1.59 |
| 4426 | 82.2 | 55 | 10.3 | 7.75 | 1.65 | 12.7 | 1.40 | 2.5 | 1.14 | 6.95 | 1.54 |

Table 3.1 Total dissolvable concentrations [$10^{-12}$mol per kg seawater] of rare earth elements at a 4460 m deep Sargasso Sea station (33°58'N, 58°05'W).

Samples were left unfiltered in order to avoid contamination. The suspended particulate REE fraction has probably an order of magnitude lower concentration (Buat-Menard, 1979), was probably retained on the Chelex columns and was thus excluded from our analyses. Extractions and separations were done in a Class 100 clean air room using hot acid leached PE, Teflon and Pyrex labware. Our values for La, Ce, Sm, Eu and Yb are in agreement with the concentration ranges recently reported by others using different methods (Piepgras, Wasserburg, and Dasch, 1979; Piepgras and Wasserburg, 1980, 1982; Elderfield and Greaves, 1982; Masuda and Ikeuchi, 1979).

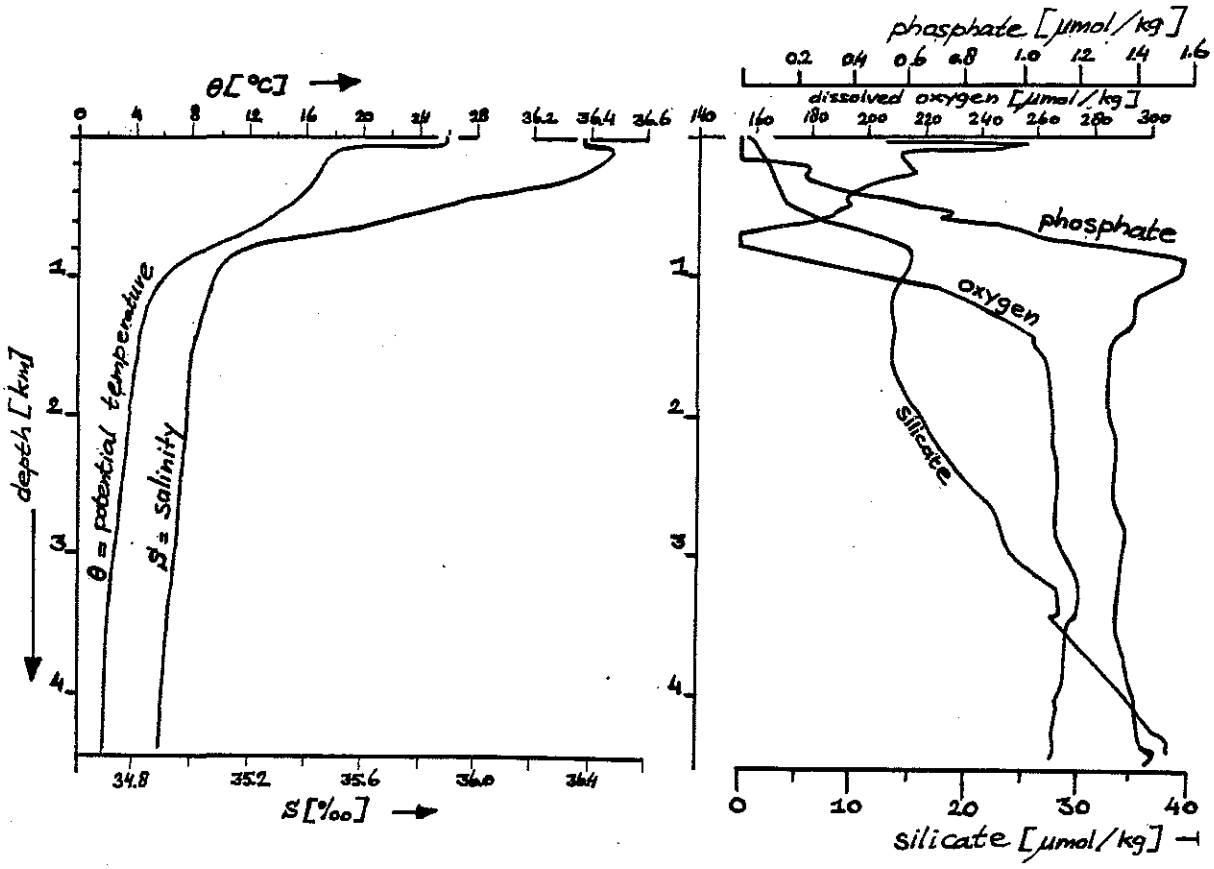


Figure 3.1. Hydrography of Oceanus 86/1 station 3 at 33°58'N, 58°,05'W in the Northwest Atlantic Ocean.

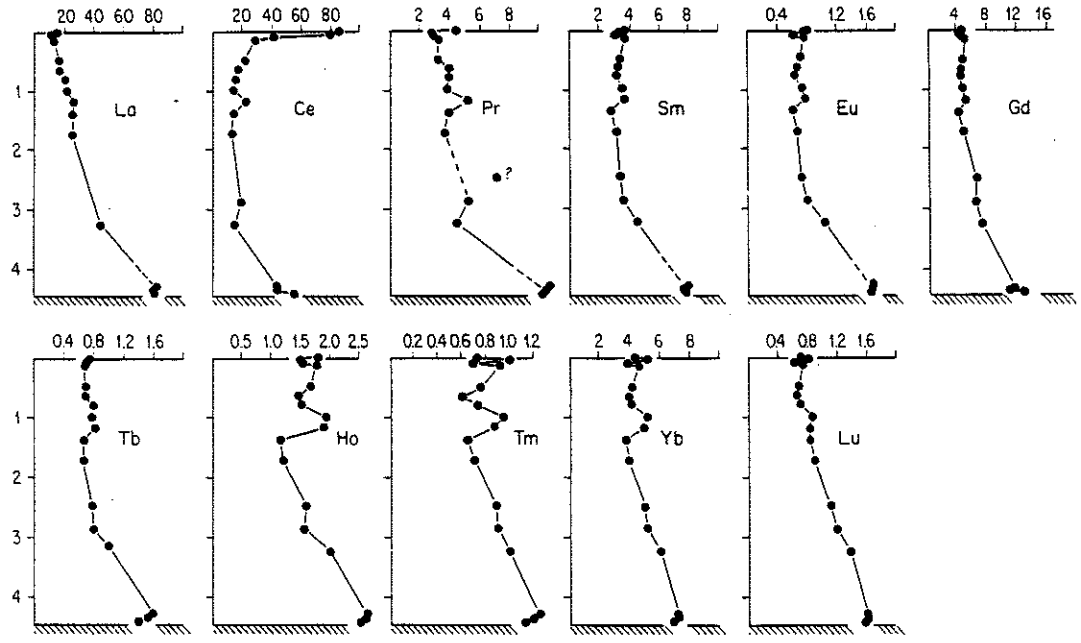


Figure 3.2. Profiles versus depth of rare earth elements in the northwest Atlantic Ocean. Some of the REE show a maximum at 1,184m depth where the hydrography is particularly complicated (BROECKER, TAKAHASHI & STUIVER, 1980; BROECKER & TAKAHASHI, 1981, EDMOND et al., 1979; SPENCER, 1972; WORTHINGTON, 1976). Mediterranean Overflow Water has occasionally been observed at similar depths in this region (WORTHINGTON, 1976), but is not clearly shown in our hydrographic data.

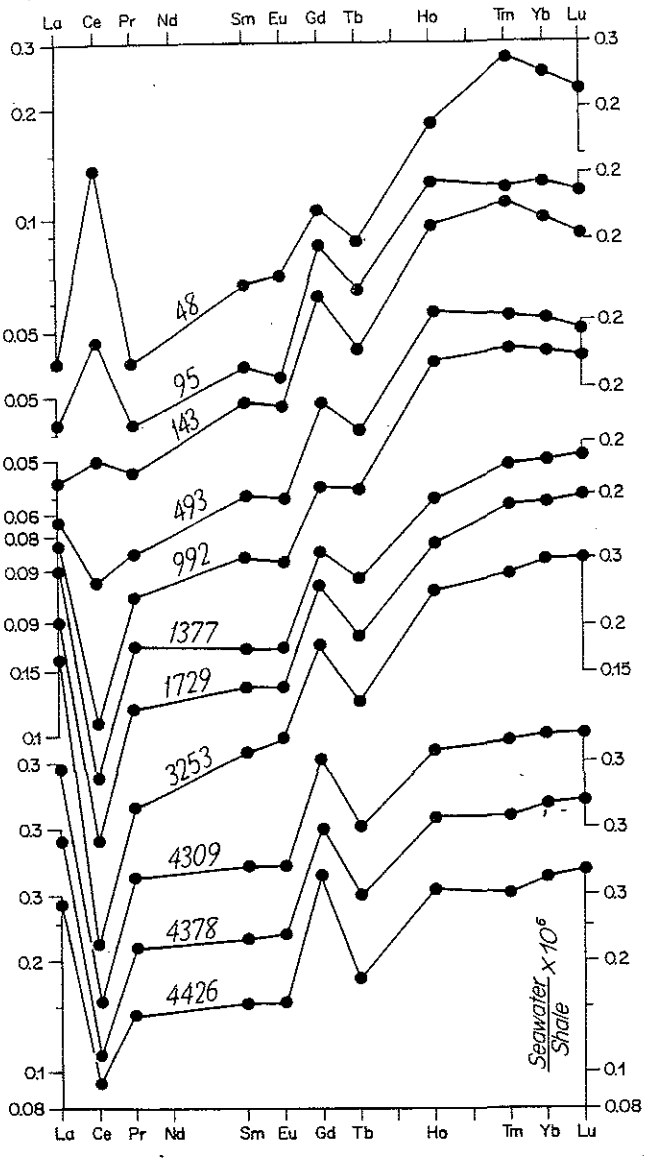


Figure 3.3. Distribution patterns of REE normalized versus shales (HASKIN & HASKIN, 1966) at selected depths. Offset vertical log- scales. Values for shales are thought to represent average abundances in the continental crust (WEDEPOHL, 1978). The limited data base (ELDERFIELD & GREAVES, 1982; Table 3.1), and the virtual absence of data for seawater dissolvable REE inputs (aeolian (RAHN, 1976; BUAT-MENARD, 1979), riverine (MARTIN et al., 1976), hydrothermal ?), do not yet allow definition of a more suitable REE normalization standard. The Gd excursions from a smooth curve are discussed in chapter 6.

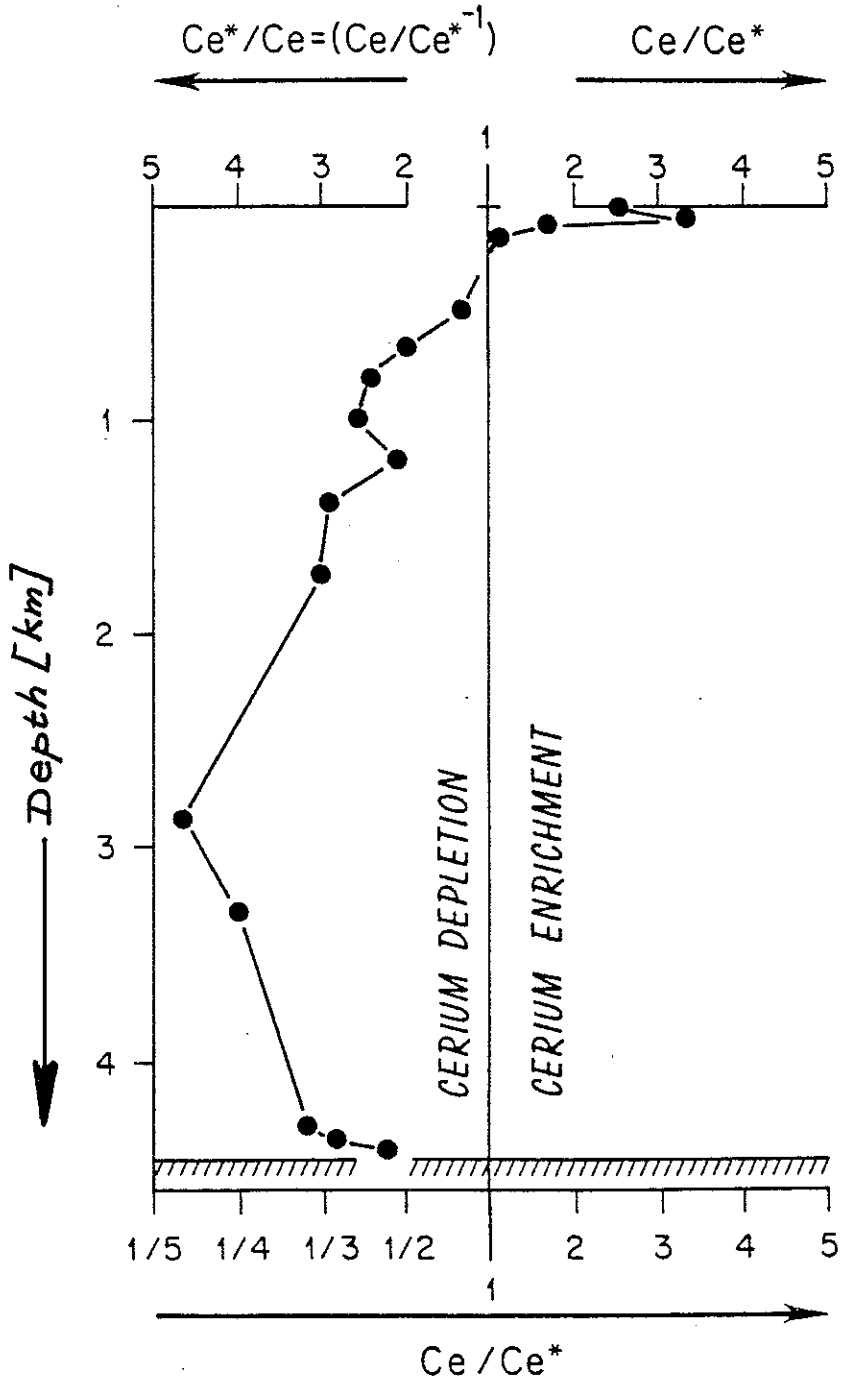


Figure 3.4. Profile versus depth of the cerium anomaly defined as Ce/Ce* (see text). Enrichment(positive anomaly) plotted as Ce/Ce*, depletion(negative anomaly) as its inverse Ce*/Ce.

# 4. RARE EARTH ELEMENT DISTRIBUTIONS in the EASTERN EQUATORIAL PACIFIC OCEAN

## 4.1. Abstract.

The first profiles of Pr, Tb, Ho, Tm, Lu, as well as profiles of La, Ce, Nd, Sm, Eu, Gd, Yb in the Pacific Ocean are reported. Concentrations of REE (except Ce) in the deep water are two- to threefold those observed in the deep Atlantic Ocean. Surface water concentrations are typically lower than in the Atlantic Ocean, especially for the heavier elements Ho, Tm, Yb and Lu. Ce is extremely depleted in the Pacific water column, but less so in the oxygen minimum zone. La acts somewhat independently from the other elements. The REE as a group, best represented by the suite Pr-Lu, are controlled by two simultaneous processes: (i)cycling like or identical to opal and calciumcarbonate, with circumstantial evidence in support of the latter as a possible carrier. (ii)adsorptive scavenging, possibly by manganese oxide phases. Combination of both apparent mechanisms, for instance scavenging of REE by adsorptive coatings on settling skeletal material, is conceivable.

## 4.2. Hydrography.

The VERTEX II site at about $18^{o}$N, $108^{o}$W was occupied during the November 10-18, 1981 period. Our samples were collected at different days at slightly different latitude and longitude due to the ships tracking of free floating sediment traps. The nearest coast is about 400 km eastward, Manzanillo, Mexico (Figure 4.1). Average water column depth in the area is around 4000m, with a depth of about 3560m at the station location.

The hydrography of the site has been described by BROENKOW & KRENZ(1982). It is an area of merging surface waters from:

(1) the California Current
(2) the Equatorial Countercurrent
(3) the Gulf of California.

Thus the VERTEX II study site is a region of surface convergence where the North Equatorial Current is formed (WYRTKI, 1967). Major subsurface water types are derived from the Pacific Subarctic water mass originating at about 50°N, and Equatorial Pacific water. The Equatorial Pacific water itself is a mixture of surface waters formed between 20°N and 18°S, Antarctic Intermediate Water (core depth at about 900m), and Antarctic circumpolar water below this depth (SVERDRUP et.al., 1942). The temperature-salinity diagram (Figure 4.2) shows several features pertinent to this discussion: the deep salinity minimum (6°C, 34.6 o/oo S) lies at a core depth of about 900m and is characteristic of Intermediate Water. The salinity maximum (12°C, 34.8 o/oo S) lies at a core depth of about 175m, and has been called Subtropic Surface Water by WYRTKI (1967). The California Current water forms a sharp salinity minimum (34.1 o/oo S) at about 70m in the northwest corner of the study area.

The most notable aspect of this area is the well developed oxygen minimum zone extending from 100m to 800m depth (Figure 4.9). Between these depths the oxygen concentration is less than 10 micromoles.kg$^{-1}$ (about 4 % saturation), but never below about 1.5 µmol.kg$^{-1}$ during this cruise. During other expeditions in the general area oxygen concentration below the 0.5 µmol.kg$^{-1}$ detection limit were often encountered, yet no hydrogen sulfide has ever been reported in these waters (CLINE & RICHARDS, 1972). The oxygen minimum waters lie between the Subtropical Subsurface and Intermediate waters in the area where the subtropical anti-cyclonic circulation does not penetrate (WYRTKI, 1967).

## 4.3. Results

Concentration values for 12 REE as determined for 10 ltr. samples of filtered seawater are listed in Table 4.1. All REE, except Ce, exhibit an increase with depth (Figure 4.3) not unlike the profiles of Ni and Pd at a nearby VERTEX II station (LEE, 1983). This was also observed for the REE in the North Atlantic Ocean (Chapter 3). However the gradient with depth is much more pronounced in the Pacific, especially for the heavier elements like Yb and Lu. In shale normalized distribution patterns for the deep water these heavy REE are very strongly enriched

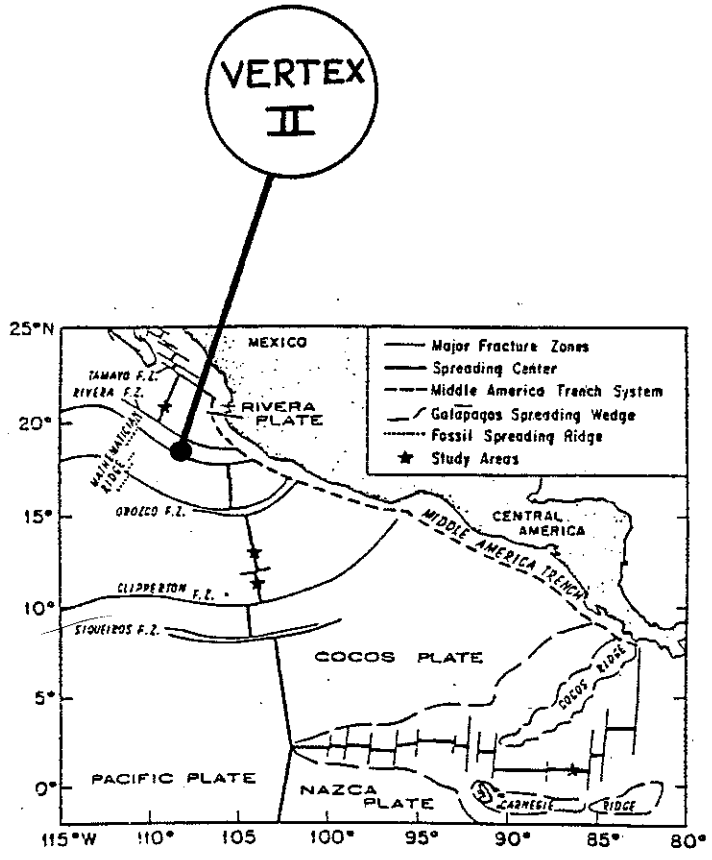


Figure 4.1. Station VERTEX II (18$^{o}$N, 108$^{o}$W) in the vicinity of the East Pacific Rise. Two areas of active hydrothermal circulation have been located at 13$^{o}$N, 104$^{o}$W and 21$^{o}$N, 109$^{o}$W. Taken from BALLARD & FRANCHETEAU(1982).

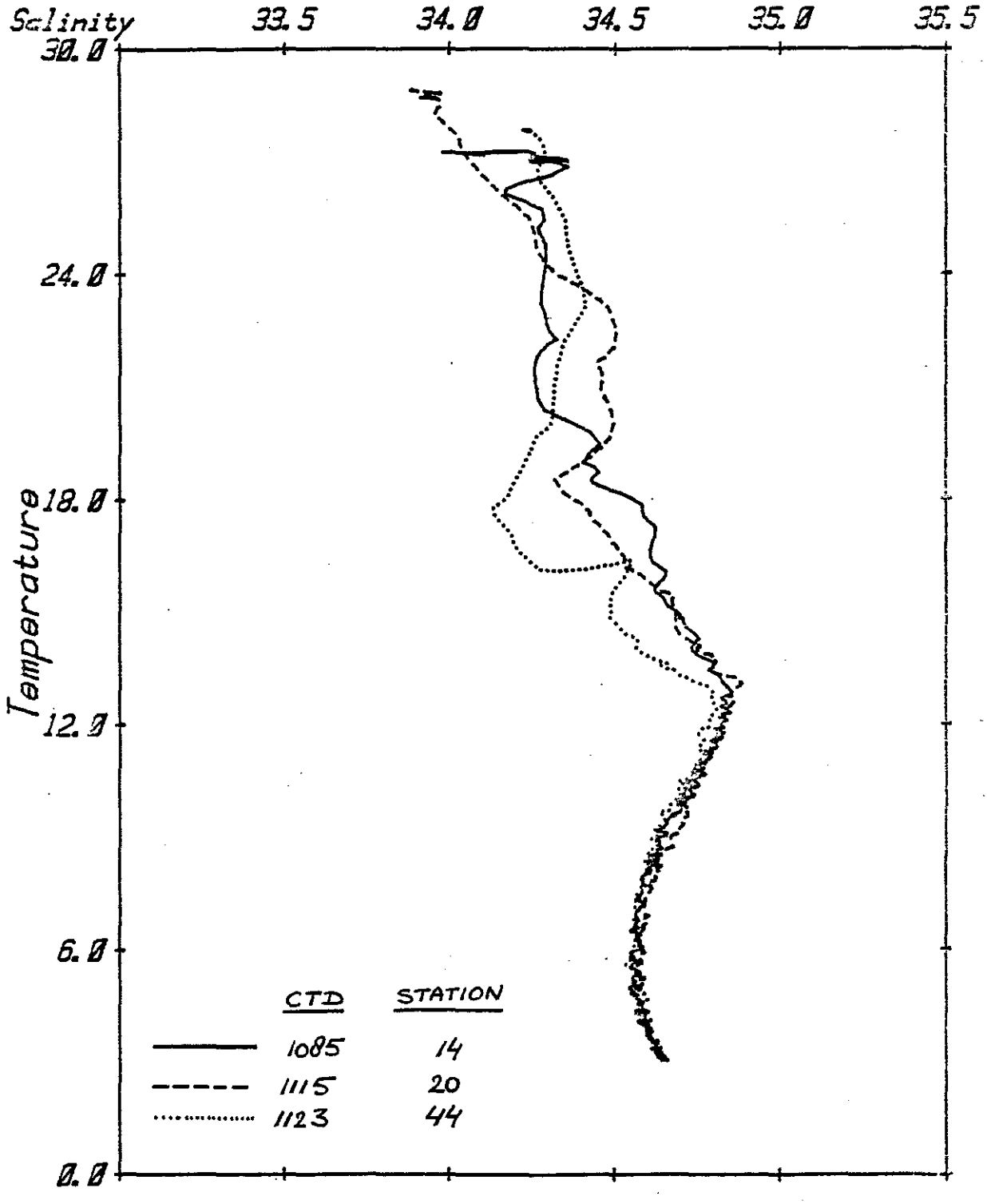


Figure 4.2. Salinity-temperature diagram at VERTEX II, November 4 to 14 1981. (Taken from BROENKOW & KRENZ, 1982).

| Depth [m] | La | Ce | Pr | Nd | Sm | Eu | Gd | Tb | Ho | Tm | Yb | Lu |
|---|---|---|---|---|---|---|---|---|---|---|---|---|
| 15 | 19 | 11 | 3.2 | 13 | 2.7 | 0.70 | 4.0 | 0.54 | 0.97 | 0.35 | 2.2 | 0.35 |
| 45 | 22 | 10 | 3.5 | 16 | 2.8 | 0.69 | 3.7 | 0.56 | 0.71 | 0.40 | 1.9 | 0.30 |
| 100 | 32 | 10 | 3.3 | 15 | 2.6 | 0.76 | 4.0 | 0.58 | 0.83 | 0.52 | 2.8 | 0.44 |
| 150 | 47 | 25 | 4.3 | 24 | 4.0 | 1.23 | 6.3 | 0.91 | 1.50 | 0.86 | 5.75 | 0.96 |
| 200 | 17 | 17 | 2.5 | 13 | 2.6 | 0.71 | 3.7 | 0.55 | 1.11 | 0.57 | 3.5 | 0.60 |
| 300 | 19 | 18 | 3.0 | 15 | 2.6 | 0.77 | 4.3 | 0.61 | 1.02 | 0.57 | 3.7 | 0.63 |
| 400 | 22 | 13 | 2.3 | 14 | 2.6 | 0.71 | 4.0 | 0.54 | 1.20 | 0.62 | 4.0 | 0.68 |
| 500 | 20 | 13 | 3.1 | 15 | 2.5 | 0.75 | 4.2 | 0.58 | 1.50 | 0.66 | 4.0 | 0.71 |
| 750 | 34 | 8.4 | 4.2 | 17 | 3.1 | 0.82 | 4.1 | 0.70 | 1.40 | 0.78 | 5.5 | 0.98 |
| 1000 | 35 | 7.4 | 7.6 | 34 | 6.4 | 1.56 | 8.6 | 1.41 | 3.52 | 1.84 | 13.2 | 2.44 |
| 1250 | 33 | 4.2 | 4.5 | 25 | 4.5 | 1.25 | 7.1 | 1.13 | 2.36 | 1.5 | 9.1 | 1.63 |
| 1500 | 44 | 11 | 6.5 | 22 | 4.7 | 1.16 | 5.2 | 0.97 | 2.05 | 1.0 | 7.3 | 1.31 |
| 1750 | 49 | 4.2 | 7.4 | 27 | 6.0 | 1.47 | 8.6 | 1.33 | 3.3 | 1.9 | 13 | 2.4 |
| 2000 | 46 | 5.3 | 5.6 | 24 | 5.2 | 1.30 | 7.2 | 1.12 | 2.8 | 1.5 | 11 | 2.0 |
| 2250 | 67 | 3.3 | 8.5 | 33 | 6.7 | 1.68 | 9.4 | 1.47 | 3.75 | 2.0 | 14 | 2.6 |
| 2750 | 63 | 2.9 | 8.9 | 42 | 9.0 | 2.32 | 13 | 2.01 | 4.4 | 2.5 | 17 | 3.1 |
| 3000 | 51 | 3.4 | 9.2 | 49 | 8.8 | 2.43 | 13 | 2.11 | 4.8 | 2.4 | 15 | 2.7 |
| 3250 | 67 | 2.9 | 7.0 | 41 | 7.7 | 2.15 | 12 | 1.81 | 4.0 | 1.95 | 13 | 2.3 |

Table 4.1 Concentrations [$10^{-12}$mol $kg^{-1}$] at given depths [m] for VERTEX II station (18°N, 108°W).

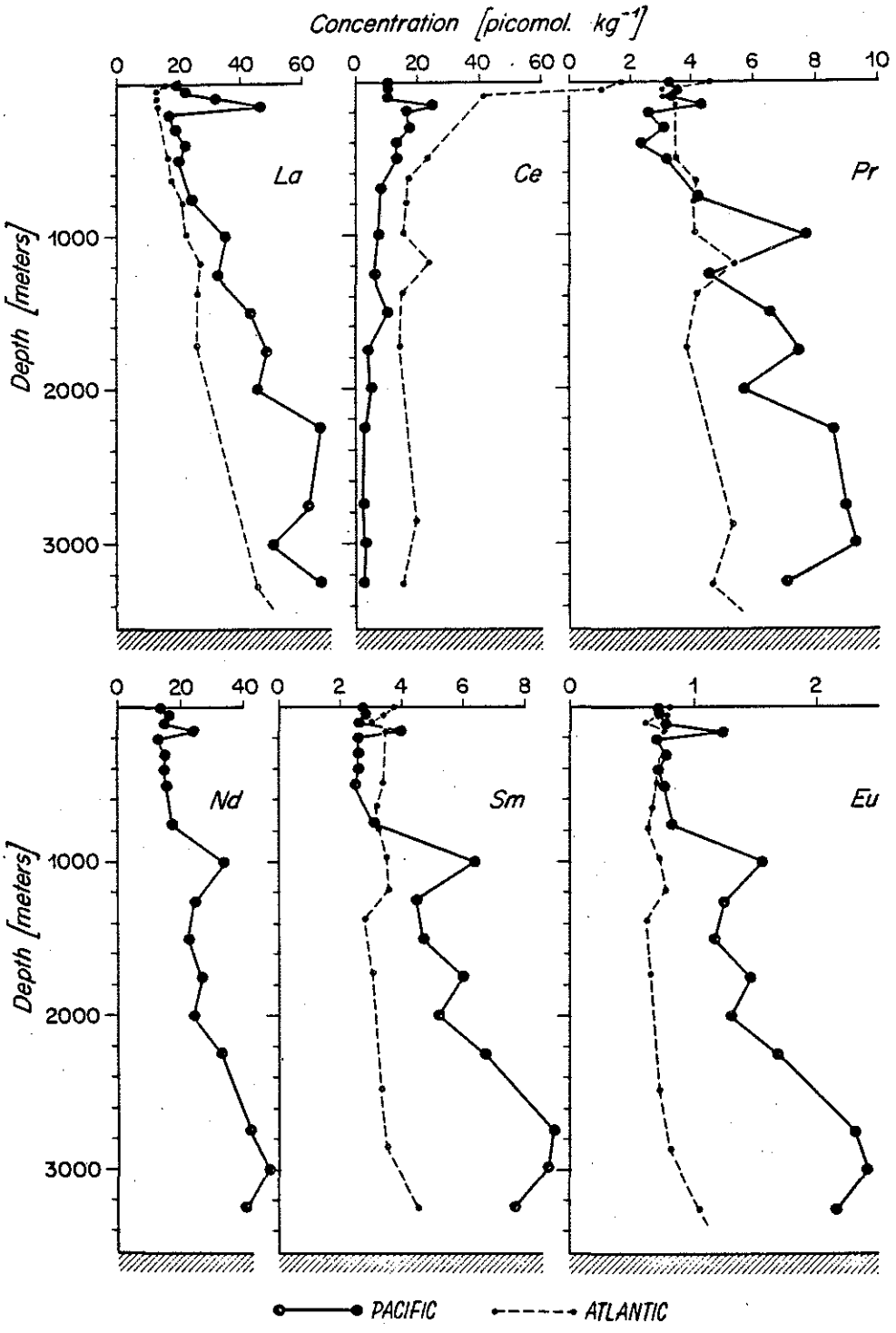


Figure 4.3. Vertical profiles of 12 Rare Earth Elements in the Eastern Equatorial Pacific Ocean. The dotted lines represent similar profiles in the Northwest Atlantic Ocean (see chapter 3).

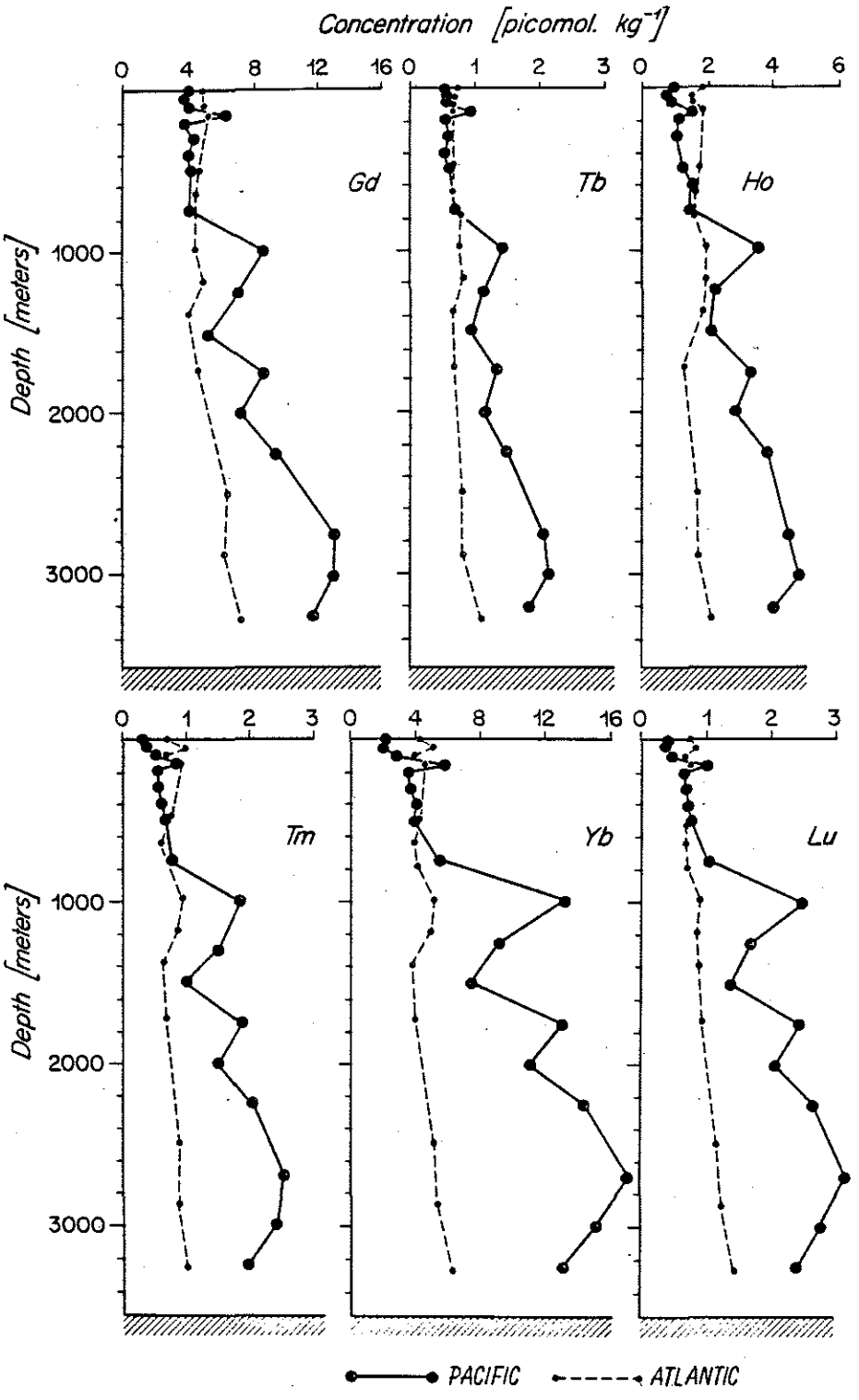


Figure 4.3. continued.

(Figure 4.4). The negative Ce anomaly observed over the whole water column increases with depth to very strong Ce depletions in the bottom waters. The Gd anomaly observed at all depths is ascribed to the unique properties of the $Gd^{3+}$-cation with exactly half filled 4f electron shell, as discussed in chapter 6. For all elements, except La and Ce (see below), the concentrations in the upper water column are at or below those in the Atlantic Ocean (Figure 4.3). These interoceanic differences are very apparent from plots of the Atlantic/Pacific concentration ratios at 'comparable' depths for each element (Figure 4.5).

The profiles in the upper 750m appear to be rather smooth, with the exception of a pronounced maximum at 150m depth. The latter may be explained either by physical, chemical or biological processes. As a hydrographic feature it roughly coincides with the salinity maximum at 175m which characterizes the core of the Subtropic Surface Water (WYRTKI, 1967). The linear trend over the 45-100-150m depth interval for La, as well as the four heavy REE (Ho, Tm, Yb, Lu), may indicate conservative mixing between S.S. Water and the overlying California Current water with a core depth of about 70m.

On the other hand this 150m maximum is only about 20m below the very pronounced oxygen minimum (Figure 4.9). Similar observations were made in the Cariaco Trench where all REE (except La and Ce) exhibit a pronounced increase just below the $O_2/H_2S$ interface (Chapter 5). At the Pacific station MARTIN and coworkers (in press) found broad, somewhat scattered maxima for Cu and Ag in the same 100-175m depth range and also a minimum at about 60m depth (Figure 4.6). Detailed sampling allowed them to demonstrate that these extrema are really connected by intermediate concentrations, and not just analytical artifacts. The same 150m depth is also marked by a distinct Fe maximum (LANDING, 1983), and sharp increases for Mn and Co which reach maximum values at about 300m depth (Figure 4.6). Scavenging of REE by Fe/Mn oxide surfaces on settling particles may explain the REE minima at 45m depth. Subsequent release of REE upon dissolution of the Fe/Mn oxide phases in the oxygen depleted zone may account for the REE maxima at 150m depth. Thus simple inorganic chemistry alone may account for the observed REE profiles in

the upper 750m of the water column. Of course the $O_2$ minimum is ultimately caused by biological processes, while the actual kinetics of the oxidation/reduction reactions may very well be controlled by bacterial mediation (EMERSON et al., 1982).

Finally more direct biological controls are also conceivable. The broad chlorophyll maximum which peaks at about 60m depth (Figure 4.6.) coincides with a grazing maximum and high heterotrophic production rates (KARL, unpubl. results). Maximum scavenging rates of $^{234}Th$ at the same depth range (BRULAND & COALE, in prep.) are consistent with the REE minima at 45m depth. High counts of dead cells at 120m (KNAUER, unpubl. results), maximum activity of cyanobacteria at 150m depth (KARL, unpubl. results) and the onset of nitrite production (LEE, C., unpubl. results) all suggest strong regeneration in that depth range, most probably accompanied by release of REE from various biogenous carriers. Depth and intensity of these zones of biological activity are also subject to diurnal variations (BROENKOW et al., 1983).

The vertical profile of Bi (LEE, 1982) also shows a distinct minimum at about 100-200m but then a very different much broader maximum over the 500-1500m range with highest values around 1000m, well below the maxima of Fe, Co and Mn (Figure 4.6).

From the 600-1000m range downward the Pacific concentrations begin to exceed the Atlantic values. Pacific deep water values are two to four times as high as in the Northwest Atlantic Ocean. At a first glance these interoceanic differences are not unlike those for the micronutrient elements. With respect to silicate the linear correlation:

$$Lu\ [pmol.kg^{-1}] = 0.0306\ Si\ [umol.kg^{-1}] + 0.435 \qquad (4.3.1)$$

for the North Atlantic Deep Water over the 981-4427m depth range was reported to be very close (r=0.994, Figure 4.7). The same correlation

$$Lu\ [pmol.kg^{-1}] = 0.036\ Si\ [umol.kg^{-1}] - 2.86 \qquad (4.3.2)$$

for the deep Pacific water (1250-3250m) is not nearly as good (r=0.8), mostly due to the scatter in the Lu-profile (Figure 4.3). Nevertheless a very similar ratio $Lu/Si = 0.03 \times 10^{-6}$ is found in both deep water

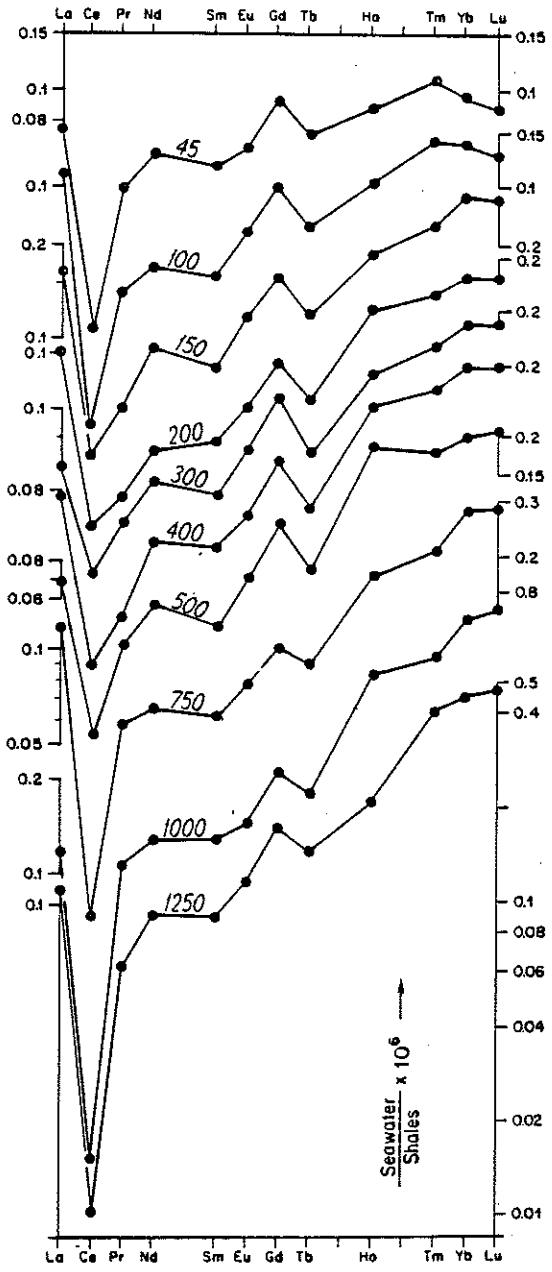


Figure 4.4. Distribution patterns of REE normalized versus shales at selected depth in the Pacific Ocean. Offset vertical log-scales. Note strong Ce depletions and heavy REE enrichments at greater depths, Gd excursions at all depths.

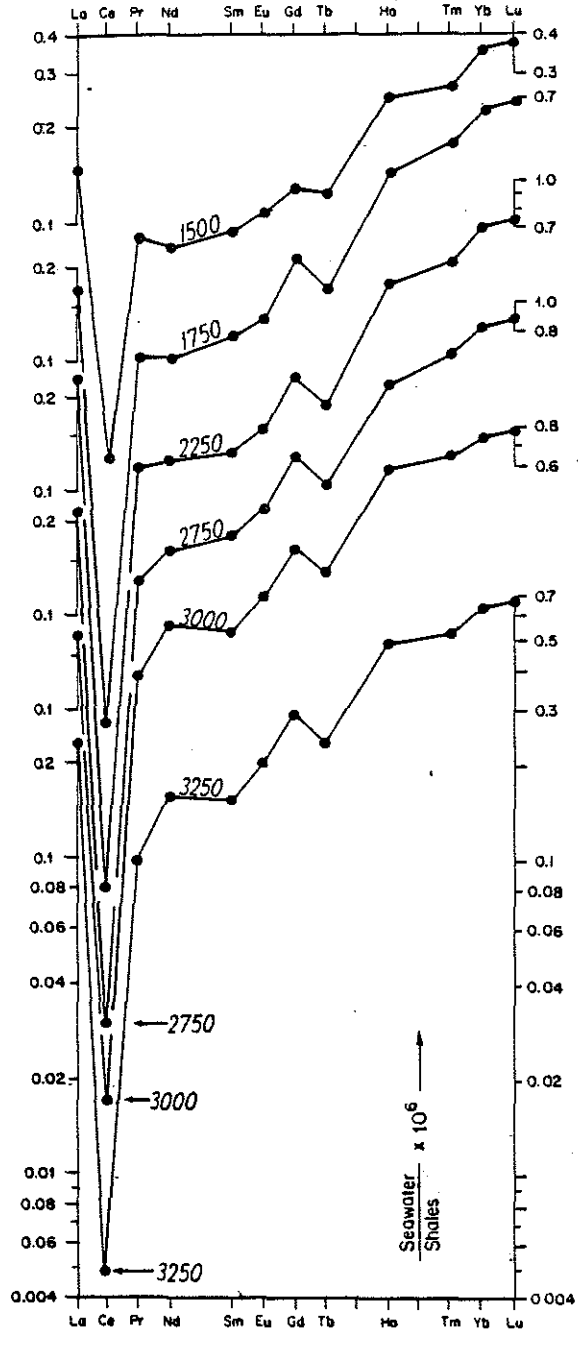


Figure 4.4. continued.

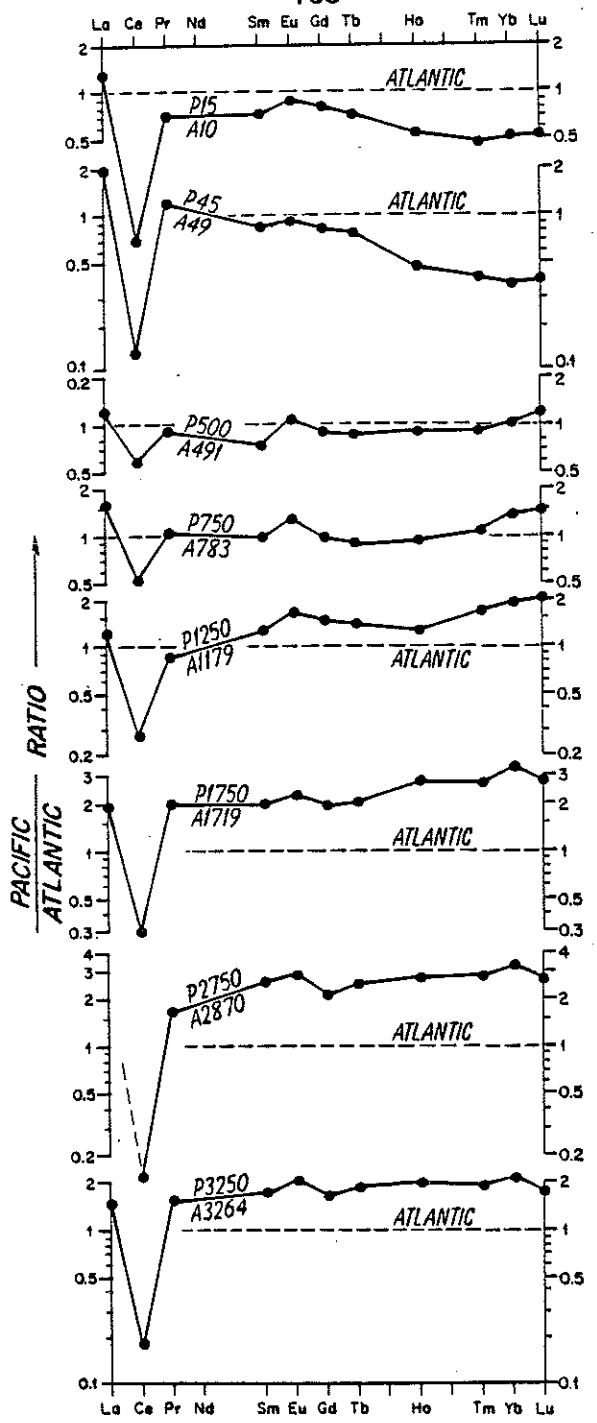


Figure 4.5. Pacific / Atlantic concentration ratios at selected representative depths. Pacific surface water is depleted relative to the Atlantic Ocean. The strong Ce depletion at this depth mostly results from the high positive Ce anomalies at the Northwest Atlantic station, which are probably not representative for average Atlantic surface waters. The breakeven point is at about 750m depth, from there downward Pacific deep water is highly enriched in all REE, except Ce which is strongly depleted.

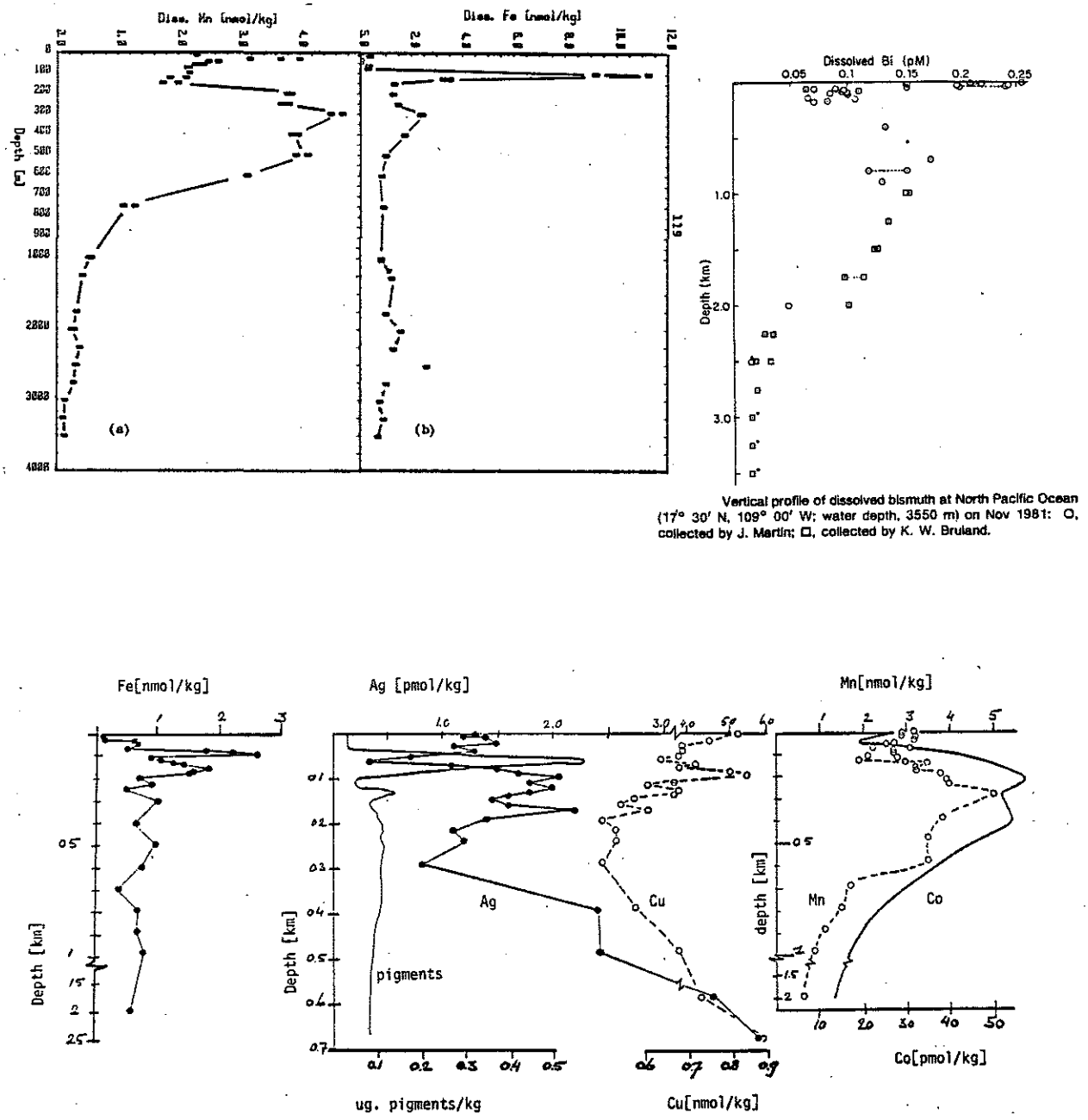


Vertical profile of dissolved bismuth at North Pacific Ocean (17° 30′ N, 109° 00′ W; water depth, 3550 m) on Nov 1981: O, collected by J. Martin; □, collected by K. W. Bruland.

Figure 4.6. Dissolved Fe, Mn (LANDING, 1983), Bi (LEE, 1982) and Fe, pigments, Ag, Cu, Mn, Co (GORDON et al., 1982; KNAUER et al., 1982; MARTIN et al., 1983; MARTIN & KNAUER, in press) at VERTEX II stations with slightly different locations, occupied at different days at the $18^{0}$N, $108^{0}$W site. Note the distinct Mn bulge at about 200-600m depth, as well as the strong Fe peak at about 100m depth in both data sets.

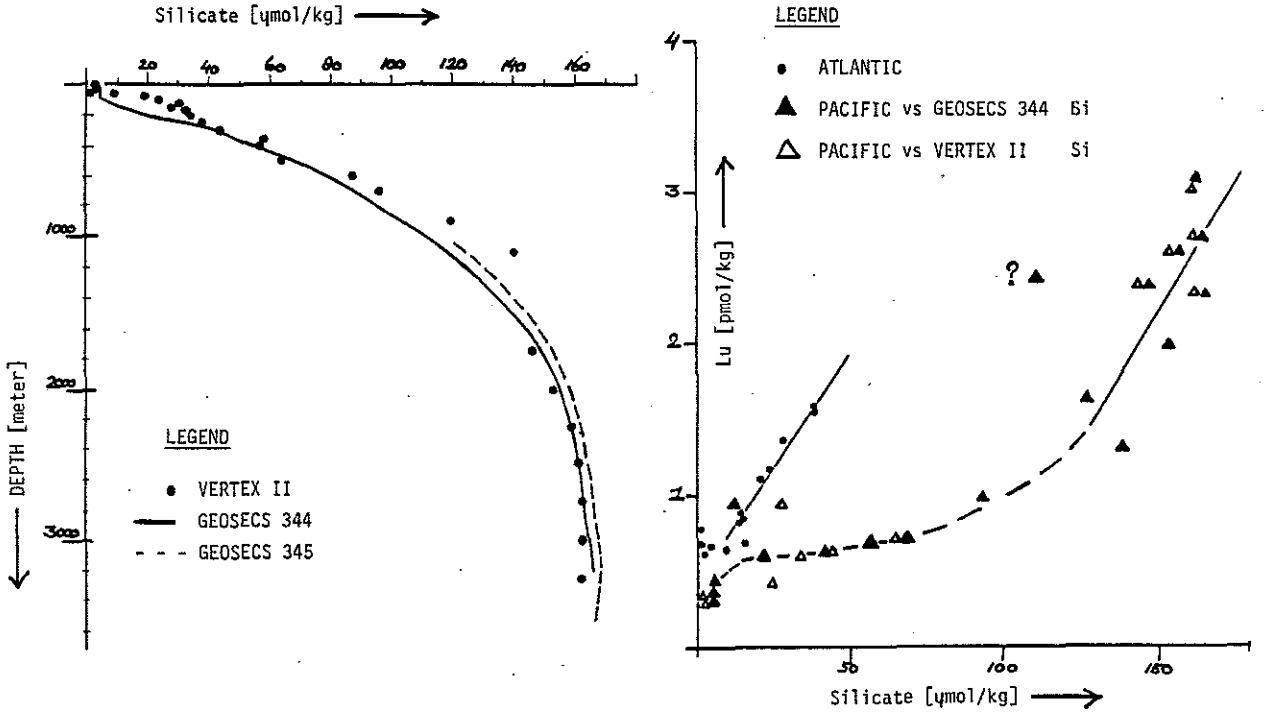


Figure 4.7. LEFT: Vertical profiles of silicate at GEOSECS stations 344 (19°30'N, 122°43'W), 345(22°31'N, 122°12'W) and VERTEX II (18°N, 108°W). Note the excursions of Si at VERTEX II, values lower in the eutrophic zone, higher in the Subtropic Surface Water, and a broad 'bulge' between about 800m and 1200m, at the depth range of the AAIW. GEOSECS data taken from CRAIG et al. (1981)

RIGHT: Lu versus Si in the Northwest Atlantic Ocean (34°N, 58°W) and the Eastern Equatorial Pacific Ocean. Pacific Si data, as interpolated along the smooth profile of GEOSECS 344, represented by black dots. Corresponding open dots represent VERTEX II samples for which Si data were also available.

masses. This correlation, albeit imperfect, suggests that the REE are at least to some degree involved in a regenerative cycle similar to the hard shell cycle of opal, calcite and aragonite in the oceans.

On the other hand there appears to be another quasi-linear Lu/Si section over the 200-750m interval (Figure 4.7), with a distinctly different slope (the Lu maximum at 1000m being disregarded). With increasing depth the Si increases dramatically in these intermediate waters, while the gradient of Lu is very small. In the upper water column of the Atlantic station the trend is similar, although less regular. Over the complete 200-3250m depth range the Pacific Lu/Si relation exhibits negative curvature, possibly suggesting preferential removal of Lu relative to Si over that 3000m depth range. Plots of lighter elements Nd, Sm, Tb and Yb versus Si are virtually identical to that of Lu/Si at the Pacific site. In contrast with the North Atlantic Deep Water there appears to be no negative curvature of the lighter REE versus Lu or Si in the deep Pacific water.

Curiously enough Lu, Yb and Tm do drop off to very low values in the upper 100m at the Pacific site, again not unlike silicate. Yet levels of intermediate REE (Nd, Sm, Eu, Tb) in the upper 100m are more or less the same as at greater (200-750m) depth.

The very strong REE-maxima at 1000m depth are somewhat disturbing. Similar maxima were also observed at the same depth range in the North Atlanic Ocean. Given above analogies with Si one is inclined to believe that these maxima are somehow associated with Antarctic Intermediate Water. At the Pacific site the AAIW indeed stretches from about 800 to 1200m, with a 900m core depth. However the origin of the broad Si 'bulge' at the same depth range has not yet been resolved Figure 4.7). The latitude of the North Atlantic station is believed to be too high for discerning AAIW from hydrographic tracers (chapter 3). Moreover its core depth would be below the depth of the observed REE maxima.

## 4.4. Discussion

### The Rare Earth Elements as a Group

Two different geochemical processes seem to have comparable impact on REE distributions within the oceans:

i) The first process is the continuous formation and dissolution of opal and calcite or aragonite skeletons. Shells are formed within the euphotic zone during plankton blooms, the latter varying in time and space. Some regeneration takes place during settling of the shells in the water column, yet most dissolution occurs at the seafloor. As a result silicate and total alkalinity, our indicators for dissolution of opal and $CaCO_3$, tend to increase towards the seafloor. Dissolution also varies in time and space, yet mixing and circulation of oceanic water masses largely cancel out such variability and leave us with very smooth lateral and vertical gradients of silicate and alkalinity. Oceanic distributions of the latter are primarily controlled by hydrography (EDMOND et al., 1979), although the ultimate driving force is of biogeochemical nature. Not surprisingly trace elements like Ba and Ra (CHAN et al., 1976,1977), Zn (BRULAND et al., 1978) and Ge (FROELICH & ANDREAE, 1981) seem associated very closely with this cycling of $CaCO_3$ (Ba?, Ra?) and opal (Ge). It is conceivable that these trace elements are taken up with a constant molar ratio versus Ca or Si when shells are being formed within the surface waters. However further studies of the skeletal materials and other particulate carrier phases are necessary.

Lacking alkalinity data for our stations only the correlation of Si with REE was discussed above. Given the analog oceanic distributions of Si and alkalinity the field data does not allow us to make a clear distinction between the opal or $CaCO_3$ phases as possible REE carriers.

However physico-chemical properties of the elements involved may serve as a guideline for further speculations. The ionic radii of trivalent REE cations, ranging from about 1.03A (La) to 0.86A (Lu) with small shifts depending on coordination number, are very close to the 1.00A radius of the $Ca^{2+}$-ion in its most commonly occurring sixfold coordination (Table 1.3.).

Substitution of Ca in calcite or aragonite seems very well possible, although incorporation of REE in opal cannot be ruled out. Preferential uptake of the heavier REE with smaller ionic radii seems consistent with the low surface water concentrations of Tm, Yb and Lu. In other words these heavier elements seem more strongly associated with the hard shell cycle than the lighter ones. This would also lead to preferential

downward transport of the heavy REE, i.e. a stronger heavy REE enrichment upon dissolution in the deep water (Figure 4.4). On the other hand La (r=1.06A) and possibly Ce (r=1.01A) and Pr (r=0.99A) as well, may simply be too large and be excluded from a $CaCO_3$ matrix. This might lead to the more erratic behaviour of La and Pr as discussed below. If this were the dominant mechanism then one would expect to find the same ratio REE/Ca [molar ratio x $10^{-6}$] in carefully cleaned shells of e.g. foraminifera, as the ratio

$$\text{REE} / \Delta\ 0.5\ \text{Alkalinity [molar ratio x } 10^{-6}]$$

observed in the deep waters of the Pacific and Atlantic stations.

The analogy with Ca is quite interesting. The latter element is very abundant in seawater and even intense formation of $CaCO_3$ shells in the eutrophic zone would lead to a barely discernable, less than 1 percent, Ca depletion of surface waters versus deep waters. In this respect Si represents the other extreme. It is strongly depleted in surface waters and often becomes the limiting nutrient in a diatom bloom. The REE, especially the heavier ones, may exhibit an intermediate behaviour. For instance, assume a constant uptake ratio Lu/Ca in $CaCO_3$ shells. Then a plankton bloom may remove a large portion, say about half, of the total dissolved Lu in the surface water. Twofold lower surface water values is what we found at the Pacific station.
Formation and subsequent removal of $CaCO_3$ shells leads to low values of alkalinity in the remaining water mass. Regions with low surface water alkalinity, e.g. the central Pacific gyres or the Circumpolar Convergence, are expected to have very low concentrations for the (heavy) REE as well, provided aeolian inputs have been small. After a calcareous plankton bloom has succumbed when the nitrate or phosphate reservoir is exhausted, low REE concentrations are left behind. In a sense such a 'leftover' amount of REE would resemble the concept of a 'preformed nutrient', provided no additional scavenging removal has taken place.

ii) The second process is the removal of trace elements from seawater by adsorptive scavenging onto settling particles (GOLDBERG, 1954; CRAIG, 1974). This process depends on such factors as seasonal production of scavenger particles during plankton blooms, aeolian input of terrestrial aerosols (e.g. clay particles), occurrence of nepheloid layers, and possible in situ formation of highly reactive Fe/Mn oxide surfaces at or near the seafloor. All these factors are known or expected to vary greatly in time and space. When scavenging is the dominant process for removal of a given element one expects to find a corresponding variabality in its oceanic distribution. This is especially true when the scavenging removal rate is fast relative to oceanic mixing and circulation. The exact nature of the scavenging mechanism varies from element to element. Moreover several classes of potential adsorptive sites (clay minerals, Fe/Mn oxide coatings, various organic functional groups) on the settling particles are possibly involved. On the one hand a very specific reaction between one element and one specific surface site can be envisioned. On the other hand there is currently a debate in the literature on the true 'Grand Unifying Theory' of scavenging removal and oceanic residence times of all chemical elements (LI, in press; TURNER & WHITFIELD, in press). Alternatively BALISTRIERI et al.(1981) relied somewhat more on field data in an attempt to constrain the options with respect to plausible surface sites. Yet they were forced to use a small group of trace elements with rather different chemical properties. In this respect the group of REE with very similar, gradually varying chemical properties would be more suitable, also because one can safely assume that they will all interact with the same type surface site. On the other hand the simultaneous involvement in a regenerative cycle (i) would considerably blur the picture.

For this process we are deprived of tracers like silicate and alkalinity, or nitrate and phosphate, the latter being indicators of the cycles of hard shells or soft tissue. Yet distributions of various Th-isotopes, $^{210}Pb$, antropogenic Pb, and possibly Al and Be as well, are thought to be largely controlled by scavenging removal. In such case a steady state (i.e. Pb excluded) comparison with conservative tracers like potential temperature or salinity leads to a first approximation of the scavenging removal (CRAIG, 1974). The relatively well studied

element Cu is of particular interest because it also seems to be affected both by a nutrient regeneration cycle and this scavenging mechanism. In principle the scavenging removal can be assessed by resolving the difference with the regenerative term. The similarity of REE profiles to those of $^{232}Th$, $^{234}Th$, $^{230}Th$, Cu, Al and Be indicates at least some control of REE distributions by scavenging removal. With this knowledge the relative importance of processes (i) and (ii) at both the Atlantic and Pacific site can now be discussed.

In the North Atlantic Deep Water silicate can be treated as a conservative element, i.e. in situ regeneration rates are negligible relative to water mass circulation. The same holds for Lu, given its linear relation with Si in the NADW (Figure 4.7). The lighter REE with larger ionic radii (see above) would be even less affected by the hard shell cycle, i.e. their regenerative input into NADW is even less likely than for Lu. Actually plots of these lighter REE versus Lu or Si exhibit negative curvature at middepth, indicative for their preferential removal either in situ or some time earlier in the life history of this NADW mass (chapter 3). Preferential scavenging removal of the lighter REE is fully compatible with stabilization of heavier REE in solution by stronger inorganic complexation (TURNER et al.,1981). Adsorptive scavenging over the whole water column seems to be the dominant (in situ) process at the North Atlantic station. In situ regeneration of REE does not occur. At this station the resemblance of deep REE profiles to silicate and alkalinity is merely an advective feature, although it does suggest REE regeneration in other locales.
In the oligotrophic surface waters there is no apparent dropoff in REE concentrations.

On the other hand the lower surface water values of Tm, Yb and Lu at the Pacific site suggest some degree of (in situ) incorporation in hard shells. This is consistent with the higher biological productivity in these waters. Plots of lighter REE versus Lu or Si in the water deeper than 1250m do not exhibit negative curvature. This may be due to the scatter in the data, but it may also indicate that scavenging removal is less dominant at this site. On the other hand when approaching the

seafloor Si remains constant, while concentrations of most REE tend to decrease (Figure 4.3). Some scavenging of REE may actually occur in these near bottom waters. In situ regeneration rates of REE, opal or calcite cannot be assessed. Yet the elevated REE concentrations in the deep Pacific versus the deep Atlantic Ocean, especially for the heavy REE, combined with the apparent Lu/Si relations in both oceans, inevitably lead to the conclusion that such regeneration is a dominant process in large parts of the worlds oceans.

Oceanic distributions of the REE as a group are governed by the competition between:

i) a regeneration and removal cycle analog or identical to those of opal and calcium carbonate.

ii) scavenging removal by settling particles

With increasing atomic number along the REE-series the first process tends to become more dominant, at the expense of the second. The relative importance of each process also varies in time and space. Circumstantial evidence supports the $CaCO_3$-cycle rather than the opal cycle as the more likely candidate for the first process. Matters are further complicated by aeolian inputs of terrestrial aerosols in certain locales(ELDERFIELD & GREAVES, 1982), or the occurrence of oxygen minima and hydrothermal sources (see below Eu) in other areas (this paper). The relative importance of riverine inputs has yet to be assessed (MARTIN et al., 1976; KEASLER & LOVELAND, 1982).

When excluding the lighter elements La, Ce (Pr) the remaining suite Nd-Lu (Pr-Lu) exhibits fairly smooth curvatures in the distribution patterns (Figure 4.4). Above conclusions are most relevant for these same elements Nd-Lu (Pr-Lu), which seem most representative of the REE as a group. Nevertheless the element Gd exhibits a rather unique anomaly which will be dealt with in chapter 6. The behaviour of La, Ce and Pr, will be discussed below.

La and Pr

GOLDBERG et al.(1963) originally suggested that the global oceanic residence times of the trivalent REE (all except Ce) would increase with atomic number, in accordance with the stabilization in solution of heavier REE by their stronger complexation (TURNER et al., 1981). Strictly spoken the lightest element La with an exceedingly high 38 percent free ion would be expected to be scavenged most rapidly, i.e. to be most depleted in REE patterns of seawater. This holds true for the upper few hundred meters of the Atlantic water column (Figure 3.2), but below there and all over the Pacific water column La is strongly enriched (Figure 4.4). For the combined data sets La and Sm do not correlate very well (r=0.87), with the average ratio La/Sm=9.1 well over the La/Sm=5.8 value for shales (Figure 4.8). Apparently La behaves rather independently from the other REE. Preferential adsorptive scavenging of the light REE, combined with release (desorption) of this light REE enriched fraction upon dissolution of the carriers at the seafloor had been proposed as the most simple explanation of the La enrichments in the bottom waters at the Atlantic site (chapter 3). The combined Atlantic and Pacific data now suggest an additional regenerative cycle (i) superimposed on this adsorption/desorption mechanism. With respect to such formation and dissolution of skeletal material the $La^{3+}$ cation with exceedingly large ionic radius may again act differently from the other REE.

The values for Pr and Sm correlate somewhat better (r=0.91) although there still is considerable scatter in the data (Figure 4.8). This may be largely due to the low precision of our Pr data. Nevertheless the average ratio Pr/Sm=1.1 is indeed below Pr/Sm=1.43 for shales, in agreement with the expected shorter residence time of Pr.

Ce, its oxidation and reduction

The behaviour of Ce in the oceans is largely controlled by its oxidation / reduction chemistry. Exact reaction mechanisms are not known, yet the equation

$$4\ CeO_2(s) + 12\ H^+ = 3\ Ce^{3+} + O_2(g) + 6\ H_2O \qquad (4.4.1)$$

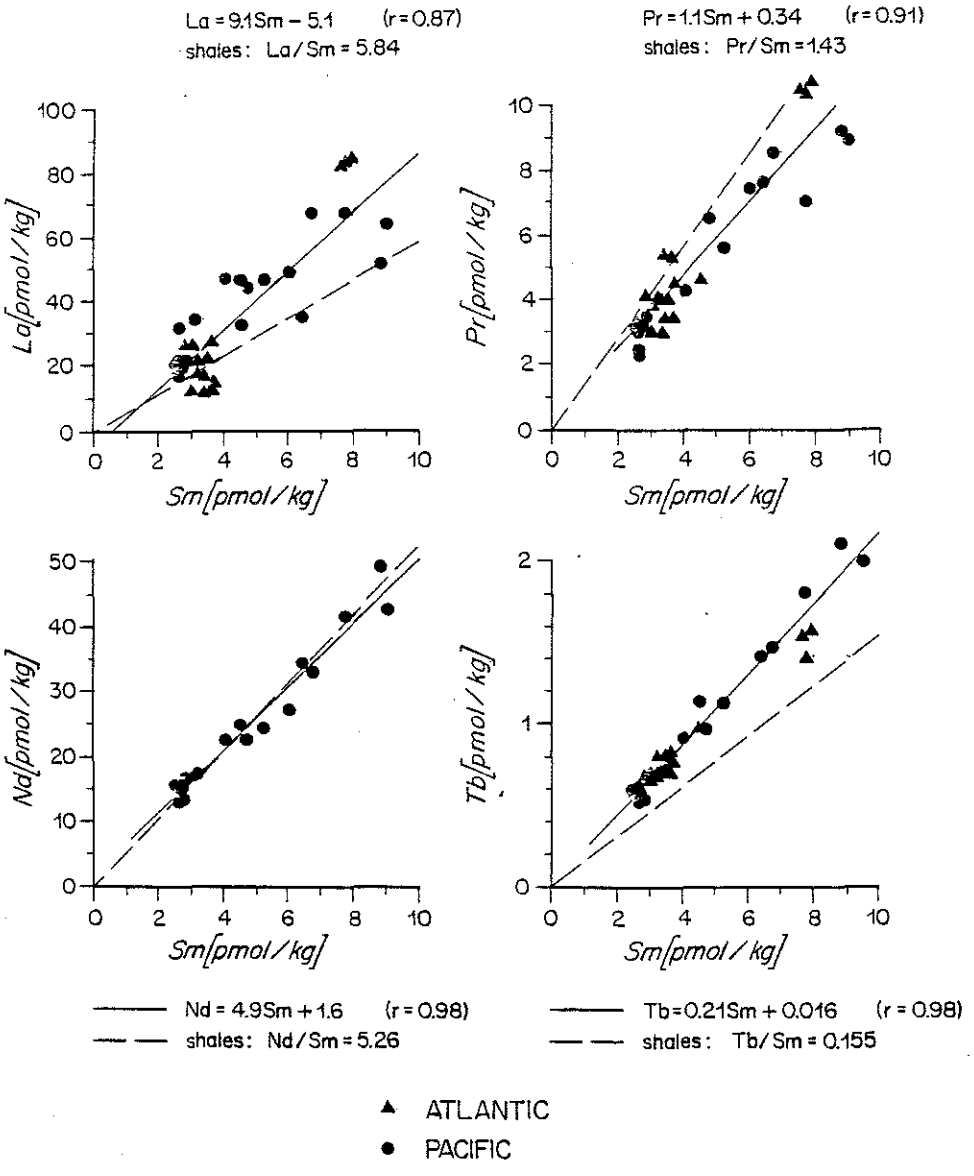


Figure 4.8. Concentrations of La, Pr, Nd and Tb plotted versus those of Sm for the Pacific (●) and Atlantic (▲) stations. The corresponding Eu-Sm relation is shown in Figure 4.11.

is useful for this discussion. Just like the other, strictly trivalent, REE the $Ce^{3+}$-cation is also affected by processes like adsorptive scavenging, a hard shell type cycling and water mass circulation. Yet the effects of its unique oxidation-reduction reaction can be singled out by definition of the Ce anomaly

$$\text{Ce-anomaly} = Ce/Ce^* = 2(Ce/Ce_{shale})/(La/La_{sh}+Pr/Pr_{sh}) \qquad (3.6.1)$$

versus neighboring elements La and Pr, where Ce* is the hypothetical concentration a strictly trivalent Ce would have. Contrary to the other REE the concentrations of Ce are extremely low over the complete Pacific water column. Levels are less than half of those found in the Atlantic Ocean (Figure 4.3). The Ce depletion is most developed at greater depth, and always more extreme than in the Atlantic Ocean (Figures 4.4, 3.3). The depletions in the Pacific range from about twofold (200m) to almost 25-fold (3250m), much stronger than in the Atlantic Ocean (Figure 4.9). At the latter station it was found that the change in oxidation state (see 4.4.1) approximately doubles the (deep water) removal efficiency for Ce. It is not surprising that deep Pacific waters, generally 'older' with respect to aeolian or riverine terrestrial inputs (no Ce anomaly), are more depleted. This also implies that authigenic phases in marine sediments of the Atlantic would on the average have stronger positive Ce anomalies than similar deposits in the Pacific Ocean. Global circulation leads to depletions of Ce, and simultaneous enrichments of the other REE, in the deep Pacific versus deep Atlantic waters (Figure 4.5).

This Ce fractionation in well oxygenated waters would lead to a positive Ce anomaly (or at least less of a Ce depletion) for the authigenic fraction of particles settling towards the seafloor. Upon regeneration of this, relatively Ce enriched, authigenic phase the released REE fraction would drive the overall Ce/Ce* in a parcel of water up to higher, i.e. less depleted, values. This is exactly what is observed in the strong $O_2$-minimum zone (200-750m) at the Pacific station (Figure 4.9). The effect of this regeneration would roughly correspond to the hatched area in the Ce/Ce* profile. Although all REE exhibit peaks at 150m depth (Figure 4.3), the maximum replenishment of Ce/Ce* appears to be at 200m depth (Figure 4.9). This phenomena is fully

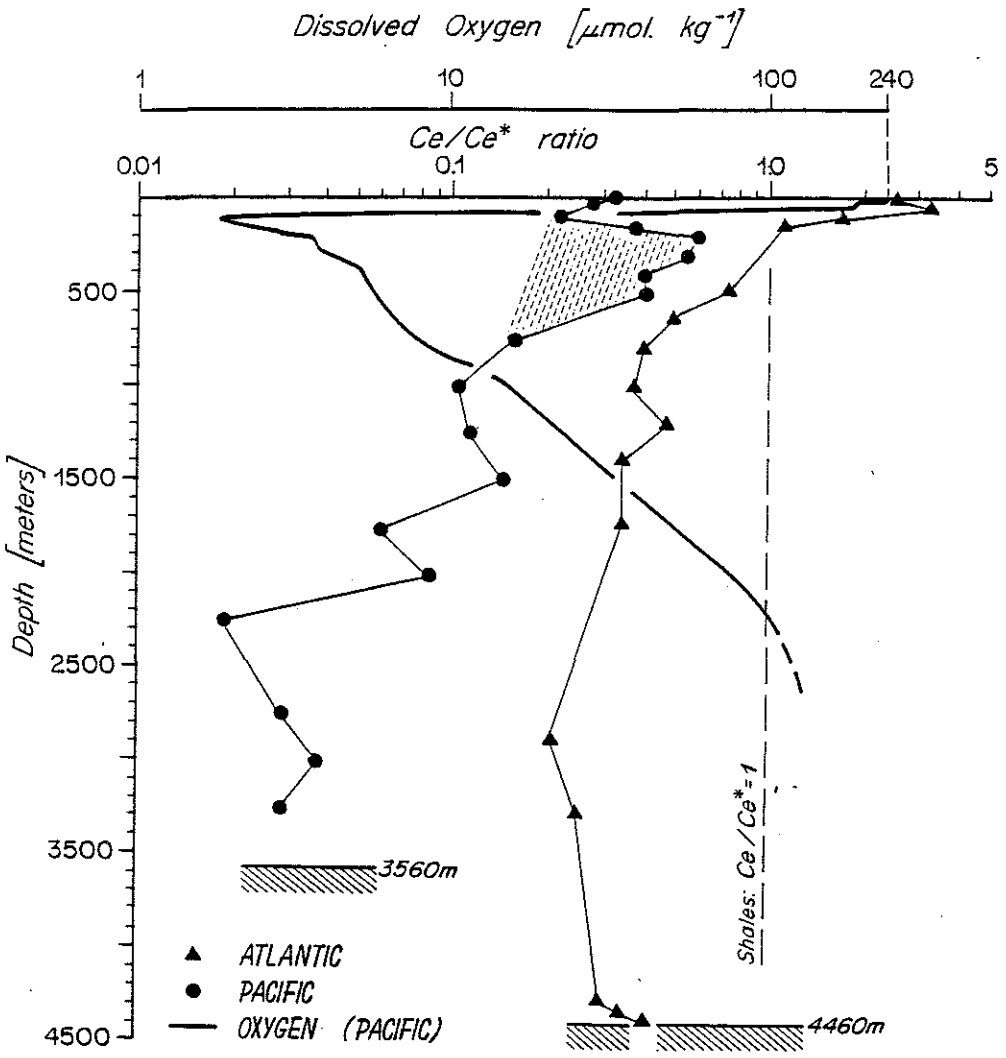


Figure 4.9. The Ce anomaly=Ce/Ce*= $2(Ce/Ce_{shale})(La/La_{sh}+Pr/Pr_{sh})$ as a function of depth at the Pacific and Atlantic stations. Also shown is the profile of dissolved $O_2$ at the Pacific site. Horizontal $^{10}$log-scales.

consistent with earlier observed positive Ce anomalies in Atlantic surface waters, a sharp gradient of the Ce anomaly near the Atlantic seafloor (Figure 4.9), as well as enhanced Ce levels in anoxic waters of the Cariaco Trench (chapter 5).

Preferential, i.e. faster, removal of Ce from oxygenated waters is considered an established fact. On the other hand our data so far does not permit us to tell whether regeneration of Ce(IV) occurs faster, as fast, or slower than for the other REE. One would speculate that all REE go through the same reaction sequence during regeneration, except for an additional reduction reaction (4.4.1) for Ce(IV). In other words, Ce(IV) regeneration could only be as fast, or slower, than regeneration of the other REE. At slower, more and more rate-limiting, kinetics of the reduction of Ce(IV) the original authigenic particulate phase has to be more and more Ce enriched in order to produce the observed 'bulge' in the Ce/Ce* profile (Figure 4.9).

This broad Ce/Ce* peak is strikingly similar to the maximum of dissolved Mn in the same $O_2$-minimum zone (Figures 4.9, 4.10). It is conceivable that an, as yet unspecified, particulate Mn-oxide serves as a REE carrier. Upon dissolution of this carrier phase under low oxygen conditions, the REE then are simply released in the ambient water mass. This is supported by observations in the completely anoxic Cariaco Trench where all REE exhibit a sharp increase just below the $O_2/H_2S$ interface (chapter 5). On the other hand regeneration of particulate organic matter serving as REE carrier may also explain both observations in the Pacific $O_2$-minimum zone and the Cariaco Trench. Nevertheless the well-known enhanced REE levels, with generally a positive Ce anomaly, in ferromanganese nodules relative to surrounding sediments (ELDERFIELD et al., 1981), tends to support a similar Mn-oxide phase as particulate carrier for scavenging the REE from the water column. The more or less inverse argument, direct formation of nodules from settling REE/Ce/Mn enriched particles, is not necessarily correct. Actually the observed positive Ce anomalies in Atlantic surface waters, as well as enhanced concentrations of both Ce and Mn in the Cariaco Trench, would be more consistent with an additional diagenetic regeneration of REE/Ce/Mn before incorporation into nodules. At least some direct adsorption of dissolved REE/Ce/Mn from bottom waters is also conceivable.

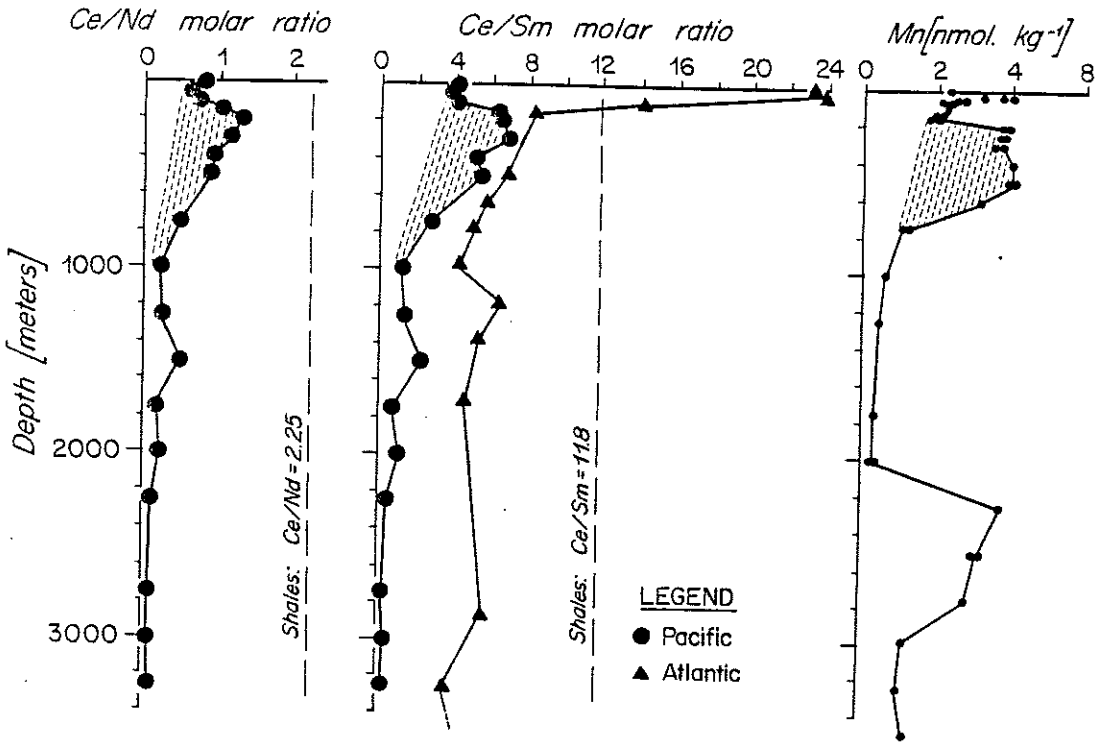


Figure 4.10. The anomalous behaviour of Ce relative to Nd and Sm in the Pacific and Atlantic Oceans. The profiles are of similar shape as for the more conventional defined Ce anomaly Ce/Ce* (see Figure 4.9). Note the similarity with the profile of dissolved Mn (Taken from LANDING, 1983).

When defining the Ce anomaly Ce/Ce* the neighboring elements La and Pr were chosen to represent the REE group. However La, and possibly Pr as well, seem to act somewhat independently from the other REE (Nd-Lu). On the other hand Nd, Sm, Eu and even heavy REE like Tb are more strongly related (Figures 4.8, 4.11). Nevertheless plots of the Ce/Nd ratio and Ce/Sm ratio as indicators of Ce excursions yield essentially the same features as the Ce/Ce* profiles (Figures 4.10, 4.9). The Ce anomaly appears to be too dominant a feature to be affected by minor excursions of La (and Pr).

Very little is known about the exact mechanisms and thermodynamic constraints for the overall reaction (4.4.1). CARPENTER & GRANT (1967) reported the disappearance of free $Ce^{3+}$-cation during the oxidation reaction, with a dramatically faster kinetics at pH=8 relative to pH=7 in seawater. Most probably an adsorption of the free $Ce^{3+}$-cation would preceed the actual oxidation reaction. Physical constraints like the diffusion of cations from the bulk solution across a laminary water layer to the solid surface may very well be rate limiting.

HIRANO & KOYANAGI (1978) have proposed hydrolysed intermediates in solution like $Ce(OH)^{2+}$, $Ce(OH)_2^+$, $Ce(OH)_3^0$, which they also suggested to be the dominant species in natural pH=8 seawater, contrary to the model results of TURNER et al.(1981). This was supposed to explain the reported lower oxidation rates in seawater at lower pH=7 (CARPENTER & GRANT, 1967), and the absence of Ce anomalies from river waters as indeed no hydrolysed Ce-species occur in fresh water (pH=6, TURNER et al., 1981).(The limited data base for river water can be found in MARTIN et al., 1976, KEASLER & LOVELAND, 1982.). Yet this would also imply hydrolysed intermediates for the adsorption of all other REE from seawater (unless the actual Ce oxidation takes place in solution, which is unlikely from a thermodynamical point of view, see below), leading to faster removal and shorter residence times of the heavy REE which are more strongly hydrolysed in seawater(Table 6.2).

In fact the generally believed truism of longer residence times for heavy REE is consistent with direct adsorption of free $REE^{3+}$ cations instead. Also the overall oxidation reaction of Ce produces protons and would still be favored at higher pH. Of course the solid Ce(IV) phase

could very well be a hydroxide $Ce(OH)_4$, a hydrated crystalline form or even more likely a solid solution of sorts, rather than simply $CeO_2$.

The oceanic water column is an open system, at best in a steady state, but definitely not in thermodynamical equilibrium. Nevertheless simple thermodynamic considerations may serve as constraints when attempting to predict in which direction reactions tend to go, without yielding any information on whether these reactions actually occur at an appreciable rate. Unless it is very strongly complexed $Ce^{4+}$ is capable of oxidizing water to oxygen:

$$4\ Ce^{4+} + 2\ H_2O = 4\ Ce^{3+} + 4\ H^+ + O_2(g) \qquad (4.4.2)$$

$$\log K = 8.6 \text{ (BAES \& MESMER, 1976)}$$

In other words dissolved $Ce^{4+}$ falls outside the stability field of water (GARRELS & CHRIST, 1965) and does not exist in aqeous solution. The above corresponds to

$$\log(Ce^{3+}/Ce^{4+}) = 8.6 + pH - 0.25 \log pO_2 \qquad (4.4.3)$$

In water at pH=8.2 and 1atm partial pressure for $O_2$ this ratio amounts to $Ce^{3+}/Ce^{4+} = 10^{17}$. This value may vary somewhat with ionic strength. On the other hand the formations of various hydrolysed species and other complexes in seawater are essentially non-redox reactions and the overall ratio Ce(III)/Ce(IV) in seawater at pH=8.2 should be about the same. At lower $O_2$ pressures, i.e. in anoxic waters, the ratio would be even higher. For acidified seawater (pH=2) with a $^{144}Ce$ internal standard spike (chapter 2) the ratio would still be around $10^{10}$. For our purposes Ce(IV) does not exist in solution.

From thermochemical data (BAES & MESMER, 1976) cerium dioxide should be very insoluble:

$$CeO_2(s) + 4\ H^+ = Ce^{4+} + 2\ H_2O \qquad (4.4.4)$$

$$\log K_s = -8.16$$

Combination with equation 4.3.2 yields

$$\log (Ce^{3+}) = 0.44 - 3pH - 0.25 \log pO_2 \qquad (4.4.5)$$

for the overall reaction 4.4.1. The constants K and $K_s$ were determined at very high Ce concentrations, in solutions of high acidity with different anionic composition than seawater. Attempts could still be made to take these effects, as well as the seawater speciation, into account. More importantly however is the notion that pure crystalline $CeO_2$ is almost certainly not the solid phase on marine suspended particles. Nevertheless the above equation predicts:

| pH | $pO_2$ | log $(Ce^{3+})$ | seawater |
|---|---|---|---|
| 8.2 | 1 atm | -24.16 | oversaturated |
| 8.2 | 0.01atm | -23.66 | oversaturated |
| 7 | 0.01atm | -20.66 | oversaturated |
| 2 | 1 atm | - 5.56 | undersaturated |

Table 4.4.1. Predicted equilibrium concentrations of $Ce^{3+}$ from equation 4.4.5. Note that acidified seawater samples with $^{144}Ce$ spikes added appear to be undersaturated, i.e. oxidation of Ce during sample storage is unlikely.

Apparently oxygenated seawater with $(Ce^{3+})$ = 1-100 pmol/kg would be oversaturated, in agreement with the observed preferential removal by oxidation of Ce from the oceanic water column. As mentioned these numerical values are of limited validity, if any. More significant is the notion that lower pH and lower $pO_2$ tend to bring $Ce^{3+}$ in solution. It is interesting to note in equation 4.3.5 that changes in

acidity have a larger effect than variations in oxygen pressure. This strong pH dependence combined with the absence of complexing anions may also explain the apparent lack of Ce anomalies in well oxygenated fresh waters.

The above predicted equilibrium concentrations (Table 4.4.1) were derived from solubility constants determined in the laboratory. The inverse would be a derivation of the apparent solubility product K' from filed measurements. From the profiles of Ce, Ce/Ce* and dissolved $O_2$ (Figures 4.3, 4.9) it seems that at about 150-750m depth the unknown solid Ce(IV)-phase goes into solution again. Given the local conditions

$$pO_2 = 10^{-3} \text{ to } 10^{-2} \text{ atm}$$
$$[Ce^{3+}] = 15 \pm 5 \times 10^{-12} \text{ mol.kg}^{-1}$$
and acidity assumed at pH=8.2

for the apparent reaction

$$Ce(IV)_{\text{unknown solid}} + 3\ H^+ = (Ce^{3+}) + 1/4\ O_2 + \text{some water}$$

one may simply derive:

$$\log[Ce^{3+}] = \log K' - 3\ pH - 0.25 \log pO_2 \qquad (4.4.6)$$

where $\log K' = 13 \pm 0.5$

Of course this is a very simplistic first approach and the numerical value of K' may shift somewhat when more field data becomes available. Nevertheless a crude relationship is obtained which indicates that high $Ce^{3+}$ concentrations are possible in even more strongly reducing environments like anoxic basins (chapter 5) or pore waters of organic rich shelf sediments (chapter 3).

Eu

Under strongly reducing conditions Eu can be reduced to Eu(II). Fractionations of Eu during hydrothermal circulation have been inferred (De BAAR et al., 1983a) from observations of Eu anomalies in continental hydrothermal barites (GUICHARD et al., 1979) and some, but not all, metalliferous deposits (COURTOIS & TREUIL, 1977; CORLISS et al., 1978). Recently strong positive Eu anomalies were indeed observed in 'undiluted' hydrothermal fluids collected at the 13$^{o}$N vents field (MICHARD et al., 1983). Concentrations of REE were reported to be about 1000-fold those found in seawater, with Eu/Sm ratios around 2.6 versus Eu/Sm=0.25 in the open ocean (Figure 4.11). All available data for Eu/Sm in open ocean water of both the Atlantic and Pacific Ocean plots essentially on a straight line, with a best fit slope Eu/Sm=0.25. Linear regression of the Atlantic dataset alone leads to a slightly lower ratio Eu/Sm=0.22, very close to Eu/Sm=0.21 for shales, the latter thought to be representative for average terrestrial inputs into the ocean basins. The Pacific ratio Eu/Sm=0.26 is slightly higher, although there is quite some overlap in the data. Although this difference is small, if significant it would be consistent with two major processes:

i) slower scavenging removal of the heavier element Eu which in seawater is complexed more strongly than Sm. This would lead to a Eu enrichment of Pacific waters, the latter assumed to be 'older' with respect to an original input of REE from terrestrial sources.

ii) a relatively larger hydrothermal input of REE into the Pacific Ocean due to the generally faster spreading rates in that basin.

The latter process is supported by the Pacific / Atlantic comparisons (Figure 4.5). At all depths Eu exhibits a small but distinct enrichment in the Pacific Ocean, relative to both its neighbors Sm and Gd in the REE series. Also the ratios Eu/Gd and Eu/Tb appear to be higher in the Pacific than in the Atlantic Ocean, rather than lower as would be expected from the first (i) scenario. However more work is needed to confirm this apparent trend of a general Eu enrichment in the Pacific Ocean.

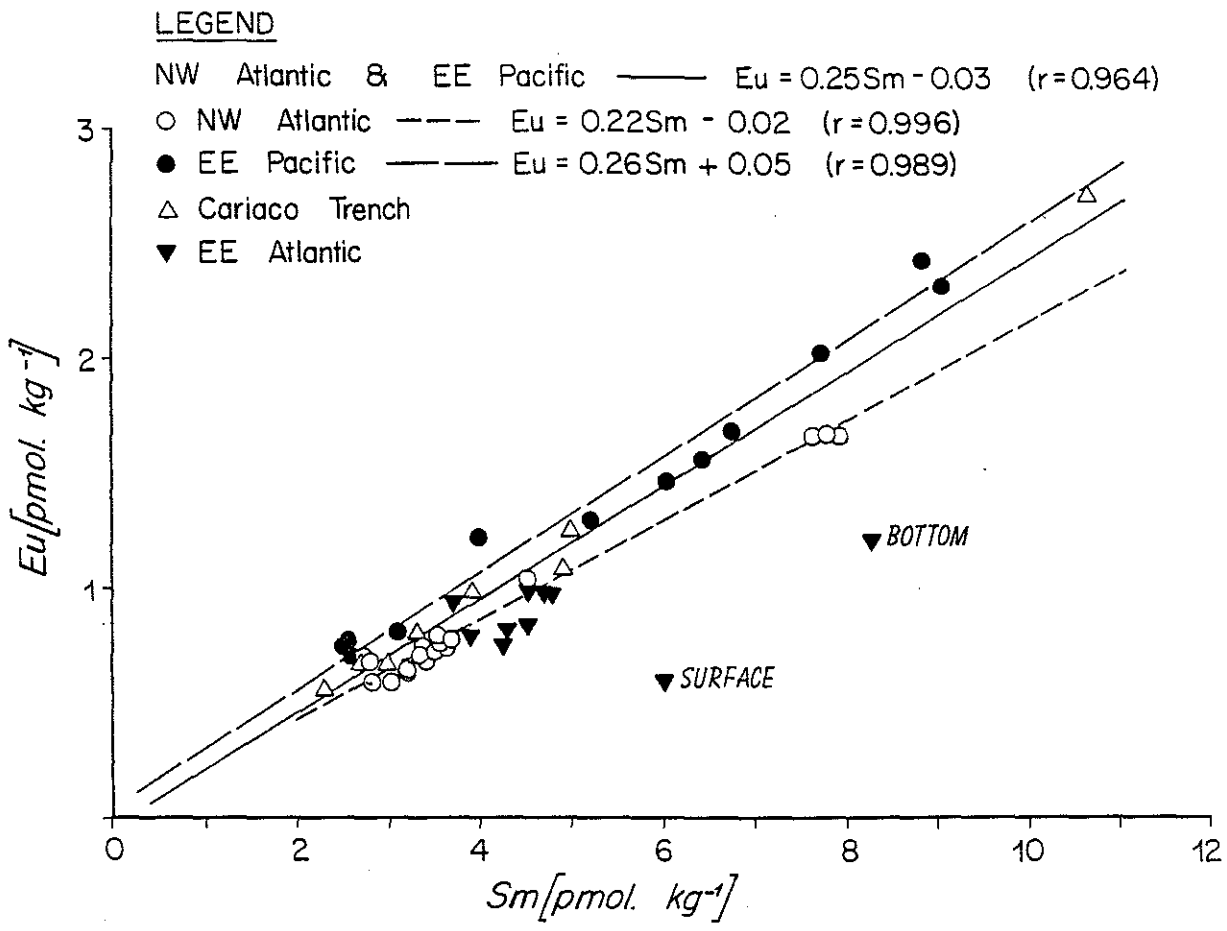


Figure 4.11. The Eu/Sm relationship in the Atlantic and Pacific Oceans and the Cariaco Trench. The two datapoints with low Eu/Sm ratio in the Eastern Atlantic Ocean (ELDERFIELD & GREAVES, 1982) probably arise from a similar Eu depletion of the original terrestrial source (RAHN, 1976), rather then from a fractionation within the ocean basin.

The distinctly higher $^{143}Nd/^{144}Nd$ ratio in the Pacific versus the Atlantic Ocean (see chapter 7.2) may also be compatible with mixing between continental sources with low $^{143}Nd/^{144}Nd$ ratios and a Mid Ocean Ridge Basalt source (hydrothermal circulation) with a higher ratio. Combined determinations of both this $^{143}Nd/^{144}Nd$ ratio and concentrations of the suite Sm, Eu, Gd in the very same samples would be helpful for assessing the relative importance of the continental versus the oceanic crust as ultimate sources for REE in the oceans.

KLINKHAMMER et al. (1983) recently reported concentration values for nine REE at two locations near spreading centers in the Pacific Ocean. Their observations:

- typically lower surface water values than in the Atlantic Ocean;
- an enrichment of deep Pacific versus deep Atlantic waters;
- a general depletion of Ce relative to the Atlantic Ocean;

are consistent with the results reported in this thesis. In the Mariana Trough they found a linear Er-Si relation, similar to the linear Lu-Si relation reported earlier for the North Atlantic Deep Water (DE BAAR et al., 1983).

A distinct positive Eu anomaly is also shown in a comparative Pacific/Atlantic plot for samples at 2500m depth (their Figure 5b). Of course both their Pacific stations are exactly at sites of hydrothermal activity, at a 2500m sampling depth close to ridge crest depth. This Eu enrichment is not necessarily representative of their samples at other depths or, for that matter, the Pacific Ocean in general. Also the Atlantic sample at 2500m depth which was used as a reference happens to exhibit a fairly distinct Eu depletion (Eu/Sm=0.19; ELDERFIELD & GREAVES, 1982) versus shales (Eu/Sm=0.21). This tends to enhance the apparent Eu enrichment of the Pacific samples. Nevertheless these apparent trends for Eu are intriguing and additional studies may further resolve the potential of the Eu anomaly as a tracer of hydrothermal processes.

## 4.5. Conclusions

Analogies with distributions of nutrients as well as certain trace elements have been used to unravel the marine geochemistry of the Rare Earth Elements. As a group, represented most clearly by the suite Nd-Lu, they appear to be controlled by two competing processes:

i) a regeneration and formation cycle analogous or identical to those of opal and calcium carbonate, with circumstantial evidence in support of the latter as a more likely carrier.
ii) removal by adsorptive scavenging, possibly in association with Mn oxide surface phases.

Combination of both these apparent mechanisms is conceivable with a reactive surface coating (Mn-oxide, phosphorous phase, organic material) on calcareous or siliceous skeletons as the scavenging agent (De BAAR et.al., 1983a).

The lightest element La, whose properties are known to differ from the other REE, also seems to act somewhat more independently in seawater.

Cerium is extremely depleted in the deep Pacific Ocean. The distribution of Ce is mostly controlled by its oxidation/reduction reactions, rather than above processes. Its cycling in the water column is very similar to the behaviour of Mn. In well oxygenated waters both elements are removed very rapidly by oxidation to insoluble (IV) states. In the oxygen minimum zone of the Eastern Equatorial Pacific both Mn and Ce are enriched due to their reduction and subsequent release from settling particles.

Positive Gd anomalies are ascribed to unique properties of the $Gd^{3+}$-ion with exactly half-filled 4f electron shell.

# 5. RARE EARTH ELEMENTS in the CARIACO TRENCH, an ANOXIC BASIN

## 5.1. Abstract.

The first profiles of REE in anoxic waters are reported. All REE are strongly affected by the chemical changes across the $O_2/H_2S$ interface. Enhanced Ce concentrations in the anoxic deep water column support the contention that Ce and Mn have a very similar marine geochemistry, both elements being largely controlled by their oxidation-reduction reactions.

## 5.2. Introduction.

The Cariaco Trench is a depression in the continental shelf north of Venezuela. It is approximately 175km long and 50km wide, and it comprises two basins, each about 1400m deep, separated by a saddle at a depth of about 900m. (Figure 5.1). The sill separating the basin from the Carribean Sea is nowhere deeper than 150m. Water above sill depth exchanges freely with the open sea, while the deeper water is isolated by the sill and by a density gradient that inhibits vertical mixing. The deep water appears to be permanently anoxic and contains appreciable levels of hydrogen sulfide. Various attempts have been made to estimate the age of the deep water within the Trench (RICHARDS & VACCARO, 1956; FANNING & PILSON, 1972; DEUSER, 1973). All these estimates are based on simple models which may be considerably flawed by their inherent assumptions. The resulting residence times vary between 22 and 300 years. The most likely value lies near 100 years (DEUSER, 1975).

The stability of the deep water column is a result of the lower temperature of the deep water, rather then of its higher salinity. Over the years of observation there appears to be an increase in the temperature of the deep water, which would eventually lead to a turnover after the vertical density gradient has been eliminated.

The deep anoxic water where $H_2S$ is observed is separated from the overlying oxygenated water by a distinct boundary. The $O_2/H_2S$ interface has been found at somewhat different depths during different expeditions. RICHARDS & VACCARO(1956) report a depth of 375m, whereas

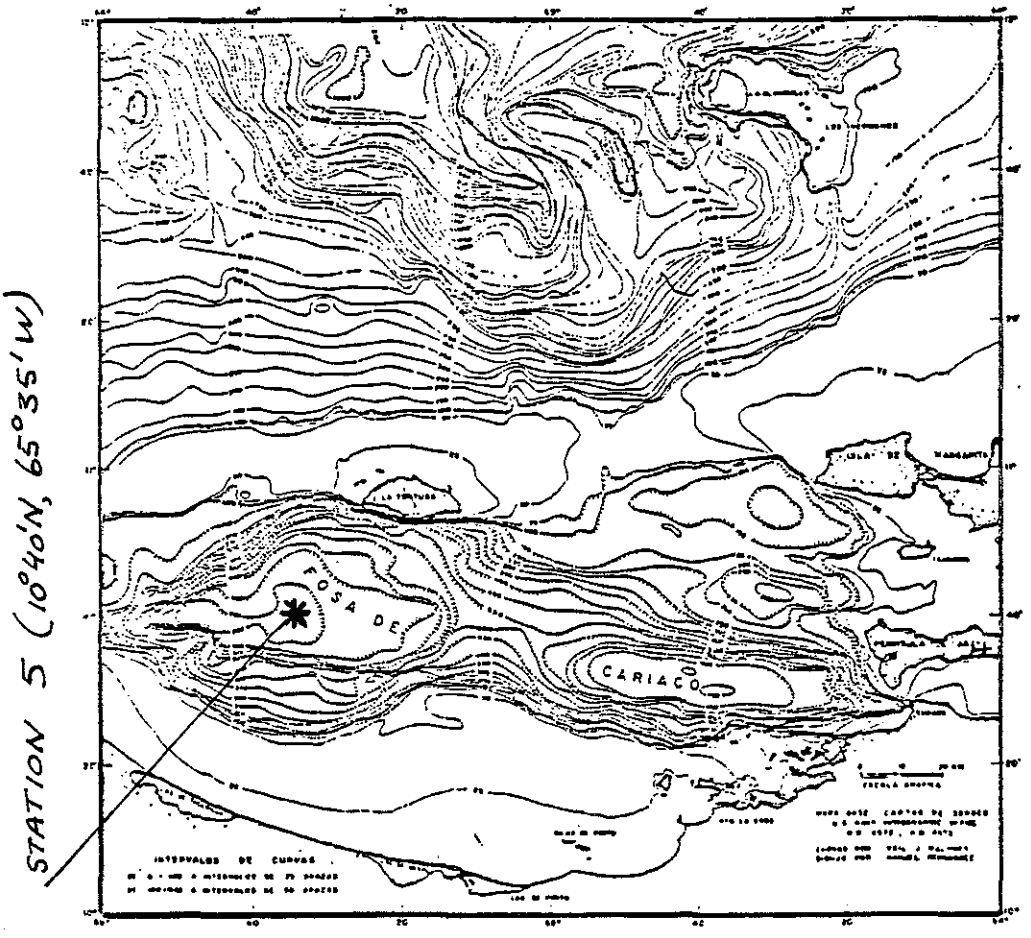


—Bathymetry of the Cariaco Basin (from Maloney, 1966).

Figure 5.1. Station occupied during cruise 99/2 aboard R.V. KNORR in the Cariaco Trench, for which results are reported in this chapter.

DEUSER (1973) later found $H_2S$ in waters as shallow as 250-300m.

The distributions of various transition elements and radionuclides are known to be affected by the chemical gradients across the $O_2/H_2S$ interface in the Cariaco Trench and other anoxic basins (SPENCER & BREWER, 1971; EMERSON et al., 1979; BACON et al.,1980; JACOBS & EMERSON, 1982). This is especially the case for Fe and Mn, which have multiple oxidation states within the marine environment. Their basic cycle consists of (BACON et al., 1980):

- upward mixing of dissolved divalent Fe and Mn from the reducing into the oxidizing environment;
- precipitation of $MnO_2$ and $Fe(OH)_3$ or similar (hydr)oxides at or just above the interface;
- settling of the precipitate;
- dissolution upon reduction in the anoxic zone.

Equilibrium considerations determine the direction of the oxidation and reduction reactions. Yet the vertical profiles are ultimately controlled by a combination of (bio)chemical kinetics and transport terms. Vertical profiles of Fe and Mn invariably exhibit a steep increase just below the $O_2/H_2S$ interface.

Anoxic sediments, anoxic basins and fjords, and the mixing zone of hydrothermal waters with ambient seawater, all have this $O_2/H_2S$ interface in common. Of these environments, the anoxic basins are more accessible, less susceptible to sampling artifacts, and also less complicated than either pore waters or hydrothermal vents. The enrichments of both Fe and Mn in anoxic basins are analogous to enhanced levels commonly found in anoxic pore waters (KLINKHAMMER, 1980b). Initial speculations about the analogy between Ce and Mn (chapter 1), as well as the observation of positive Ce anomalies in Atlantic surface waters (chapter 3), led us to believe that high Ce levels can be found both in pore waters and anoxic basins. Of course the precipitation of mono- or polysulfides, carbonates and other phases may further complicate the distributions of dissolved Ce, Fe and Mn in anoxic environments. These latter removal mechanisms would be even more important for elements with only one oxidation state like Cu, Cd, Ni and Co. In anoxic basins such 'non-redox' elements might also be carried along in the above described downward transport of Fe/Mn oxides across the $O_2/H_2S$ interface.

5.3. Results.

During cruise 99/2 aboard RV KNORR in November 1982 station 5 was occupied for about one week at a location over the deepest point of the western basin of the Cariaco Trench (1398m depth; $10^{o}40'N$, $65^{o}35'W$). Both temperature and salinity decrease smoothly with depth and remain essentially constant below about 600m (Figure 5.2). The salinity maximum at about 100m has been observed previously (BACON et al., 1980) and appears to be a seasonal feature (OKUDA et al., 1969). The deep water temperatures were indeed higher compared to previous expeditions, confirming the warming trend which would eventually cause a turnover of the basin.

The $O_2/H_2S$ interface was found to be at 300m depth, with a variability less than $\pm$10m between different hydrocasts (Figure 5.3). The interface itself may be envisioned as a discrete surface whose depth varies somewhat as a function of lateral position and time. In the anoxic zone the sulfide concentrations increase with depth until maximum values of about 50 umol.kg$^{-1}$ near the bottom. This is in clear contrast with the less reducing environment in the $O_2$-minimum zone at the Eastern Equatorial Pacific site where $O_2$ always remained detectable and $H_2S$ has never been found. On the other hand $H_2S$ concentrations as high as 300 umol.kg$^{-1}$ have been reported for the bottom waters of the Black Sea.

The nutrients silicate and phosphate exhibit fairly normal depth profiles (Figure 5.4). There is some indication of a phosphate maximum and minimum at and just below the $O_2/H_2S$ interfaces but these extrema are not as distinct as reported for the Black Sea (BREWER & MURRAY, 1973).

The results of the first REE analyses of 8 out of 31 filtered water samples are listed in Table 5.1. Unfortunately two overall reagent blanks were found to have high levels of the light REE, especially La and Ce. For various reasons it is not clear whether a blank correction should be applied. Nevertheless these initial results exhibit distinct trends which, at least in a qualitative sense, would not change upon application of blank corrections.

| Depth (m) | La | Ce | Pr | Nd | Sm | Eu | Gd | Tb | Ho | Tm | Yb | Lu |
|---|---|---|---|---|---|---|---|---|---|---|---|---|
| 80 | 62 | 20 | 4 | 20 | 5 | 1.26 | 6.3 | 1.05 | 1.9 | 0.84 | 5.3 | 0.85 |
| 209 | 76 | 12 | 3.4 | 10 | 3 | 0.66 | 3.7 | 0.54 | 1.1 | 0.52 | 3.8 | 0.63 |
| 294 | 68 | 22 | -- | 10 | 2.3 | 0.56 | 3.1 | 0.48 | -- | 0.46 | 2.8 | 0.48 |
| 308 | 56 | 35 | 1.9 | 12 | 2.7 | 0.7 | 3.4 | 0.56 | 0.91 | 0.46 | 3.1 | 0.48 |
| 318 | 56 | 42 | 2.1 | 17 | 3.9 | 0.98 | 4.8 | 0.76 | 1.28 | 0.58 | 3.7 | 0.60 |
| 398 | 53 | 55 | 3.3 | 19 | 4.9 | 1.09 | 5.0 | 0.81 | 1.54 | 0.69 | 3.9 | 0.62 |
| 794 | 19.2 | 62 | 3.14 | 14.6 | 3.3 | 0.81 | 3.2 | 0.54 | 0.79 | 0.33 | 2.4 | 0.35 |
| 1194 | 113 | 58 | 10.7 | 47 | 10.6 | 2.71 | 13.6 | 1.95 | 2.6 | 1.10 | 7.2 | 1.13 |
| Duplicate overall reagent blanks: | | | | | | | | | | | | |
| I | 5.9 | 8.7 | -- | 5.2 | 0.39 | 0.078 | -- | -- | -- | -- | 0.071 | 0.0091 |
| II | 13.5 | 8.6 | -- | 5.4 | 0.44 | 0.085 | -- | -- | -- | -- | 0.087 | 0.0116 |
| mean | 9.7 | 8.65 | (0.86) | 5.3 | 0.42 | 0.081 | -- | -- | -- | -- | 0.079 | 0.0104 |

Table 5.3.1. Measured concentrations of REE [$10^{-12}$mol/kg$^{-1}$] and duplicate overall blanks for filtered water in the Cariaco Trench and overlying waters.

The blanks for Pr were not measured. The mean value Pr = 0.86 was estimated by interpolation between mean values of La and Pr. These mean values for La, Ce, Pr, Nd, Sm blanks were used for calculation of the blank corrected data points (open diamonds) in Figures 5.6 and 5.7

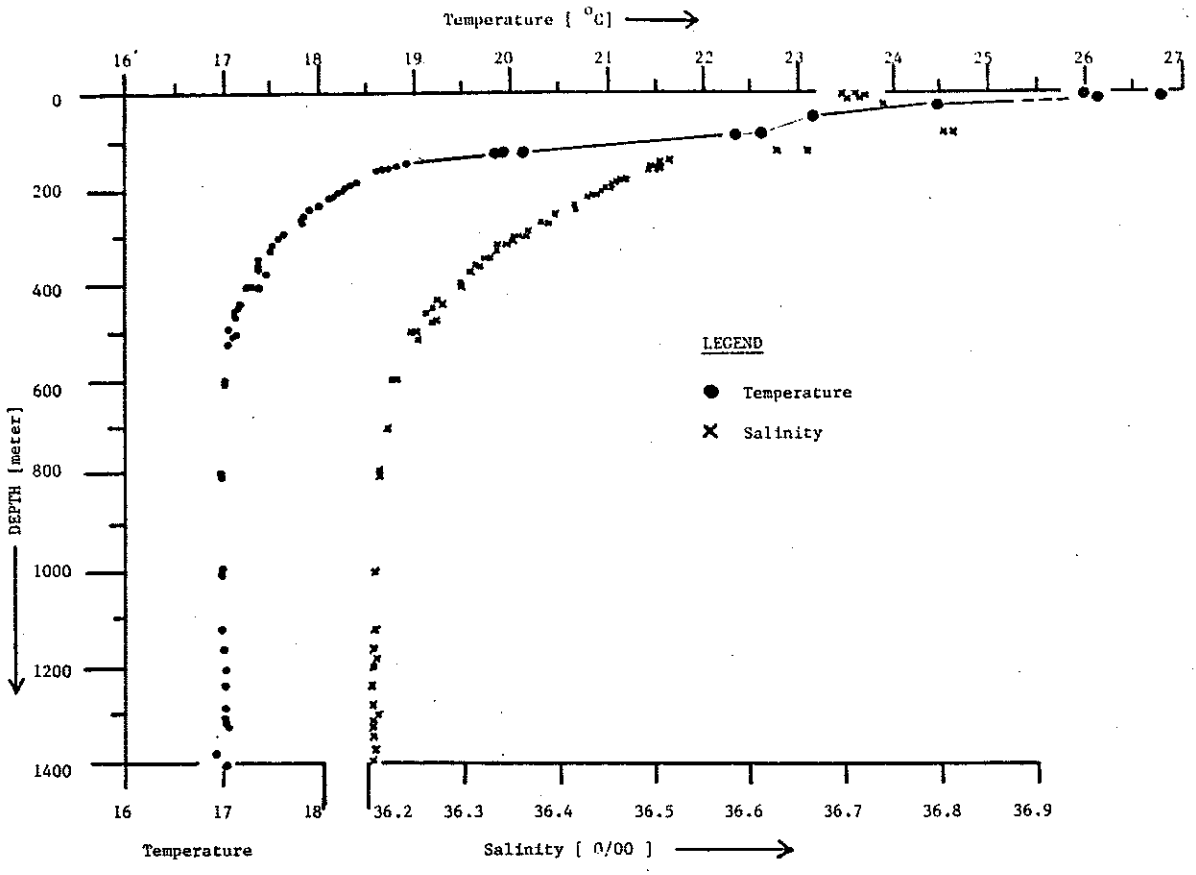


Figure 5.2. Vertical profiles of temperature and salinity at station 5. Data courtesy Deborah Shafer, WHOI.

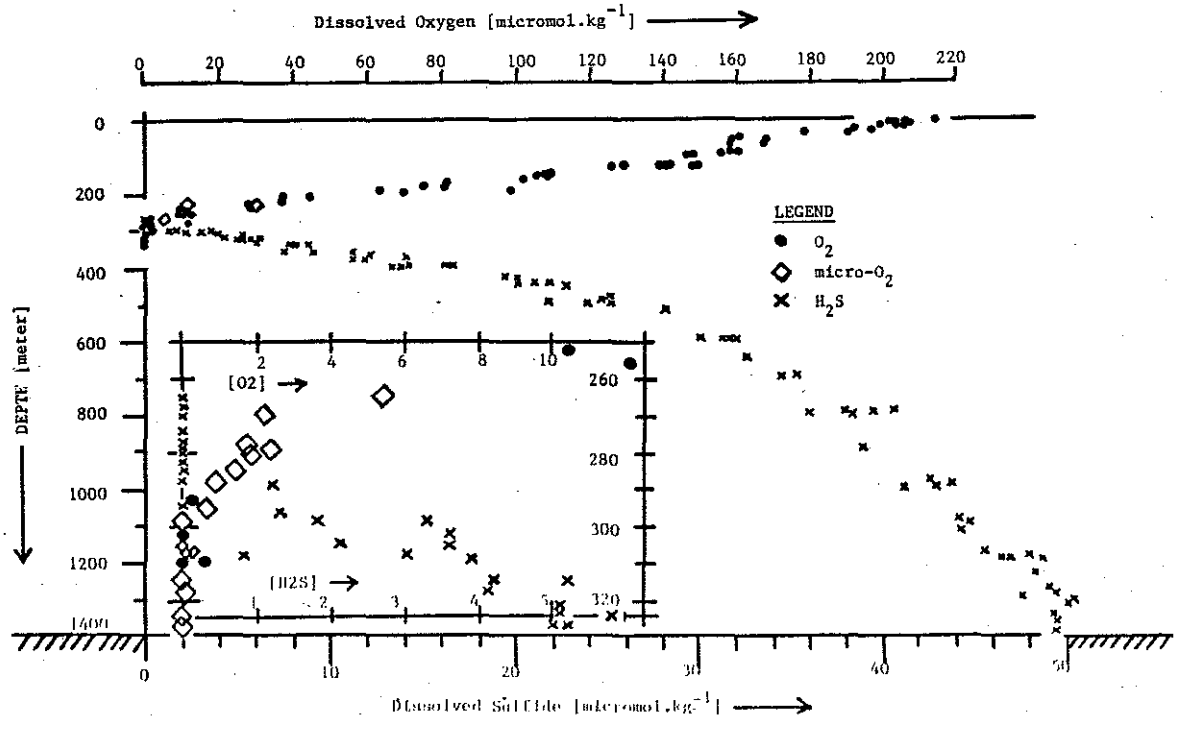


Figure 5.3. Vertical profiles of dissolved $O_2$ and $H_2S$ at station 5. Insert: the $O_2/H_2S$ interface at expanded scales. Shipboard $O_2$-data courtesy Rebecca Belastock, WHOI. Shipboard micro-$O_2$ data courtesy David Hastings, $H_2S$ data courtesy Lucinda Jacobs (Univ. of Washington).

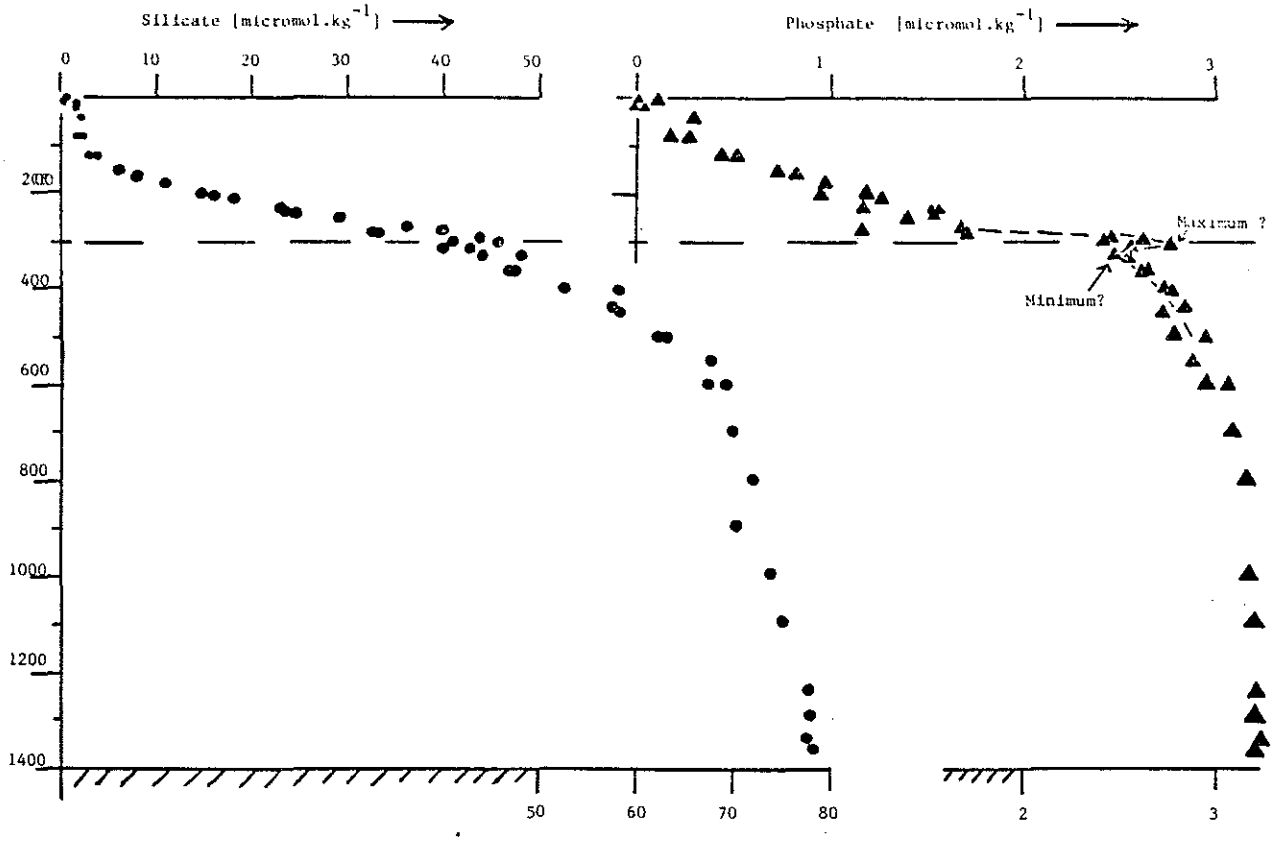


Figure 5.4. Vertical profiles of silicate and phosphate at station 5. Data courtesy Zofia Mlodzinska.

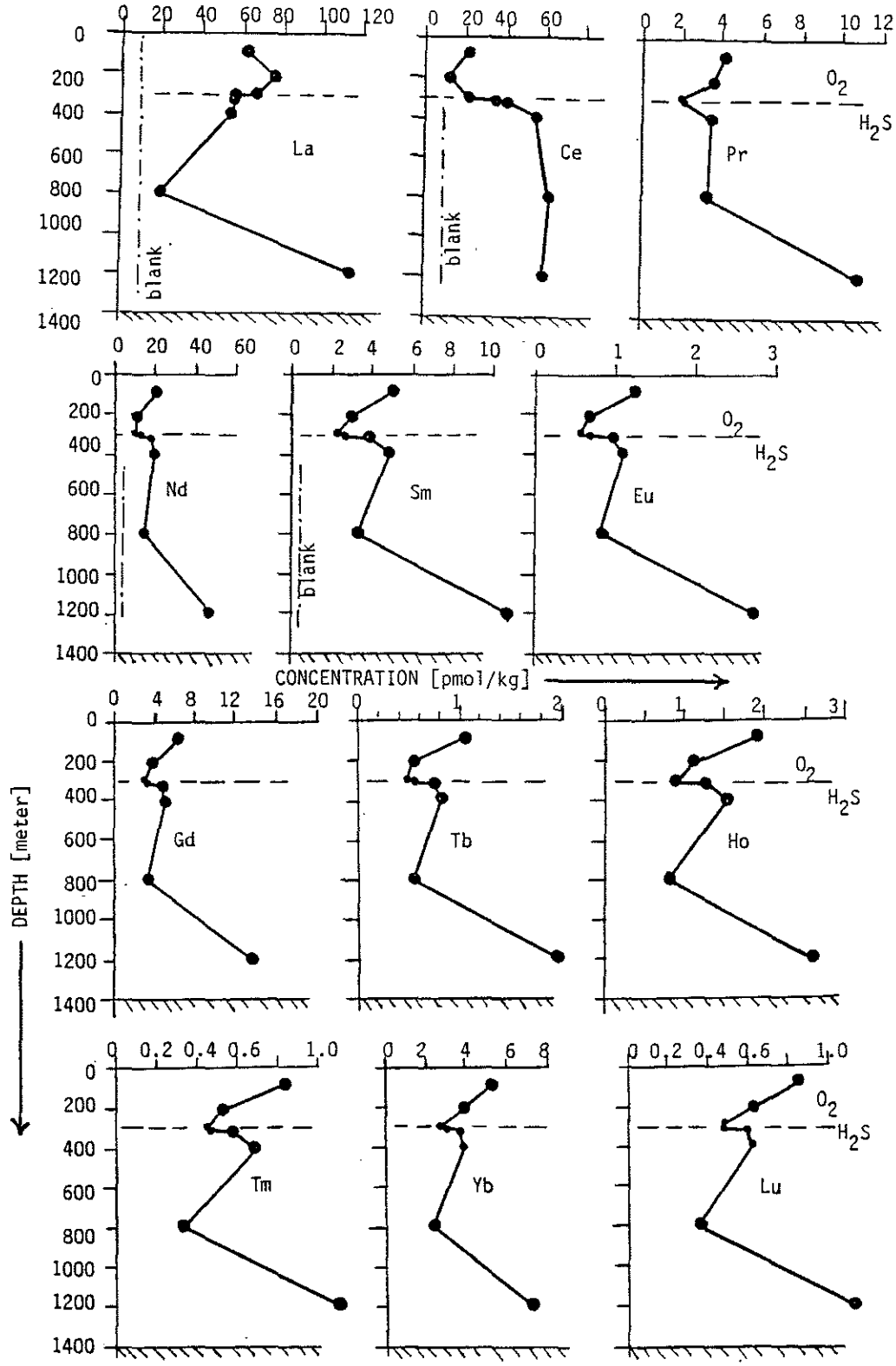


Figure 5.5. Vertical profiles of 12 REE [$10^{-12}$mol.kg$^{-1}$] at station 5.

Vertical profiles of all REE are strongly affected by the $O_2/H_2S$ interface (Figure 5.5). The suite Nd-Lu invariably shows a steep increase into the anoxic zone. This trend is even stronger for Ce. On the other hand La (and Pr) shows a distinct decrease instead. In other terms Ce behaves very differently indeed from its neighbors La and Pr in the REE-series. At greater depths (400-800-1200m) Ce remains essentially constant while the other REE exhibit strong minima at 800m (except Pr, Nd) and high levels at 1200m depth. The enhanced Ce concentrations in the anoxic water support our earlier scenario for Ce mobilization in reducing pore waters of organic rich shelf sediments (chapter 3). It is also consistent with the broad Ce-anomaly maximum in the $O_2$-minimum zone at the Eastern Equatorial Pacific site (chapter 4).

## 5.4. Discussion.

The sharp increase of all elements (except La and Pr) below the $O_2/H_2S$ interface could very well be explained by dissolution of settling Fe/Mn oxides, the latter serving as carriers of REE. These Fe/Mn (hydr)oxides which are continuously formed just above the interface are most likely finely dispersed. Their large 'fresh' surface area may be a very efficient scavenger for adsorption of REE. Positive Ce anomalies in this settling suspended phase would lead to the observed dramatic Ce increase upon dissolution below the interface. Future analyses of suspended particles collected at the same depths may confirm this explanation. However the dropoff for La and Pr just below the interface seems inconsistent with above reasoning, unless La and Pr are preferentially removed from anoxic waters, for instance, by sulfide precipitation. Such removal, controlled by equilibrium solubility products, would be consistent with the minima at 800m depth but incompatible with the high REE values at 1200m depth where sulfide concentrations are actually higher.

Although more data points are needed in the deep water some speculations about controlling mechanisms can be expressed. Here again a combination of regeneration and scavenging removal may be operative. Regeneration at or near the seafloor combined with vertical mixing would yield a linear increase between e.g. 400m and 1200m depth. Additional

scavenging removal over the same depth range of trivalent REE would cause a midepth minimum, e.g. at about 800m. Under anoxic conditions the scavenging removal rate of $Ce^{3+}$ should not exceed the removal rates of La and Pr. Yet Ce does not exhibit a minimum at 800m depth. Within this framework the absence of such a Ce minimum can only be explained by preferential Ce regeneration. In other words, (preferential) regeneration and scavenging of Ce cancel each other out and the resulting profile looks like that of a conservative tracer (Figure 5.2). For all other elements the scavenging rate at middepth appears to exceed the regeneration rate. The above scenario is of course extremely simplistic, as horizontal transport terms have been neglected. Lateral transport along isopycnal surfaces to and from the margins of the anoxic basin is conceivable. Occasional spills of Carribean Sea bottom water with appropriate density over the sill may also lead to changes in the vertical profiles.

The REE patterns versus shales (Figure 5.6) are not inconsistent with the above speculations. The 800m depth sample is the only one which exhibits a positive Ce anomaly. In all samples the suite Pr-Lu follows the expected trend of a more or less gradual enrichment with increasing atomic number. The consistent positive excursion of Gd will be discussed in chapter 6. The lightest element La again seems to act independently from the other REE, as observed previously (chapter 4). At all depths La is strongly enriched, and in this respect a blank correction would not make much difference (Figure 5.6). At 318m and 398m depth Ce falls exactly on a straight line between La and Pr. This behaviour might be representative for a hypothetical Ce(III) which would not undergo redox reactions, i.e. Ce* in equation 3.6.1. Then the fractionations of strictly trivalent REE in seawater would seem to develop into a pattern with the actual minimum at Pr, rather than at the lightest element La. This erratic behaviour of La(III), and possibly Ce(III) as well, combined with the analytical uncertainties, would cast some doubt on the Ce-anomaly profile (Figure 5.7., left). However profiles of the molar ratios Ce/Nd and Ce/Sm, with or without blank corrections, are of similar shape as the Ce/Ce* profile (Figure 5.7). All three graphs clearly suggest a preferential increase of Ce in the anoxic zone.

5.5. Conclusions.

i) Additional analyses of filtered water and suspended particulates at different sampling depth is required, especially for the lighter REE with currently an analytical uncertainty due to blank problems.

ii) Enhanced Ce concentrations in the anoxic zone support the contention that Ce and Mn have a very similar marine geochemistry, both elements being largely controlled by their oxidation-reduction reactions.

iii) All REE are strongly affected by the chemical changes across the $O_2/H_2S$ interface.

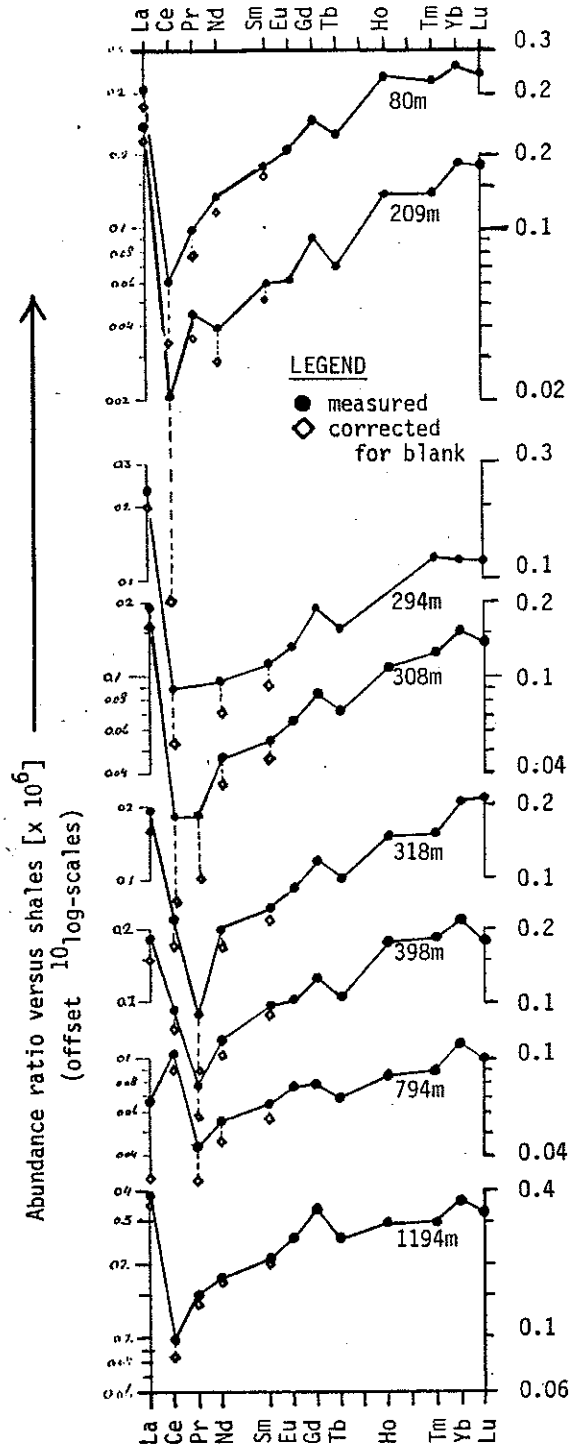


Figure 5.6. Distribution patterns of REE normalized versus shales at station 5. The filled dots represent measured values, the open diamonds correspond to blank corrected values.

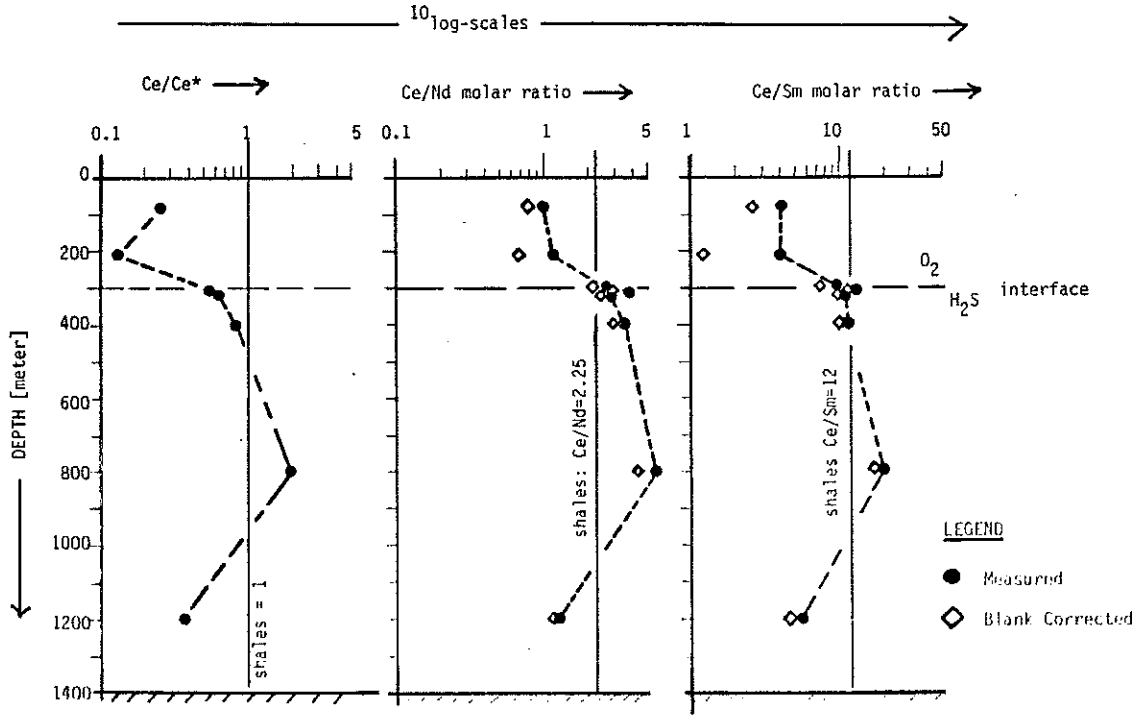


Figure 5.7. Vertical profiles of the Ce anomaly

$$Ce/Ce^* = 2(Ce/Ce_{shale})/(La/La_{sh} + Pr/Pr_{sh})$$ (left panel)

and molar ratios Ce/Nd, Ce/Sm at station 5. Filled dots represent measured values, open diamonds correspond to blank corrected values.

# 6. GADOLINIUM ANOMALIES IN SEAWATER

## 6.1. Abstract.

An observed Gd anomaly in seawater is consistent with the unique chemical behaviour of the Gd(III) cation with exactly half filled 4f electron shell. An anomalously strong complexation of Gd(III) in seawater is also predicted by the TURNER-WHITFIELD-DICKSON-model. Apparently Gd behaves more like the heaviest REE. Its observed anomaly tends to support scavenging as the dominant removal mechanism of REE(III) from the oceans.

## 6.2. Introduction.

At all three stations the vertical profiles of Gd look very similar to those of its neighboring elements (Sm), Eu and Tb in the series (Figures 3.2, 4.3, 5.6). Yet after normalization versus shales a distinct positive Gd anomaly was found in the REE distribution patterns of almost all samples (Figures 3.3; 4.4; 5.6; 6.8). This enrichment of Gd versus neighboring elements Eu and Tb may be an artefact caused by:

i) faulty analytical standards
ii) systematic analytical errors
iii) normalization versus shales.

On the other hand it may also be a geochemically significant feature arising from:

iv) true Gd fractionations in seawater, consistent with the predicted anomalous speciation of Gd in seawater (TURNER et al.,1981).

Before venturing into the last, undoubtedly most exciting, explanation (6.6), the first three options have to be explored(6.3; 6.4; 6.5).

## 6.3. Analytical Standards

Standards made up from pure metals were used for the Pacific Ocean and Cariaco Trench data sets (see section 2.14). For the Northwest Atlantic Ocean profiles an older standard mixture, made up from REE-oxides, was used. The new standards do potentially have a higher

accuracy. Nevertheless both standards are expected to agree within a few percent, although an intercalibration has not yet been performed. It is highly unlikely that both independently prepared standard mixtures would have such a large and similar Gd offset leading to the 'too' high Gd values in all data sets.

The seawater data taken from ELDERFIELD & GREAVES(1982) is also based on 'oxide' standards. More recently 'pure metal' standards have also been used in their laboratory, and apparently no large differences between the two type standards were found. Next year the various standards at their and our laboratory will be intercalibrated.

6.4. Systematic analytical errors.

Gd is one of the more difficult REE for determination by neutron activation analysis (see section 2.13). Concentration values based on the 97keV and 103keV peaks of long-lived isotope $^{153}$Gd usually agree within ten percent, with each value yielding a positive Gd anomaly. The reported concentrations represent a simple arithmetic mean of both values.
Various type systematic errors are conceivable. For instance a small unnoticed peak of another (REE)radionuclide may be hiding under a Gd peak. In order to minmize such effects the standard mixture was made up in elemental ratios which generally mimic the sample composition. However the 'difficult' element Gd is enriched in the standards. With an unnoticed hidden peak this relatively larger Gd-contribution to the total peak in the standard spectra would lead exactly to the systematically 'too' high Gd values in the samples. It is unlikely though that both peaks of $^{153}$Gd(97, 103keV) would sit on top of two hidden peaks of similar size. The sample spectra are very 'clean' and appear devoid of any peaks of elements other than the REE. Moreover we found no possible candidates for hidden peaks in the 97-103 keV range when carefully searching the literature and gamma-ray energy tables for minor gamma peaks of (REE)radionuclides other than $^{153}$Gd.
Systematic errors in peak integration were avoided by checking the net peak areas calculated by GAMANL versus the areas recorded directly from the TN1710 analyzer (see 2.12).

Finally concentrations based on the weak but interference-free 363keV peak of short lived isotope $^{159}Gd$ agree within $\pm$ 20% of the $^{153}Gd$ derived values, and also yield positive Gd anomalies. Chances of systematic errors in all three peaks of two different Gd isotopes are very small.

6.5. Normalization.

The necessity of normalization has been outlined in section 1.3. After some evaluation two top contenders emerged for the status of normalization standard:

i) A weighted mean of abundances in chondritic meteorites(EVENSEN et al., 1979), representative of the relative REE distribution in the bulk earth.
ii) An arithmetic mean of abundances in three composites made up from North American, European and Russian Platform shales(HASKIN & HASKIN, 1966).

The latter is more relevant for our work because it represents:

- average crustal abuncance
- average abundance in terrestrial and marine sediments
- aeolian or riverine input of terrestrial material into the ocean basins.

Moreover the Eu depletion of seawater(Eu/Sm=0.22-0.26) and shales (Eu/Sm=0.22) are very similar (Figure 4.11) compared to chondrites (Eu/Sm=0.37). In other words there appears to be no Eu anomaly in typical seawater/shale ratios. This is important when defining the Gd anomaly relative to its neighbors Eu and Tb in the series.

Simple elemental ratios Gd/Sm, Gd/Eu and Gd/Tb are consistently higher in seawater than in shales (Figure 6.1). Given the gradual enrichment of heavy REE in seawater higher Gd/Sm and Gd/Eu ratios are of course expected. However the very same HREE enrichment would lead to lower rather than the observed higher Gd/Tb ratios. The ratio Gd/Ho, Ho being the next measured element, is indeed lower in seawater than in shales (Figure 6.1). There appears to be a crossover somewhere between Tb

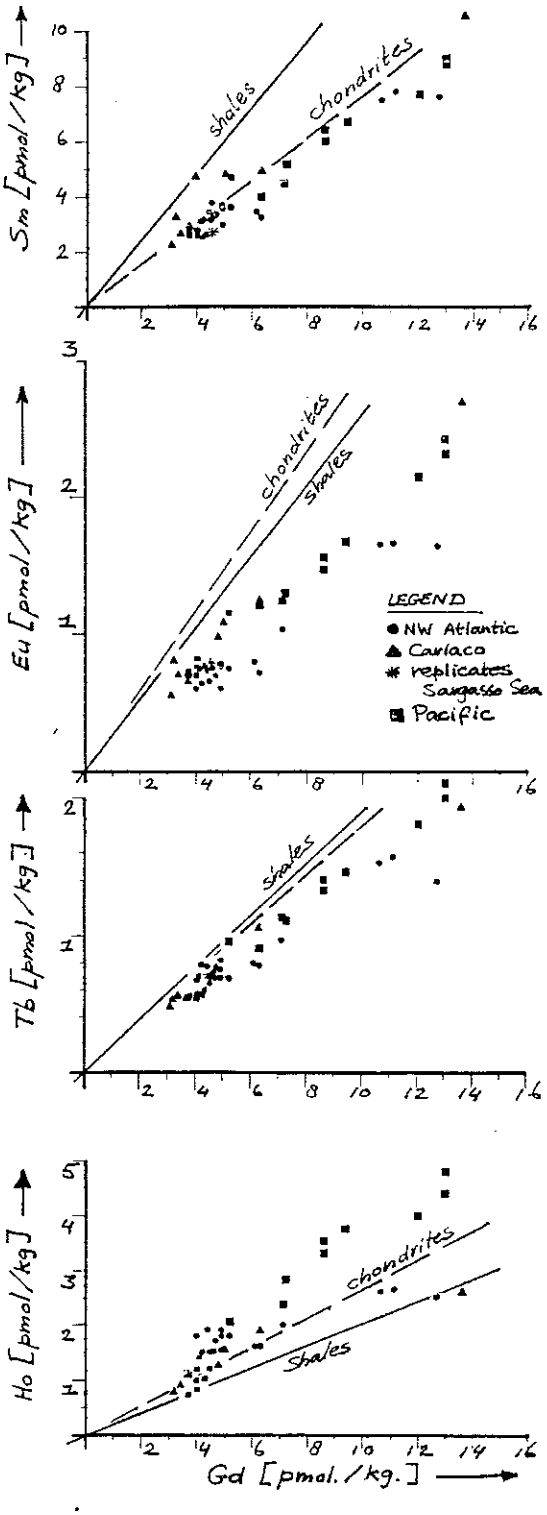


Figure 6.1. Elemental molar ratios Gd/Sm, Gd/Eu, Gd/Tb, Gd/Ho in the Northwest Atlantic Ocean and the Cariaco Trench and for the Pacific Ocean.

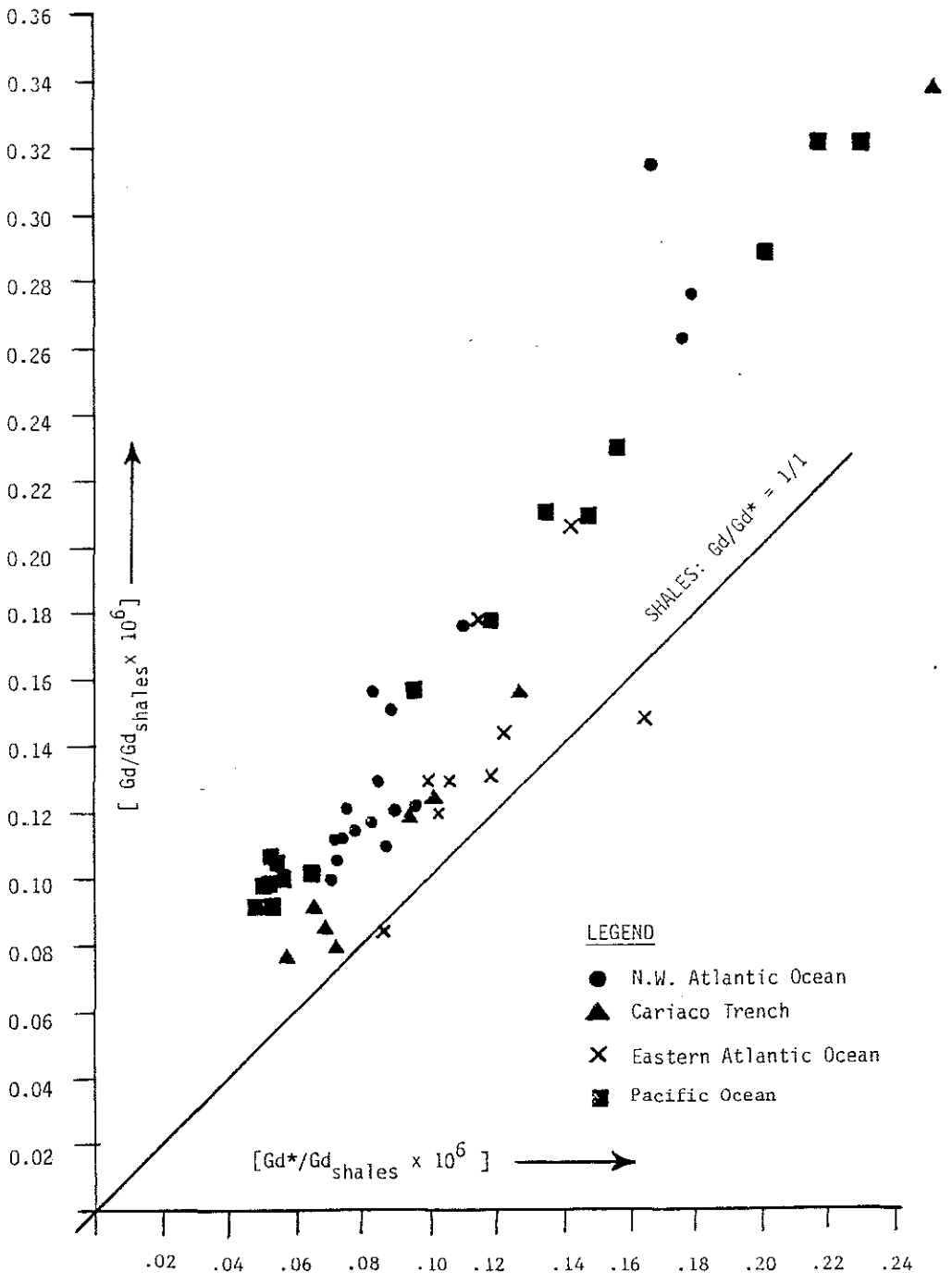


Figure 6.2. Shale-normalized measured values $Gd/Gd_{shales}$ in the Northwest Atlantic Ocean, the Cariaco Trench and the Pacific Ocean plotted versus the expected value

$$Gd^* = 1/2\ (Eu/Eu_{sh} + Tb/Tb_{sh})$$

as interpolated between neighboring elements Eu and Tb also normalized versus shales. The data for the Eastern North Atlantic Ocean (ELDERFIELD & GREAVES, 1982) was plotted versus

$$Gd^* = 1/3\ (2\ Eu/Eu_{sh} + Dy/Dy_{sh})$$

and Ho where the Gd/REE ratio shifts from too high values back to expected lower ratios than in shales. In other words, in seawater Gd seems to fit better in the heavier Dy-Ho range than in between Eu and Tb where it belongs according to atomic number.

This unusual behaviour of Gd can be better resolved by definition of a Gd anomaly:

$$(Gd/Gd^*)_{sh}=2(Gd/Gd_{sh})/(Eu/Eu_{sh} + Tb/Tb_{sh}) \qquad (6.5.1)$$

where Gd* represents the 'normal' behaviour of Gd as interpolated between neighboring elements Eu and Tb. When measured Gd-values are plotted versus Gd* almost all data points fall above the Gd/Gd*=1/1 line for shales (Figure 6.2). ELDERFIELD & GREAVES(1982) did not measure (monoisotopic) Tb, and there appears to be no distinct Gd anomaly in their REE patterns versus shales. However for their samples we calculated Gd* by using the next element Dy instead. In this way the linear interpolation stretches a longer span of the curved REE distribution pattern, and the resulting values of Gd* are slightly less significant. Nevertheless most of their data also fall above the 1/1 line.

Alternatively the same approach can be used for normalization versus chondrites instead of shales. Seawater has a strong Eu depletion relative to chondrites (see above). Determination of Gd/Gd* by linear interpolation between $Eu/Eu_C$ and $Tb/Tb_C$ would invariably yield a positive yet meaningless Gd anomaly. Therefore the next element Sm is used instead:

$$(Gd/Gd^*)_C=3(Gd/Gd_C)/(Sm/Sm_C + 2\ Tb/Tb_C) \qquad (6.5.2)$$

In this way the same trend, although not as distinct, is found as before versus shales (Figure 6.3). Whether normalizing versus shales or chondrites, Gd seems consistently enriched in seawater relative to the adjacent elements Sm, Eu, Tb (and Dy).

The vertical profiles of above defined Gd anomalies are scattered but there is a trend of stronger anomalies at greater depths, consistent with a more developed fractionation in deeper, older, water masses (Figure 6.4).

The ambiguities of normalization standards may be avoided by comparing concentrations in different waters. For instance, one might expect to find an enhanced Gd anomaly in (older) Pacific waters. However, when comparing the Pacific versus the Atlantic data, any small effects for Gd would be obscured by a minor but distinct Eu anomaly at almost all depths (Figure 4.5).

## 6.6. Gd fractionations in seawater.

In the earlier chapters it was found that two competing mechanisms probably control the distributions of REE(III) in seawater (section 4.3):

i) incorporation in crystal lattices of calcareous skeletons
ii) scavenging by adsorbing surfaces of settling particles.

The corresponding fundamental properties for fractionation of the REE(III) cations are:

i) different ionic radii
ii) different relative affinity of chemical bonding with either the adsorbing surface or the stabilizing complexers in seawater solution.

Of course both properties depend largely on the electron shell filling of the REE(III)-cations. The concept of ionic radius is closely tied in with the type and strength of chemical bonding, and in a sense the above distinction between the two properties is misleading. Nevertheless the effects of both properties will be adressed.

### Ionic radii

The famous lanthanide-contraction with increasing atomic number (chapter 1) corresponds to a gradual decrease in ionic radii from 1.03A for La(III) to 0.8 A for Lu(III) in sixfold coordination (Table 1.3. ). With respect to Gd it is interesting to note a small but distinct discontinuity in the contraction between Gd and Tb. Sixfold coordinated Ca(II) has an ionic radius of exactly 1.00A and substitution of Ca by REE(III) in calcite or aragonite is possible. Of course there are difficulties with maintaining charge balance. Also the REE(III)-O bonds are more covalent than the Ca(II)-O bonds and ideally these as well as

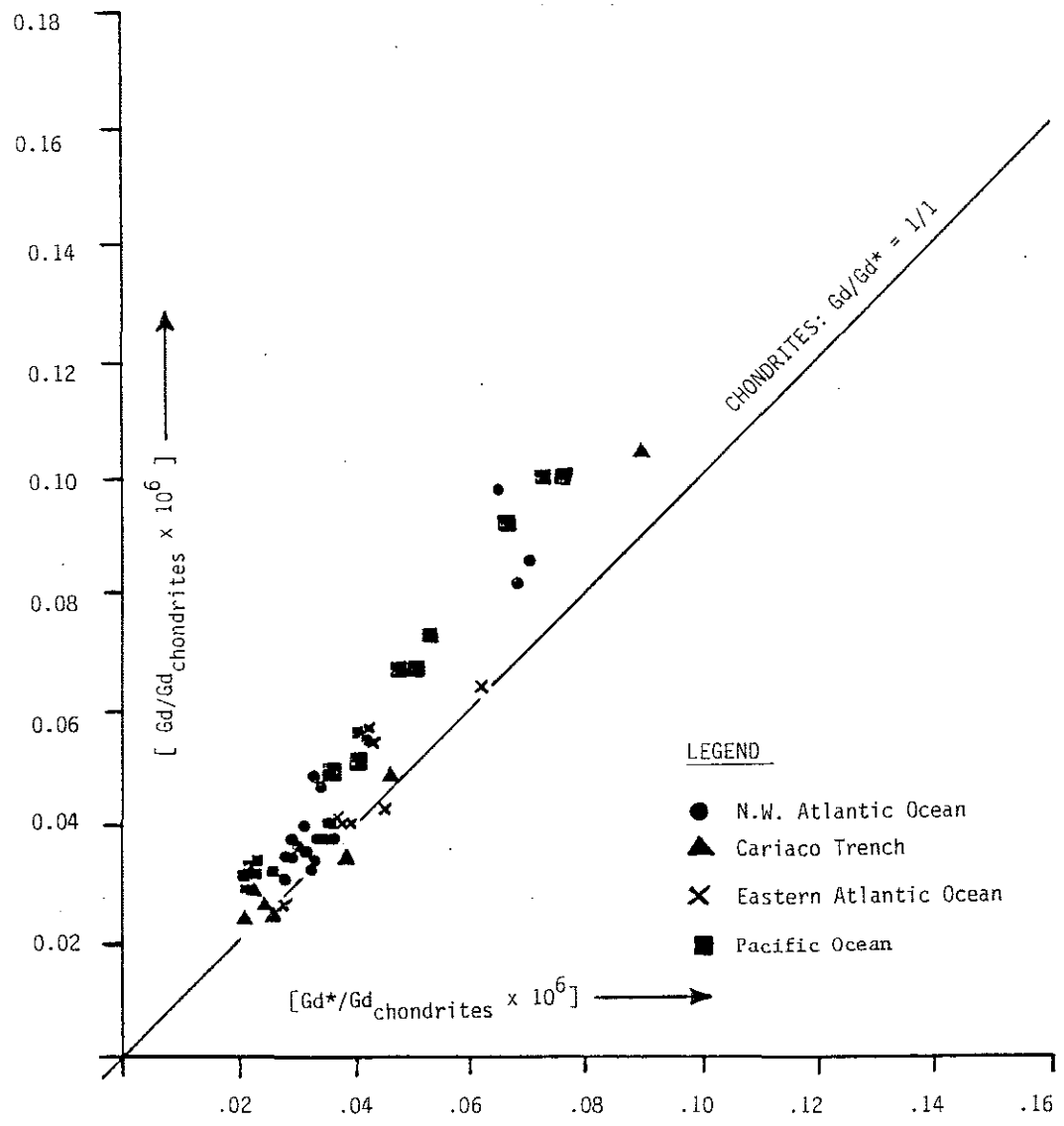


Figure 6.3. Chondrite-normalized measured values of $Gd/Gd_{chondrites}$ in the Northwest Atlantic Ocean, the Cariaco Trench and the Pacific Ocean plotted versus expected values

$$Gd^* = 1/3\ (Sm/Sm_c + 2\ Tb/Tb_c)$$

as interpolated between Sm and Tb, also normalized versus chondrites. The data of the Eastern Atlantic Ocean (ELDERFIELD & GREAVES, 1982) was plotted versus

$$Gd^* = 1/2\ (Sm/Sm_c + Dy/Dy_c)$$

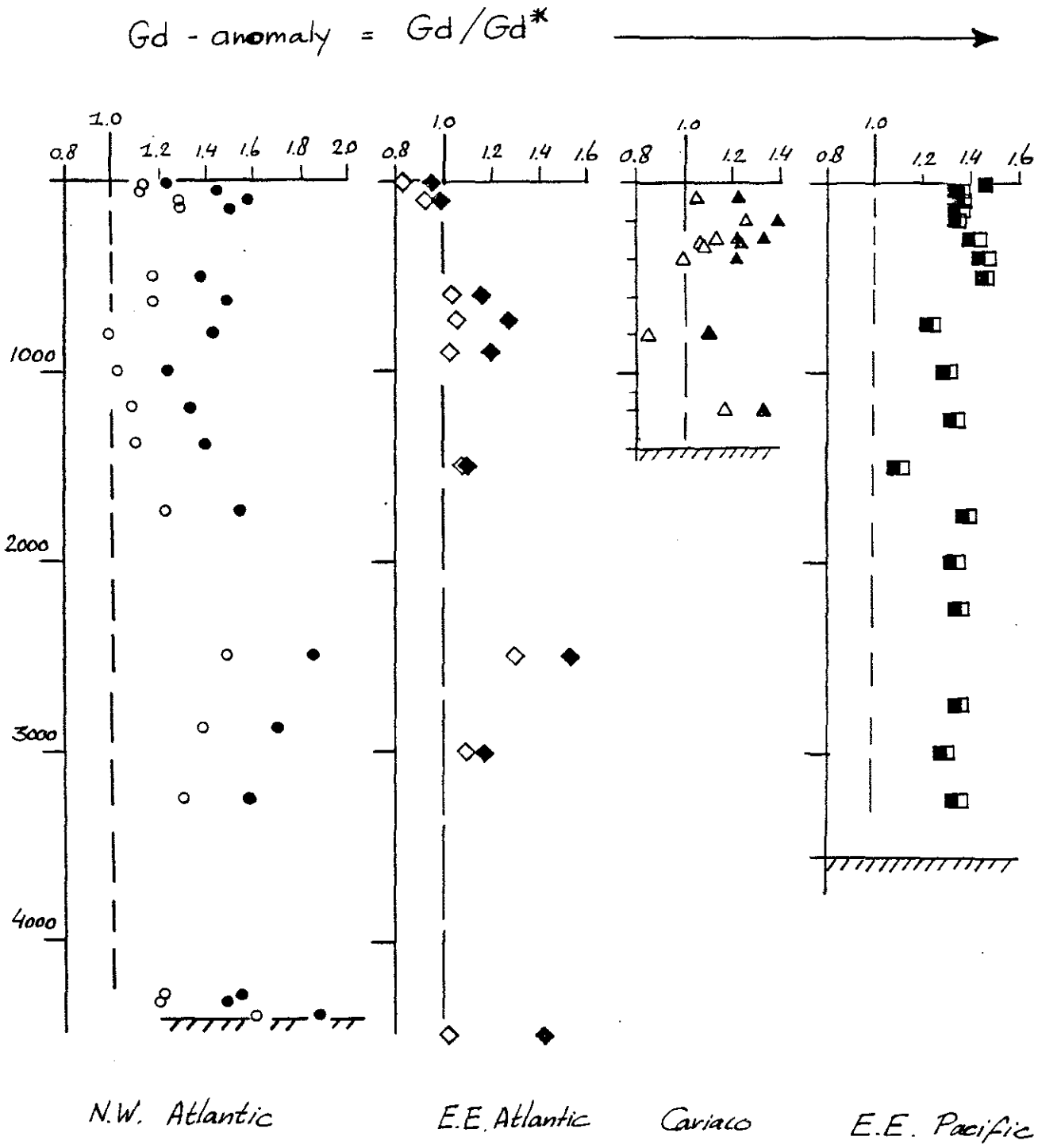


Figure 6.4. Vertical profiles of Gd/Gd* in the Northwest Atlantic Ocean, the Eastern Atlantic Ocean (ELDERFIELD & GREAVES, 1982), the Cariaco Trench and the Pacific Ocean. Filled symbols normalized versus shales, open symbols normalized versus chondrites.

crystal field effects have to be taken into account. Nevertheless it is conceivable that the heavier REE(III) with smaller ionic radii are taken up in crystal lattices of for instance calcite, whereas lighter REE(III) with larger ionic radii than Ca(II) simply do not fit and are excluded from the shells. This would lead to a preferential downward transport of the heavy REE. Upon dissolution of the skeletons the deep water would be HREE enriched, with higher levels in the deep Pacific versus the deep Atlantic Ocean.

Unfortunately there is no acceptable data on REE concentrations in uncontaminated calcium carbonate skeletons of planktonic organisms from which distribution coefficients versus bulk seawater could be calculated. However some speculations are possible from analogies with substitution of Ca(II) by REE(III) in the formation of igneous rocks. Of course the various types of igneous rock minerals do not only differ greatly among themselves, but are also very different from biogenic calcite. Nevertheless, in the crystallisation of a calcium mineral like clinopyroxene from a melt there is a preferential uptake of heavy REE in the crystal phase. There appears to be a site on the clinopyroxene crystal matrix with a radius in the same range as the radii of REE (III) ions. The heavy REE (III) with radii smaller than that of the site may substitute for Ca(II) without significant fractionation. Yet the larger light REE (III) are discriminated against to a degree increasing with increasing radii (Figure 6.5). The resulting REE fractionation typically exhibits a linear increase from La to Eu, and a horizontal trend for the heavy REE, Tb to Lu. In other words, there appears to be a break at Gd. Similar distribution coefficients for biogenic calcite versus seawater could produce a similar pattern with a distinct break at Gd. The quasi linear increase of the light REE is more or less observed in seawater. However the increasing trend continues for the heavy REE in seawater, rather than the horizontal trend in clinopyroxene. Moreover at Gd we did not observe a simple break in the curve but rather a true anomaly peak with Eu and Tb at its base.

For the calcite/seawater system the above described clinopyroxene type fractionation is at least conceivable. However, other fractionation patterns, for instance similar to those of plagioclase or olivine, are just as plausible (Figure 6.5).

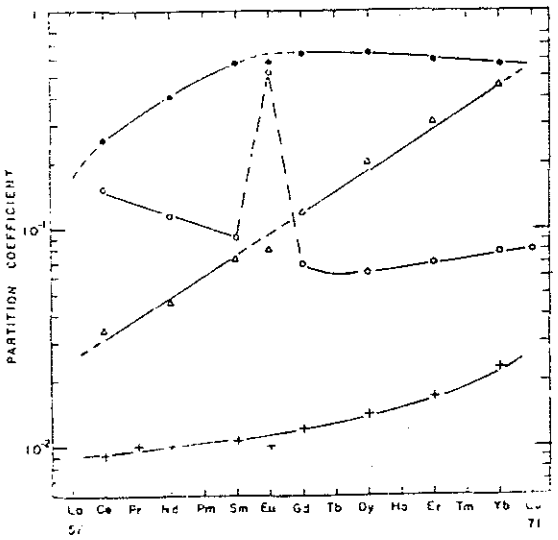


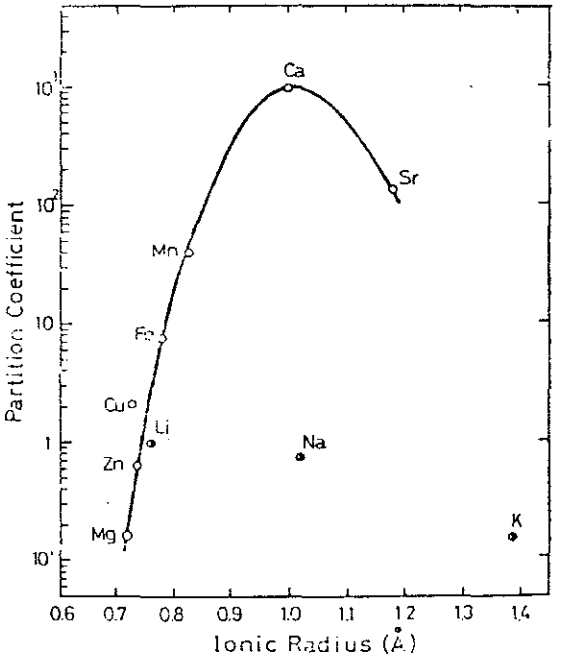


Figure 6.5. ABOVE: Average REE partition coefficients of phenocrysts (concentration in mineral phenocryst divided by concentration in matrix): closed circle Ca-clinopyroxene; open circle, plagioclase feldspar; open triangle, orthopyroxene; cross, Mg-rich olivine. Taken from SCHETZLER & PHILPOTTS (1963). One of the chapters in the new volume on Rare Earth Geochemistry edited by HENDERSON (in preparation) should provide a review of REE distribution coefficients.

BELOW: Partition coefficient versus ionic radius for inner shell layer aragonite and solution phase of a marine bivalve mollusc. Taken from ONUMA et al., 1979). A similar shape curve with generally lower $K_d$=values and a maximum at Gd could be envisioned as partial explanation for the observed Gd anomalies.

Of course multiple fractionations along above lines, possibly combined with additional fractionation due to scavenging removal, could also lead to any type REE pattern, including the observed Gd anomaly, in seawater. Alternatively one can envision a fractionation pattern between calcite and seawater with maximum distribution coefficient for the best fitting element, (e.g. Gd) whereby both smaller and larger REE(III) are discriminated against. Such trend has been reported for distribution coefficients of divalent cations between aragonite and seawater (Figure 6.5).

While the substitution of Ca(II) by REE(III) in biogenic $CaCO_3$ cannot be excluded as a cause for Gd anomalies in seawater, there is no evidence at all to support such mechanism.

Chemical Bonding.

In analogy with a model by BACON & ANDERSON (1982) the scavenging removal of trace elements from seawater is envisioned as a two step process:

i) equilibration of REE(III) between inorganic complexes in solution and surface sites on small suspended particles (Figure 6.6)

ii) periodic removal of small suspended particles, the latter being swept out either by settling biogenic debris from surface waters or by zooplankters at all depths which are packaging fine suspended particles into large projectiles(e.g. fecal pellets) to be sent downward.

Every time when part of the small particles have been swept out (ii), the remaining REE(III) will re-equilibrate between dissolved species and left-over small particles. Fractionations within the REE-series are thought to occur exclusively in this equilibration step. Different REE(III)-ions may have different bonding energies either with the solid phase or with the various anions in solution. Without constraints on the plausible surface sites (e.g. Fe/Mn-oxides, clays, organic functional groups) and lacking information on their binding constants with REE(III) it is hard to predict whether the solid phase does control REE fractionations. On the other hand there is a convincing line of evidence in support of fractionations resulting from differential REE(III) speciation patterns in seawater.

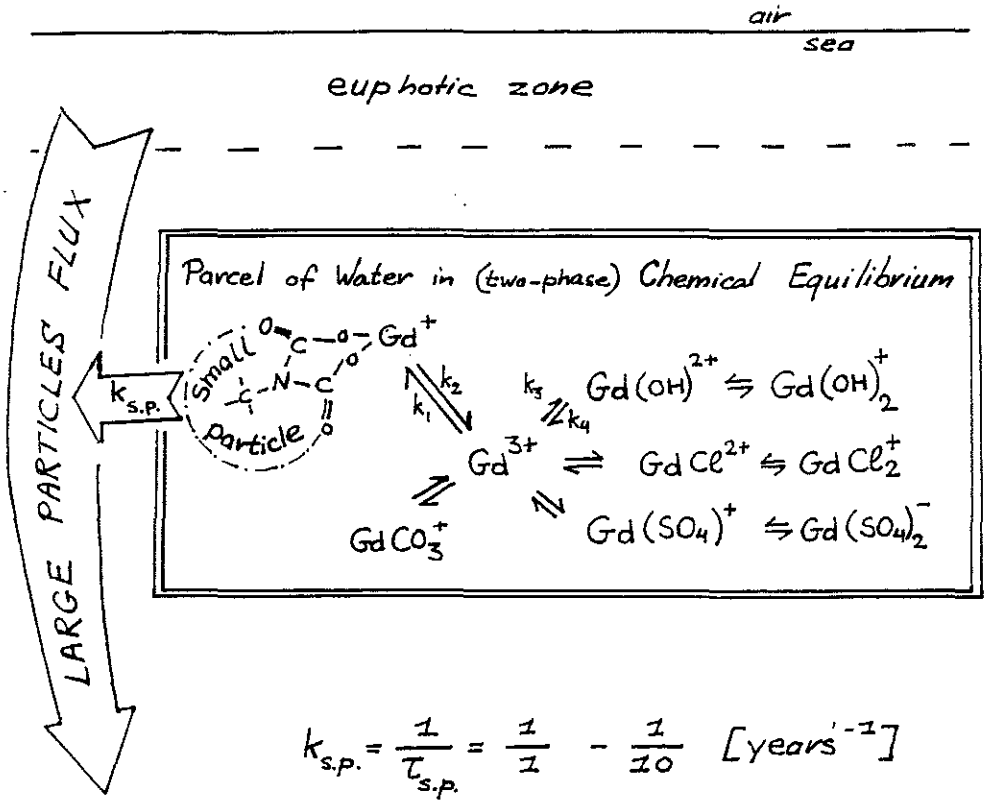


$$k_{s.p.} = \frac{1}{\tau_{s.p.}} = \frac{1}{1} - \frac{1}{10} \quad [years^{-1}]$$

$hours^{-1} \ll k_3, k_4 \ll seconds^{-1}$

$days^{-1} \ll k_1, k_2 \ll hours^{-1}$

$k_1, k_2, k_3, k_4 \ggg k_{s.p.} \longrightarrow$ equilibrium control

$$\frac{1}{\text{residence time (scavenging)}} = \frac{1}{\tau_{REE}} = \frac{1}{\tau_{s.p.}} \times \frac{[REE]_{s.p.}}{[REE]_{total}} = \frac{1}{10} \times \frac{1}{50} = \frac{1}{200} \; [yr^{-1}]$$

where 1/50 = 2% of REE on fine suspended particles in equilibrated parcel of water, as example.

Figure 6.6. Sketch depicting the equilibration and periodic scavenging removal of REE(III)-ions in a parcel of seawater. Most of the time the parcel of water may be considered a subsystem in chemical equilibrium, with only intermittent disturbance when the fine particles are occasionally being removed.

First the unique fundamental properties of the Gd(III) ion will be highlighted. Then the ambiguities encountered when predicting the behaviour of Gd(III) in aqueous solution will be discussed. Finally the remarkable agreement between such a speciation model and the field measurements will be demonstrated.

Gd (Z=64) is the 8th element in the series of 15 REE ($_{57}$La to $_{71}$Lu). This location halfway along the series leads to an exactly half-filled inner 4f electron shell for the Gd(III)-cation (Table 1.1). There appears to be a special stability associated with the exactly half-filled 4f shell. The sum of the first three ionization potentials exhibits a distinct minimum at Gd (Figure 6.7). The relatively larger decrease in ionic radii between Gd and Tb has been mentioned above, but is also indicative for similar discontinuities in for instance hydration and complexation constants.

Similar, but considerably weaker, energetic advantages have been invoked for exactly 1/4 filled (between Nd and Pm) and 3/4 filled (between Ho and Er) 4f shells of the REE(III)ions. These combined discontinuities between the third and the fourth, exactly at the seventh (Gd), and between the tenth and eleventh 4f electron filling are known as tetrad effects (NUGENT, 1970; SIEKIRSKI, 1971; DZURINSKII, 1980). An example is depicted in Figure 6.7. Of course the stronger effect exactly at Gd would be better detectable than the weaker effects in between Ho-Er and Nd-Pm, not in the least because Pm does not exist in nature and Er has not been measured in our samples.

When attempting to translate the above unique properties of Gd into predictions for aqueous solution, the effects of hydration have to be taken into account. In a fundamental sense metal ions simply dissolved in water are already complexed in that they have formed aquo-ions. The process of forming what more conventionally are called complexes is really one of displacing one set of ligands, which happen to be water molecules, by another set (COTTON & WILKINSON, 1972). Thus it is only logical to first look at these aquo-ions, (i.e. hydration) before evaluating the formation of complex ions. The tremendous experimental and

theoretical problems of the hydration concept in (sea)water have been outlined by WHITFIELD(1975). With respect to the REE(III) the Gd(III)-ion has an exactly spherically symmetrical ligand field which in itself might lead to a unique hydration pattern. There is however a large number of other factors and concepts involved. As a result there appears to be no simple explanation of tetrad effects as observed in certain type aqueous solutions (WILLIAMS, 1982). Prediction of tetrad effects for hydration in other aqueous solutions (e.g. seawater), is probably even more difficult. Nevertheless there is some indication that the lighter members La(III) to Nd(III) have a ninefold coordination, whereas the series Gd(III) to Lu(III) is generally eightfold coordinated. In other words, there would again be a break at about Gd. However all above evidence is based on measurements in strong solutions, and different REE(III) hydration numbers may be dominant in very dilute media like seawater.

The formation of complexes in seawater undoubtedly exerts a control on the distribution of many trace elements in the oceans. However it is extremely difficult to quantify this speciation in a meaningful way. Speciation models for inorganic complexation in seawater can be constructed from equilibrium constants measured under laboratory conditions, to be found in compilations like those of SILLEN & MARTELL (1976) or BAES & MESMER (1976). Of course the oceans are not an equilibrium system. Especially when dealing with elements involved in biological cycles or slow redox reactions, the equilibrium assumption could lead to misleading predictions. On the other hand, the formation of inorganic complexes in solution has relatively fast kinetics, and this subsystem may, at least in principle, well be described by equilibrium models. However several other problems still remain (BYRNE, 1983):

- activity coefficients are usually only interpolated as a function of ionic strength, while in fact they also depend on the anion type (e.g., chloride, chlorate, nitrate) of the bulk solution.
- double ligand species are usually ignored
- models are usually defined at 1atm and 25$^{o}$C, whereas oceanic conditions vary between 0-30$^{o}$C and 1-500atm. The well known pressure dependence of the carbonate ion [$CO_3^{2-}$] concentration is a case in point. With respect to the REE(III) ions, their predominant carbonate species would shift accordingly.

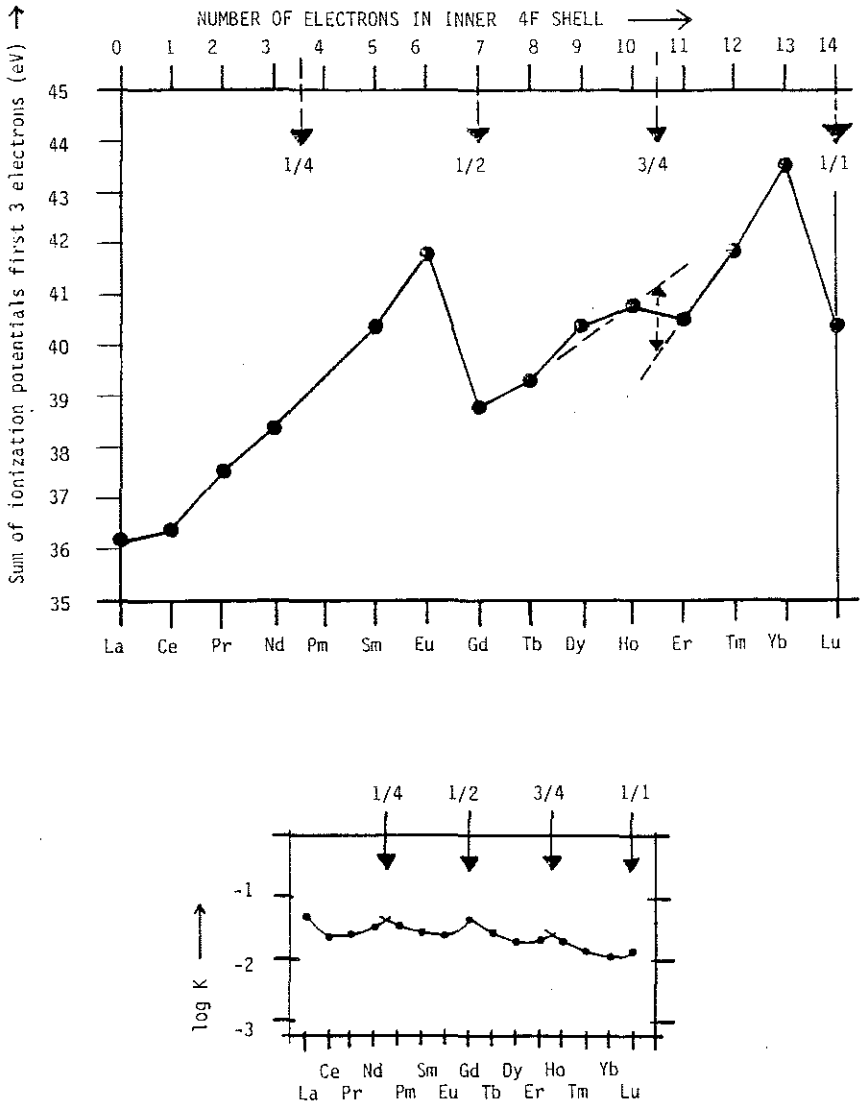


Figure 6.7. ABOVE: The sum of the first three ionization potentials of the rare earth elements. Note the marked decrease at half-filled (Gd) and completely filled (Lu) 4f electron shells. A minor discontinuity may occur between Ho and Er, yet no such discontuinuity appears between Nd and Pm. Taken from FAKTOR & HANKS (1969).

BELOW: An example of a tetrad effect. Variation of log K with atomic number Z where K is the equilibrium distribution constant between an aqueous solution of LiBr and HBr and a solution of di(ethylhexyl) chloromethyl phosphonate in benzene. Taken from PEPPARD et al. (1969).

When dealing with just one element, for instance Cu, these sources of error combined with different choices of constants may lead to very different predictions in the various models (HANSON et al., 1983). On the other hand the relative trends for a group of elements like the REE are, at least in qualitative sense, less susceptible to these errors.

Despite the above pitfalls and the uncertainties of hydration various speciation models have been developed for trace elements in seawater. A major problem with respect to the REE is the fact that so far no formation constants have been available for the important REE(III)-carbonate complexes. TURNER, WHITFIELD & DICKSON (1981) attempted to solve this deficiency by relying on a general correlation between constants for oxalates and carbonates. Clearly a more detailed study of REE(III)-complexes in seawater is badly needed. Yet for the time being the best available model (TURNER et al., 1981) leads to some interesting predictions. In their results a very distinct Gd anomaly appears for almost every dissolved species, including the free $Gd^{3+}$-ion itself (Table 6.1, Figure 6.8). This being the case there is a striking resemblance between the total amount of REE(III) complexes and the shale normalized pattern observed in seawater (Figure 6.8). In other words, not only do the heavier REE indeed appear to be more stabilized due to their generally stronger complexation in seawater (GOLDBERG et al., 1963), but a minor anomaly in Gd speciation is also reflected in our measurements.

MASUDA & IKEUCHI (1979) expected to find such a Gd anomaly (or actually a full-fledged tetrad effect) in seawater. Although their analysis of nine REE in one seawater sample did not provide firm proof, our data now corroborates their expectations with respect to the Gd anomaly.

## 6.7. Discussion

For a given parcel of water the fractionation of REE may take place as a single batch process. For instance, assume a flat shale pattern for the REE input, i.e., the initial total REE content. Subsequently REE(III) are distributed between the solid and liquid phases, with the distribution coefficient proportional to the percentage free ion

(Table 6.1). After the solid phase (fine suspended particles) has been taken out the remaining REE in the parcel of water would have the observed pattern with a positive Gd anomaly. The authigenic phase of settling large particles (sediment trap material) or marine sediments would then have the complementary (inverted) pattern with a Gd depletion.

On the other hand, the two-step removal model (Figure 6.6) would amount to multiple removal and equilibration steps. For instance a small particle residence time of 1-10 years and a REE(III) residence time in the 500-year range would correspond to 50-500 equilibrations. This would be analogous to a chromatography column with 50-500 theoretical plates, each one of them in equilibrium. The behaviour of such systems can be described by the RAYLEIGH distillation equation, also commonly used for unraveling REE fractionations in the upper mantle. Starting with a shale type pattern one would only need very small differences in distribution coefficients in order to arrive at the observed seawater pattern within 50-500 equilibration steps. In other words, one does not necessarily need the big difference in speciation as predicted by the TURNER-WHITFIELD-DICKSON-model. Given enough fractionations a difference as small as 1 percent between Gd and the other REE would yield the observed Gd anomalies. With the unique fundamental properties of Gd(III) it is most likely that such a difference, whether small or large, would indeed exist. With multiple removal steps the removed material, i.e. the authigenic phase of sediment trap material, would have a REE pattern barely distinguishable from the parcel of water. In contrast to a single batch extraction the REE pattern would not be the inverse of the seawater pattern. The absence of a Gd depletion from sediment trap material (yet to be analyzed) would not necessarily disprove our observation and interpretation of Gd anomalies in seawater. More or less the same argument could be made with respect to the authigenic phase of marine sediments. Moreover any authigenic signal would often get lost in the dominant shale pattern of the major detrital component of deep sea sediments.

| Cation | Free | OH | F | Cl | SO4 | CO3 |
|---|---|---|---|---|---|---|
| La(III) | 38 | 5 | 1 | 18 | 16 | 22 |
| Ce(III) | 21 | 5 | 1 | 12 | 10 | 51 |
| Pr(III) | 25 | 8 | 1 | 12 | 13 | 41 |
| Nd(III) | 22 | 9 | 1 | 10 | 12 | 46 |
| Sm(III) | 18 | 10 | 1 | 8 | 11 | 52 |
| Eu(III) | 18 | 13 | 1 | 10 | 9 | 50 |
| Gd(III) | 9 | 5 | 1 | 4 | 6 | 74 |
| Tb(III) | 16 | 11 | 1 | 8 | 11 | 52 |
| Dy(III) | 11 | 8 | 1 | 5 | 6 | 68 |
| Ho(III) | 10 | 8 | 1 | 5 | 5 | 70 |
| Er(III) | 8 | 12 | 1 | 4 | 4 | 70 |
| Tm(III) | 11 | 21 | 1 | 5 | 6 | 55 |
| Yb(III) | 5 | 9 | 1 | 2 | 3 | 81 |
| Lu(III) | 5 | 21 | 1 | 1 | 1 | 71 |

Table 6.1. The equilibrium speciation of dissolved REE(III) cations in seawater at pH=8.2, 25$^{o}$C and 1 atm pressure (TURNER, WHITFIELD & DICKSON, 1981).

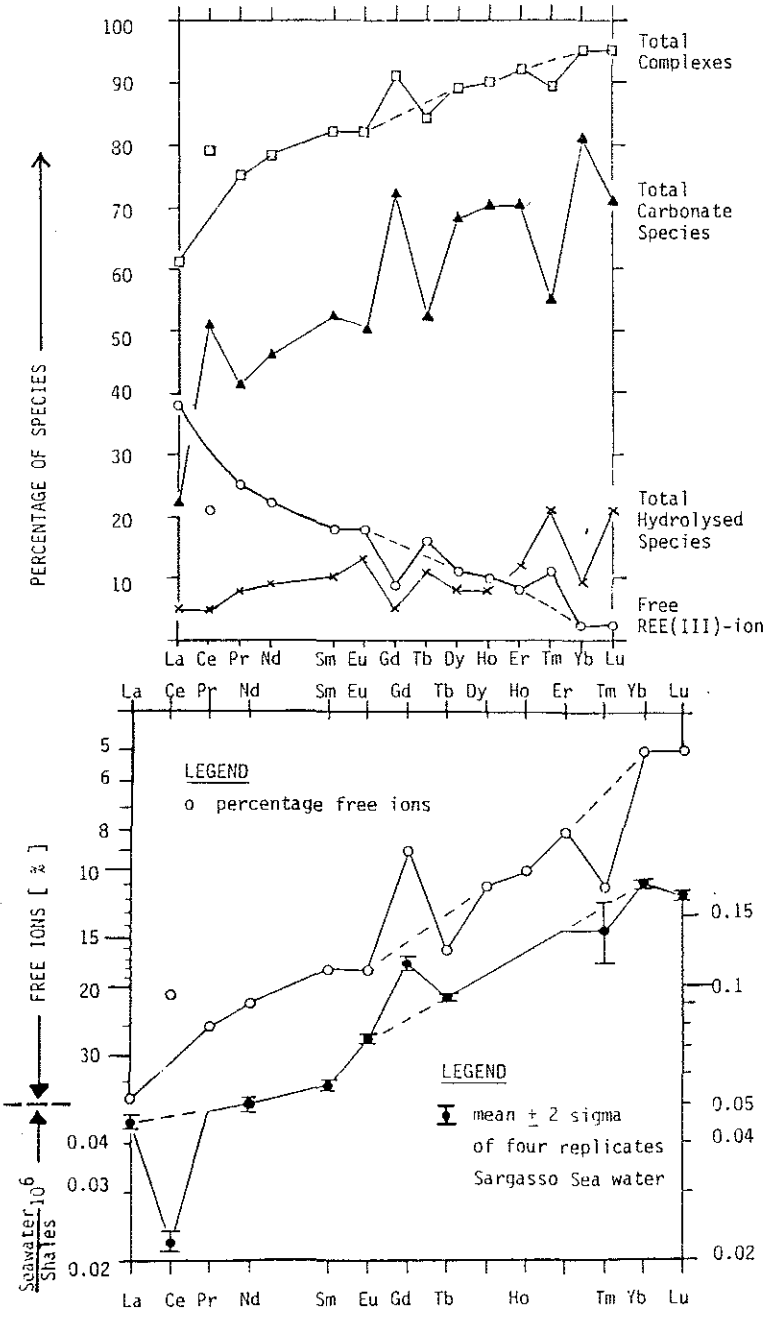


Figure 6.8. ABOVE: Percentages of various species of REE(III) in seawater as predicted by the model of TURNER, WHITFIELD & DICKSON (1981). Note the strong Gd excursions.

BELOW: The mirror image (log-scale) of above percentage free REE(III)-ions compared with the shale-normalized distribution pattern for four replicates of Sargasso Sea surface water. The light REE(III) with a higher percentage free ion are more depleted in seawater. The Gd anomaly in seawater is compatible with a similar anomaly in the percentage free ions.

## 6.8. Conclusions

1) Seawater, normalized versus either shales or chondrites, consistently exhibits a positive Gd anomaly.

2) The well known anomalous physical and chemical properties of the Gd(III) cation with exactly half filled 4f electron shell could very well lead to the observed Gd fractionation in seawater.

3) The Gd anomaly is compatible with the predicted speciation of REE(III) in seawater, in combination with scavenging removal as the dominant control of REE distributions in the oceans.

3) Some hypothetical fractionation of Gd due to uptake in calcareous skeletons is at least conceivable. Yet there is no evidence in support of this mechanism.

4) The absence of Gd anomalies from deep sea sediments or sediment trap material (yet to be measured) would not necessearily disprove the earlier conclusions.

# 7. SUMMARY

## 7.1. Conclusions

Distributions of dissolved REE in ocean waters are dominated by their internal cycling within the ocean basins. The ultimate external sources (riverine, aeolian, hydrothermal) and sinks (authigenic minerals) would generally have very little impact on the spatial distribution of REE in oceanic water masses, although on two occasions a terrestrial aerosol source (ELDERFIELD & GREAVES, 1982) and a hydrothermal source (MICHARD et al., 1983) have been identified.

In reference to the working hypotheses stated in chapter 1 (section 1.4), various conclusions can be drawn:

Analogies with distributions of other properties within the oceans suggest that the REE as a group are controlled by two simultaneous processes:

i) cycling like or identical to opal and calcium-carbonate, with circumstantial evidence in suport of the latter as a possible carrier.

ii) adsorptive scavenging, possibly by manganese-oxide phases on settling particles.

The latter mechanism is strongly supported by the parallels between REE(III) speciation in seawater and the 'typical' seawater REE pattern. This general correspondence is highlighted by the very distinct excursions of Gd in both Gd(III)-speciation and the observed seawater REE patterns.

Combination of both apparent mechanisms, for instance scavenging of REE by adsorptive coatings (Mn-oxides) on settling skeletal material, is very well conceivable. Upon dissolution of the shells at or near the seafloor, the adsorbed REE fraction would again be released into the bottom waters.

The observations of

- positive Ce anomalies in Northwest Atlantic surface waters (Ch.3),
- enhanced Ce anomalies and Mn levels in the $O_2$-minimum zone of the Eastern Equatorial Pacific Ocean (Ch.4), and
- enhanced Ce concentrations in anoxic waters (Ch.5)

all support the contention that a vigorous cycling driven by oxidation and reduction reactions dominates both Ce and Mn in the ocean basins.

When disregarding kinetic hindrance and at a constant pH=8.2 of seawater the element Ce appears to be fractionated between environments with partial oxygen pressure above respectively below a certain threshold level, probably at or about 0.001-0.010 atmosphere (chapter 4). At higher $pO_2$ levels dissolved Ce(III) is removed by formation of insoluble Ce(IV) forms. As a result Ce tends to be depleted in open ocean waters and normal or enriched in waters below the $pO_2$ threshold. In analogy with surfaces of constant salinity, potential temperature or density one may envision surfaces of constant Ce anomaly (i.e. constant Ce/Ce*). In a hypothetical 'equilibrium ocean' the 'no-anomaly' surface (Ce/Ce* = 1) would coincide with the $O_2$-threshold surface, the latter generally lying below the sediment water interface. However, the ocean is an open system and definitely not in equilibrium. Transport terms which are fast relative to slow kinetics of the Ce oxidation (reduction) reaction, would cause uncoupling of the 'no-anomaly' surface and the $pO_2$-threshold surface. For instance positive Ce anomalies were found in well oxygenated surface waters (chapter 3). Matters seem further complicated by the observed stronger Ce depletion in the Pacific compared to the Atlantic Ocean. With the Pacific water column generally more depleted it is more difficult to generate 'normal' (Ce/Ce*=1) or enriched Ce levels by in situ regeneration, i.e. reduction. Strictly speaking, the aforementioned transport terms may be seen as the ultimate driving force behind this interoceanic difference. In other words, going from the Atlantic into the Pacific basin the $O_2$ threshold surface tends to coincide with lower and lower (more depleted) Ce anomaly surfaces.

If these observations are indeed characteristic for the Pacific and Atlantic Oceans, then the Atlantic Ocean with less of a Ce-depletion would appear to be the major recipient of the, presumably unfractionated, external terrestrial REE input, the latter with a flat (no Ce depletion)

shale pattern. This, combined with the fact that about 70% of the world's rivers drain into the Atlantic Ocean, would suggest that the dissolved river load is an important source of REE in the ocean basins.

## 7.2. Neodymium Isotopic Ratios in the Ocean Basins

The Atlantic, Indian and Pacific Oceans have distinctly different populations of 143Nd/144Nd ratios in ferromanganese deposits (PIEPGRAS & WASSERBURG, 1982). Corresponding values were reported in the overlying water column of the Atlantic and Pacific Oceans. The ratios tend to increase from the North Atlantic to the Indian and the Pacific Ocean. Values are at or below the ratios for continental crust, within the range of continental crust and continental flood basalts, but always lower than typical Mid Ocean Ridge Basalts values.

One could argue that Nd, and the other REE, in seawater are ultimately derived from continental weathering, with subsequent riverine or aeolian transport into the ocean basins. Each continent, or more specifically, drainage basin or aerosol source region, would then have a distinctly different 143Nd/144Nd isotopic ratio, leading to correspondingly different ratios between the various oceanic 'catch' basins.

However, recent 143Nd/144Nd results for suspended matter in major rivers and some aerosols are surprisingly uniform and fall within the range of the North Atlantic ferromanganese deposits (GOLDSTEIN & O'NIONS, 1982). Most of the Nd in the suspended matter and aerosols is probably incorporated within crystal lattices and thus represents a highly refractory pool. On the other hand the values for ferromanganese deposits may be more representative of the reactive pool of Nd and other REE. Nevertheless it is unlikely that the dissolved, i.e. reactive, component of a given river would have 143Nd/144Nd ratios very different from its suspended load. GOLDSTEIN & O'NIONS (1982) suggested instead that the observed difference between ocean basins may be compatible with two end member mixing between a continental source with low 143Nd/144Nd values and a mantle derived source through hydrothermal circulation at mid ocean ridges. In other words, low ratios in the North Atlantic point

at a mostly continental source, while higher values in the Pacific reflect the more active (submarine) volcanism within the latter ocean basin. Along the lines of this argument the 143Nd/144Nd ratios might serve as a tracer of hydrothermal influence in the water column, or possibly as a paleoindicator of mid ocean ridge spreading rates. Of course matters are more complicated by the weathering of various type flood basalts with intermediate Nd ratios. Interaction of hydrothermal fluids with deep sea sediments might also shift their presumed high (MORB) Nd ratio to lower (continental) values.

PIEPGRAS & WASSERBURG (1980,1982) have repeatedly advocated the use of 143Nd/144Nd ratios as a water mass tracer. With this in mind they have determined 143Nd/144Nd values in Drake Passage which indeed fall nicely in between their seawater values for the Atlantic and Pacific Oceans.

An ideal water mass tracer should be conservative, i.e. its content in a water body should only be changed by linear mixing with another water body, and not by biogeochemical processes such as biological growth, regeneration or scavenging by settling particulates.

However, the 143Nd/144Nd differences between oceans can only be maintained by a (bio)geochemical removal mechanism of Nd with, at least in Antarctic circumpolar waters, much shorter time scales (e.g. 50-250 years) than the suggested timescales ranging from about 500 to 2000 years for interoceanic mixing. Paradoxically the same mechanism which has to maintain the 143Nd/144Nd differences between water masses, would also invalidate its use as a water mass tracer. This required non-conservative behaviour of Nd has also been demonstrated in this work (for Nd and analog elements Pr, Sm, Eu; chapters 3 and 4). Only when the hydrographic time scales are short relative to the Nd removal rates the 143Nd/144Nd ratio could be treated as a quasi conservative tracer, provided that the various end members have different isotope signatures. For example, one might use the 143Nd/144Nd ratio for tracing the spreading of Mediterranean Overflow Water in the Atlantic Ocean (PIEPGRAS & WASSERBURG, 1983).

Not surprisingly the conclusions drawn by PIEPGRAS & WASSERBURG (1982) from a multi box model (which also is rather elaborate relative to the small data set) seem to disagree with the salt and water balances for

exchange between the Atlantic and Pacific Oceans. The recent observations of Nd isotopes in ocean basins are very exciting and 143Nd/144Nd isotopic ratios indeed have potential as a tracer of sorts. However a thorough study of the exchange of Nd and other REE between seawater, suspended particulates and surface sediments is required before further claims are made about specific tracer application(s) of 143Nd/144Nd ratios.

## 7.3. REE in Authigenic Minerals.

In analogy with other elements the open ocean distributions (ch.3, 4) of the REE suggest that the reactive pool (about 10 % ?) of REE in marine sediments is strongly affected by diagenesis, in contrast with the conclusions of FLEET(1983). The REE distributions in an anoxic basin also suggest active diagenesis (chapter 5). The Ce data is consistent with a major diagenetic source of Ce and other REE in ferromanganese nodules, rather than a direct seawater source (ELDERFIELD et al., 1981). Studies of REE diagenesis, supported by careful physical and chemical separation methods, are required for understanding the modes of formation and REE sources of many authigenic deposits.

The continuous redistribution of Ce within the modern ocean, combined with the likelihood of active diagenesis, cast serious doubts (see also GRAF, 1978; HOLLAND, in press) on the use of Ce anomalies as paleoindicators of oxic versus anoxic conditions in ancient oceans (FRYER, 1977; AHMAD & CONRADY, 1983; WRIGHT et al., 1983; LIU & SCHMITT, ).

On the other hand the Eu/Sm ratio, possibly combined with 134Nd/144Nd, would have potential as a tracer for modern and ancient processes of submarine hydrothermal circulation. For instance in hydrothermal deposits right at or just beyond the ridge crest one would expect to find higher values of both Eu/Sm and 143Nd/144Nd indicative of a truly hydrothermal REE fraction. The leachable REE fraction of deep sea sediment cores may very well exhibit variations of both Eu/Sm and $^{143}Nd/^{144}Nd$, possibly indicative of similar variations in hydrothermal circulation, c.q. seafloor spreading rates.

8. BIBLIOGRAPHY

AHMAD, R. & M.C. CONRADY (1983). Rare earth element geochemistry of ichtyoliths(fish debris): Implications for possible changes in the chemistry of ancient oceans. Trans. Am. Geophys. Union, 64(18): 245.

ALLER, L.H. (1961). The abundance of the elements. Wiley Interscience 283p.

ALTSCHULER, Z.S. (1980). The geochemistry of trace elements in marine phosphorites. Part I. Characteristic abundances and enrichment. Spec. Publ. Soc. econ. Paleontol. Mineral. 29: 19-30.

ANDERSON, R.F. & A.P. FLEER (1982). Determination of Natural Actinides and Plutonium in Marine Particulate Material. Anal. Chem., 54:1142-1147

ANDREAE, M.O. (1979). Arsenic speciation in seawater and interstitial waters: the influence of biological-chemical interactions on the chemistry of a trace element. Limnol. Ocean., 24(3):440-452.

ANDREAE, M.O. (1981). Determination of Antimony(III), Antimony(V), and Methylantimony species in Natural waters by Atomic Absorption Spectrometry with Hydride Generation. Anal. Chem., 53: 1766-1771.

BACON, M.P. & R.F. ANDERSON (1982). Distribution of Thorium Isotopes Between Dissolved and particulate Forms in the Deep Sea. J. Geophys. Res., 87(C3): 2045-2056.

BACON, M.P., P.G. BREWER, D.W. SPENCER, T.W. MURRAY & T. GODDARD (1980). Lead - 210, polonium - 210, manganese and iron in the Cariaco Trench. Deep-Sea Res., 27A: 119-135.

BAES, C.F. & R.E. MESMER (1976). The hydrolysis of cations. Wiley: 489p.

BAINBRIDGE, A.E. (1981) GEOSECS Atlantic Expedition, Volumes 1 and 2. IDOE/NSF, US Govt. Printing Office, Washington D.C. 20402

BALASHOV, Y.A. & L.M. KHITROV (1961). Distribution of the rare earths in the waters of the Indian ocean. Geochem Int. 9: 877-890 (translation).

BALISTRIERI, L., P.G. BREWER & J.W. MURRAY (1981). Scavenging residence times and surface chemistry. Deep Sea Res., 28: 101.

BALLARD, R.D. & J. FRANCHETEAU (1982). The Relationship Between Active Sulfide Deposition and the Axial Processes of the Mid-Ocean Ridge. Marine Techn. Soc. J., 16(3):8-22

BARRETT, T.J., H. FRIEDRICHSEN & A.J. FLEET (1983) Elemental and stable isotopic composition of some metalliferous and pelagic sediments from the Galapagos Mounds Area, DSDP Leg 70. Ch. 16 in: Init. Reps. DSDP, Vol. LXX: 315-323

BENDER, M.L., G.P. KLINKHAMMER & D.W. SPENCER (1977). Manganese in seawater and the marine manganese balance. Deep-Sea Res., 24: 799-812.

BERNAT, M. (1975). Les isotopes de l'Uranium et du Thorium et les terres rares dans l'environment marin. Cah. Orstom, Ser. Geol. 7(1): 65-83.

BEVINGTON, P.R. (1969). Data Reduction and Error Analysis for the Physical Sciences. McGraw-Hill, New York, xv + 336p.

BIORAD-LABORATORIES (1978). Chelex-100 Chelating Ion Exchange Resin for Analysis, Removal or Recovery of Trace Metals. Prod. Inf. sheet 2020.

BLOKH, A.M.(1961) Rare earths in the remains of Paleozoic fishes of the Russian platform. Geochemistry, 5: 404-415

BONNOT-COURTOIS, C. (1981). Distribution des terres rares dans le depots hydrothermaux de la zone FAMOUS et des Galapagos - comparaison avec les sediments metalliferes. Mar. Geol., 39: 1-14.

BONNOT-COURTOIS, C. (1981) Distribution des terres rares dans le depots hydrothermaux de la zone FAMOUS et des Galapagos - comparaison avec les sediments metalliferes. Mar. Geol., 39: 1-14

BONNOT-COURTOIS, C. (1980) Le comportement des terres rares au cours de l'alteration sous-marine et ses consequences. Chem Geol., 31: 119-131

BOROUGHS, H., W.A. CHIPMAN & T.R. RICE (1957) Laboratory experiments on the uptake, accumulation and loss of radionuclides by marine organisms. In: The effects of Atomic Radiation on Oceanography and Fisheries, NAS/NRC Publ. 551, Washington D.C.:80-87

BOWEN, V.T. & T.T. SUGIHARA (1965). Oceanographic Implications of Radioactive Fall-out Distributions in the Atlantic Ocean: From 20 N to 25 S, from 1957 to 1961. J. Mar. Res., 23(2): 123-145.

BOYLE, E.A. (in preparation) Manganese Carbonate Overgrowths on Foraminifera tests.

BOYLE, E.A.(1981). Cadmium, Zinc, Copper, and Barium in Foraminifera tests. Earth planet. Sci. Letts., 53:11-35

BOYLE, E.A., F. SCLATER & J.M. EDMOND (1976). On the marine geochemistry of cadmium. Nature, 263: 42-44.

BOYLE, E.A., F.R. SCLATER & J.M. EDMOND (1977). The distribution of dissolved copper in the Pacific. Earth planet. Sci. Letts., 37: 38-54.

BREWER, P.G. & D.W. SPENCER (1975). Minor element models in coastal waters. Ch. 4 In: T. Church. (Ed.) Marine Chemistry in the coastal environment, Am.Chem.Soc. Symposium Ser., 18: 80-96.

BREWER, P.G. & J.W. MURRAY (1973). carbon, nitrogen and phosphorus in the Black Sea. Deep-Sea Res., 20: 803-818.

BREWER, P.G., D.W. SPENCER, C.L. SMITH, S. KADAR, D. SHAFER and A.P. FLEER, (1978). The distribution and chemical composition of particulate matter in the Atlantic Ocean. Technical Report. WHOI.

BROECKER, W.S. & T. TAKAHASHI (1980). Hydrography of the Central Atlantic. - III. The North Atlantic Deep-Water Complex. Deep-Sea Res., 27: 591-613.

BROECKER, W.S. & T.H. PENG (1982). Tracers in the Sea. Eldigio Press of Columbia University, Palisades, NY: 690p.

BROECKER, W.S. & T.TAKAHASHI (1981). Hydrography of the central Atlantic - IV. Intermediate waters of Antarctic origin. Deep-Sea Res., 28A(3): 177-193.

BROECKER, W.S., T. TAKAHASHI & M. STUIVER (1980). Hydrography of the central Atlantic - II. Waters beneath the Two-Degree Discontinuity. Deep-Sea Res., 27: 397-419.

BROENKOW, W. & R. KRENZ (1982). Oceanographic Results from the VERTEX II particle interceptor trap experiment off Manzanillo, Mexico. MLML Technical Publ. 82-1; Moss Landing, Calif.

BROENKOW, W.W., A.J. LEWITUS, M.A. YARBROUGH & R.T. KRENZ (1983) Particle fluorescence and bioluminescence distributions in the eastern tropical Pacific. Nature, 302: 329-331

BRULAND, K.W. & K.H. COALE (in prep.) $^{234}$Th: Rates of Surface Water Scavenging in the California Current.

BRULAND, K.W. (1980).-Oceanographic Distributions of Cadmium, Zinc, Nickel, and Copper in the North Pacific. Earth planet. Sci. Letts., 47:176-198

BRULAND, K.W. (1983). Trace Elements in Seawater. Ch. 3 in: RILEY, J.P. (Ed.) Chemical Oceanography, Vol. 8; Academic Press.

BRULAND, K.W., G.A. KNAUER & J.H MARTIN (1978). Zinc in north-east Pacific waters. Nature, 271: 741-743.

BRULAND, K.W., R.P. FRANKS, G.A. KNAUER, J.H. MARTIN (1979). Sampling and analytical methods for the determination of copper, cadmium, zinc, and nickel at the nanogram per liter level in seawater. Anal. Chem. Acta, 105: 233-245.

BUAT-MENARD, P. & R. CHESSELET (1979). Variable influence of the atmospheric flux on the trace metal chemistry of oceanic suspended matter. Earth Planet. Sci. Letts., 42: 399-411.

BUAT-MENARD, P. (1979). Influence de la retombee atmospherique sur la chimie des metaux en trace dans la matiere en suspension de l'Atlantique Nord. These, Univ. de Paris VII: 434.

BURBIDGE, E.M., G.R. BURBIDGE, W.A. FOWLER & F HOYLE (1957). Synthesis of the elements in stars. Rev. Mod. Phys., 29: 547-650.

BURNEY, G.A. & R.M. HARBOUR (1974). Radiochemistry of Neptunium. Nuclear Sciences Series, NAS/NRC, USAEC Techn. Inf. Ctr.; NTIS, Vol. NAS-NS-3060: 239p.

CALLAHAN, C.M., J.M. PASCUAL & M.G. LAI (1966). The concentration of trace elements from seawater by ion exchange. U.S. Naval Radiological Defense Laboratory, Dept. of Commerce, NTIS, AD-647661: 32p.

CAMERON, A.G.W. (1973). Abundances of the elements in the solar system. Space Science Rev., 15: 121-146.

CARPENTER, J.H. & V.E. GRANT (1967). Concentration and state of Cerium in coastal waters. J. Mar. Res., 25(3): 228-238.

CHAMBERLIN, T.C. (1897). The method of multiple working hypotheses. J. Geol., 5: 837-848. Reprinted in Science, 148: 754-759, 1965.

CHAN, L.H., D.DRUMMOND, J.M. EDMOND & B. GRANT (1977) On the barium data from the Atlantic GEOSECS expedition. Deep-Sea Res., 24: 613-649

CHAN, L.H., J.M. EDMOND, R.F. STALLARD, W.S. BROECKER, Y.C. CHUNG, R.F. WEISS & T.L. KU (1976) Radium and barium at GEOSECS stations in the Atlantic and Pacific. Earth Planet. Sci. Letts., 32: 258-267

CHEN, J.H. & G.J. WASSERBURG (1981). Isotopic Determination of Uranium in Picomole and Subpicomole Quantities. Anal. Chem., 53: 2060-2067.

CHIPMAN, W.A. (1958). Accumulation of Radioactive Materials by Fishery Organisms. Proc. Gulf. and Caribbean Fish. Inst.: 97-110.

CHRISTELL, R., S. FORBERG & T WESTERMARK (1961). Some experiments on the use of the chelating ion exchanger Dowex A-1 in nuclear chemistry. J. Inorg. Nucl. Chem., 19: 187-189.

CLAYTON, D.D. (1968). Principles of Stellar Evolution and Nucleosynthesis. McGraw-Hill: 612p.

CLINE, J.D. & F.A. RICHARDS (1972). Oxygen deficient conditions and nitrate reduction in the Eastern Tropical North Pacific Ocean. Limnol. Oceanogr., 17(6):885-900

CORLISS, J.B., M. LYLE, J. DYMOND & K. CRANE (1978) The chemistry of hydrothermal mounds near the Galapagos Rift. Earth Planet. Sci. Letts., 40: 12-24

CORMACK, D. & V.T. BOWEN (1967) Lanthanide interactions with particles in seawater. I. Standard clay minerals; II. Open ocean suspensoids and sediments. Unpublished NYO Reports 2174-53 and 54.

COTTON, F.A. & G. WILKINSON (1972). The Lanthanides, also Scandium and Yttrium. In: Advanced Inorganic Chemistry, 3rd. edition. Wiley: 1056-1076.

COURTOIS, C. & M. HOFFERT (1977). Distribution des terres rares dans les sediments superficiels du Pacifique sud-est. Bull. Soc. geol. Fr., 19: 1245-1251.

COURTOIS, C. & M. TREUIL (1977) Distribution des terres rares et de quelques elements en trace dans les sediments recents des fosses de la Mer Rouge. Chem. Geol., 20: 57-72

CRAIG, H. (1974). A scavenging model for trace elements in the deep sea. Earth planet. Sci. Letts., 23: 149-159.

CRAIG, H., W.S. BROECKER & D. SPENCER (1981) GEOSECS Pacific Expedition, Vols 3 and 4. IDOE/NSF, US Govt. Printing Office, Washington D.C. 20402

CROCK, J.G. & F.E. LICHTE (1982). Determination of Rare Earth Elements in Geological Materials by Inductively Coupled Argon Plasma/Atomic Spectrometry. Anal. Chem., 54:1329-1332

DANIELSSON, L.G., B. MAGNUSSON & S. WESTERLUND (1978). An improved metal extraction procedure for the determination of trace metals in seawater by atomic absorption spectrometry with electrothermal atomization. Anal. Chimica Acta, 98: 47-57.

DAWSON, R. & E.K. DUURSMA (1974) Distribution of radioisotopes between phytoplankton, sediment and seawater in a dialysis compartment system. Neth. J. Sea Res., 8: 339-353

DE BAAR, H.J.W, M.P. BACON & P.G. BREWER (1982). Rare Earth Elements in the Northwest Atlantic Ocean. Trans. Am. Geophys. Union (Eos), 63: 352.

DE BAAR, H.J.W., M.P. BACON & P.G. BREWER (1983a). Rare-earth distributions with a positive Ce anomaly in the Western North Atlantic Ocean. Nature, 301: 324-327.

DE BAAR, H.J.W., P.G. BREWER & M.P. BACON (1983b). Trace Metal Equilibria and Rare Earth Distributions in Sea Water. Trans Am. Geophys. Union (Eos), 64: 249.

DE BAAR, H.J.W., M.P. BACON & P.G. BREWER (1983c) Rare Earth Elements in the Eastern Equatorial Pacific Ocean. Trans. Am. Geophys. Union (Eos), 64 (52, Dec. 27 issue)

DE BAAR, H.J.W. (in press) Neutron Activation Analysis of Rare Earth Elements in Seawater. In: Proceedings of International Symposium on the Use and Development of Low and Medium Flux Research Reactors. MIT, Cambridge, October 1983. Special Volume Atomkernenergy & Atomtechnik.

DENECHAUD, E.B., P.A. HELMKE & L.A. HASKIN (1970). Analysis for the Rare-earth Elements by neutron activation and Ge(Li) spectrometry. J. Radioanal. Chem., 6: 97-113.

DEPAOLO, D.J. & G. WASSERBURG (1976). Inferences about Magma Sources and Mantle Structure from variations of 143Nd/144Nd. Geophys. Res. Letts., 3(12): 743-746.

DEPAOLO, D.J. & G.J. WASSERBURG (1976). Nd Isotopic Variations and Petrogenic Models. Geophys. Res. Letts., 3(5): 249-252.

DEUSER, W.G. (1973). Cariaco Trench: Oxidation of Organic matter and Residence Time of Anoxic Water. Nature, 242: 601-603.

DEUSER, W.G.(1975). Reducing environments. Chapter 16 in: J.P. Riley & G. Skirrow (Eds.) Chemical Oceanography, Vol. 3; Academic Press: 1-38.

DUFFIELD, J. & G.R. GILMORE (1979). An optimum method for the determination of rare earth elements by neutron activation analysis. J. Radioanal. Chem., 48:135-145.

DUURSMA, E.K. & D. EISMA (1973) Theoretical, experimental and field studies concerning reactions of radioisotopes with sediments and suspended particles of the sea. part C: applications to field studies. Neth. J. Sea Res., 6(3): 265-324

DZURINSKII, B.F. (1980) Tetrad Effects. Russian J. Inorg. Chem. (in english), 41: 25.

EDMOND, J.M., C. MEASURES, R.E. McDUFF, L.E. CHAN, R. COLLIER, B. GRANT, L.I. GORDON & J. CORLISS (1979). Ridge crest hydrothermal activity and the balances of themajor and minor elements in the ocean: the Galapagos data. Earth planet. Sci. Letts., 46: 1-18.

EDMOND, J.M., S.S. JACOBS, A.L. GORDON, A.W. MANTYLA & R F. WEISS (1979). Water Column Anomalies in Dissolved Silica Over Opaline Pelagic Sediments and the Origin of the Deep Silica Maximum. J. Geophys. Res., 84(C12):7809-7826

ELDERFIELD, H. & M. GREAVES (1983). Determination of the Rare Earth Elements in Seawater. In: C.S. Wong, E. Boyle, K.W. Bruland, J.P. Burton & E.D. Goldberg (Eds.): Trace Metals in Seawater. Plenum Press, New York: 427-446.

ELDERFIELD, H. & M.J. GREAVES (1982). The rare earth elements in seawater. Nature, 296:214-219

ELDERFIELD, H. & V.W. TRUESDALE (1980). On the biophilic nature of iodine in seawater. Earth planet. Sci. Letts., 50: 105-114.

ELDERFIELD, H. (1977). The form of manganese and iron in marine manganese deposits. In: G.P. Glasby (Ed.): Marine manganese deposits. Elsevier: 269-290.

ELDERFIELD, H., C.J. HAWKESWORTH, M.J. GREAVES & S.E. CALVERT (1981). Rare earth element geochemistry of oceanic ferromanganese nodules and associated sediments. Geochim. Cosmochim. Acta, 45:513-528

ELDERFIELD, H., C.J. HAWKESWORTH, M.J. GREAVES & S.E. CALVERT (1981) Rare earth element geochemistry of oceanic ferromanganese nodules and associated sediments. Geochim. Cosmochim. Acta, 45: 513-528

EMERSON, S., R.E. CRANSTON & P.S. LISS (1979). Redox species in a reducing fjord: equilibrium and kinetic considerations. Deep-Sea Res., 26(8A): 859-878.

EMERSON, S., S. KALHORN, L. JACOBS, B.M. TEBO, K.N. NEALSON & R.A. ROSSEN (1982). environmental oxidation rate of manganese(II): bacterial catalysis. Geochim. Cosmochim. Acta, 46: 1073-1079.

EVENSEN, N.M., P.J. HAMILTON & R.K. O'NIONS (1978) Rare-earth abundances in chondritic meteorites. Geochim. Cosmochim. Acta, 42: 1199-1212

FAKTOR, M.M. & R. HANKS (1969) Calculation of the third ionisation potentials of the lanthanons. J. inorg. Nuclear Chem., 31: 1649-1659.

FANNING, K.A. & M.E.Q. PILSON (1972). A model for the anoxic zone of the Cariaco Trench. Deep-Sea Res., 19: 847-863.

FLEET, A.J. (1983). Aqueous and Sedimentary Geochemistry of the Rare Earths. Chapter 2 in: P. Henderson (Ed.): Rare Earth Element Geochemistry, Elsevier.

FOWLER, S.W., M. HEYRAUD, L.F. SMALL & P.G. BENAYOUN (1973). Flux of $^{141}Ce$ through a Euphausiid Crustacean. Mar. Biol., 21: 317-325.

FREY, F.A. (1983) Rare Earth Element Abundances in Upper Mantle Rocks. In: Henderson, P. (Ed.), Rare Earth Element Geochemistry, Elsevier: in press

FRIEDLANDER, G., J.W. KENNEDY & J.M. MILLER (1966). Nuclear and Radiochemistry. 2nd edition. Wiley: xi + 585p.

FROELICH, P.N., M.L. BENDER, N.A. LUEDTKE, G.R. HEATH & T. DeVRIES (1982). The Marine Phosphorus Cycle. Am. J. Sci., 282:474-511.

FROELICH, P.N.,Jr. & M.O.ANDREAE (1981) The marine geochemistry of Germanium: Ekasilicon. Science, 213: 205-207

FRYER, B.J. (1977) Trace element geochemistry of the Sokoman Iron Formation. Can. J. Earth Sci., 14: 1598-1610

GARRELS, R.M. & C.L. CHRIST (1965). Solutions, Minerals and Equilibria. Freeman, Cooper & Cy., San Francisco: xiii + 450p.

GLASBY, G.P. (1973) Mechanisms of enrichment of the rarer elements in marine manganese nodules. Mar. Chem., 1: 105-125

GLASBY, G.P., R.R. KEAYS & P.C. RANKIN (1978) The distribution of rare earth, precious metal and other trace elements in Recent and fossil deep-sea manganese nodules. Geoch. J., 12(4): 229-243

GOLDBERG, E.D., M. KOIDE, R.A. SCHMITT & R.H. SMITH (1963). Rare-earth distributions in the marine environment. J. Geophys. Res., 68: 4209-4217.

GOLDSTEIN, S. & R.K. O'NIONS (1982). Nd isotope studies of river particulates, atmospheric dusts and pelagic sediemnts. Trans. Am. Geophys. Union (Eos), 63(18): 352.

GORDON, R.M., J.H. MARTIN & G.A. KNAUER (1982). Iron in Northeast Pacific waters. Nature, 299: 611-612

GRAF, J.L. (1977) Rare Earth Elements as Hydrothermal Tracers During the Formation of Massive Sulfide Deposits in Volcanic Rocks. Econ. Geol., 72(4): 527-548

GRAF, J.L. (1978) Rare earth elements, iron formations and seawater. Geochim. Cosmochim. Acta, 42: 1845-1850

GUEGUENIAT, P., J.P. AUFFRET & Y. BARON (1979). Evolution de la radioactivite artificielle gamma dans des sediments littoraux de la Manche pendant les annees 1976-1977-1978. Oceanologica Acta, 2:165-179

GUICHARD, F., T.M. CHURCH, M. TREUIL & H. JAFFREZIC (1979). Rare earths in barites: distribution and effects on aqeous partitioning. Geochim. Cosmochim. Acta, 43: 983-997.

HAMMOND, C.R. (1981). The Elements. In: R.C. Weast (Ed.) CRC Handbook of Chemistry and Physics, 62nd ed.; CRC Press, Boca, Florida: B2-B48.

HANSON, A.K., R.W. ZUEHLKE & D.R KESTER(1983). Copper speciation in Marine Waters: A Comparison of Analytical Results and Equilibrium Model Predictions. Trans. Am. Geophys. Union (Eos), 64(18): 249.

HARPER, T., T. INOUYE & N.C. RASMUSSEN (1968). GAMANL, A computer program applying Fourier transforms to the analysis of Gamma spectral data. MIT, AEC Contract Report AT(30-1)-3944.

HASKIN, L.A., F.A. FREY, R.A. SCHMITT & R.H. SMITH (1966). Meteoritic, solar and terrestrial rare earth distributions. Physics & Chemistry of the Earth, 7:169-321

HASKIN, L.A., M.A. HASKIN, F.A. FREY & T.R. WILDEMAN (1968). Relative and absolute terrestrial abundances of the rare earths. In: L.H. Ahrens (Ed.): Origin and Distribution of the Elements. Pergamon Press: 889-912.

HASKIN, M.A. & L.A. HASKIN (1966). Rare earths in European shales: a redetermination. Science, 154: 507-509.

HAYES, D.W. (1969). A study of the distribution of the lanthanide elements in the Gulf of Mexico using neutron activation analysis. Ph.D. thesis, Texas A&M University: viii + 168p.

HEFT, R.E. & W.H. MARTIN (1977) NADAC and MERGE - computer codes for processing neutron activation analysis data. Univ. Calif., Lawrence Livermore Lab., Livermore, Calif., UCRL-52249, 50p.

HEITNER-WIRGUIN, C. & G. MARKOVITS (1963). Kinetics of ion exchange in the chelating resin BIO-CHELEX 100. I. The exchange of the alkaline earth ions. J. Phys. Chem., 67: 2263-2266.

HEMING, R.F. & P.C. RANKIN (1979). Ce-anomalous lavas from Rabaul caldera, Papua New Guinea. Grochim. Cosmochim. Acta, 43:1351-1355

HENDERSON, P. (1982) Inorganic Geochemistry. Pergamon Press, Oxford: xv + 353p.

HENDERSON, P.(Ed.)(1983) Rare Earth Element Geochemistry. Elsevier Publishing Comp., Amsterdam, in press

HERRMANN, A.G. (1970). Yttrium and Lanthanides. In: H.K. Wedepohl. ed., Handbook of Geochemistry, V. II/5, 39: 57-71: B1-09.

HETHERINGTON, J.A. & D.F. JEFFERIES (1974). The distribution of some fission produced radionuclides in sea and estuarine sediments. Neth. J. Sea Res., 8(4): 319-338.

HIRANO, S., & T. KOYANAGI (1978). Study on the Chemical Forms of Radionuclides in Seawater - I. Chloride, sulfate and hydroxide complexes of $^{144}Ce$. J. Ocean. Soc. Jap., 34: 269-275.

HIROSE, A. & D. ISHII (1978). Determination of uranium in Sea water by preconcentration on Chelex 100 and neutron activation. J. Radioanal. Chem., 46: 211-215.

HOGDAHL, O.T. (1966-1968). Distribution of the Rare Earth Elements in seawater. NATO Research Grant No. 203, Semiannual Progress Reports Nos. 3,4,5,6. Central Inst. Ind. Res., Blindern, Norway. (Unpublished).

HOGDAHL, O.T., S. MELSON & V.T. BOWEN (1968). Neutron activation analysis of lanthanide elements in seawater. In: R.A. Baker. ed., Trace inorganics in water. Adv. Chem. Series 73, ACS, Washington, D.C., 308-325.

HOLLAND, H.D. (in press) The Chemical Evolution of the Atmosphere and Oceans. Princeton University Press

HOLYNSKA, B. (1974). The use of chelating ion exchanger in conjunction with radioisotope X-ray spectrometry for determination of trace amounts of metals in water. Radiochem. Radioanal. Letts., 17: 313-324.

HOOD, D.W. (1966) Rare Earth Distributions in Waters of the Gulf of Mexico. Section IV in: The Chemistry and Analysis of Trace Metals in Seawater. Texas A&M Project 276; AEC Contract No. AT-(40-1)-2799

HUMPHRIS, S.E. (1983). The Mobility of the Rare-Earth Elements in the Crust. Chapter 8 in: Henderson, P. (Ed.), Rare Earth Element Geochemistry, Elsevier, in press

HYDES, D.J. (1979) Aluminum in seawater: control by inorganic processes. Science, 205: 1260-1262.

JACOBS, L. & S. EMERSON (1982). Trace Metal Solubility in an Anoxic Fjord. Earth planet. Sci. Letts., 60: 237-252

KAUFMAN, A., R.M.TRIER & W.S. BROECKER (1973). Distribution of $^{228}Ra$ in the world ocean. J. Geophys. Res., 78: 8827-8848.

KEASLER, K.M. & W.D. LOVELAND (1982). Rare earth element concentrations in some Pacific Northwest rivers. Earth planet. Sci. Letts.,61:68-72

KHALIL, Y.F. (1982). Neutron Flux Determination by Foil Irradiation in Several Facilities in the M.I.T. Nuclear Reactor. Report on subject 22.39, under D. Lanning, Dept. of Nuclear Engineering, MIT, Cambridge, Mass., USA.

KINGSTON, H.M. (1979). Quantitative ultratrace transition metal analysis of high salinity waters utilizing chelating resin separation: application to energy-related environmental samples. Nat. Bureau of Standards. EPA-600/7 -79-174: 72p.

KINGSTON, H.M., I.L. BARNES, T.J. BRADY & T.C. RAINS (1978). Separation of Eight Transition Elements from Alkali and Alkaline Earths Elements in Estuarine and Seawater with Chelating Resin and their Determination by Graphite Furnace Atomic Absorption Spectrometry. Anal. Chem., 50(14): 2064-6070.

KLINKHAMMER, G. & H. ELDERFIELD(1982). Rare Earths in the Pacific. Trans. Am. Geophys. Union (Eos),63(45): 989.

KLINKHAMMER, G.P. & M.L. BENDER (1980). The distribution of Manganese in the Pacific Ocean. Earth planet. Sci. Letts., 46: 361-384.

KLINKHAMMER, G.P. (1980c) Determination of Manganese in Seawater by flameless atomic absorption spectrometry after pre-concentration with 8-hydroxyquinoline in chloroform. Anal. Chem., 52: 117-120

KLINKHAMMER, G.P. (1980a). Observations of the distributions of manganese over the East Pacific Rise. Chem. Geol., 29: 211-226.

KLINKHAMMER, G.P. (1980b). Early diagenesis in sediments from the eastern equatorial Pacific: II Pore water metal results. Earth Planet. Sci. Letts., 49: 81-101

KNAUER, G.A., J.H. MARTIN & R.M. GORDON (1982). Cobalt in Northeast Pacific waters. Nature, 297: 49-51

KNAUSS, K. & T.L KU (1983) The elemental composition and decay-series radionuclide content of plankton from the East Pacific. Chem. Geol., 39: 125-145

KOCHENOV, A.V. & V.V. ZINOV'EV (1960). Distribution of rare earth elements in phosphatic remains of fish from the maikop deposits. Geochemistry(USSR, english translation): 860-873.

KOLESOV, G.M., V.V. ANIKYEV & V.S. SAVENKO (1975) On the Geochemistry of Rare Earth Elements in the Waters of the Black Sea. Geochem. Int. (in english): 82-88

KORKISCH, J. & G. ARRHENIUS (1964). Separation of Uranium, Thorium, and the Rare Earth Elements by Anion Exchange. Anal. Chem., 36: 850-854.

KORKISCH, J.H. (1969). Modern Methods for the Separation of Rarer Metal Ions. Pergamon Press, Oxford: xi + 620p.

KRAUS, K.A. & F. Nelson (1955). Anion Exchange Studies of the Fission Products. Proc. 1st U.N. Intern. Conf. Peaceful Uses Atomic Energy, GENEVA, Vol. 7: 113-125. Reprinted in: WALTON, H.F. (Ed.): Ion-Exchange Chromatography, Benchmark Papers in Analytical Chemistry /1. Dowden, Hutchinson & Ross, distr. by Halsted Press (div. of Wiley):161-175.

LAAJOKI, & SAIKKONEN (1977) On the geology and geochemistry of the Precambrian iron formations in Vayrylankyla, sotuh Puolanka area, Finland. Bulletin 292, Geol. Survey of Finland.

LAI, M.G. & H.A. GOYA (1966) A rapid ion exchange method for the concentration of cobalt from seawater. U.S. Naval Radiological Defense Laboratory, Dept. of Commerce, NTIS, AD-648485: 20p.

LANDING, W.M. & K.W. BRULAND (1980). Manganese in the North Pacific. Earth planet. Sci. Letts., 49: 45-56.

LANDING, W.M. & K.W. BRULAND (1981). The vertical distribution of iron in the Northeast Pacific. Trans. Am. Geophys. Union (Eos), 62(45): 906.

LANDING, W.M. (1983). The Biogeochemistry of Manganese and Iron in the Pacific Ocean. Ph.D thesis, Univ. Calif., Santa Cruz: 202p.

LEDERER, C.M. & V.S. SHIRLEY (Eds.)(1978). Table of Isotopes, seventh edition. Wiley, New York.

LEE, C., N.B. KIM, I.C. LEE & K.S. CHUNG (1977). The use of a chelating resin column for preconcentration of trace elements from seawater in their determination by neutron activation analysis. Talanta, 24: 241-245.

LEE, D.S. (1982). Determination of bismuth in environmental samples by flameless atomic absorption spectrometry with hydride generation. Anal. Chem., 54: 1682-1686.

LEE, D.S. (1983) Palladium and nickel in north-east Pacific waters. Nature, 305: 47-48

LEE, D.S.(1983). Bismuth, Nickel and Palladium in Northeast Pacific Waters. Novel Analytical Methods in Marine Chemistry. Ph.D. thesis, Scripps Institute of Oceanography, San Diego.

LEYDEN, D.E. & A.L.UNDERWOOD (1964). Equilibrium Studies with the Chelating Ion-Exchange resin Dowex A-1. The J. of Phys. Chem., 68(8): 2093-2097.

LI, Y.H. (in press). Ultimate Removal Mechanisms of Elements from the Ocean. Geochim. Cosmochim. Acta.

LI, Y.H., H.W. FEELY & J.R. TOGGWEILER (1980). 228Ra and 228Th concentrations in GEOSECS Atlantic surface waters. Deep-Sea Res., 27A: 545-555.

LIU, Y.G. & R.A. SCHMITT (198 ). Chemical Profiles in Sediment and Basalt Samples from DSDP Leg 74, Hole 525A, Walvis Ridge. Submitted to Initial Reports of the Deep Sea Drilling Project, Vol. 74.

LUTTRELL, G.H., C.MORE & C.T. KENNER (1971). Effect of pH and Ionic Strength on Ion Exchange and Chelating Properties of an Iminodiacetate Ion Exchange Resin with Alkaline Earth Ions. Anal. Chem., 43: 1370-1375.

MARTIN, J.H. & G.A. KNAUER (1983). VERTEX: Manganese transport through oxygen minima. Submitted to Earth planet. Sci. Letts.

MARTIN, J.H. & G.A. KNAUER (1983) VERTEX: Manganese transport with $CaCO_3$ Deep-Sea Res., 30: 411-425

MARTIN, J.H., G.A. KNAUER & R.M. GORDON (1983). Silver distributions and fluxes in north-east Pacific waters. Nature, 305: 306-309

MARTIN, J.M., O. HOGDAHL & J.C. PhILIPPOT (1976). Rare earth element supply to the ocean. J. Geophys. Res., 81(18): 3119-3124.

MASUDA, A. & Y. IKEUCHI (1979). Lanthanide tetrad effect observed in marine environment. Geochem. J., 13: 19-22.

MASUDA, A.(1965). The Abundance ratios between the average basic rock and chondrites as a function of reciprocal ionic radii. Tectonophysics, 2: 299-317.

MASUDA, A., N. NAKAMURA & T. TANAKA (1973). Fine structure of mutually normalized rare-earth patterns of chondrites. Geochim. Cosmochim. Acta, 37:239-248

MEASURES, C.I. & J.D. BURTON (1980). The vertical distribution and oxidation states of dissolved Selenium in the Northeast atlantic Ocean and their relationship to biological processes. Earth planet. Sci. Letts., 46: 385-396.

MEASURES, C.I. & J.M. EDMOND (1982). Beryllium in the water column of the central North Pacific. Nature, 297: 51-53.

MICHARD, A., F. ALBAREDE, G. MICHARD, J.F. MINSTER & J.L. CHARLOU (1983) Rare-earth elements and uranium in high-temperature solutions from East Pacific Rise hydrothermal vent field (13°N). Nature, 303:795-797

MIYAKE, Y., Y. SUGIMURA & T. UCHIDA (1972). A new method of spectrophotometric determination of Uranium in seawater and Uranium content with 234U/238U ratio in the Pacific Water. Records of Oceanographic Works in Japan, 11(2): 53-63.

MOODY, J.R. & E.S. BEARY (1982). Purified reagents for trace metal analysis. Talanta, 29: 1003-1010.

MOORE, R.M. (1977). Trace Metals, Dissolved Organic matter, and their Association in Natural Waters. Ph.D Thesis, Univ. Southampton (U.K.): 175p.

MOORE, R.M. (1978). the distribution of dissolved copper in the eastern Atlantic Ocean. Earth planet. Sci. Letts., 41: 461-468.

MORRIS, L.R., R.A. MOCK, C.A. MARSHALL & J.H. HOWE (1959). Synthesis of Some Amino Acid Derivatives of Styrene. J. Amer. Chem. Soc. 81: 377-382.

MURRAY, J.W. & P.G. BREWER (1977). Mechanisms of removal of manganese, iron and other trace metals from seawater. In: G.P. Glasby, ed., Marine Manganese Deposits, Elsevier: 291-326.

NAGATSAKU, S., H.SUZUKI & K.NAKAJIMA (1971). Activation analysis of Lanthanide elements in natural water. Radioisotopes, 20(7): 305-309.

NAGAYA, Y. & K.NAKAMURA (1974) A field study of physico-chemical states of artificial radionuclides in seawater. J. Oceanogr. Soc. Jap., 30: 179-184

NAGAYA, Y., M. SHIOZAKI & Y. SETO (1965) Some fallout radionuclides in deep waters around Japan. J. Radiat. Res., 6: 23-31

NAKAMURA, N. (1974). Determination of REE, Ba, Fe, Mg, Na and K in carbonaceous and ordinary chondrites. Geochim. Cosmochim. Acta, 38: 757-775

NEEDELL, G.J. (1980). The distribution of dissolved silica in the deep western North Atlantic Ocean. Deep-Sea Res., 27A: 941-950.

NUGENT, L.J. (1970). Theory of the tetrad effect in the lanthanide(III) and actinide(III) series. J. Inorg. Nucl. Chem., 32: 3485-3491.

OKUDA, T., B.R. GAMBOA & A.J. GARCIA (1969). Seasonal variations of hydrographic conditions in the Cariaco Trench. Boletin del Instituto Oceanografico de la Universidad de Oriente, 8: 21-27.

ONUMA, N., F. MASUDA, M. HIRANO & K. WADA (1979). Crystal structure control on trace element partition in molluscan shell formation. Geochem.J.,13:187-189

OSTERBERG, C., W.G. PEARCY & H. CURL (1964) Radioactivity and its relationship to oceanic food chains. J. Mar. Res., 22(1): 2-12

OSTERBERG,C., A.G. CAREY & H. CURL (1963). Acceleration of sinking rates of radionuclides in the ocean. Nature, 28: 1276-1277.

PATCHETT, P.J. & M. TATSUMOTO (1980). A routine high precision method for Lu-Hf isotope geochemistry and chronology. Contrib. Mineral. petrol., 75: 263-267.

PEPPARD, D.F., G.W. MASSON & S. LEWEY (1969). A tetrad effect in the liquid-liquid extraction ordering of lanthanides(III). J. Inorg. Nucl. Chem., 31: 2271-2272.

PIEPGRAS, D.J. & G.J. WASSERBURG (1982) Isotopic Composition of Neodymium in Waters from the Drake Passage. Science, 217:207-214

PIEPGRAS, D.J. & G.J. WASSERBURG (1980). Neodymium Isotopic Variations in Seawater. Earth planet. Sci. Letts., 50, 128-138

PIEPGRAS, D.J. & G.J. WASSERBURG (1983) Influence of the Mediterranean outflow on the isotopic composition of Neodymium in waters of the North Atlantic. J. Geophys. Res., 88: 5997-6006

PIEPGRAS, D.J., G.J. WASSERBURG & E.J. DASCH (1979). The isotopic composition of Nd in different ocean masses. Earth Planet. Sci. Lett., (2): 223-236.

PIPER, D.Z. (1974b) Rare Earth Elements in ferromanganese nodules and other marine phases. Geochim. Cosmochim. Acta, 38: 1007-1022

PIPER, D.Z. (1974a). Rare earth elements in the sedimentary cycle: a summary. Chem. Geol., 14: 285-304.

QUINBY-HUNT, M.S. & K.K. TUREKIAN (1983) Distribution of Elements in Sea Water. Trans. Am. Geophys. Union (Eos), 64(14): 130-131

RAHN, K.A. (1976). The Chemical composition of the Atmospheric Aerosol. Graduate School Oceanography, Univ. Rhode Island, Technical Report: xi + 265p.

RANKIN, P.C. & G.P. GLASBY (1979) Regioanl Distribution of Rare Earth and Minor Elements in Manganese Nodules and Associated sediemnts in the Southwest Pacific and other localities. In: J.L. BISCHOFF & D.Z. PIPER (Eds.), Marine Geology and Oceanography of the Pacific Manganese Nodule Province. Plenum Press: 681-698

RICE, T.R. & V.M. WILLIS (1959) Uptake, Accumulation and loss of radioactive cerium-144 by marine planktonic algae. Limnol. Ocean., 4(3): 277-290

RICE, T.R. (1963) The role of phytoplankton in the cycling of radionuclides in the marine environment. In: SCHULTZ, V. & A.W. KLEMENT (Eds.), Radioecology, Reinhold, N.Y.: 179-185

RICHARDS, F.A. & R.F. VACCARO (1956). The Cariaco Trench, an anaerobic basin in the Caribbean Sea. Deep-Sea Res., 3: 214-228

RICHARDS, F.A. (1975). The Cariaco Basin (Trench). Oceanogr. Mar. Biol. Ann. Rev., 13: 11-67.

RILEY, J.P. & D. TAYLOR (1968a). Chelating resins for the concentration of trace elements from sea water and their analytical use in conjunction with atomic absorption spectroscopy. Anal. Chim. Acta, 40: 479-485.

RILEY, J.P. & D. TAYLOR (1968b). The determination of manganese in seawater. Deep-Sea Res., 15: 629-632.

RILEY, J.P. & D. TAYLOR (1968c). The use of chelating ion exchange in the determination of molybdenum and vanadium in seawater. Anal. Chimica Acta, 41: 175-178.

RILEY, J.P. & D. TAYLOR (1972). the concentrations of cadmium, copper, iron, manganese, molybdenum, vanadium and zinc in part of the tropical north-east Atlantic Ocean. Deep-Sea Res., 19: 307-317.

RILEY, J.P.(1975). Analytical Chemistry of Seawater. Chapter 19 in: J.P. Riley & G. SKIRROW (Eds.) Chemical Oceanography, Vol. 3; Academic Press: 285-286.

ROBERTSON, A.H.F. & A.J. FLEET (1976). The origins of rare earths in metalliferous sediments of the Troodos Massif, Cyprus. Earth planet. Sci. Letts., 28: 385-394.

ROBINSON, M.K., R.A. BAUER & E.H. SCHROEDER (1979) Atlas of the North Atlantic - Indian Ocean monthly mean temperatures and mean salinities of the surface layer. Naval Oceanographic Office Ref. Publ. No. 18, Dept. of the NAVY, Washington D.C. 20373

SCHINDLER, P.W. (1975). Removal of trace metals from the oceans: a zero order model. Thalassia Jugoslavica, 11(1/2): 101-111.

SCHNETZLER, C.C. & J.A. PHILPOTTS (1968). Partition coefficients in rare earth elements and barium between igneous matrix materials and rock-forming mineral phenocrysts,- I. In: AHRENS, L.H.(Ed.): Origin and Distribution of Elements, Pergamon Press:929-938.

SCHREIBER, H.D., H.V. LAUER, JR., & T. THANAYASIRI (1980). the redox state of cerium in basaltic magma's: an experimental study of iron-cerium interactions in silicate melts. Geochim. Cosmochim. Acta., 44: 1599-1612

SCLATER, F.R., E. BOYLE & J.M. EDMOND (1976). On the Marine Geochemistry of Nickel. Earth planet. Sci. Letts., 31: 119-128.

SHANNON, R.D. (1976). Revised effective ionic radii and systematic studies of interatomic distances in halides and chalcogenides. Acta Cryst. A, 32: 751-767.

SHIGEMATSU, T., M. TABUSHI, T. AOKI, O. FUJINO, Y. NISHIKAWA & S GODA (1967). Activation analysis of Lanthanum and Europium in Seawater and Lake water. Bull. Chem. Res. Kyoto Univ., 45: 307-317.

SHIMIZU, H. & A. MASUDA (1977). Cerium in chert as indication of marine environment of its formation. Nature, 266:346-348

SIEKIRSKI, S. (1971). The shape of the lanthanide contraction as reflected in the changes of the unit cell volumes, lanthanide radius and the free energy of complex formation. J. Inorg. Nucl. Chem., 33: 377-386.

SMITH, R.M. & A.E. Martell (1976). Critical Stability Constants, V. 4: Inorganic Complexes. Plenum Press, New York, XIII: 257.

SPENCER, D.W. & P.G. BREWER (1971). Vertical advection diffusion and Redox Potentials as Controls on the Distribution of Manganese and Other Trace Metals Dissolved in Waters of the Black Sea. Jour. Geophys. Res. 76, 24: 5877-5892.

SPENCER, D.W. (1972). Geosecs II, the 1970 North Atlantic station: hydrographic features, oxygen and nutrients. Earth planet. Sci. Letts.,16; 91-102.

SPIRN, R.V. (1965). Rare-Earth Distributions in the Marine Environment. Ph.D. Thesis, M.I.T.: 165p.

STEINNES, E.(1971). Epithermal Neutron Activation Analysis of Geological Material. In: A.O. Brunfelt & E. Steinnes (Eds.) Activation Analysis in Geochemistry and Cosmochemistry. Scandinavia University Books, Oslo.:113-128.

STRELOW, F.W.E. (1963). The separation of Uranium from Scandium, Yttrium, Rare Earths, Thorium, Beryllium, Magnesium, Copper, Manganese, Iron, Aluminium and other elements by cation-exchange chromatography. Joernaal van die Suid-Afrikaanse Chemiese Instituut, XVI: 38-47.

STRELOW, F.W.E. (1960). An ion exchange selectivity scale of cations based on equilibrium distribution coefficients. Anal. Chem., 32: 1185-1188.

STRELOW, F.W.E., R. RUTHEMEYER & C.J.C. BOTHMA (1965). Ion exchange selectivity scales for cations in nitric acid and sulfuric acid media with a sulfonated polystyrene resin. Anal. Chem., 37(1): 106-111.

SUESS, H.E. & H.C UREY (1956). Abundances of the Elements. Rev. Mod. Phys. 28: 53-74.

SUGIHARA, T. & V.T. BOWEN (1962). Radioactive rare earths from fallout for study of particle movement in the sea. In: Radioisotopes in the physical sciences and industry. IAEA, Vienna: 57-65.

SVERDRUP, H.U., M.W. JOHNSON & R.H. FLEMING (1942). The Oceans. Their Physics, Chemistry and General Biology. Prentice-Hall, Inc., Englewood Cliffs, N.J.: x +1087p.

TANAKA, T. & A. MASUDA (1982) The La-Ce geochronometer: a new dating method, Nature, 300: 515-518

TEMPLETON, D.H. & C.H. DAUBEN (1954). Lattice parameters of some rare-earth compounds and a set of crystal radii. J. Am. Chem. Soc., 76: 5337-5239.

THIRLWALL, M.F. (1982). A Triple-Filament Method for rapid and precise Analysis of Rare-Earth Elements by Isotope Dilution. Chem. Geol., 35:155-166

THOMPSON, L.C. (1961). Complexes of the Rare Earths. I. Iminodiacetic Acid. Inorganic Chemistry, 1(3): 490-493.

THOMPSON, L.C., B.L. SHAFER, J.A. EDGAR & K.D. MANNILA (1967). Complexes of the Rare Earths, N-Substituted Iminodiacetic Acids. In: P.R. Fields, and T. Moeller, (Symp. Chairmen), eds. Lanthanide/Actinide Chemistry, Adv. Chem. Series, 71: 169-179.

TOTH, J.R. (1980). Deposition of submarine crusts rich in manganese and iron. Geol. Soc. Am. Bull., I, 91: 44-54.

TUG, S. & M. STEINBERG (1982) Distribution of Rare-Earth Elements (REE) in size fractions of recent sediments of the Indian Ocean. Chem. Geol., 37: 317-333

TUREKIAN, K.K., A. KATZ & L. CHAN (1973) Trace element trapping in pteropod tests. Limnol. Ocean., 18: 240-249

TURNER, D.R. & M. WHITFIELD (in press). Inorganic Controls on the Biogeochemical Cycling of the Elements in the Oceans.

TURNER, D.R., M. WHITFIELD & A.G. DICKSON (1981). The equilibrium speciation of dissolved components in freshwater and seawater at 25 C and 1 atm pressure. Geochim. Cosmochim. Acta, 45:855-881

VOBECKY, M. (1980). Nuclear Interference Contribution of Uranium in Lanthanum Determination by the NAA Method. Radiochem. Radioanal. Letts., 45: 147-152.

VON DAMM, K.L. (1983). Chemistry of Submarine Hydrothermal Solutions at 21°North, East Pacific Rise and Guaymas Basin, Gulf of California. Ph.D. thesis, WHOI/MIT.

WALKER, F.W., G.J. KIROUAC & F.M. ROURKE (1977). Chart of the Nuclides, Twelfth Edition. General Electric Company, San Jose, Calif.: 52p.

WALSH, J.N., F. BUCKLEY & J. BARKER (1981). The Simultaneous Determination of the Rare-Earth Elements in Rocks using Inductively Coupled Plasma Source Spectrometry. Chem. Geol., 33: 141-153

WASSERBURG, G.J., S.B. JACOBSON, D.J. DEPAOLO, M.T.M. McCULLOCH & T. WEN (1981). Precise determination of Sm/Nd ratios, Sm and Nd isotopic abundances in standard solutions. Geochem. Cosmochim. Acta, 45: 2311-2323.

WEDEPOHL, K.H. (1978). Handbook of Geochemistry, volume II/5 Springer, Berlin.

WHITFIELD, M. (1975). Sea Water as an Electrolyte Solution. Chapter 2 in: J.P. Riley & G. Skirrow (Eds.): Chemical Oceanography, Vol. 1, Academic Press, London: 44-172.

WILDEMAN, T.R. & L. HASKIN (1963). Rare earth elements in Ocean Sediments. J. Geophys. Res., 70: 2903-2910.

WILLIAMS, R.J.P.(1982). The Chemistry of Lanthanide Ions in Solution and in Biological Systems. Structure & Bonding (Springer, Berlin), 50:80-119

WILSON, T.R.S. (1975). Salinity and the Major Elements of Seawater. Chapter 6 in: J.P. Riley & G. Skirrow (Eds.) Chemical Oceanography, Vol. 1; Academic Press: 365-408.

WONG, C.S., E. BOYLE, K.W. BRULAND, J.D. BURTON & E.D. GOLDBERG (Eds.)(1983) Trace Metals in Seawater. Plenum Press, New York: xiv + 920p.

WONG, G.F. (1980). the stability of dissolved inorganic species of iodine in seawater. Mar. Chem., 9: 13-24.

WORTHINGTON, L.V. (1976). On the North Atlantic circulation. The Johns Hopkins Oceanographic Studies, No. 6, Baltimore, 110p.

WORTHINGTON, L.V. (1981). The water Masses of the World Ocean: Some Results of a Fine-Scale Census. In: B.A. Warren & C. Wunsch (Eds.) Evolution of Physical Oceanography, MIT Press, Cambridge, Mass.: 42-69.

WRIGHT, J., R.S. SEYMOUR & H.F. SHAW (1983) REE and Nd isotopes in conodont apatitie: variations with geological age and depositional environment. In: D.L. CLARK (Ed.): "Conodont Biofacies and Provincialism" (N-C GSA Symposium, 1983), 15: 247

WYRTKI, K.(1967). Circulation and Water Masses in the Eastern Equatorial Pacific Ocean. Int. J. Oceanol. & Limnol., 1(2):117-147

# 9. APPENDIX

## 9.1. LANT/03: a program in BASIC for calculation of REE concentrations in seawater from net gamma peak areas; with listing of parameters LANT/04

```
10  REM BASIC PROGRAM "LANT/03"
20  REM VERSION "LANT/04" IS LIST OF PARAMETERS
30  REM LAST REVISION NOVEMBER 2, 1983
40  REM ******************************************************
50  REM ****MAIN PROGRAM**** CALLS SUBROUTINES TO COMPUTE
60  REM LANTHANIDE CONCENTRATIONS IN SEAWATER
70   DIM A0(20,15),B0(20,15),B1(20),V1(20)
80   DIM C0(15),C1(15),C2(15),T1(15),T2(15)
90   DIM D0(20),D1(20),D2(20)
100   DIM E1$(15)4,E2$(15)6,F1$(20)6,F2$(20)4
110 PRINT "HI THERE;HOW NICE OF YOU TO WAKE ME UP"
120 PRINT "no thank you;coffee is not good for my system"
130 PRINT "WHAT DAY IS IT ANYWAY?"
140 INPUT "ENTER MONTH/DAY/YEAR(E.G. 12/31/81)";G1$
150 PRINT "MY NAME IS LANT/03;WHO ARE YOU?"
160 INPUT "ENTER YOUR NAME(<16 DIGITS)";G2$
170 PRINT "************************************************"
1000 REM ****CALLING OF CALCULATION SUBROUTINES****
1010 GOSUB *30
1020 GOSUB *70
1030 GOSUB *80
1040 IF N3=N2 THEN 1060
1050 GOSUB *90
1060 IF N3=N1 THEN 1100
1070  GOSUB *100
1080 IF P2=13 THEN 1100
1090 GOSUB *110
1100 IF M3=M2 THEN 1140
1110 IF P3=13 THEN 1140
1120 GOSUB *120
1130 GOTO 1040
1140 PRINT "END OF PROGRAM LANTH01;WAS NICE MEETING YOU" ~
1150 PRINT "************************************************"
1160 PRINT "DEPRESS 'RESET' AND 'RUN (EXEC)' FOR NEXT RUN."
2000 DEFFN *30
2010 REM ****DECISION TREE FOR MODE OF DATA INPUT****
2020 PRINT "YOU HAVE FIVE OPTIONS FOR THE INPUT DATASET"
2030 PRINT "10    OLD=EXISTING DATAFILE"
2040 PRINT "30    OLD DATAFILE TO BE MODIFIED TEMPORARILY"
2050 PRINT "50    OLD DATAFILE TO BE MODIFIED PERMANENTLY AND"
2060 PRINT "        STORED BACK INTO SAME DISKFILE"
2070 PRINT "    (THIS OPTION ALSO ALLOWS WRITING A NEW DATASET"
2080 PRINT "    INTO OLD FILE;THUS ERASING OLD DATASET)"
2090 PRINT "70    OLD DATAFILE TO BE MODIFIED PERMANENTLY AND"
2100 PRINT "        STORED INTO NEW DISKFILE"
2110 PRINT "90    BRANDNEW DATASET TO BE STORED INTO NEW DISKFIL
E"
2120 INPUT "ENTER 10/30/50/70/90 ";P4
2130 IF P4>80 THEN 2180
2140 LIST DC F
2150 PRINT "WHICH OF ABOVE EXISTING FILES DO YOU NEED?"
2160 INPUT "ENTER NAME IN QUOTES";R1$
2170 GOSUB *60
2180 IF P4<60 THEN 2220
2190 LIST DC F
2200 PRINT "ABOVE FILES DO ALREADY EXIST"
2210 INPUT "ENTER DIFFERENT NEW FILE NAME(<8DIGITS)IN QUOTES";R2
$
2220 IF  P4<20 THEN 2280
```

```
2225 IF P4>80 THEN 2270
2230  P1=13
  40 PRINT "DO YOU ONLY HAVE TO MAKE A FEW CHANGES?"
2250 INPUT "ENTER 11 FOR ONLY A FEW CHANGES";P1
2260 IF P1=11 THEN 2280
2270 GOSUB '40
2280 GOSUB '170
2290 IF P4<50 THEN 2310
2300 GOSUB '50
2310 RETURN
2490  DEFFN' 40
2500   REM ****INPUT OF DATA****
2510   PRINT  "DATA INPUT LANTHANIDES"
2520 INPUT "ENTER MONTH/DAY/YEAR OF IRRADIATION";G3$
2530 INPUT "ENTER M/D-M/D/YR(EG.10/29-11/3/81)OF COUNT SET";G4$
2540 INPUT "ENTER ORDER(FIRST,SECOND..)OF COUNT SET";G5$
2550   PRINT  "YIELD TRACER, YES(1) OR NO(0)?"
2560   INPUT  "ENTER NUMBER(EITHER 1 OR 0)OF YIELD TRACERS";M1
2570  PRINT "NUMBER OF IRRADIATION PRODUCED ISOTOPES?"
2580   PRINT  "(MULTIPLE PEAKS OF SINGLE ISOTOPE COUNT AS"
2590   PRINT  "SINGLE PEAKS OF MULTIPLE ISOTOPES)"
2600   PRINT  "(EXCLUDE YIELD TRACER, IF ANY !)"
2610   INPUT  "ENTER NUMBER(0-20)OF ISOTOPES";M2
2620   M3=M1 + M2
2630   INPUT "ENTER NUMBER(0-20)OF STANDARD SPECTRA";N1
2640   INPUT  "ENTER NUMBER(0-10)OF SAMPLE SPECTRA";N2
2650  N3=N1+N2
2660   INPUT  "ENTER REFERENCE TIME TO(MINUTES)";TO
2670   P1=11
2680   INPUT  "ENTER 13 FOR CORRECTIONS IN ABOVE";P1
2690   IF P1=13 THEN 2520
2700   IF N3=N2 THEN 2870
2710   FOR N=1 TO N1
2720    PRINT "***********************************************"
2730     PRINT "STANDARD N=";N
2740     INPUT "ENTER STANDARD NUMBER(#DIGITS<5)";E1$(N)
2750     INPUT "ENTER AMOUNT OF LA(PMOL)(DIGITS<6)";E2$(N)
2760     PRINT "COUNT TIME CT=";CO(N)
2770     INPUT  "ENTER COUNT TIME CT(SECONDS)";CO(N)
2780     PRINT "LIFE TIME LT=";C1(N)
2790     INPUT  "ENTER LIFE TIME LT(SECONDS)";C1(N)
2800     PRINT "HAYDEN CLOCK TIME=";T1(N)
2810     INPUT  "ENTER HAYDEN CLOCK TIME(MINUTES)";T1(N)
2820     PRINT  "ANY CORRECTIONS FOR STANDARD ";N;" ?"
2830     P1=11
2840     INPUT  "ENTER 13 FOR CORRECTIONS";P1
2850     IF P1=13 THEN 2730
2860   NEXT N
2870   IF  N3=N1 THEN 3050
2880   FOR N=N1+1 TO N3
2890     PRINT  "SAMPLE N=";N
2900     INPUT  "ENTER SAMPLE NUMBER";E1$(N)
2910     INPUT "ENTER SAMPLE DEPTH(E.G. 1228M)";E2$(N)
2920     PRINT "COUNT TIME CT=";CO(N)
2930     INPUT "ENTER COUNT TIME CT(SECONDS)";CO(N)
2940     PRINT "LIFE TIME LT=";C1(N)
2950     INPUT "ENTER LIFE TIME LT(SECONDS)";C1(N)
2960     PRINT "HAYDEN CLOCK TIME=";T1(N)
2970     INPUT  "ENTER HAYDEN CLOCK TIME(MINUTES)";T1(N)
2980     PRINT "KILOGRAM SEAWATER=";C2(N)
```

```
2990      INPUT  "ENTER KILOGRAM SEAWATER";C2(N)
3000      PRINT  "ANY CORRECTIONS FOR SAMPLE "¦N¦" ?"
3010      P1=11
3020      INPUT  "ENTER 13 FOR CORRECTIONS",P1
3030      IF  P1=13 THEN  2890
3040    NEXT N
3050    IF  M3=M2 THEN 3130
3060    INPUT  "ENTER NAME OF YIELD TRACER(E.G. 144CE)";F1$(1)
3070    INPUT "ENTER KEV OF YIELD TRACER";F2$(1)
3080    PRINT "1/LAMBDA="¦DO(1)
3090    INPUT "ENTER 1/LAMBDA(MINUTES)OF YIELD TRACER";DO(1)
3100    PRINT "CHECK ABOVE YIELD TRACER INPUT"
3110    P1=11
3120    INPUT "ENTER 13 FOR CORRECTIONS";P1
3130     P2=11
3140      PRINT "DO YOU NEED SHALE NORMALIZATION?"
3150      INPUT "ENTER 13 IF NOT TRULY NEEDY";P2
3160    FOR M=M1 + 1 TO M3
3170      PRINT "NUMBER OF ISOTOPE :"¦M
3180      INPUT "ENTER NAME OF ISOTOPE";F1$(M)
3190      INPUT "ENTER KEV OF ISOTOPE";F2$(M)
3200      PRINT " 1/LAMBDA OF"¦F1$(M)¦" IS "¦DO(M)
3210      INPUT "ENTER 1/LAMBDA(MINUTES)OF ISOTOPE",DO(M)
3220      IF P2=13 THEN 3260
3230      PRINT "SHALE CONCENTRATION="¦D2(M)
3240      INPUT "ENTER SHALE CONCENTRATION(UMOL/KG)ELEMENT",D2(M)

3250      PRINT "PMOL IN STANDARDS="¦D1(M)
3260      INPUT "ENTER PMOL OF ELEMENT IN STANDARDS",D1(M)
3270      P1=11
3280        PRINT "CHECK ABOVE DATA OF ISOTOPE:"¦M
3290        INPUT "ENTER 13 FOR CORRECTIONS",P1
3300      IF P1=13 THEN 3170
3310    NEXT M
3320    REM INPUT OF GAMANL DERIVED NET PEAK AREAS
3330    FOR M=1 TO M3
3340      PRINT " "
3350      PRINT "****NEXT ISOTOPE****NEXT ISOTOPE****NEXT ISOTOPE
****"
3360      PRINT " "
3370      FOR  N=1 TO N3
3380        PRINT " "
3390        PRINT " "
3400        PRINT "ISOTOPE: "¦M¦" SPECTRUM: "¦N¦"  AREA:  "¦AO(M,
N)
3410        INPUT "            ENTER GAMANL PEAK AREA";AO(M,N)
3420        P1=11
3430        INPUT "ENTER 13 FOR CORRECTION",P1
3440        IF P1=13 THEN 3400
3450     NEXT N
3460    NEXT M
3470    RETURN
3480 DEFFN'70
3490 REM ****PRECOMPUTATION OF CO,T1,T2 FOR ALL N3 SPECTRA****
3500 REM INPUT N1,N2,N3,TO,T1(N),CO(N),C1(N),C2(N)
3510 REM OUTPUT T2(N),NEW CO(N),NEW T1(N)
3520 REM FOR STANDARDS KG.SEAWATER=C2(N)=1.000
3530 REM PROGRAM PARAMETER P3 IS FIRST SET TO 11(UNCORRECTED)
3540 P3=11
3550 IF N3=N2 THEN 3590
```

```
3560 FOR N=1 TO N1
3570   C2(N)=1
3580 NEXT N
3590 FOR N=1 TO N3
3600   T1(N)=T1(N)-T0
3610   T2(N)=T1(N)+C0(N)/60
3620   C0(N)=(C0(N)/C1(N))/C2(N)
3630 NEXT N
3640 RETURN
3650 DEFFN'80
3660 REM ****COMPUTATION OF NUMBER OF ATOMS A0(M,N) AT TIME T0
3670 REM FOR ALL M3 ISOTOPES IN ALL N3 SPECTRA****
3680 REM INPUT M3,N3,A0(M,N),C0(N),T1(N),T2(N),D0(M)
3690 REM OUTPUT NEW A0(M,N)
3700 FOR  N=1 TO N3
3710   FOR M=1 TO M3
3720     A0(M,N)=A0(M,N)*C0(N)/(EXP(-T1(N)/D0(M))-EXP(-T2(N)/D0(
M)))
3730     B0(M,N)=A0(M,N)
3740   NEXT M
3750   IF M3=M2 THEN 3790
3760    REM DIVIDING YIELD TRACER BY C2 WAS INCORRECT;THUS;
3770    A0(1,N)=A0(1,N)*C2(N)
3780    B0(1,N)=A0(1,N)
3790 NEXT N
3800 PRINT "A0(M,N) AT T0;NOT CORRECTED FOR YIELD TRACER"
3810 GOSUB '130(0,INT(M3/4),1,N3)
3820 PRINT "DO YOU NEED HARD COPY PRINTOUT?"
3830 P1=11
3840 INPUT "ENTER 13 IF NOT TRULY NEEDY",P1
3850 IF  P1=13 THEN 3910
3860 SELECT PRINT 01D
3870 GOSUB '160
3880 PRINT "A0(M,N) AT T0;NOT CORRECTED FOR YIELD TRACER"
3890 GOSUB '130(0,INT(M3/4),1,N3)
3900 SELECT PRINT 005
3910 RETURN
3920 DEFFN'90
3930 REM ****COMPUTATION OF MEAN VALUE B1(M)(1/PICOMOL)AND ITS
3940 REM STANDARD DEVIATION V1(M)(%) OF A0(M,N)/D1(M) FOR
3950 REM ALL N1 STANDARD SPECTRA(ONLY FOR M2 ISOTOPES)****
3960 REM INPUT M1,M3,N1,A0(M,N),D1(M)
3970 REM OUTPUT B1(M),V1(M)
3980 FOR M=M1+1 TO M3
3990   B1(M) = 0
4000   FOR N=1 TO N1
4010     B1(M)=B1(M)+A0(M,N)/D1(M)
4020   NEXT N
4030   B1(M)=B1(M)/N1
4040   IF N1=1 THEN 4110
4050   V3=0
4060   FOR N=1 TO N1
4070      V2=A0(M,N)/D1(M)-B1(M)
4080     V3=V3+V2*V2
4090   NEXT N
4100   V1(M)=(100/B1(M))*SQR(V3/(N1-1))
4110 NEXT M
4120 GOSUB '150
4130 PRINT "DO YOU NEED HARD COPY PRINTOUT OF B1(M),V1(M)?"
4140 P1=11
```

```
4150 INPUT "ENTER 13 IF NOT TRULY NEEDY",P1
4160 IF P1=13 THEN 4210
4170 SELECT PRINT 01D
4180 GOSUB '160
4190 GOSUB '150
4200 SELECT PRINT 005
4210 RETURN
4220 DEFFN'100
4230 REM ****CALCULATION OF CONCENTRATION(PICOMOL/KG)
4240 REM OF M2 ISOTOPES IN N2 SAMPLES****
4250 REM INPUT M1,M3,N1,N3,P3,A0(M,N),B1(M)
4260 REM OUTPUT B0(M,N),NEW A0(M,N)
4270 FOR N=N1+1 TO N3
4280   FOR M=M1+1 TO M3
4290     A0(M,N)=A0(M,N)/B1(M)
4300   NEXT M
4310 NEXT N
4320 P1=11
4330 IF P3=13 THEN 4350
4340 PRINT "CONCENTRATION(PICOMOL/KG),NOT CORRECTED FOR YIELD TR
ACER"
4350 IF P3=11 THEN 4370
4360 PRINT "CONCENTRATION(PICOMOL/KG),YIELD TRACER CORRECTED"
4370 GOSUB '130(0,INT(M3/4),N1+1,N3)
4380 IF P1=15 THEN 4460
4390 PRINT "DO YOU NEED HARD COPY PRINTOUT OF CONCENTRATIONS?"
4400 INPUT "ENTER 13 IF NOT TRULY NEEDY",P1
4410 IF P1=13 THEN 4470
4420 P1=15
4430 SELECT PRINT 01D
4440 GOSUB '160
4450 GOTO 4330
4460 SELECT PRINT 005
4470 RETURN
4480 DEFFN'110
4490 REM ****NORMALIZATION VERSUS SHALES OR OTHER MEAN
4500 REM CRUSTAL ABUNDANCE DATASET D2(M)****
4510 REM INPUT M1,M3,N1,N3,A0(M,N),D2(M)
4520 REM OUTPUT NEW SHALE NORMALIZED A0(M,N)
4530 FOR M=M1+1 TO M3
4540   FOR N=N1+1 TO N3
4550     A0(M,N)=A0(M,N)/D2(M)
4560   NEXT N
4570 NEXT M
4580 P1=11
4590 IF P3=13 THEN 4610
4600 PRINT "RATIO SAMPLE*E^6/SHALE,NOT CORRECTED FOR YIELD TRACE
R"
4610 IF P3=11 THEN 4630
4620 PRINT "RATIO SAMPLE*E^6/SHALE,CORRECTED FOR YIELD TRACER"
4630 GOSUB '130(0,INT(M3/4),N1+1,N3)
4640 IF P1=15 THEN 4720
4650 PRINT "DO YOU NEED HARD COPY OF RATIOS VS. SHALES?"
4660 INPUT "ENTER 13 IF NOT TRULY NEEDY",P1
4670 IF P1=13 THEN 4730
4680 P1=15
4690 SELECT PRINT 01D
4700 GOSUB '160
4710 GOTO 4590
4720 SELECT PRINT 005
```

```
4730 RETURN
4740 DEFFN'120
4750 REM ****YIELD TRACER CORRECTION OF BO(M,N)****
4760 REM INPUT M1,M3,N1,N3,BO(M,N)
4770 REM OUTPUT P3,CORRECTED AO(M,N)
4780 REM FIRST PROGRAM PARAMETER P3 IS ADJUSTED
4790 P3=13
4800 FOR M=M1+1 TO M3
4810   FOR N=1 TO N3
4820     AO(M,N)=BO(M,N)/BO(1,N)
4830   NEXT N
4840 NEXT M
4850 PRINT "AO(M,N) AT TO,CORRECTED FOR YIELD TRACER"
4860 GOSUB '130(0,INT(M3/4),1,N3)
4870 P1=11
4880 PRINT "DO YOU NEED HARD COPY PRINTOUT?"
4890 INPUT "ENTER 13 IF NOT TRULY NEEDY";P1
4900 IF P1=13 THEN 4960
4910 SELECT PRINT 01D
4920 GOSUB '160
4930 PRINT "AO(M,N)AT TO,CORRECTED FOR YIELD TRACER"
4940 GOSUB '130(0,INT(M3/4),1,N3)
4950 SELECT PRINT 005
4960 RETURN
4970 DEFFN '130(K1,K2,N4,N5)
4980 REM    ****CRT PRINTOUT OF DATA MATRIX****
4990  REM MAXIMUM OF N=12 SPECTRA FIT THE SCREEN
5000 FOR K=K1 TO K2
5010   PRINT "    "
5020   PRINT "STANDARD OR";TAB(16);F1$(4*K+1);TAB(24);F1$(4*K+2)
;TAB(35);F1$(4*K+3);TAB(46);F1$(4*K+4)
5030  PRINT "SAMPLE",TAB(16);F2$(4*K+1);TAB(24);F2$(4*K+2);TAB(3
5);F2$(4*K+3);TAB(46);F2$(4*K+4)
5040   FOR N=N4 TO N5
5050     PRINTUSING 5090,E1$(N),E2$(N),AO(4*K+1,N),AO(4*K+2,N),A
O(4*K+3,N),AO(4*K+4,N)
5060   NEXT N
5070   STOP "ENTER CONTINUE(EXEC)FOR NEXT FOUR ISOTOPES"
5080 NEXT K
5090 %#### ###### ###.##^^^^ ###.##^^^^ ###.##^^^^ ###.##^^^^
5100 RETURN
5110 DEFFN' 50
5120 REM ****STORAGE OF INPUT DATA INTO DISK FILE****
5130 IF  P4>60 THEN 5150
5140 DATA LOAD DC OPEN F R1$
5150 IF  P4<60 THEN 5170
5160 DATA SAVE DC OPEN F 30, R2$
5170 DATA SAVE DC G3$,G4$,G5$,M1,M2,M3,N1,N2,N3,P2,TO,E1$(),E2$(
),CO(),C1(),C2(),T1(),F1$(),F2$(),DO(),D2(),D1(),AO()
5180 DATA SAVE DC END
5190 DATA SAVE DC CLOSE
5200 RETURN
5210 DEFFN' 60
5220 REM ****LOADING INPUT DATA FROM DISK FILE INTO MEMORY****
5230 DATA LOAD DC OPEN F R1$
5240 DATA LOAD DC G3$,G4$,G5$,M1,M2,M3,N1,N2,N3,P2,TO,E1$(),E2$(
),CO(),C1(),C2(),T1(),F1$(),F2$(),DO(),D2(),D1(),AO()
5250 RETURN
5260 DEFFN'150
5270 REM ****CRT PRINTOUT OF B1(M) AND V1(M)****
```

```
5280 REM INPUT M1,M3,P3,F1$(M),F2$(M),B1(M),V1(M)
5290 IF P3=13 THEN 5310
5300 PRINT "B1(M) AND V1(M),NOT CORRECTED FOR YIELD TRACER"
5310 IF P3=11 THEN 5330
5320 PRINT "B1(M) AND V1(M),CORRECTED FOR YIELD TRACER"
5330 PRINT "ISOTOPE/KEV   B1   V1(%)  ISOTOPE/KEV  B1  V1(%)"
5340 PRINT "  "
5350 FOR M=1 TO 10
5360   PRINTUSING 5380,F1$(M),F2$(M),B1(M),V1(M),F1$(M+10),F2$(M
+10),B1(M+10),V1(M+10)
5370 NEXT M
5380 %###### #### ##.##^^^^ ##.## ###### #### ##.##^^^^ ##.##
5390 RETURN
5400 DEFFN'160
5410 REM ****PRINTING OF DATES****
5420 STOP "TURN ON PRINTER,LINEFEED NEW PAGE,CONTINUE(EXEC)"
5430 PRINT "DATE WANG PROGRAM RUN    ",G1$
5440 PRINT "NAME WANG OPERATOR       ",G2$
5450 PRINT "DATE OF IRRADIATION      ",G3$
5460 PRINT "DATE(S)OF COUNT SET      ",G4$
5470 PRINT "ORDER OF COUNT SET       ",G5$
5480 PRINT "  "
5490 RETURN
5500  DEFFN '170
5510  REM ***PRINTOUT(CRT&PRINTER)OF INPUT DATASET***
5520  P3=11
5530  PRINT " "
5540  PRINT "M1=";M1;" M2=";M2;" N1=";N1;" N2=";N2;" TO=";TO
5550  FOR N=1 TO N3
5560    PRINTUSING 5580,N,CO(N),C1(N),T1(N),C2(N)
5570  NEXT N
5580  %##  ######  ######  ######.#  ##.###
5590  IF P3=13 THEN 5610
5600  STOP "WRITE DOWN CORRECTIONS,IF ANY,THEN CONTINUE(EXEC)"
5610  PRINT " "
5620  FOR M=1 TO 10
5630    PRINTUSING 5650,D0(M),D2(M),D1(M),D0(M+10),D2(M+10),D1(M
+10)
5640  NEXT M
5650  %#########.### ###.### ###.### #######.### ###.### ###.###
5660  IF P3=13 THEN 5680
5670  STOP "WRITE DOWN CORRECTIONS,IF ANY,THEN CONTINUE(EXEC)"
5680  PRINT " "
5690  PRINT "INPUT NET PEAK AREA A0(M,N)"
5700  GOSUB '130(0,INT(M3/4),1,N3)
5710  IF P3=13 THEN 5810
5720  P3=13
5730  STOP "ENTER FINAL CORRECTIONS,THEN CONTINUE(EXEC)"
5740  PRINT "DO YOU NEED HARD COPY PRINTOUT OF INPUT DATA?"
5750  P1=11
5760  INPUT "ENTER 13 IF NOT TRULY NEEDY";P1
5770  IF P1=13 THEN 5820
5780  SELECT PRINT 010
5790  GOSUB '160
5800  GOTO 5530
5810  SELECT PRINT 005
5820  RETURN
```

```
10  REM LANT/04, LIST OF PARAMETERS FOR PROGRAM LANT/03
20  REM USE VERSION "LANT/03" FOR ACTUAL CALCULATIONS
30  REM PROGRAMMER   HEIN DE BAAR
40  REM LAST REVISION NOVEMBER 2, 1983
50  REM ************************************************
60  REM ****DESCRIPTION OF PROGRAM LANT/03****
70  REM ACTIVITY AT TIME (T-T0)AFTER END OF IRRADIATION
80  REM   -DN/DT=LAMBDA*N=LAMBDA*N0*EXP(-LAMBDA(T-T0))
90  REM WHERE N0 IS NUMBER OF ATOMS OF RADIOISOTOPE AT T0
100  REM INTEGRATE LINE 160 WITH BOUNDARIES (N1,T1)(N2,T2)
110  REM N1-N2=N0(EXP(-LAMBDA(T1-T0))-EXP(-LAMBDA(T2-T0)))
120  REM   WHERE (N1-N2)=NUMBER OFCOUNTS,I.E.NET PEAK AREA
130  REM FINALLY INCLUDE DEAD TIME CORRECTION CT/LT
140  REM   N0=CT/LT*(N1-N2)/(EXP(-LAMBDA(T1-T0))-EXP(-LAMBDA(T2-
T0)))
150  REM ABOVE N0 AND N1-N2 ARE NOT EFFICIENCY CORRECTED
160  REM DIVIDE BY ABSOLUTE DETECTOR EFFICIENCY IN ORDER TO
170  REM OBTAIN ABSOLUTE 'REAL' VALUES FOR N0 AND N1-N2
180 REM BASIC ANALOG OF LINE 140 IS LANT/03 LINE 3720 WITH
190 REM   T1,T2,C0 SUBSTITUTED IN PROGRAM LINES 3600,3610,3620
200 REM     WHERE C0 DIVIDED BY KG.SEAWATER FOR SAMPLE SPECTRA
210 REM SUBROUTINE 40 PUTS IN NEW OR MODIFIED DATA
220 REM SUBROUTINE 50 STORES INPUT DATA INTO DISKFILE
230 REM SUBROUTINE 60 LOADS EXISTING INPUT DATA INTO MEMORY
240 REM SUBROUTINES 70 AND 80 COMPUTE NUMBER OF ATOMS AT T0
250 REM SUB 90 COMPUTES NUMBER OF ATOMS RADIOISOTOPE PER MOLE
260 REM   ELEMENT IN EACH STANDARD,THEN TAKES MEAN OF STANDARDS
270 REM SUB 100 THEN COMPUTES CONCENTRATIONS IN SAMPLES
280 REM SUB 110 COMPUTES SHALE NORMALIZED VALUES IF DESIRED
290 REM SUBROUTINE 120 MAKES YIELD TRACER CORRECTION ON
300 REM   OUTPUT OF SUB 80,THEN PROGRAM STEPS AGAIN THROUGH
310 REM   SUBS 90,100 AND 110
320 REM THUS ONE OBTAINS BOTH YIELD TRACER CORRECTED AND
330 REM   UNCORRECTED CONCENTRATIONS(PICOMOL/KG SEAWATER)
340 REM SUBROUTINE 130 PRINTS A0(M,N)ON CRT OR LINE PRINTER
350 REM SUBROUTINE 150 PRINTS B1 AND V1 ON CRT OR LINE PRINTER
360 REM SUBROUTINE 160 PRINTS G1$,G2$,G3$,G4$,G5$
370 REM SUBROUTINE 170 PRINTS INPUT DATASET
380 REM ****PARAMETERS LISTING****
390 REM M    INTEGER LABEL OF EACH SINGLE ISOTOPE,MULTIPLE
400 REM      PEAKS OF SINGLE ISOTOPE TREATED AS SINGLE PEAKS
410 REM      OF MULTIPLE ISOTOPES
420 REM      M>M1 ACTIVATION PRODUCED ISOTOPE
430 REM M1   NUMBER (0 OR 1)OF YIELD TRACER ISOTOPES
440 REM M2   NUMBER OF ACTIVATION PRODUCED ISOTOPES
450 REM M3   =M1+M2<21
460 REM N    INTEGER LABEL OF EACH SINGLE SPECTRUM
470 REM      N>N1 SPECTRUM OF SAMPLE OR BLANK
480 REM N1   NUMBER OF STANDARD SPECTRA
490 REM N2   NUMBER OF SAMPLE (AND BLANK) SPECTRA
500 REM N3   =N1+N2<16
510 REM
520 REM A0(M,N)    NUMBER OF COUNTS COLLECTED OVER TIME
530 REM     INTERVAL T1-T2,I.E.NET PEAK AREA FROM GAMANL OUTPUT
540 REM A0(M,N)   =NUMBER OF ATOMS PER KG SEAWATER AT T0, AFTER
550 REM             PROGRAM LINE 3720
560 REM A0(M,N)   =CONCENTRATION(PICOMOL/KG)OF SAME ELEMENT AS
570 REM              ISOTOPE M IN SAMPLE N (N>N1),AFTER
580 REM              PROGRAM LINE 4290
590 REM A0(M,N)   =RATIO SAMPLE*E^6/SHALE,AFTER LINE 4550
```

```
600 REM A0(M,N)    =YIELD TRACER CORRECTED NUMBER OF ATOMS AT
610 REM               T0,AFTER PROGRAM LINE 4820
620 REM A0(M,N)    =YIELD TRACER CORRECTED ANALOGS OF ABOVE
630 REM               LINES 560,580,610
640 REM B0(M,N)   =NUMBER OF ATOMS PER KG SEAWATER AT T0, NOT
650 REM             CORRECTED FOR YIELD TRACER
660 REM B1(M)     (1/PICOMOL) MEAN VALUE FOR N1 STANDARDS OF
670 REM             B0(M,N)/D1(M,N)
680 REM              CORRECTED FOR YIELD TRACER
690 REM C0(N)     (SECONDS)  CT=COUNT TIME OF SPECTRUM N
700 REM C1(N)     (SECONDS)  LT=LIFE TIME OF SPECTRUM N
710 REM C2(N)     KILOGRAM SEAWATER OF SAMPLE N (N>N1)
720 REM            ASSIGN SIMILAR VALUE FOR BLANKS
730 REM C3(N)     =(C0(N)/C1(N))/C2(N)
740 REM D0(M)     (MINUTES)= 1/LAMBDA=HALFLIFE/LN2
750 REM D1(M,N)   (PICOMOL) AMOUNT OF SAME ELEMENT AS ISOTOPE
760 REM             M IN STANDARD N WHERE M>M1
770 REM D2(M)     (MICROMOL/KG) CONCENTRATION IN SHALE OR
780 REM             OTHER NORMALIZER WHERE M>M1
790 REM T0        (MINUTES)REFERENCE TIME POINT,E.G.END OF
800 REM             IRRADIATION;RESTRICTION T0<T1(N) FOR ANY N
810 REM T1(N)     (MINUTES)HAYDEN CLOCK TIME AT BEGIN OF COUNT
820 REM T1(N)     (MINUTES)=T1(N)-T0 AFTER PROGRAM LINE 3600
830 REM T2(N)     (MINUTES)=END OF COUNT INTERVAL,SEE LINE 3610
840 REM V1(M)     (%)STANDARD DEVIATION OF B1(M)
850 REM **PROGRAM PARAMETERS**
860 REM P1        INPUT RETURN;P1=13 CORRECTION;P1=11 CONTINUE
870 REM          HARD COPY PRINTOUT? P1=11=YES;P1=13=NO
880 REM P2        SHALE NORMALIZATION? P2=11=YES;P2=13=NO
890 REM P3        PREVENTS MULTIPLE YIELD TRACER CORRECTION
900 REM             LOOPS (SEE PROGRAM LINES 1110,3540,4790)
910 REM          SELECTS PROPER HEADINGS (CORRECTED/UNCORRECTED)
920 REM P4        SELECTS DESIRED MODE FOR DATA INPUT(LINE 2120)
930 REM **ALPHANUMERICS**
940 REM E1$(N)    SPECTRUM NUMBER (MAXIMUM 4 DIGITS)
950 REM E2$(N)    SAMPLE DEPTH (M) OR AMOUNT OF LA IN STANDARD
960 REM F1$(M)    NAME OF ISOTOPE (MAXIMUM 6 DIGITS)
970 REM F2$(M)    KEV OR CHANNEL NUMBER (MAXIMUM 4 DIGITS)
980 REM G1$       MONTH/DAY/YEAR OF LANTH01 PROGRAM RUN
990 REM G2$       NAME OF OPERATOR
1000 REM G3$       M/D/YR OF IRRADIATION
1010 REM G4$       M/D-M/D/YR OF COUNT SET
1020 REM G5$       ORDER OF COUNT SET
1030 REM R1$      NAME OF EXISTING DATAFILE
1040 REM R2$      NAME OF NEW DATAFILE
```

## 9.2. Removal Rates of the Rare Earths in the North Atlantic Deep Water

Assessment of the relative importance of in situ chemical processes versus lateral transport is a classical problem in marine chemistry. Given only one station in an area with complex dynamic hydrography one will not arrive at a firm answer to this question for the rare earths.Yet by following the two schools of thought the two extreme cases for behaviour of these elements can be evaluated.

The deep water column (992-4426m) exhibits a fairly linear O-S relationship(r=0.995,N=35; Figure 3.1). All REE-S plots over this depth range exhibit a negative curvature.With decreasing atomic number this curvature increases from Lu to Sm, but then drops off again towards Pr and Lu. This degree of REE-S curvature can be expressed semi-quantitatively with the constant $\psi/w$ (Figure 9.2.1., upper graph). This constant is determined using the formalisms of CRAIG (1974). First a best value $z^* = 1.2 \pm 0.4$ was established by curve fitting to the profiles of both salinity and potential temperature over the 992-4426m depth range. Then, using both the best value 1.2 as well as the lower and upper limits $z^*=0.8$ and $z^*=1.6$, best values for $\psi/w$ were assessed by curve fitting to the profiles of each rare earth element. Under assumption of (1) a steady state mean (southward) flow of the NADW, (2) with constant flow rate over the depth interval and (3) identical REE patterns of its various source waters, the relative degree of curvature $(\psi/w)_{REE}/(\psi/w)_{Lu}$ evolves into a constant $\psi/\psi_{Lu}$ for the relative net removal rate of REE at this station (Figure 9.2.1). This would suggest that the absolute net removal rates for Tb,Eu and Sm are respectively 2.3, 2.6 and 2.8 times as fast as for Lu. This trend is consistent with above mentioned adsorptive removal of free ionic $REE^{3+}$-ions from seawater. Due to adsorption alone the rare earths remaining in seawater become HREE enriched, while the authigenic flux on settling particles carries the inverse, LREE enriched, pattern. Regeneration of this particulate fraction reintroduces a LREE enriched pattern into seawater. The difference between gross adsorption and regeneration eventually determines the net removal rate of each rare earth element. The shape of the REE pattern for a given sample is a composite of the linear HREE enriched and LREE enriched patterns and

reflects the relative importance of respectively gross adsorption and regeneration. Therefore the gross adsorption of a much higher percentage free $La^{3+}$-ion is counteracted by strong preferential regeneration. As a result the net removal rate of Lu is only 2.3 times faster than for Lu, and actually slower than for Sm and Eu(Figure 9.2.1).In lieu of above kinetic approach one can also conceive of a rapid, quasi-equilibrium, reversible exchange between the dissolved and particulate forms in the water column. Then the LREE would spend relatively more time in the particulate form, thus being transported downward more rapidly, and their profiles would indeed have the observed steeper gradient with depth.

Alternatively we have sought to explain all features at this station strictly by lateral transport. With close enough sampling a REE pattern can be assigned to the core of each water mass. Vertical dissipation between two adjacent water masses would show up as a linear mixing line between the tow endmembers. Then the REE pattern at 3253m represents the core of the Denmark Strait Water. Higher concentrations and a slightly different REE pattern in the bottom water can only be explained by admixture of a southern component(AABW). Minima for most REE at 2870m and 1729m roughly coincide with respectively Iceland-Scotland Water and Labrador Sea Water. Most REE show a maximum at 1184m which one would like to ascribe to the Mediterranean overflow. Yet the hydrographic data do not yield evidence for this water type. On the other hand concentration values and REE patterns reported for MOW are not unlike our 1184m sample. With only 17 sampling depths mixing lines between adjacent water masses cannot be established.

Below 990m depth a good correlation ($r=0.997, P<0.001$) exists between Lu and silicate. The latter is generally considered a conservative tracer within the Northwest Atlantic basin. Thus Lu and other REE might just as well be treated as conservative elements.Of course the lighter REE again display a negative curvature versus silicate but that may simply be ascribed to different LREE depletion patterns in the various source waters (DSW,ISW,LSW) for the NADW.Yet in order to obtain these various LREE depleted patterns from a flat input pattern one eventually still has to invoke the inverse trend for net removal rates.

No firm assessment can be made of the importance of lateral transport versus in situ chemical processes. Yet some speculative hypotheses may serve as subjects of future falsification:

The correlation with deep water silicate as well as proposed long residence times imply that the distribution of Lu in the Northwest Atlantic Ocean is dominated by lateral transport. A similar statement can be made for the lighter rare earths. This in itself would not invalidate the scenario for relative net removal rates. For example an arbitrarily assigned 90-95 % control by lateral transport for Lu would amount to a control by in situ chemical processes of only 5-10 % for Lu but 14-28 % for Sm. Only in the case of cerium the chemical terms may become significant at this station. An extreme upper limit can be set by assuming a 100 % chemical control of cerium in the deep water. Then the Lu distribution would still be dominated for (100 - 100/4.3)= 80 % by lateral transport.

On a global scale lateral transport would cancel out. The controls on a 'typical' REE profile would be as follows. A regenerative flux from shelf sediments in combination with a possible aeolian or riverine terrestrial influx determines the surface water concentration. Extensive regeneration at the seafloor,most probably due to desorption from dissolving opal or calcite carriers, sets the value in the bottom water. Vertical dissipation would yield a linear mixing trend, but the eventual curvature of the profile is set by the balancing act between global upwelling and scavenging removal. The scavenging term itself is the net result of gross adsorption, desorption and regeneration. Settling particles, probably opal or calcite, would act as the scavenging agents. For cerium this internal cycling is considerably enhanced by additional oxidation/reduction reactions.

In order to accomodate the REE patterns for seawater one seemingly has to invoke an identical trend for the mean oceanic residence times. The latter are supposedly in the same order of hundreds of years as the timescales for interoceanic mixing. Their inverse, the mean oceanic removal rate, would then indeed resemble the trend in relative scavenging removal rates as observed locally at this station (Figure 2.9.1). Yet in a steady state the output should match the input. In other words, all REE

must have the same mean oceanic residence time. Then the observed local scavenging removal in the Northwest Atlantic would have to be counteracted by intense regeneration of authigenic deposits in other locales, and the mean global REE pattern for seawater would be flat like shales. However these deposits have been formed over much longer geological time scales during which a steady state is rather unlikely. The construction of a realistic steady state mass balance for dissolved REE in seawater may prove to be difficult, if not impossible.

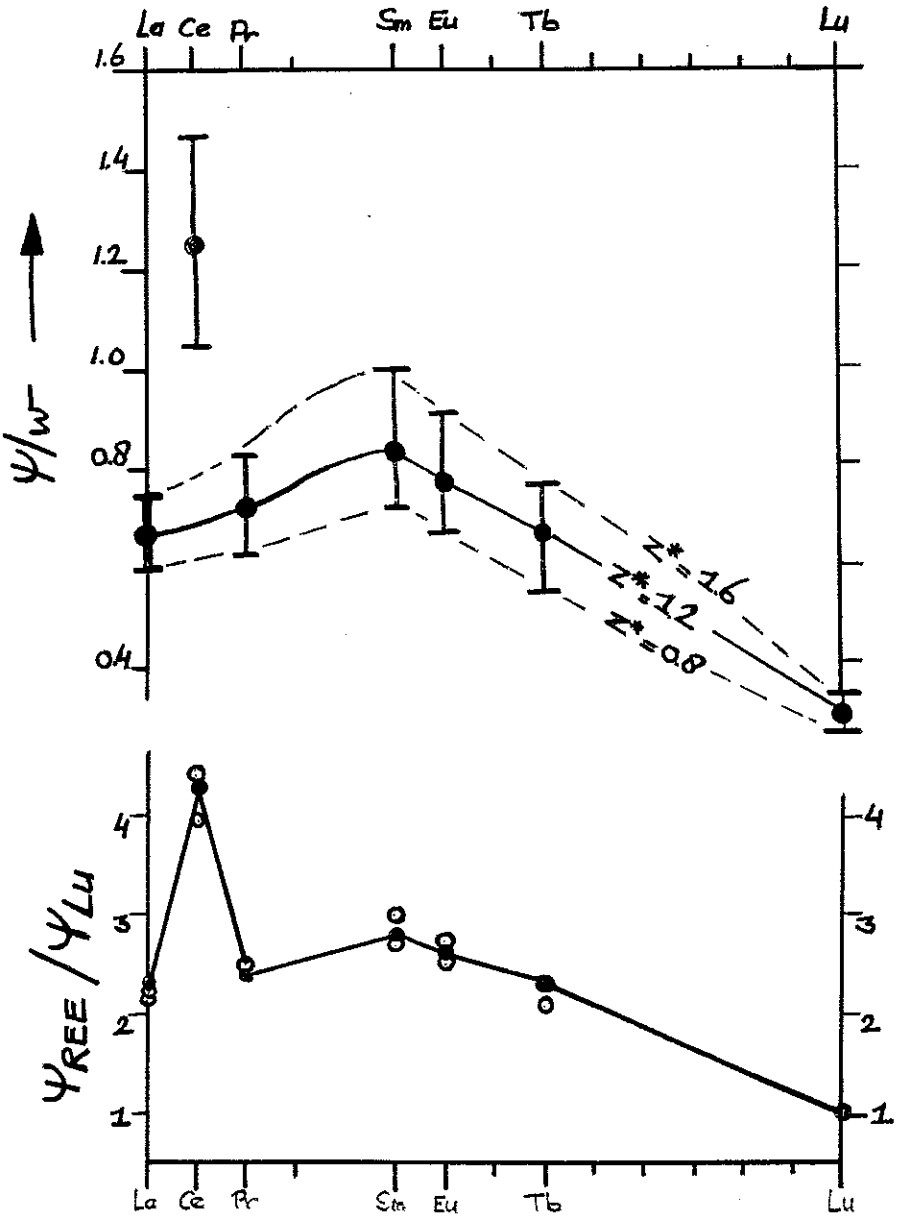


Figure 9.2.1. ABOVE: The negative curvature of REE-Salinity plots as quantified by $\psi/w$ in the equation $z^*C'' + \psi/w\, C = C'$ with $z^*$ determined after CRAIG (1974). The trend resembles the inverse of the REE patterns of the deeper samples at the N.W. Atlantic station and is not greatly affected by variations of $z^*$ between its lower and upper limits.

BELOW: Ratios $\psi / \psi_{Lu}$ in the bottom graph suggest net removal rates which are 2.3(La), 4.3(Ce), 2.4(Pr), 2.8(Sm), 2.6(Eu), and 2.3(Tb) times as fast as for Lu.